PICES Scientific Report No. 20
2002

PICES-GLOBEC INTERNATIONAL PROGRAM ON CLIMATE CHANGE AND CARRYING CAPACITY

REPORT OF 2001 BASS/MODEL, MONITOR and REX Workshops, and THE 2002 MODEL/REX Workshop

Edited by
Harold P. Batchelder (CCCC IP), Gordon A. McFarlane (BASS), Bernard A. Megrey (MODEL), David L. Mackas (MONITOR), William T. Peterson (REX)

August 2002
Secretariat / Publisher
North Pacific Marine Science Organization (PICES)
c/o Institute of Ocean Sciences, P.O. Box 6000, Sidney, B.C., Canada. V8L 4B2
E-mail: secretariat@pices.int Home Page: http://www.pices.int

-

TABLE OF CONTENTS

EXECUTIVE SUMMARY

This report summarizes the results of three PICES-GLOBEC Climate Change and Carrying Capacity (CCCC) Task Team (TT) workshops held at the PICES Tenth Annual Meeting in October 2001, in Victoria, British Columbia, Canada and a joint MODEL/REX workshop held in Nemuro, Japan, in January 2002. The three workshops during the Annual Meeting were: 1) a 1-day joint BASS/MODEL workshop to *review ecosystem models for the subarctic Pacific gyres*, 2) a 1-day MONITOR workshop to *review progress in monitoring the North Pacific*, and 3) a 1-day REX workshop on *temporal variations in size-at-age for fish species in coastal areas around the Pacific rim*. Each of these workshops addressed the core activities of these Task Teams; moreover, they continue a trend of having joint workshops of multiple Task Teams, which provides opportunities to broaden the scope of the discussions and lead to synthesis. This trend to multi-Task Team workshops is timely because during the coming year, and particularly at the PICES Eleventh Annual Meeting (Qingdao, People's Republic of China), CCCC will be examining progress achieved during the past decade, documenting its successes and failures in answering the scientific questions posed initially, and evaluating whether the current structure of Task Teams and Advisory Panels is the most suitable to carry CCCC research forward into the next decade.

The joint BASS/MODEL workshop focused on two ECOPATH equilibrium models describing energy flow through the eastern and western subarctic gyres, and explored the dynamics of energy flow in these two systems using ECOPATH/ECOSIM formulations. The equilibrium models suggest that biomass in the western subarctic gyre (WSA) is higher than in the eastern subarctic gyre (ESA). Biomasses of several species (flying squid, pomfret, chaetognaths and salmon) were higher in the WSA than in the ESA. A conclusion of these ECOPATH investigations was that estimates of diet compositions for many of the species were poorly known. Several recommendations regarding future research resulted from the workshop, including improving the quality of available input data sets (like diet). BASS and MODEL plan to continue their joint work on this project by linking the ECOPATH/ECOSIM higher trophic model to the NEMURO model of lower trophic levels dynamically. Since the NEMURO model is forced by ocean conditions (mixed layer depth, temperature, insolation, etc.), this linking of models will provide a method for exploring the results of various climate change scenarios on higher trophic levels in the WSA and ESA.

The MONITOR workshop was focused on reviewing the need and capability of sustained, long-term monitoring of ocean and ecosystem conditions in the PICES region, especially considering the recent emphasis within PICES on producing a North Pacific Ecosystem Status Report. Presentations at the workshop summarized some of the tools that are available now or could be put into place to assist this effort - including both regional networks of coastal observing systems, Continuous Plankton Recording (CPR) across the gyres, and data management. Among other recommendations, MONITOR would like to develop a closer liaison with regional (Gulf Ecosystem Monitoring [GEM]) and international (Data Buoy Cooperation Panel [DBCP], Coastal Global Ocean Observing System [C-GOOS]) providers of ocean data, and extend CPR observations of the subarctic gyres to other ancillary data types beyond zooplankton biomass and species composition.

The REX workshop summarized historical datasets on salmon and herring populations across the Pacific, with additional contributions on a few other species. Several key themes that emerged from the workshop were: 1) the importance of understanding the spatial coherence and scales of size-at-age patterns, 2) the search for mechanistic (causal) as opposed to correlational explanations of common temporal trends between the environmental variables and size-at-age data, and 3) the influence of density-dependence and the mechanisms through which it affects size-at-age changes through time.

The fourth report is the result of a joint MODEL/REX workshop that brought scientists involved in developing the NEMURO model together with experts on saury and herring growth. The principal objective was to include a fish growth model into the lower trophic level NEMURO model. For efficiency, the group focused on modeling the growth of a single fish using input data on prey abundances and temperature provided by the NEMURO model. A previously published clupeid bioenergetics model (from the Atlantic) was adapted to two different important fish in the North Pacific, Pacific herring and Pacific saury. These two species have contrasting life histories and growth rates; however, by tuning the parameters of the model to each species, growth curves were obtained that match observations reasonably well. A few longer term, multicohort (where each year one fish is modeled) simulations of the saury model indicated some interannual variability in growth as a result of environmental forcing of temperature and prey fields.

The four Task Teams of CCCC are beginning to coordinate their activities in ways that will hopefully provide answers to many of the CCCC scientific questions, and to develop or coordinate an ecosystem monitoring network. This network will provide information to PICES that is essential in preparing regularly updated North Pacific Ecosystem Status Reports. The final recommendations from each of the CCCC Task Teams can be found in the PICES 2001 Annual Report.

Harold P. Batchelder and Makoto Kashiwai
CCCC-IP Co-Chairmen

BASS/MODEL WORKSHOP TO REVIEW ECOSYSTEM MODELS FOR THE SUBARCTIC PACIFIC GYRES

(Co-convenors: Gordon A. McFarlane, Andrei S. Krovnin, Bernard A. Megrey and Michio J. Kishi)

Workshop objectives

The BASS/MODEL workshop on higher trophic level modeling (March 5-6, 2001, Honolulu, U.S.A.) recommended to convene a 1-day workshop to evaluate the results of the inter-sessional workshop (for details see PICES Scientific Report No. 17, 2001) and initiate hypothesis testing using the models developed.

This follow-up BASS/MODEL workshop was held October 5, 2001, immediately preceding the PICES Tenth Annual Meeting in Victoria, British Columbia, Canada. The objectives of the workshop were to:

- assess the results of the March 2001 workshop,
- review progress on model development and updated models; and
- begin to develop scenarios to test key hypotheses.

Review of baseline models

The two ECOPATH/ECOSIM baseline models developed at the March 2001 workshop on higher trophic level modeling should be viewed as work in progress. Estimates of biomass, productivity to biomass, consumption rate to biomass and diet composition were compiled from the literature and from research data provided by PICES member countries. In general, information available for 1990 (or 1990-1993) was used such that the two models could be viewed as representative of the early 1990s conditions. In total, 56 species groups (with three detrital groups) were included in the models, however some species were not common to both regions. Minke whales, common dolphin, Japanese sardines and anchovies were present in the Western Subarctic Gyre (WSA) model, but not in the Eastern Subarctic Gyre (ESA) model. Conversely, elephant seals were present in the ESA model only. Many of the estimates are at best only guesses. Some observations were derived from coastal ecosystems and therefore may not be applicable to gyre ecosystems.

In general, the total biomass estimated for the WSA was higher than for the ESA. Major differences between the two model regions include higher biomasses of flying squid and Pacific pomfret in the ESA, higher biomass of chaetognaths in the WSA, and higher salmon biomass in the WSA (pink salmon) than in the ESA (sockeye salmon). Marine mammal biomass estimates were identical for each region since they were derived from basic-scale North Pacific estimates. No biomass estimates of forage fish and micronektonic species groups were available from the literature or from research survey data, so these were evaluated by top-down balancing of each model. Biomass estimates for lower trophic level plankton groups were derived from outputs of the NEMURO model that had been calibrated for Ocean Station P in the ESA.

Productivity values were derived from mortality rates. Consumption rates were obtained from diet composition and laboratory descriptions of calories/gram for prey species. Both production and consumption estimates were weighted by residence time for migratory species. The estimates for lower trophic levels (e.g. large zooplankton) were taken from other ECOPATH models and, in some cases, from the NEMURO model.

All information on diet composition was poor. Marine mammal diets were not as detailed as fish diets. Salmon diets were specific and detailed with many stomachs sampled over large areas and seasons, however, only summer estimates were available for the WSA. The major difference between the WSA and ESA were the seasonal differences in the diet of salmon since WSA included sockeye salmon in May. Early spring diet estimates for the early 1990s were not

available for the ESA. Physical forcing inputs to the NEMURO model can be generated to produce phytoplankton and zooplankton outputs. Maximum photosynthetic rates, zooplankton growth efficiencies and microbial loops can be modified and initiated to provide various climate change scenarios. These outputs can be used in ECOSIM.

Update of ECOPATH/ECOSIM models

Kerim Aydin reviewed the updated ECOPATH/ECOSIM baseline models. Figures 1 and 2 show composite images of the food webs for the eastern and western Pacific subarctic gyres. These models were initially constructed from data assembled at the March 2001 BASS/MODEL workshop and updated by including results of lower trophic level modeling by the MODEL Task Team and upper trophic level data from a wide range of sources on both sides of the Pacific.

Future adjustments to the models based on additional data presented at the Victoria workshop will be incorporated into the final versions of these models and presented at an inter-sessional BASS/MODEL workshop to be convened in April 2002. This will lead to a PICES Scientific Report

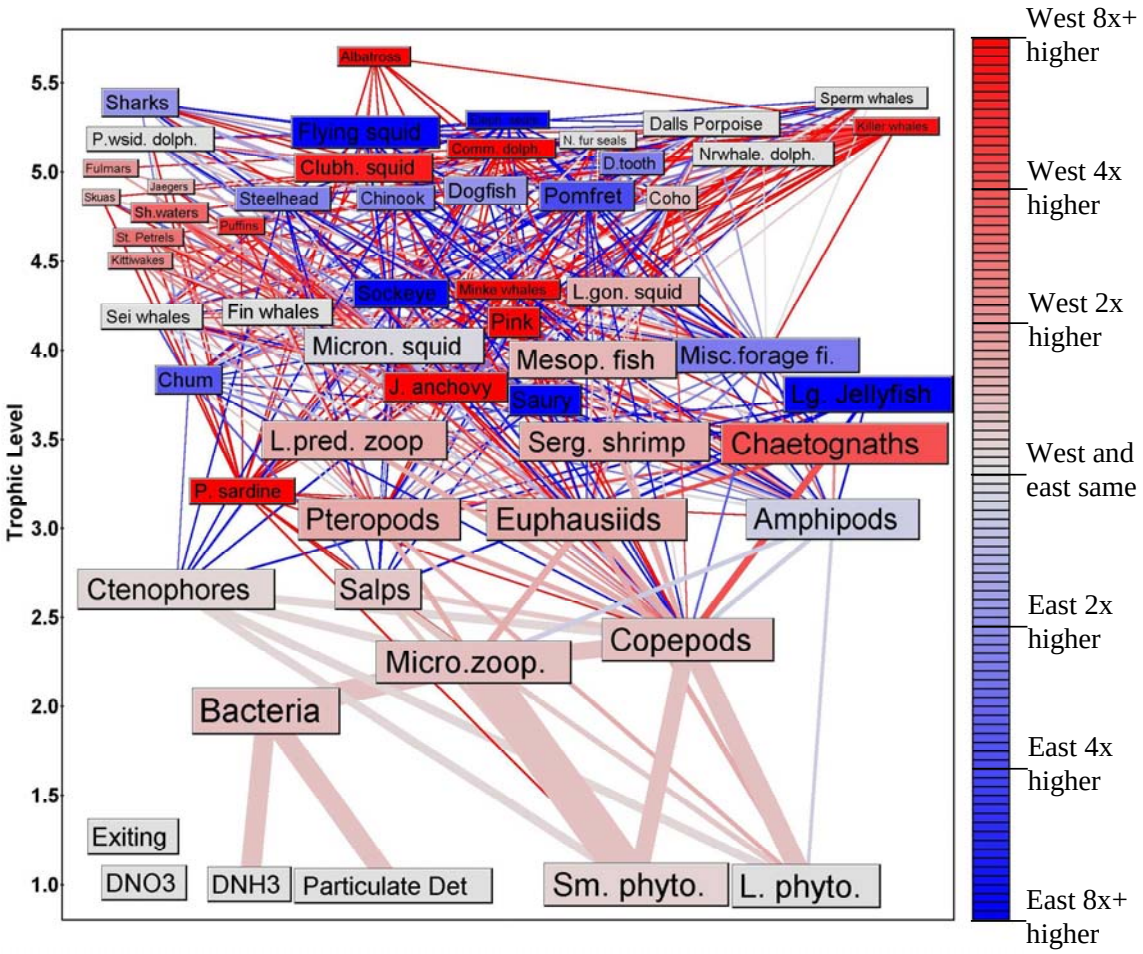

Fig. 1 A combined quantitative food web of the eastern and western Pacific subarctic gyres constructed from data assembled at the March 2001 BASS/MODEL workshop and presented at the PICES Tenth Annual Meeting. Species in both the western and eastern gyres are shown. The area of each compartment is proportional to log of average biomass density (t/km^2), and the width of each connecting flow is proportional to the square root of the averaged yearly flow volume (t/km^2/year). Coloration shows the ratio of west *vs*. east biomass density and flow volume: where the ratio of west/east is higher (red) and where the ratio of east/west is higher (blue).

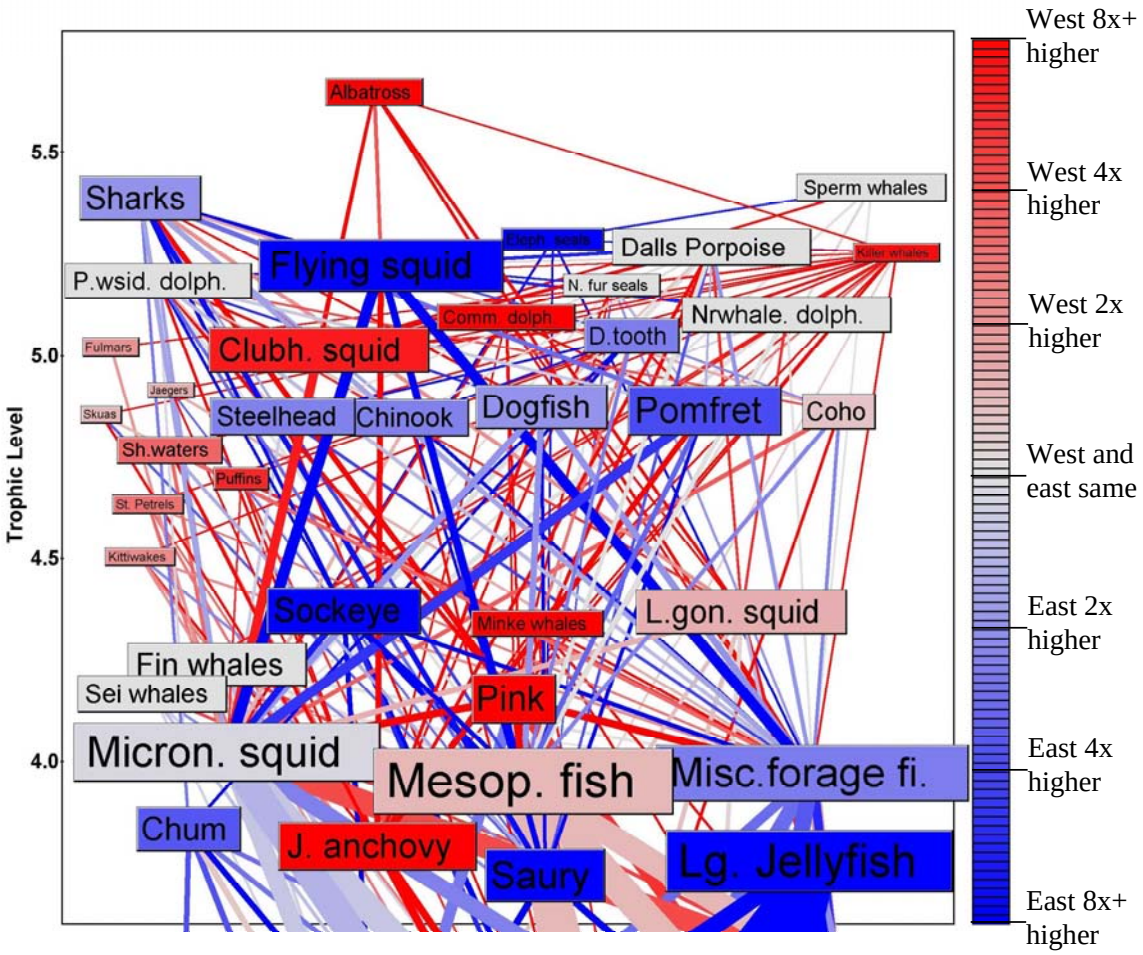

Fig. 2 An enlargement of the upper trophic level flows and biomass densities shown in Figure 1. Minor flows (the lowest 10% (cumulative) of prey mortality and predator diet) are removed for clarity. See Figure 1 for explanation of coloration.

to document the models and assess the overall state of knowledge of food web interactions and critical dynamic links in subarctic gyre ecosystems. In addition, the April 2002 meeting will focus on the potential to incorporate dynamic simulations of climate into these models.

This continuing synthesis highlighted some key areas for future research, for example, the exploration of dynamics of the intermediate trophic levels such as micronektonic squid, small forage fish, and mesopelagic fish (Fig. 2). The biology of these species is currently poorly understood and yet central to the functioning of the subarctic food web.

Another key direction for future work lies in developing methods to integrate gyre processes with boundary currents and near-shore processes. Specifically, concurrently examining the dynamics of boundary current species such as the Pacific sardine and Japanese anchovy in relation to the dynamics of the salmon-dominated subarctic gyre ecosystems that were simulated by these models, will increase our understanding of North Pacific-wide climate systems and their interrelations with coastal systems.

Recent improvements to NEMURO model

Bernard Megrey reviewed recent progress and improvements on the NEMURO lower trophic level modelling efforts.

Diagnostic calculations

Several diagnostic calculations were added to the NEMURO model. These included Production/ Biomass (P/B) ratios for phytoplankton and zooplankton, Food Consumption/Biomass (C/B) ratios for small, large and predatory zooplankton, and Ecotrophic Efficiency (a measure of how much primary production transfers up the food web to the zooplankton species and ultimately to higher trophic level species).

Validation to Station P

The NEMURO model was parameterized for Ocean Station P and output was compared to data collected from that site. Results were favourable. NEMURO provides reasonable C/B and P/C ratios. Annual primary production from the model (149 $gC/m^2/yr$) is only 6% higher than the best current estimate (140 $gC/m^2/yr$) by Wong *et al.* (1995). Average chlorophyll concentration from the model (0.42 mg/m^3) is only 5% higher than the long-term value (0.4 mg/m^3) measured by Wong *et al.* (1995). An f-ratio (assuming that the production of the large phytoplankton is primarily fuelled by "new" nitrogen) is in a good agreement with the estimate by Wong *et al.* (1995): 0.23 and 0.25 respectively.

Zooplankton vertical migration

Results without ontogenetic migration of predatory zooplankton (ZP) show a large diatom bloom around day 73 (Fig. 3, top panel). The prevailing view is that there is no spring bloom at Station P. Thus the bloom is an artifact of the "box" nature of the model. Adding ZP migration, decreases biomass of phytoplankton by a factor of 2 (Fig. 3, bottom panel) and generates more reasonable diagnostics. The estimates of Ecotropic Efficiency are not significantly affected.

Microbial loop

Inclusion of a microbial loop had only a small impact on the standing stocks of small and large zooplankton (Fig. 4). Predatory zooplankton were reduced by about one half, reducing potentially available biomass for fish production. These differences are due to the decreased net trophic efficiency of the system because a large portion of the primary production passes through a microbial

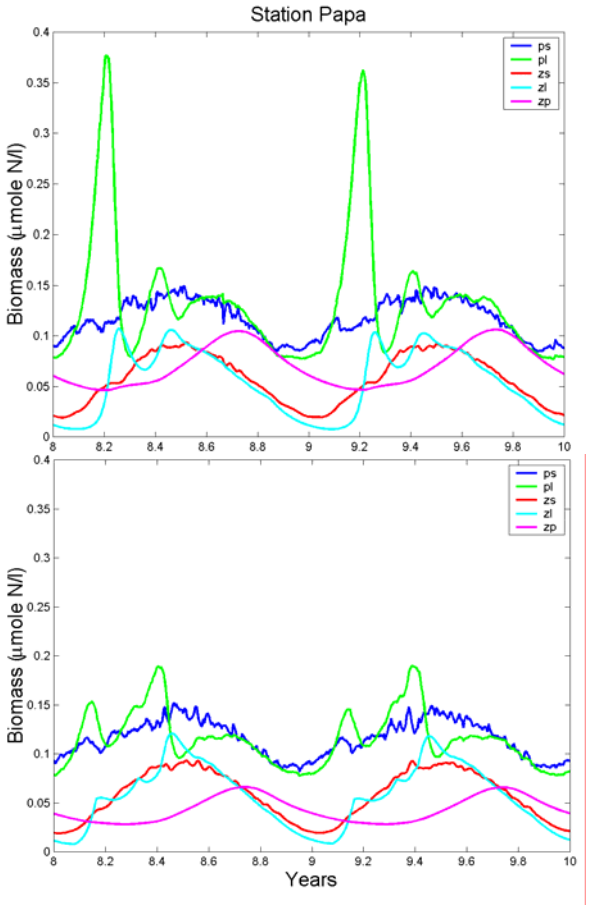

Fig. 3 Comparison of NEMURO output with (bottom panel) and without (top panel) ontogenetic migration of large zooplankton.

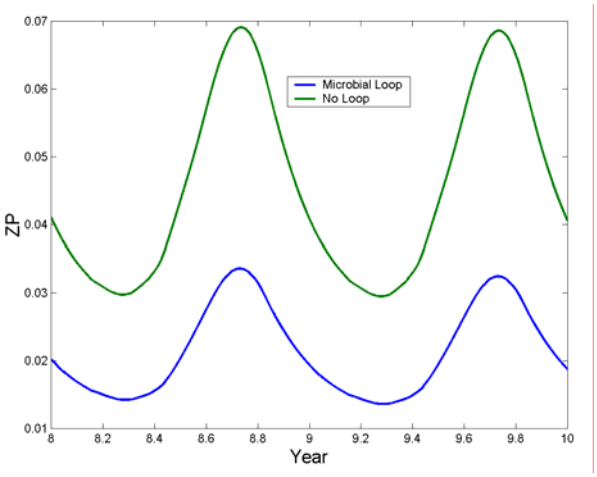

Fig. 4 Comparison of NEMURO output with and without the microbial loop approximation.

community before entering the zooplankton community.

Recent progress

MODEL Task Team also conducted a sensitivity analysis and data assimilation for Station A7 and added carbon fluxes to the LTL model.

The most recent improvements to the NEMURO model include:

- Acquired SST time series from Station P 1951-1988;
- Acquired equations to permit calculation of light at the surface;
- Modified primary production equations to explicitly include mixed layer depth (MLD) to permit simulation of regime shift scenarios.

In addition, S. Lan Smith presented work being conducted in support of the NEMURO model, and this overview is appended as Endnote 2.

Hypothesis testing scenarios

The following scenarios were suggested:

- Examine impact of changes in primary and secondary production on each gyre. Do they respond similarly or differently?
- Examine seasonality of changes in each system;
- Examine the role of primary production increases on sockeye salmon abundance;
- Examine role of predation in the regulation of population abundance:
  - shark/salmon
  - marine mammal/salmon
- Examine role of marine birds in each gyre;
- Examine role of forage fish in each gyre;
- Examine species competition for prey, e.g. pink/sockeye salmon; pomfret/squid, etc.

Recommendations

1. Convene a joint BASS/MODEL workshop in April 2002 to continue hypotheses testing of the models developed at the 2001 workshop and refined at the Tenth Annual Meeting;
2. Parameterize the western gyre model, in particular finalize the boundary to exclude the transition area;
3. Calibrate and validate the NEMURO model to Station A, which is more appropriate for the western gyre;
4. For both the eastern and western gyre models, incorporate time series (from the NEMURO model) for light, SST, etc. to generate primary productivity and zooplankton time series;
5. Hypotheses to be tested should be developed prior to the inter-sessional workshop and should focus on climate change scenarios;
6. Complete final data synthesis (including marine birds and mammals) prior to the inter-sessional workshop;
7. Following the inter-sessional workshop; prepare the two baseline models for publication as a PICES scientific Report, including the results of hypotheses testing, and a data inventory;
8. PICES provide a means of accessing these models, and other workshop products on the web;
9. BASS/MODEL/REX Task Teams convene a joint session (with GLOBEC) at the PICES Eleventh Annual Meeting to examine "Approaches for linking basin scale models to coastal ecosystem models";
10. Given the limited data on diet of many species inhabiting the gyres, PICES should encourage researchers to collect and collate diet data for species in these areas and sponsor the development of "Diet database" which would be peer-reviewed and citable.

References

Wong, C.S., Whitney, F.A., Iseki, K., Page, J.S., and Zeng, J. 1995. Analysis of trends in primary productivity and chlorophyll-a over two decades at Ocean Station P (50˚N 145˚W) in the Subarctic Northeast Pacific Ocean. *In* R.J. Beamish (ed.) Climate Change and Northern Fish Populations. Canadian Special Publication in Fisheries and Aquatic Sciences 121: 107-117.

Endnote 1

Simulating the cycling of organic matter using a nitrogen-based oceanic ecosystem model: carbon to nitrogen ratios

S. Lan Smith[1], Yasuhiro Yamanaka[2] and Michio J. Kishi[3]

[1] Frontier Research System for Global Change, Global Warming Division, 3173-25 Showa Machi, Kanazawa-ku, Yokahama, Kanagawa 236-0001, Japan. E-mail: lanimal@jamstec.go.jp

[2] Graduate School of Environmental Earth Science, Hokkaido University, N10W5 Kita-Ku, Sapporo, Japan. 060-0810 E-mail: galapen@ees.hokudai.ac.jp

[3] Hokkaido University, Graduate School of Fisheries Sciences, 3-1-1 Minato-cho, Hakkodate 041-8611, Japan. E-mail: kishi@salmon.fish.hokudai.ac.jp

Efforts are beginning to include oceanic ecosystem models in global simulations of the carbon cycle, to improve the representations of primary production and of the resulting oceanic uptake of carbon dioxide. Coupling complicated ecosystem models with three dimensional physical models to obtain meaningful simulations poses several challenges. Before proceeding to a three dimensional implementation, we undertook this study using a one dimensional model to address challenges relevant to simulating the fate of dissolved and particulate organic matter.

We embedded a formulation for the cycling of dissolved organic matter (DOM) via the microbial food web (MFW) into a nitrogen-based oceanic ecosystem model [the NEMURO model developed by the PICES program; see Yamanaka *et al.* (2001)]. The formulation of Anderson and Williams (1999) for the cycling of dissolved organic carbon (DOC) was converted to a nitrogen-based formulation including the same three fractions of DOM: labile (L-), semi-labile (S-) and refractory (R-), as dissolved organic nitrogen (DON). With this ecosystem model, coupled to a one dimensional physical model, we simulated the Hawaii Ocean Time-series Station ALOHA for 1997 and 1998.

We compared our simulations to data for nitrate, silicate, DON, DOC, PON, and POC. Despite the deficiencies of the physical model, the ecosystem model reasonably simulated the vertical distribution of total DON, without tuning of parameters for this site. Only the sinking velocity of POM was reduced to 10 m per day from the default value of 50 m per day from NEMURO for the North Pacific. This was done consistently with the findings of Kawamiya *et al.* (1997) and Hurtt and Armstrong (1996), that slower sinking rates are necessary to simulate substropical locations. Parameters for the ecosystem model were based on those of Kishi *et al.* (2001)'s simulation of a site in the northwestern Pacific, and parameters for the DOM model were based on those of Anderson and Williams (1999).

While the average vertical profiles of nutrients and DOM were well simulated, seasonal variations were not well resolved by this one dimensional model. The model simulated too steep a decline in DON with depth below the photic zone, as did Anderson and Williams' model. The simulated C:N ratio of DOM was also too low in the near surface waters. We found that the assumption of Redfield stoichiometry was inconsistent with the data for non-refractory DOM and for POM at Station ALOHA. Data from other locations also reveal C:N ratios higher than Redfield values. To use nitrogen-based models such as this to simulate the carbon cycle with confidence, we must improve their representations of the C:N ratios of DOM and POM. These issues of stoichiometry are also relevant to the PICES program's goal of coupling lower trophic level models to models of fish production. Accurate simulations of fish production and biomass will require correct stoichiometries in these models.

References

Anderson, T.R., and Williams, P.J.B. 1999. Global Biogeochemical Cycles 13 (2): 337-349.

Hurtt, G.C., and Armstrong, R.A. 1996. Deep-Sea Res. 43 (2-3): 653-683.

Kawamiya, M., Kishi, M.J., Yamanaka, Y., and Suginohara, N. 1997. J. Oceanogr. 53: 397-402.

Kishi, M.J., Motono, H., Kashiwai, M., and Tsuda, A. [in press]. J. Oceanogr.

Yamanaka, Y., Yoshie, N.A., Fujii, M., Aita-Noguti, M., and Kishi, M.J. [in press]. Journal of Oceanography.

Endnote 2

List of participant

Canada

Jacqueline R. King
Gordon A. McFarlane
R. Ian Perry
Marc Trudel

Japan

Makoto Kashiwai
Toshio Katsukawa
Michio J. Kishi
Takahiro Ida
Kohei Mizobata
Sei-ichi Saitoh
Hiroaki Sato
S. Lan Smith
Akihiko Yatsu
Hiroshi Yoshinari

Russia

Natalia Klovatch
Andrei S. Krovnin
Alexei Orlov

U.S.A.

Kerim Aydin
Patricia Livingston
Thomas Loughlin
Bernard A. Megrey
Thomas C. Wainright
Francisco E. Werner

MONITOR WORKSHOP TO REVIEW PROGRESS IN MONITORING THE NORTH PACIFIC

(Co-convenors David L. Mackas and Sei-Ichi Saitoh)

A half-day workshop was convened by the MONITOR Task Team on the afternoon of October 6, 2001, immediately preceding the PICES Tenth Annual Meeting in Victoria, British Columbia, Canada. The overall workshop goal was to familiarize participants with the range of present monitoring activities in the PICES region, and with both near-future and longer-term plans and opportunities.

The group heard and discussed seven presentations on the March 2001 PICES/CoML/IPRC workshop in Honolulu, on ongoing or soon-to-begin time series data collection programs in the North Pacific, and on some of the challenges and opportunities in archival and analysis of historic time series data. Presentation titles and topics are very briefly summarized in the following bulleted paragraphs. Extended abstracts for some presentations follow.

- **Overview of the Workshop on "Impact of climate variability on observation and prediction of ecosystem and biodiversity changes in the North Pacific"** (Patricia Livingston, Alaska Fisheries Science Center, NOAA, U.S.A.; Pat.Livingston@noaa.gov)

A 3-day workshop co-sponsored by PICES, the Census of Marine Life program (through Alfred P. Sloan Foundation) and the International Pacific Research Center, was held March 7-9, 2001, in Honolulu. The workshop (proceedings published as PICES Scientific Report No. 18) catalogued existing time series observation programs in the North Pacific, and discussed plans for future North Pacific operational monitoring activities, and the roles of international organizations and programs with interests in these activities. An important outcome of the meeting was a proposal for a regularly-updated "North Pacific Ecosystem Status Report", coordinated through PICES, and perhaps involving the development of "Regional Analysis Centres" to facilitate analysis of ongoing time series.

- **Progress report from the PICES Continuous Plankton Recorder (CPR) pilot project** (Sonia Batten, Sir Alistair Hardy Foundation, UK; soba@wpo.nerc.ac.uk)

This report summarized for a broader audience the material previously presented to the CPR Advisory Panel (see Endnote 1 to the MONITOR Task Team report in the 2001 PICES Annual Report). The CPR is towed behind commercial ships of opportunity and samples mesozooplankton abundance and species composition in the upper layer. Group discussion focused on potential value-added measurements which might be included, *e.g.* ship-mounted sensors for temperature, salinity, fluorescence, nutrients, ocean color, and acoustic backscatter; depth profiles of temperature and/or salinity using expendable probes; visual observations of seabirds and marine mammals; and collation of measurements along the CPR track with broader surrounding spatial coverage from satellites and drifting buoys.

- **Updates on GEM (Exxon Valdez Oil Spill Trustee Council's "Gulf Ecosystem Monitoring" Initiative) and U.S. GOOS plans in the North Pacific** (Phillip Mundy, Exxon Valdez Oil Spill Restoration Office, U.S.A.; phil_mundy@oilspill.state.ak.us)

A large endowment fund is now in place to support (on a permanent basis) long-term time series observations in the coastal ocean off Alaska. Requests for proposals are being issued, and monitoring activities, both partnered and fully-funded, will increase steadily through the remainder of this decade. GEM is a regional program within the larger PICES area. GEM welcomes PICES expertise (and example) in the optimal design of the program. U.S. GOOS is developing additional regional programs centered in the Gulf of Maine, the California Current, and the Gulf of Mexico.

- **A proposal for a North Pacific Action Group of the international WMO/IOC Data Buoy Cooperation Panel** (Ron McLaren, Environment Canada; ron.mclaren@ec.gc.ca)

A network of moored and drifting buoys provides real-time meteorological and near-surface oceanographic data from various locations throughout the ocean. Coverage in the oceanic North Pacific is very sparse. A proposed North Pacific Action Group, sponsored collaboratively by PICES and the International Data Buoy Cooperation Panel, would provide a forum for sharing information on deployment opportunities and data use.

- **Review of Mexican oceanographic IMECOCAL program** (Gilberto Gaxiola, Centro de Investigación Científica y de Educación Superior de Ensenada, Mexico; ggaxiola@cicese.mx)

IMECOCAL (Investigaciones Mexicanas de la Corriente de California) is a new program which extends the spatial coverage of the present CalCOFI program to the southern part of the California Current off Baja California (roughly 22-32ºN). The program completes quarterly cruises, coordinated in time with CalCOFI surveys, and samples a broad range of hydrographic, planktonic and fisheries oceanographic variables. Training of graduate students is an important component of the program. Data reports and a more detailed program description are posted at the IMECOCAL web site (http://ecologia.cicese.mx/~imecocal).

- **Report on the August 2001 NEAR-GOOS Workshop** (Yoshioki Oozeki, National Research Institute of Fisheries Science, Japan; oozeki@affrc.go.jp)

The NEAR-GOOS Ocean Environment Forecasting Workshop was held August 27-31, 2001, in Seoul, Republic of Korea. The overall workshop goal was to discuss the status and need of a forecasting capability in the NEAR-GOOS region. NEAR-GOOS obtains operational physical oceanographic and meteorological time series in the marginal seas of Northeast Asia. There is a strong emphasis on rapid availability of data, some in real time, and more detailed data as "delayed mode" through the Japan Oceanographic Data Center. NEAR-GOOS databases are not yet set up to handle biological and chemical data, and PICES advice for practical and useful data collection systems for these variables would be useful.

- **Building global ocean profile and plankton databases for scientific research** (Sydney Levitus, National Oceanographic Data Center, NOAA, U.S.A.; Sydney.Levitus@noaa.gov)

The Global Oceanographic Data Archaeology and Rescue (GODAR) project (historical data) and the IOC World Ocean Database project (new data) were described and evaluated for the PICES audience. Quality screening methods, and transcription and formatting protocols are important issues for these large databases. The presentation described some useful approaches, and also gave examples of applications.

PICES Continuous Plankton Recorder pilot project

Sonia D. Batten
Sir Alistair Hardy Foundation for Ocean Science, 1, Walker Terrace, The Hoe, Plymouth, UK. PL1 3BN
E-mail: soba@wpo.nerc.ac.uk

Background

The Continuous Plankton Recorder (CPR) is towed behind commercial ships of opportunity and samples mesozooplankton abundance and species composition in the surface ~10 m. During 2000 and 2001, a total of 12 transects were carried out in the North Pacific (Fig. 1). Samples have been processed up to spring 2001, together with a pilot transect in summer 1997. The north-south (N/S)

route was operated by an oil tanker and the east-west (E/W) route by a container vessel. Over 95% of planned sampling was successfully achieved and some additional temperature data were collected on most of the north-south transects.

Results summary

Species distribution data through 2000 were presented for the north-south transect for key copepod species. One significant finding was that the surface development duration of *Neocalanus plumchrus* copepodites varied along the transect by up to 5 weeks, and was probably influenced by temperature (Batten *et al*., in press). This species spends only about 3 to 4 months in the surface waters but is probably the most important copepod, in terms of biomass, in the Gulf of Alaska in spring/early summer.

The April 2000 transect was selected for a more intensive spatial analysis. Instead of every fourth sample being processed (which is the normal practice), almost every sample was processed. Autocorrelations of abundance against distance for the most common taxa were carried out and showed that the decorrelation length scale is about 60 km. This analysis suggests that the current routine sampling resolution of the CPR (sample spacing of 72 km) is appropriate for the Gulf of Alaska.

As expected, an analysis of the mesozooplankton community on the east-west transect revealed distinguishable differences in community structure between geographic regions such as the Bering Sea, Aleutian shelf and the Gulf of Alaska. This result supports the idea that CPR data can be used to detect shifts in community composition on a temporal as well as a spatial basis. With currently available data, interannual comparisons are limited, however, comparison of mesozooplankton abundance between the pilot north-south sampling in summer 1997 with the same period in 2000 showed large changes, with zooplankton abundances in 1997 about 5 times higher in the open Gulf of Alaska. Although interpretation needs to be tempered by the limited sampling available for 1997, the results may be related to the 1997/98 El Niño event.

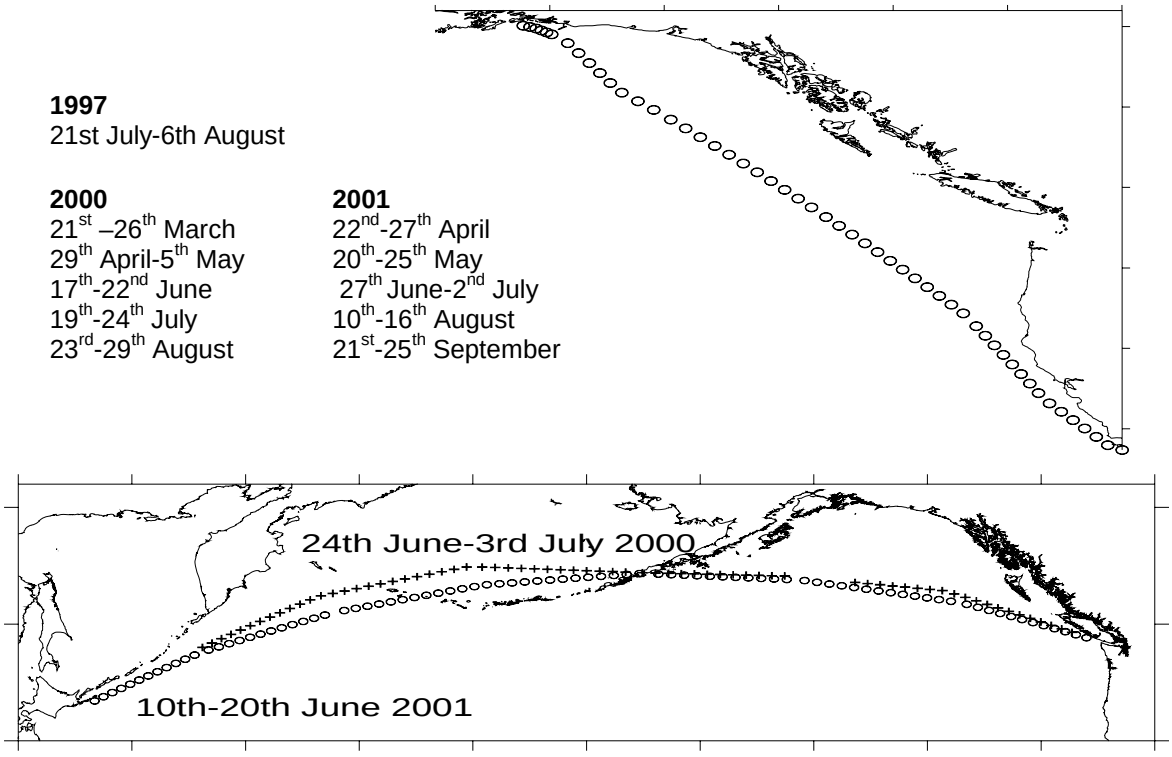

Fig. 1 Upper panel shows the N/S transect, run 5 times in 2000 and 2001, and once in 1997. Lower panel shows the E/W transect, run once in 2000 and 2001. Symbols indicate sample positions.

Group discussion

The main focus of the discussion was the possible future enhancement of the CPR program. Value-added measurements were proposed which might be included, e.g. ship-mounted sensors for temperature, salinity, fluorescence, nutrients, ocean colour, and acoustic backscatter; depth profiles of temperature and/or salinity using expendable probes; visual observations of seabirds and marine mammals; and collation of measurements along the CPR track with broader surrounding spatial coverage from satellites and drifting buoys.

The fitting of a thermosalinograph to the vessel was given a high priority since much of the physical processes occurring in the North Pacific are salinity-driven. There was also enthusiasm for adding sea-bird/mammal observers to the vessel as a potential way to obtain trophic interaction information (including inferences on intermediate levels such as squid and forage fish).

There was support within the group for holding an inter-sessional workshop on the design and implementation of a possible ship-of-opportunity monitoring package, which might include many of the parameters listed above.

Reference

Batten, S.D., Welch, D.W., and Jonas, T. Latitudinal differences in the duration of development of *Neocalanus plumchrus* copepodites. Fisheries Oceanography. (in press).

GEM (Exxon Valdez Oil Spill Trustee Council's "Gulf Ecosystem Monitoring" initiative) and U.S. GOOS plans in the North Pacific

Phillip R. Mundy
Exxon Valdez Oil Spill Restoration Office, #401-645 G Street, Anchorage, AK 99501-3451, U.S.A.
E-mail: phil_mundy@oilspill.state.ak.us

A new endowment has been put in place by the Exxon Valdez Oil Spill Trustee Council to fund (on a permanent basis) long-term time series observations in the coastal ocean of the Gulf of Alaska. The Gulf of Alaska Ecosystem Monitoring and Research Program (GEM) is one of three U.S. government endowments established within the past five years to provide for marine research and long-term monitoring in Alaskan waters. GEM is a regional program focusing primarily on the northern Gulf of Alaska within the larger PICES area. The first GEM invitation for proposals will be issued in August 2002, for funding in calendar year 2003, however two pilot projects are already underway. The oceanographic mooring at station 1 of the Seward Line (GAK-1), and the continuous plankton recorder (CPR), operated on a vessel of opportunity between Valdez and Long Beach, are being evaluated on a trial basis for their abilities to contribute to the permanent monitoring program. Recommendation of the PICES CPR Advisory Panel were instrumental in obtaining the support of GEM for the CPR project. GEM welcomes, and hopes to rely upon, PICES expertise and recommendations in the optimal design and implementation of the GEM program. Starting in 2003, GEM monitoring activities, both partnered and fully-funded, will increase steadily through the remainder of this decade, until the annual income stream is fully allocated.

GEM design and implementation is being closely coordinated with the newly constituted North Pacific Research Board (NPRB), which administers an endowment supporting marine research in all Alaskan waters. NPRB has indicated interest in partnering with GEM on an extended CPR project during calendar year 2002, and is expected to issue an invitation for proposals sometime next year. The third research endowment which GEM is following closely is the Northern Fund of the Pacific Salmon Treaty, which is now amassing capital, and which

presently has no plans to start funding work. The three funds together should contribute in excess of U.S. $20 million annually to research and monitoring in the PICES area when all are fully operational, about 2004.

In addition to the help received from PICES, GEM development is being assisted by the steering committee of the U.S. Global Ocean Observing System (U.S. GOOS). U.S. GOOS is providing recommendations on the basic components of an observing system to support modeling of climatic and oceanographic processes in the coastal environment. The Steering Committee is also assisting development of other regional marine observing programs centered in the Gulf of Maine, the California Current, and the Gulf of Mexico. In the long-term, U.S. GOOS hopes to contribute to marine research in the PICES region by providing the scientific basis for a continuing appropriation from the U.S. Congress for a system of ocean observing tools consisting of Argo profiling floats, a remotely telemetered drifting buoy array, coastal moorings, GPS-capable tide gauge stations, volunteer observing ship transects, and data management and assimilation that will support oceanographic modeling and forecasting.

A proposal for a North Pacific Action Group of the international Data Buoy Cooperation Panel

Ron McLaren and Brian O'Donnell
Meteorological Service of Canada, Pacific and Yukon Region, Environment Canada, #700-1200 W. 73rd Avenue, Vancouver, B.C. Can ada. V6P 6H9. Email: ron.mclaren@ec.gc.ca

Established in 1985, the Data Buoy Cooperation Panel (DBCP) is an official joint body of the Intergovernmental Oceanographic Commission (IOC) and the World Meteorological Organization (WMO). The Panel consists of representatives of the WMO and member states of the IOC interested in participating in its activities.

The most important task of the DBCP is to co-ordinate drifting and moored buoy programmes at the international level, with a view to increase the number of buoys deployed and maintain high quality archived and real time oceanic and atmospheric data. The Panel encourages the free exchange of data and international co-operation by the formation of regional and global Action Groups, such as the European Group on Ocean Stations and the International South Atlantic Buoy Program. An Action Group within the DBCP is an independent self-funded body that maintains an observational buoy programme providing meteorological and oceanographic data for real time and/or research purposes in support of relevant WMO and IOC programs. The goals of an Action Group are to provide good quality and timely data to users, to encourage the distribution of data via the GTS and to promote the exchange of information on buoy activities and technology.

Action groups exist for the North Atlantic, South Atlantic, Arctic, Indian and Antarctic oceans. The work of Action Groups is reflected in the number of buoy observations in their relevant areas of responsibility. Compare with other regions, the North Pacific is relatively undersampled. At the October 2000 meeting of the DBCP, Canada made a commitment to determine the level of interest within the scientific community currently doing research in the North Pacific Ocean to form an Action Group for this area.

The demonstrated success of other Action Groups would indicate that the co-operative efforts of agencies already working in the North Pacific, could contribute substantially to increasing the number of oceanographic and meteorological observations over what is currently available.

PICES members are encouraged to discuss the formation of such an Action Group with their colleagues within their own, or other oceanographic or meteorological agencies, who might be able to contribute to and benefit by

membership in an Action Group for the North Pacific. Additional information on the work of the Panel, as well as technical information on buoys and other ocean buoy programs can be found at the DBCP web site located at http://dbcp.nos.noaa.gov/dbcp/.

The Mexican oceanographic North Pacific program: IMECOCAL

Gilberto Gaxiola-Castrol and Sila Najera-Martinez
Centro de Investigación Científica y de Educación Superior de Ensenada (CICESE), Carr. Tijuana-Ensenada, Km. 107, Ensenada 22800, Baja California, Mexico. E-mail: ggaxiola@cicese.mx

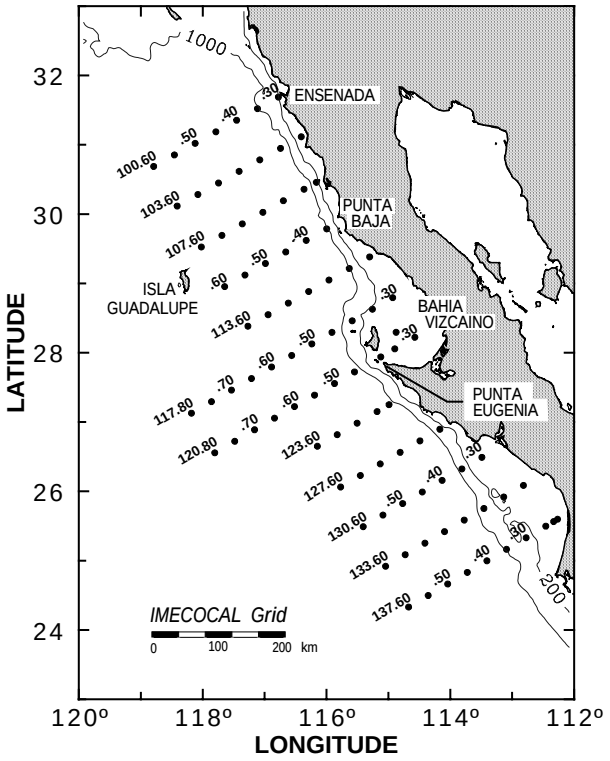

Fig. 2 IMECOCAL surveys station locations.

In September 1997, a consortium of seven Mexican academic institutions began a new oceanographic program off Baja California Mexico, as named IMECOCAL (Investigaciones Mexicanas de la Corriente de California). The IMECOCAL program was initiated with a 3-year grant from the Inter-American Institute of Global Change Research (IAI), and a four-year grant from the National Council of Science and Technology (CONACYT-Mexico). This grant was extended to five more years, covering the oceanographic surveys at least until 2004. Some funds came from the National Science Foundation (NSF-USA), under a joint grant with the Scripps Institution of Oceanography (SIO-UCSD).

The main goal of the IMECOCAL program is to understand how physical processes regulate the changes in the pelagic ecosystem of the southern region of the California Current. For that objective we are developing a long-term monitoring project to study the climatic and oceanographic variability effect in this region, maintaining core oceanographic measurements during the surveys, and collecting sea level and atmospheric data on island and land stations (Fig. 2). We are conducting modelling studies to explore plankton and small pelagic fish response to regional and global physical forcing as well as to local anthropogenic perturbations on the coastal areas. Also, we are looking to develop a new generation of research oceanographers for the program, with fellowships for graduate students doing their thesis in physical oceanography, plankton, paleoecology, small pelagic fisheries, nutrient chemistry, primary production, and climate change.

We followed the CalCOFI (California Cooperative Fisheries Investigations) sampling grid off Baja California, which was abandoned in the 1980s by U.S. marine scientists. Quarterly IMECOCAL cruises are conducted using the CICESE *R/V Francisco de Ulloa*, in January, April, July, and October. These cruises are coordinated in time with the CalCOFI surveys, in order to have an integrated description of the pelagic ecosystem of the California Current, from Point Conception, California, to the southern region of Baja California. The core oceanographic observations at each station include CTD profiles to a 1000-meter depth to measure temperature, salinity, dissolved oxygen, and fluorescence, and 200-meter Rosette casts to collect water samples with 5-litre Niskin bottles.

Water is analysed to determine dissolved oxygen, nutrients (NO_3, NO_2, SiO_2, PO_4), phytoplankton pigments (chlorophyll *a*, and phaeopigments), phytoplankton cell counts, particle and phytoplankton light absorption, and pigment phytoplankton composition (HPLC analysis). Oblique bongo net tows (505-micrometer mesh) are taken from the first 200-meters, using one cod-end to estimate zooplankton (biomass and group analysis), and the other for ichthyoplankton abundance. In addition, 100-meter vertical CALVET net tows are made to capture macrozooplankton, including ichthyoplankton (fish eggs and larvae). Casts for *in situ* primary production determinations as well as irradiance and radiance profiling are carried out daily at the mid-day stations. Also, photosynthesis-irradiance curves are made, to have the first systematic phytoplankton photosynthetic data in the southern California Current region. These data are expected to be used, together with bio-optical and satellite (SeaWiFS) information to estimate primary production over meso- and larger-scales. Occasionally we using a SIMBAD to determine near-surface water leaving radiance, in order to develop local pigment algorithms for remote colour sensors in collaboration with colleagues at SIO-UCSD.

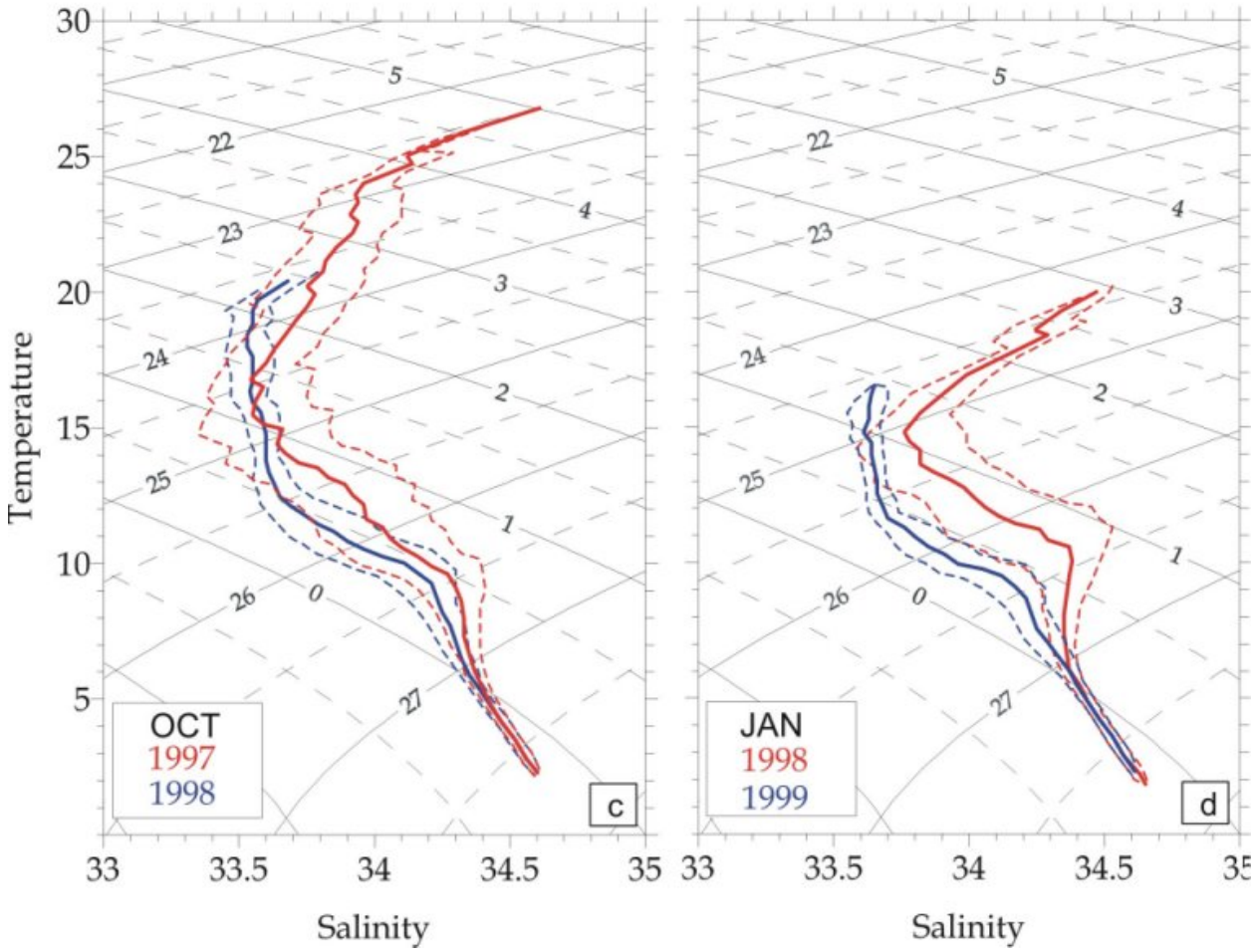

Fig. 3 T-S diagrams in the IMECOCAL zone measured during the El Niño: October 1997 to January 1998 (red lines) and the La Niña: October 1998 to January 1999 (blue lines). Redrawn from Reginado Durazo.

Near-surface temperature, salinity, and chlorophyll-fluorescence (Fig. 3) are monitored continuously underway, simultaneously with an acoustic Doppler current profiler (ADCP). A CUFES (Continuous Underway Fish Egg Sampling) system is used between stations, and

when the vertical net tows are made. This system allows to enhance our understanding of the small-scale distribution of fish eggs in this region of the California Current (Fig. 4). Together with the CalCOFI program, we are studying the transboundary production and abundance small pelagic fish in relation to the environmental variability.

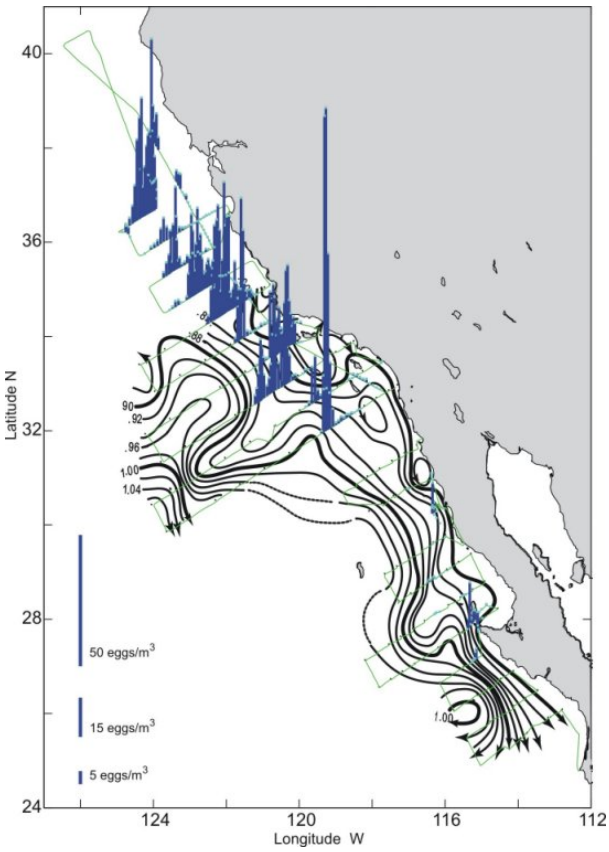

Fig. 4 Distribution of sardine eggs (CUFES data) compared to zooplankton biomass from CalCOFI (Ron Lynn) and IMECOCAL (Bertha Lavaniegos and Timothy Baumgartner) data in April, 2000.

In addition to the monitoring surveys, IMECOCAL maintains sea level pressure gauges at an oceanic island (Guadalupe Island, 29°N, 118°W), and at an onshore location (San Quintin Bay, ~31°N). These paired instruments permit to monitor the sea surface pressure gradient between the island and the coastal station in order to provide a measure of the along-shore mean flow in the region. The instruments have been operating since January 1999 in collaboration with the Mexican Navy. Also, meteorological stations are maintained at several locations along the Peninsula of Baja California.

Preliminary information derived from our 1997-2002 surveys is held in a database for the program collaborators and the international scientific community. We already have important results from our study area; derived from the seventeen surveys, the three meteorological stations, and the two sea level gauge stations. About 60% of the samples are analysed, generating twelve data reports, more than ten scientific contributions, and four MSc theses. Fourteen graduate students are working on their thesis related to information collected on the surveys, and six scientific papers should be published during the next two years. We expect to complete the database of all the core data by the end of this year. For more information about sharing data, please contact with our Data Manager (loyasa@cicese.mx), and visit our web site (http://www.ecologia.cicese.mx/~imecocal).

IMECOCAL Collaborators

Timothy Baumgarter[1], Daniel Loya[1], Bertha Lavaniegos[1], Reginaldo Durazo[2], Martin Hernandez[3], Joaquin Garcia[1], Yanira Green[4], Tomas Campos[4], Jose Gomez[1], Eduardo Millan-Nuñez[1], Ruben Lara-Lara[1], Carmen Bazan-Guzman[1], Virgilio Arenas[6], Sergio Aguiñiga[3], Rene Funes[3], Affonso da Silveira Mascarenhas Jr[2], Sergio Hernandez[5], Salvador Lluch-Cota[5], Ricardo Saldierna[3].

[1]Centro de Investigación Científica y de Educación Superior de Ensenada (CICESE); [2]Universidad Autónoma de Baja California (UABC); [3]Centro Interdisciplinario de Ciencias del Mar (CICIMAR); [4]Instituto Nacional de la Pesca (INP); [5]Centro de Investigaciones Biologicas del Noroeste (CIBNOR); [6]Universidad Nacional Autónoma de México (UNAM).

Building global ocean profile and plankton databases for scientific research

Sydney Levitus
National Oceanographic Data Center, World Data Center for Oceanography, E/OC5, #4362-1315 East West Highway, Silver Spring, MD 20910-3282, U.S.A. E-mail: Sydney.Levitus@noaa.gov

Founded in the International Geophysical Year (IGY), the World Data Center (WDC) System was established to prevent the loss of valuable scientific data gathered during the IGY by providing a permanent archive for these data. During the past ten years, the World Data Center for Oceanography, Silver Spring, has expanded its role by including all oceanographic data received as part of its archive, and by leading projects to increase the comprehensiveness of its electronic database. This presentation describes efforts at the WDC to develop global, comprehensive, integrated, scientifically quality-controlled electronic ocean profile-plankton databases that are available internationally without restriction. A description of upper ocean temperature changes using the data from World Ocean Database 1998 will be given.

IOC Global Oceanographic Data Archaeology and Rescue (GODAR) project

Data archaeology is the process of locating historical ocean data at risk of loss due to media decay. In contrast, data rescue is the digitization, quality control, and entry of historical data into global, regional, national comprehensive, integrated, electronic databases.

The GODAR project was approved in 1993 and is on-going. International cooperation within the project continues to be excellent. All countries contacted are contributing data. Six regional GODAR workshops have been held worldwide that encompass all countries that make oceanographic measurements (Table 1). These meetings were attended by approximately 175 oceanographic data managers and scientists and have resulted in the identification of substantial amounts of data that are at risk of loss due to media decay (magnetic tape and paper).

Table 1 List of GODAR meetings.

GODAR I	Obninsk	Russia	May, 1993
GODAR II	Tianjin	China	Mar., 1994
GODAR III	Goa	India	Dec., 1995
GODAR IV	Malta		Apr., 1995
GODAR V	Cartagena	Colombia	Apr., 1996
GODAR VI	Accra	Ghana	Mar., 1997

The International GODAR Review Meeting held in Silver Spring, Maryland, U.S.A., in July 1999 concluded that the project is successful with more than 2 million temperature profiles, and 600,000 plankton observations collected. The next phase is to add 'sea level' data to the project.

Current GODAR projects include MEDBLACK and MEDAR/MEDATLAS by European Community and IOC/IODE GODAR-WESTPAC by countries bordering the western Pacific. The Japan Oceanographic Data Center takes the lead in the GODAR-WESTPAC project.

Data collected as a result of the GODAR project were made available, both on-line and on CD-ROM, as part of World Ocean Atlas 1994, World Ocean Database 1998, and World Ocean Database 2001 (available March 2002).

IOC World Ocean Database project

The IOC World Ocean Database Project was approved in July 2001. Its goal is the development of global and regional, comprehensive, integrated, scientifically quality-controlled ocean profile and plankton databases. The project hopes to encourage the exchange of modern ocean profile and plankton data, and to emphasize the development of regional atlases and quality control procedures.

REX WORKSHOP ON TEMPORAL VARIATIONS IN SIZE-AT-AGE FOR FISH SPECIES IN COASTAL AREAS AROUND THE PACIFIC RIM

(Co-convenors: William T. Peterson and Douglas E. Hay)

A one-day REX Workshop on *Temporal variations in size-at-age for fish species in coastal areas around the Pacific Rim* was convened October 5, 2001, immediately preceding the PICES Tenth Annual Meeting in Victoria, British Columbia, Canada. The workshop was very popular with more than 50 scientists attending. In total, 11 papers were presented by speakers from Canada, Japan, Russia and the United States. Four presentations discussed salmon size-at-age, five considered herring (one paper was on sardine-herring comparison), one - sablefish and one - chub mackerel. In addition, several posters presented data on size-at-age of other herring stocks as well as data for pollock and yellowfin flounder.

The keynote paper by Nikolay Naumenko summarized vast amounts of data on length-at-age and weight-at-age for 19 populations of herring from the western Bering Sea. The overall conclusion of his work was that herring growth is controlled by two main factors, food abundance (zooplankton biomass) and total fish biomass (density-dependent effects). A similar conclusion was reached by other authors as well.

Several general themes were common to many papers. One was the need to understand better the spatial scales of co-variation in size-at-age for species of fish with populations distributed along great distances of the coast. Prime candidates for such analysis are of course the salmonids and herring. Peterman showed that there was strong co-variation in size-at-age time series for sockeye salmon from Bristol Bay and Fraser River; however there was even stronger co-variation at regional scales. Eight Bristol Bay stocks were far better correlated with each other than with Fraser stocks; the same was true for 20 Fraser River stocks. This suggests the hypothesis that similar stocks are more likely to occupy a similar habitat (*i.e.*, feed in the same region of the ocean). Though no data of this type were presented for other salmon species, it is known from ongoing work (NOAA/NMFS/Northwest Fisheries Science Center) that coho salmon from the Columbia River system and coastal Oregon streams tend to spend their entire lives in continental shelf waters off Washington and Oregon state. Also, there are indications that some Sacramento River chinook salmon reside chiefly in coastal waters off central California (MacFarlane). A recommendation of the workshop participants was that REX scientists should purse analysis of co-variation and spatial autocorrelation of size-at-age of other salmon stocks and of herring stocks. An alternate approach would be to use cluster analysis, as shown by Naumenko.

The second common theme was the high degree of correlation between time series of size-at-age and various environmental (explanatory) variables. Temnykh showed the declining trends in size-at-age for Okhotsk pink salmon from the 1970s through 1985. However after 1985, pinks have gotten heavier. This is in contrast to other North American pinks which continued to grow smaller through the 1990s. She noted correlation between size-at-age of pink salmon stocks from the Sea of Okhotsk and sardine and zooplankton biomass. The period of time when pink salmon were small in size was the time when sardines were abundant and zooplankton biomass was low. The simultaneous collapse of the Japanese sardine and increased size of pink salmon, though not necessarily causal, suggests the possibility of some common forcing mechanism related to zooplankton. Positive correlations between zooplankton biomass and both length-at-age and weight-at-age were found for several herring populations as well including the Korf-Karaginsk (western Bering Sea) stock (Naumenko; Balykin and Buslov), Prince William Sound (Brown), and stocks from British Columbia (Schweigert; Tanasichuk). Finally, Tarasyuk showed that biomass of yellowfin sole from the Tatar Strait (Japan/East Sea) was correlated with zooplanton biomass.

Temporal and special changes in pattern in size-at-age were examined relative to climate variability and climate change. Good correlations were also found with climatic variables such as the Pacific Decadal Oscillation, Aleutian Low Pressure Index, or water temperature alone (Peterman, MacFarlane, Brown, Schweigert, Bonk, Tarasyuk). Competition with other pelagic species was suggested as a possible mechanism explaining changes in growth of chub mackerel (Watanabe). Ecosystem change was implicated as a factor explaining stock fluctuations in Hokkaido-Sakhalin herring whereas the co-occurring sardines stocks appear to be largely density dependent (Watanabe).

Many papers demonstrated density dependence of size-at-age. When population size was large, size-at-age was small and *vice versa*. Discussion at the workshop centered on the need to think more and work harder at identifying mechanisms that might control density dependence, with studies of the forage base being one of the prime candidates.

Discussion was also focused on the need to make better use of existing samples to study size- and weight-at age through use of scales and otoliths to generate new data sets on size- and weight-at-age. There are many data on length and weight of fishes but not as much data on age and weight at length. Through analysis of otoliths and scales, one could determine age of fishes that have already been measured.

Finally, the workshop participants discussed the value of comparative studies and of course - this is what REX workshops are all about – providing a forum for discussion on differences in population size, growth, and life history characteristics of species that are distributed widely around the Pacific Rim. This led to the recommendation that PICES scientists need to do more comparisons of populations that are distributed in the coastal zones around the basin, but also need to compare response of fish, nekton and zooplankton populations that are found within the deeper waters of the Kuroshio, Kuroshio Extension, Transition Zone and the California Current. Interesting, this thought arose independently of the inter-sessional symposium proposed on comparative studies of North Pacific transitional areas (the symposium was held April 23-25, 2002, in La Paz, Mexico).

The following section contains extended abstracts of papers given at the workshop.

Spatial patterns of covariation in size-at-age of British Columbia and Alaska sockeye salmon stocks and effects of abundance and ocean temperature

Brian J. Pyper[1], Randall M. Peterman[1], Michael F. Lapointe[2] and Carl J. Walters[3]

[1] School of Resource and Environmental Management, Simon Fraser University, Burnaby, B.C., Canada. V5A 1S6. E-mail: peterman@sfu.ca

[2] Pacific Salmon Commission, 600-1155 Robson St., Vancouver, B.C., Canada. V6E 1B5. E- mail: lepointe@psc.org

[3] Fisheries Centre, University of British Columbia, Vancouver, B.C., Canada. V6T 1Z4. E-mail: c.walters@fisheries.ubc.ca

Introduction

Body lengths of adult Pacific sockeye salmon (*Oncorhynchus nerka*) have decreased significantly in recent years, reducing the reproductive potential of spawners and the economic value of harvests. To understand the causes of these important trends, we pursued three objectives. Firstly, we quantified the extent of spatial covariation among age-specific body sizes of numerous stocks in the Northeast Pacific. The observed spatial scale of covariation could suggest the causes of that variation. Secondly, we compared the extent of covariation among body size and survival rate of sockeye salmon to determine whether these two variables were influenced by similar processes. Thirdly, we tested hypotheses about the relative importance of

intraspecific competition and oceanographic conditions on size of adult sockeye salmon. This paper summarizes material already published; see Pyper *et al*. (1999) and Pyper and Peterman (1999) for details.

Methods

We used 72 time series of body length at a given adult age for 31 sockeye stocks from five geographically distinct regions in British Columbia (Fraser River and Skeena River) and Alaska (Upper Cook Inlet, Copper River and Bristol Bay). Ages included were 1.1, 1.2, 1.3, 2.2 and 2.3 fish.

Patterns of covariation. To examine patterns of covariation among length-at-age data both within and between regions, we calculated Pearson product-moment correlation coefficients for pairwise comparisons among the 72 time series of lengths. Size data were aligned to have return years in common (year in which they returned to their natal streams), because Rogers and Ruggerone (1993) and McKinnell (1995) suggest that interannual variability in body size of recruits is largely determined by growth in their final year at sea. However, to estimate the importance of conditions in early ocean life, we also computed correlations after aligning the data series to have a common ocean entry year (OEY) but a different return year (*e.g.* using size data for 1.2 and 1.3 adults).

Positive autocorrelation and time trends were present in many of the time series of body length, indicating that low-frequency (*i.e.*, slowly-changing) variability is important. However, such autocorrelation and time trends increase the chance that statistically significant but spurious correlations will occur in standard inference tests. Therefore, we used two approaches to examine correlations. Firstly, we computed them using the original time series and based significance tests on the method recommended by Pyper and Peterman (1998), which adjusts degrees of freedom to account for autocorrelation and maintains Type I error rates near the specified α in the presence of autocorrelation. Secondly, we first-differenced the time series (subtracting each data point from the next) to remove the low-frequency variation and re-computed correlations. Comparing the results from these two approaches allowed us to quantify the potential importance of low-frequency causes of the positive covariation that we found.

***Effects of oceanographic conditions and intraspecific competition*.** We also used principal components analysis (PCA) to further examine spatial and temporal covariation among lengths for 1967-1997. The PCA was done on 13 regional average length-at-age series, which better depicted the "signal" shared by given age classes and stocks in each region. This method reduced patterns of variability shared by each age class and region to a few defining time series (principal components). Copper River data were omitted due to missing data.

We then used the dominant principal component (PC1) to test hypotheses about the causes of variation in sockeye growth rate. Because our covariation results indicated that adult body size was affected primarily by conditions in the last year of ocean life, we generated indices of oceanographic conditions and intraspecific competition during the final year at sea. These indices were consistent with the area of overlap in ocean distributions of B.C. and Alaska sockeye, which roughly encompasses the Alaskan Gyre and is occupied by sockeye salmon from North America but not Asia (French *et al*. 1976). We used total ocean abundance of maturing North American sockeye salmon as an index of intraspecific competition, based on annual adult recruits (catch plus escapement) summed across the major B.C. (Fraser, Skeena, and Nass River) and Alaska stocks (Copper River, Cook Inlet, and Bristol Bay), which together account for the vast majority of sockeye abundance in the Gulf of Alaska (see Peterman *et al*. 1998 for details).

To reflect ocean conditions that might affect growth, we generated time series of annual sea-surface temperature (SST) deviations from the long-term mean. We used monthly SST data (ºC) on a 5-by-5 degree latitude-longitude grid across the area stated above of general overlap in ocean distributions of B.C. and Alaska sockeye (see Pyper and Peterman 1999 for details). Deviations were computed for a given grid cell and month by subtracting its long-term mean SST for 1947

through 1997. These deviations were then averaged to create two time series, with each corresponding to a different period preceding the return (generally in July) of sockeye salmon to their rivers: 1) winter months (November through February), and 2) a combination of winter and spring months (November through June). Climatic forcing during winter months is thought to be an important determinant of ocean productivity in the subsequent spring and summer (*e.g.*, Brodeur and Ware 1992), while in spring, maturing sockeye are feeding and growing at high rates before and during migrations back to their natal streams.

We then used multiple regression to examine relationships among the dominant pattern of covariation for length (PC1), total sockeye abundance in millions of fish (A), and ocean temperature (SST) for either November-February or November-June:

$$PC1 = a + b_1A + b_2SST + \varepsilon$$

Because of positive autocorrelation in the residuals, we simultaneously computed maximum likelihood estimates of the lag-1 autocorrelation coefficient and regression parameters. Due to time trends in the data, we first computed regressions using the original data and then repeated the regressions using detrended data (deviations from a linear time trend fit to each data series) to test for effects at shorter time scales.

Results and discussion

Patterns of covariation. There was widespread positive covariation among the 72 body-length time series, aligned by return year, across ages and across stocks. Of the 2,556 correlations, 91.4% were positive (and 43%, or 1,006, of the positive ones were significant at $p<0.05$, whereas only 3 negative cases were significant). There was strong evidence of positive covariation in age-specific body size among sockeye stocks even between distant regions, as indicated by the predominance of positive correlations in these comparisons (*e.g.*, Bristol Bay vs. Fraser River; Fig. 1C). However, there was a stronger positive covariation among body length of stocks within regions (*e.g.*, among the 8 stocks in Bristol Bay and among the 20 in the Fraser River; Fig. 1A and 1B). Generally, the percent of variation in length shared by stocks in the same region was about twice that shared by stocks from different regions (see Pyper *et al.* (1999) for detailed results).

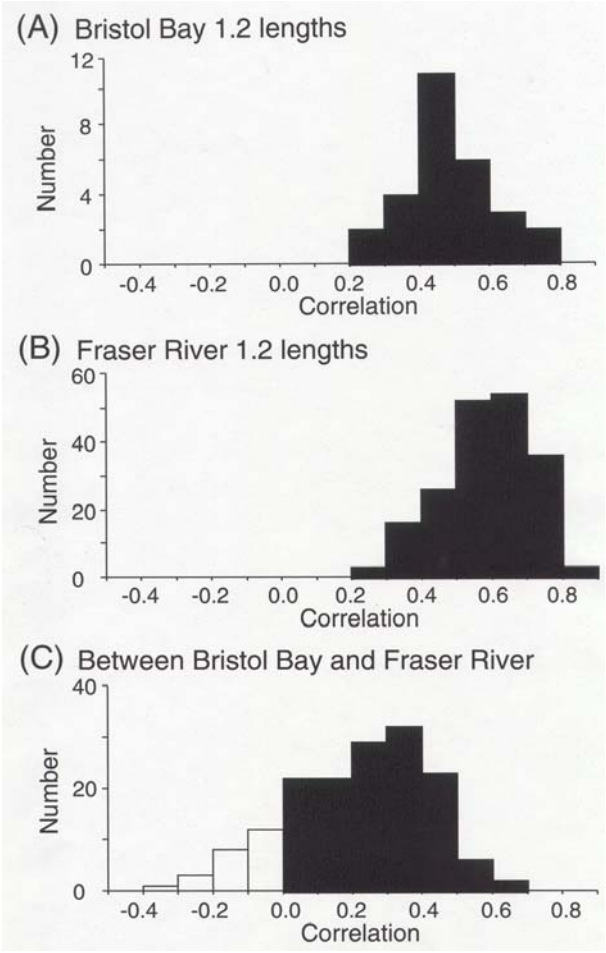

Fig. 1 Histograms of correlations between lengths of age 1.2 sockeye: A) among Bristol Bay stocks (all 28 correlations positive; 23 significant at $p<0.05$); B) among Fraser River stocks (all 190 correlations positive; 161 significant); and C) between Bristol Bay and Fraser River stocks (136 of 160 correlations positive; 25 significant positive correlations). Open bars represent negative correlations; solid bars are positive correlations. Reprinted from Pyper *et al*. (1999).

Correlations using first-differenced data support the suggestion from the PCA reported below that slowly changing, low-frequency patterns of variability, such as the declining time trends in body size, were important sources of covariation

among average lengths of stocks. After autocorrelation and time trends in the 72 stock-specific length series were removed by first-differencing, widespread positive covariation was still evident both within and between regions. However, correlations were consistently and often substantially lower than those computed using the original data. The average of the 2,556 correlations was reduced from 0.37 to 0.23, the number of negative correlations increased to 578, and the number of significant ($p<0.05$) positive correlations decreased to 745. Thus, there is little evidence that the general patterns of covariation in lengths could be solely a spurious result of unrelated time trends; instead, to the extent that the observed covariation in length-at-age of sockeye salmon arises from shared processes, such processes appear to be largely characterized by low-frequency patterns of variability.

In contrast to the above analyses, when the body-length time series were aligned to share the same ocean entry year (OEY) but to have a different return year (RY), the correlations among stocks decreased dramatically (*e.g.* for Bristol Bay stocks, the average correlation in the original data series decreased from 0.67 when lined up by RY to 0.29 when lined up by OEY). This decrease was even greater when possible confounding effects of autocorrelation were removed from both analyses (see Pyper *et al*. 1999). Like other analyses, (Rogers and Ruggerone 1993; McKinnell 1995), these findings imply that variable growth conditions during early marine life are not nearly as important a determinant of temporal variation in final sockeye body length as conditions during late marine life.

Comparison of body size and survival rates. We found weak and inconsistent correlations between average length and survival rate, suggesting that different processes drive interannual variability in these components of recruitment. This conclusion is further supported by evidence that environmental processes influence these two variables at different spatial scales. Whereas both adult body size and survival rate show strong positive covariation among stocks within regions, only body size shows strong between-region covariation (*e.g.*, compare Fig. 1C here with Fig. 1C of Peterman *et al*. 1998). These differences in spatial characteristics of covariation suggest that models for body size or forecasting annual salmon abundance (reflecting survival rates and changing age-at-maturity schedules) should be based on appropriate measures of environmental conditions that reflect this information about spatial scales. For example, we found that large, basin-scale SST was significantly associated with variation in body size (see below), whereas Mueter *et al*. (2001) found that smaller, regional-scale SST was much more important in explaining variation in survival rates of salmon.

Effects of oceanographic conditions and intraspecific competition. Principal components analysis (PCA) of the 13 age-specific regional body length series defined the temporal characteristics of variation shared among regions. The PCA yielded three principal components with eigenvalues greater than one; the best one accounted for 65% of the total variance and the other two combined accounted for only 19%. The time series (scores) of this dominant component, PC1, had an obvious declining trend from 1967-1997 ($p<0.001$; linear regression with autocorrelated error) (Fig. 2A). All 13 length series correlated strongly with PC1 (range 0.64 to 0.89), suggesting that much of the covariation among lengths of Alaska and B.C. sockeye salmon resulted from a similar declining trend over this period.

The multiple regression for the PC1 (reflecting shared variation among body size) using the original data was highly significant (multiple $r^2 = 0.71$, $p << 0.001$), as was the estimated slope on abundance ($b_1 = -0.03 \pm 0.005$ [± 1 standard error], $p << 0.001$) (Fig. 2B). The slope on November-February SST was also significant ($b_2 = -0.72 \pm 0.29$, $p = 0.014$) (Fig. 2C). Partial r^2 values were 0.56 for abundance and 0.18 for SST.

The multiple regression using detrended data (to remove possible confounding due to time trends in the original data) showed similar results. Both abundance and November-February SST were significant ($b_1 = -0.035 \pm 0.007$, $p << 0.001$ and $b_2 = -0.87 \pm 0.31$, $p = 0.004$). Overall, the multiple $r^2 = 0.54$, $p << 0.001$, and multicollinearity was

negligible (r = 0.04). Partial r^2 values were 0.48 for abundance and 0.23 for SST.

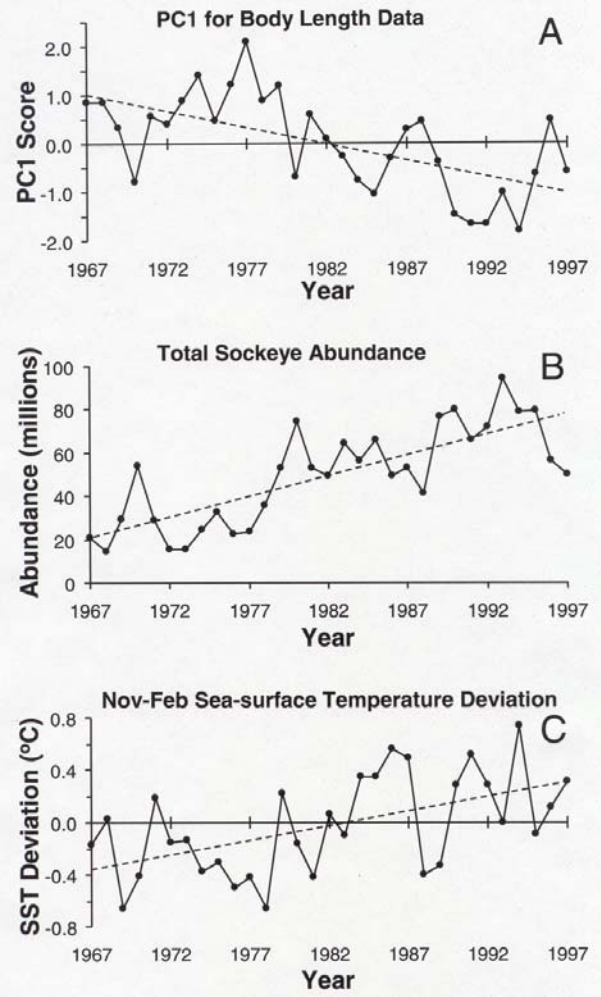

Fig. 2 (A) Scores for the dominant principal component (PC1) of length-at-age data for B.C. and Alaska sockeye salmon -- lower values of PC1, for example, reflect the tendency toward reduced body length that is shared among these stocks; (B) Total annual abundance of adult recruits (catch plus escapement) of the major B.C. and Alaska sockeye stocks; and (C) Average yearly winter (November through February) sea-surface temperature (SST) deviations in °C from the long-term (1947-1997) mean for those months (6.8°C) for the Northeast Pacific Ocean over the region where distributions of B.C. and Alaska sockeye salmon overlap. Dotted lines are the fitted linear time trends used to detrend the data. Reprinted from Pyper and Peterman (1999).

Because November-February and November-June SST data were highly correlated (r = 0.86), all results for the latter were similar to those for November-February, with the exception that November-June SST was not significant in either the multiple regression with original data (p = 0.11) or with detrended data (p = 0.08).

These results indicate that reduced adult body length of both B.C. and Alaska sockeye salmon are associated with increases in total sockeye abundance in the Northeast Pacific and November-February sea-surface.

Abundance and SST together account for 71% of the variability in the first principal component (PC1) of body length among the major sockeye stocks of the northeastern Pacific Ocean during 1967-1997. Furthermore, abundance appears to have a much greater effect on body size than temperature. Its partial r^2 was considerably larger (0.56 vs. 0.18), and when data in each series were transformed into standard deviation units so that slopes were in the same units, the standardized slope for abundance (-0.68) was greater than the slope for SST (-0.27). This indicates that for each standard deviation increase, abundance had about 2.5 times the contribution to reducing adult body size as did November-February SST.

In addition, both abundance and SST were significantly related to the dominant pattern of variability in body length at both long and short time scales (*i.e.*, in the original, as well as detrended data). Thus, although it is possible that relationships among the original data might be coincidental due to their co-occurring time trends (*i.e.*, that some other omitted variable actually explains the trend in PC1), the evidence in support of the effects of abundance and SST was strengthened by their very similar slopes in both the original data analysis and the analysis once time trends were removed.

Although several authors have documented increased secondary productivity in the northeastern Pacific Ocean in recent decades (*e.g.*, zooplankton and squid - Brodeur and Ware 1992, 1995), which should improve growth rates for sockeye salmon, abundance of sockeye recruits also increased (Fig. 2B). We therefore

hypothesize that increased food supply was more than offset by increased sockeye abundance, which resulted in greater competition and smaller body size in recent years.

Acknowledgments

We are extremely grateful to the numerous biologists and technicians in various management agencies who gathered, processed, and provided the time series of data analyzed here. Funding was provided by a grant to R.M. Peterman from the Natural Sciences and Engineering Research Council of Canada.

References

Brodeur, R.D., and Ware, D.M. 1992. Long-term variability in zooplankton biomass in the subarctic Pacific Ocean. Fisheries Oceanog. 1: 32-38.

Brodeur, R.D., and Ware, D.M. 1995. Inter-decadal variability in distribution and catch rates of epipelagic nekton in the Northeast Pacific ocean. *In* R.J. Beamish (Ed.) Climate change and northern fish populations. Can. Spec. Publ. Fish. Aquat. Sci. 121, pp. 329-356.

French, R., Bilton, H., Osaka, M., and Hartt, A. 1976. Distribution and origin of sockeye salmon (*Oncorhynchus nerka*) in offshore waters of the North Pacific Ocean. INPFC Bulletin 34.

McKinnell, S. 1995. Age-specific effects of sockeye abundance on adult body size of selected British Columbia sockeye stocks. Can. J. Fish. Aquat. Sci. 52: 1050-1063.

Mueter, F.J., Pyper, B.J., and Peterman, R.M. 2001. Effects of coastal sea surface temperatures on survival rates of sockeye, pink, and chum salmon stocks from Washington, British Columbia, and Alaska. Poster #S11-203 in Session S11: "Results of GLOBEC and GLOBEC-like programs," at the PICES Tenth Annual Meeting, Victoria, B.C., October, 5-13, 2001.

Peterman, R.M., Pyper, B.J., Lapointe, M.F., Adkison, M.D., and Walters, C.J. 1998. Patterns of covariation in survival rates of British Columbia and Alaskan sockeye salmon (*Oncorhynchus nerka*) stocks. Can. J. Fish. Aquat. Sci. 55: 2503-2517.

Pyper, B.J., and Peterman, R.M. 1998. Comparison of methods to account for autocorrelation in correlation analyses of fish data. Can. J. Fish. Aquat. Sci. 55: 2127-2140 plus the erratum printed in Can. J. Fish. Aquat. Sci. 55: 2710.

Pyper, B.J., and Peterman, R.M. 1999. Relationship among adult body length, abundance, and ocean temperature for British Columbia and Alaska sockeye salmon, 1967-1997. Can. J. Fish. Aquat. Sci. 56: 1716-1720.

Rogers, D.E., and Ruggerone, G.T. 1993. Factors affecting marine growth of Bristol Bay sockeye salmon. Fisheries Research 18: 89-103.

Pyper, B.J., Peterman, R.M., Lapointe, M.F., and Walters, C.J. 1999. Patterns of covariation in length and age at maturity of British Columbia and Alaska sockeye salmon (*Oncorhynchus nerka*) stocks. Can. J. Fish. Aquat. Sci. 56: 1046-1057.

Influences of the 1997-1998 El Niño and 1999 La Niña on juvenile chinook salmon in the Gulf of the Farallones

R. Bruce MacFarlane, Steven Ralston, Chantell Royer, and Elizabeth C. Norton
NOAA Fisheries, Southwest Fisheries Science Center, Santa Cruz Laboratory, 110 Shaffer Road, Santa Cruz, CA 95060, U.S.A. E-mail: Bruce.MacFarlane@noaa.gov

El Niño, the warm phase of El Niño/Southern Oscillation (ENSO) events, has been shown to produce dramatic effects on marine communities. Alterations in physical oceanographic properties of the marine environment can be observed as far north as Alaska. Less is known of the influences of La Niña, the cool phase of ENSO events that follows an El Niño. During the 1982-83 El Niño, anomalous plankton distributions, altered fish community structure, and reduced fish catch

occurred in coastal waters of southern California (Simpson, 1992). Along the central California coast, the 1992-93 El Niño corresponded to delayed phytoplankton blooms, changes in the abundance and distribution of invertebrates, improved recruitment of southern fish species, but recruitment failure in the northerly rockfish species (Lenarz *et al*. 1995). More recently, the largest decline in macrozooplankton abundance off central and southern California in the 50-year series of CalCOFI cruises was recorded during the 1997-98 El Niño (Lynn *et al*. 1998).

In addition to ecosystem impacts, changes in physiology and behavior of fishes, including salmon, have been noted during ENSO events. Poor growth and low condition, ascribed to low fat content, were found in adult rockfish off central California during 1992-93 (Lenarz *et al*. 1995). And in a study of widow (*Sebastes entomelas*) and yellowtail rockfish (*S. flavidus*) in coastal waters of central and northern California, Woodbury (1999) reported reduced otolith growth, a conservative measure of somatic growth history, during the 1982-83 El Niño. Reduced condition and growth of sockeye salmon (*Oncorhynchus nerka*) in the Gulf of Alaska during the 1997-98 El Niño event were related to feeding on zooplankton, prey of lower caloric content than squid, their primary food in 1998 following the El Niño (Kaeriyama *et al.* 2000). In a review of El Niño effects on fisheries, Mysak (1986) detailed other impacts to sockeye, including changes in migration patterns and the timing of returns to streams. Lower survival in juvenile coho salmon (*O. kisutch*) following ocean entry, great mortality in adult coho, and reduced size in both coho and chinook salmon (*O. tshawytscha*) were described off Oregon during the 1982-83 El Niño (Pearcy and Schoener 1987).

We report here the results of a study of juvenile chinook salmon in the Gulf of the Farallones, an embayment on the central California coast. The Gulf of the Farallones, a broad expanse of continental shelf extending from Pt. Reyes to Pillar Pt. out to the Farallon Islands, receives freshwater outflow through the Golden Gate from the Sacramento and San Joaquin Rivers and their tributaries in California's Central Valley. It is also the point of ocean entry for an estimated 50-60 million chinook salmon smolts spawned from four runs (fall, late fall, winter, spring) in streams and hatcheries in the Central Valley. The purpose of the information presented here is to document juvenile salmon development, and how it was influenced by the environment in the Gulf of the Farallones during the 1997-98 El Niño and 1999 La Niña.

Juvenile salmon were captured by surface trawl at locations in the Gulf of the Farallones in June to October of 1998 and 1999. El Niño was evident in the Gulf of the Farallones in August 1997 and persisted to August 1998 (Fig. 3). By late 1998, La Niña was apparent and continued into spring 2000. Plankton samples were taken by Tucker Trawl at 5 m and 15-25 m below the surface to estimate secondary productivity and zooplankton composition.

Relative growth for juveniles caught in 1998 and 1999 was estimated by microstructural analysis of otoliths. Growth rates and size-at-age of juvenile chinook salmon can be estimated by measuring daily otolith increment widths (Bradford and Geen 1987). We calculated mean otolith increment widths as an index for somatic growth between increments 160 and 260, representing the first 100 days after leaving the estuary. Juvenile salmon exited San Francisco Estuary at 160±1 days old in 1998 and at 168±3 days old in 1999. Growth rate indices for salmon caught in 1998, during the El Niño period, were significantly greater than for fish collected in 1999 ($P<0.0001$). Mean growth rates of otolith increments were 3.37±0.03 μm in fish sampled in 1998 and 3.02±0.03 μm in 1999 (Fig. 4).

Whole body concentrations of triacylglycerols (TAG), the primary metabolically-available form of stored energy in salmonids and other fishes, differed between the two years. Upon entering the Gulf of the Farallones, juvenile salmon had greater levels of TAG in 1999 than in 1998, 30.5±3.1 mg/g and 11.5±1.8 mg/g wet weight, respectively. However, lipid stores of salmon in the gulf were depleted to a greater extent in 1999. Juveniles collected from the gulf in 1999 had TAG levels of 4.4±1.4 mg/g, whereas those from 1998 were 7.9±1.0 mg/g. These data support previous research that found depleted TAG

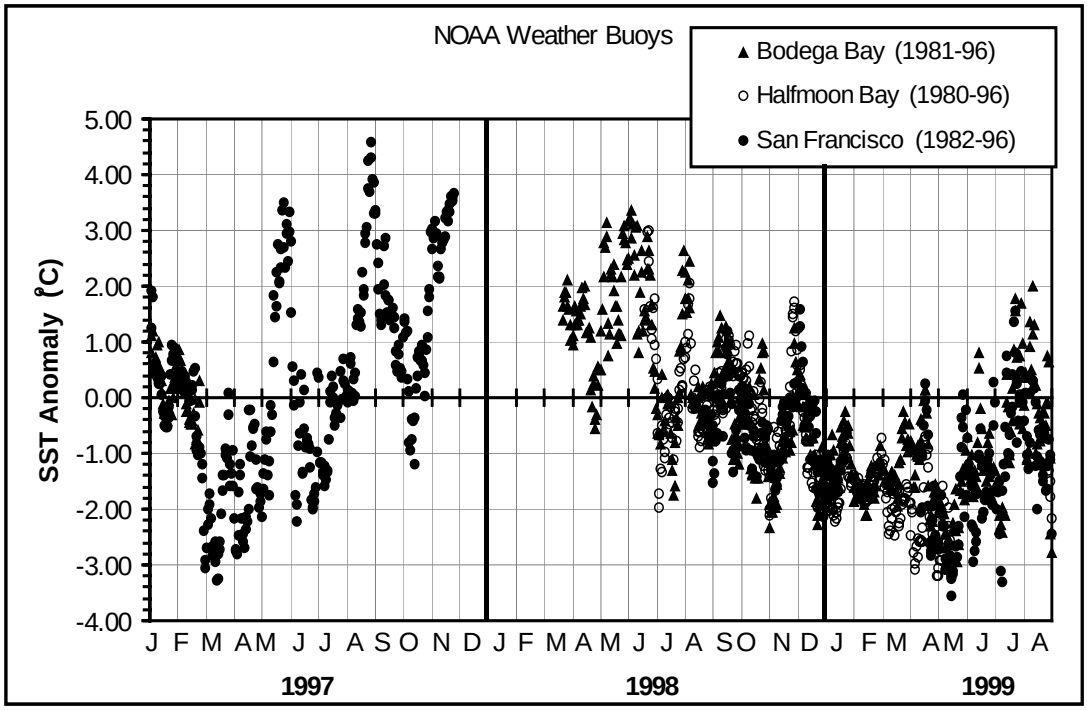

Fig. 3 Sea surface temperature anomalies from buoys at Bodega Bay, San Francisco, and Half Moon Bay. Anomalies were calculated from longer-term averages shown in parentheses in the legend. All three buoys were out of operation from December 1997 to mid-March 1998 when El Niño conditions were most evident.

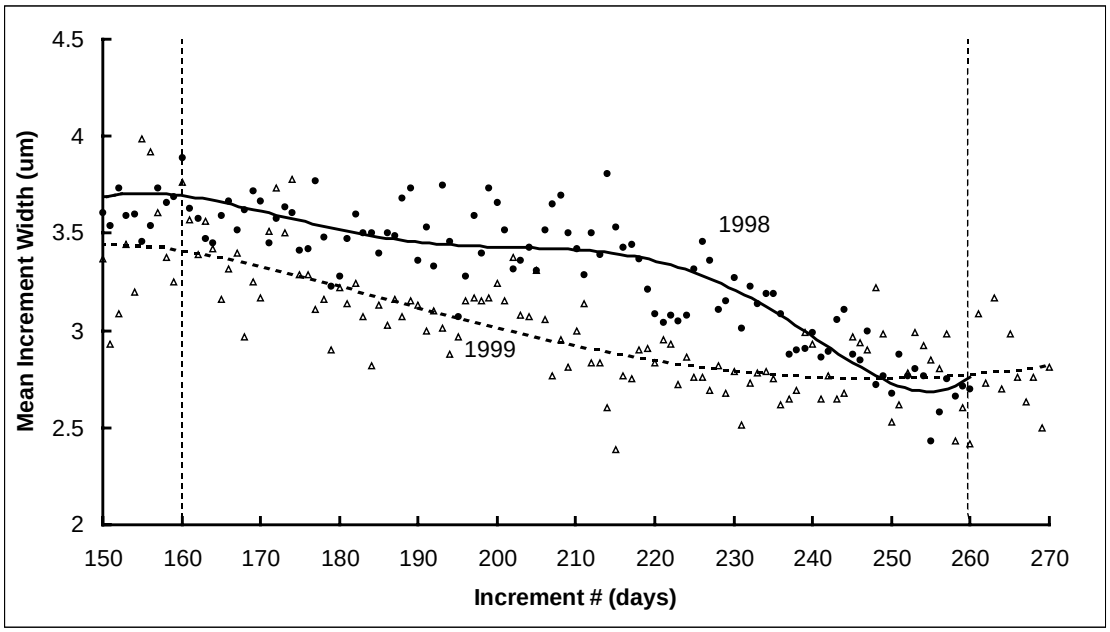

Fig. 4 Mean otolith increment widths for juvenile chinook salmon from the Gulf of the Farallones in 1998 (solid circles) and 1999 (open triangles). Lines represent least squares fit of daily mean increment widths; solid line - 1998, dashed line - 1999. Vertical dashed lines at 160 and 260 increments represent estimated first 100 days in the ocean after leaving the San Francisco Estuary.

concentrations in juvenile salmon after exiting the estuary (MacFarlane and Norton, 2002).

Juvenile salmon in the Gulf of the Farallones not only grew faster and maintained a greater TAG concentration during the 1998 El Niño period, their condition (Fulton's K-factor) was better as well. In 1998, mean K increased to 1.42±0.01 for gulf salmon from 1.03±0.01 at ocean entry, compared with a change from 1.04±0.01 at ocean entry to 1.32±0.01 in the gulf during 1999.

Although there were differences in growth, energy status, and condition between the two years, feeding data did not resolve the disparity. This is not unexpected because stomach contents reflect only recent feeding, whereas growth and lipid accumulation integrate metabolic processes over longer time scales. Stomach fullness was estimated to be 45.5% in juveniles sampled in 1998 and 56.7% in 1999. In both years, fish were the primary food item, comprising greater than 50% of the stomach contents volume. Decapod early life stages were of secondary importance, especially for salmon later in the season in August to October.

The marine environment in the Gulf of the Farallones differed between the two years. From May through August, mean sea surface temperatures were about 1.0°C warmer in 1998 and about 1.3°C cooler in 1999 than long-term averages (Fig. 3). The 1997-98 El Niño was characterized by heavy precipitation in California and this was evident in freshwater outflow from the Central Valley. Freshwater outflow into the gulf averaged 2,940 cubic meters per sec (m^3/s) from January to June 1998, whereas outflow in 1999 was much reduced during the dryer La Niña to 1,330 m^3/s.

The Gulf of the Farallones is buffered from large-scale oceanic influences because it is in the upwelling shadow of Pt. Reyes to the north, bounded by the Farallon Islands and associated marine banks on the west, and subjected to the effects of freshwater outflow from San Francisco Bay. Although El Niño typically produces enhanced poleward flow of the California Current, near-surface current data from an Acoustic Doppler Current Profiler in May and June 1998 did not reveal such a pattern. Currents in the gulf were forced by tidal circulation and persistent northwesterly winds, which also produced positive upwelling index anomalies throughout the summer and fall of 1998 (April - November mean monthly anomaly for 39°N 125°W: +44.5±25.6). As expected, strong northwesterly winds during the summer and fall of the 1999 La Niña event resulted in intense upwelling with a mean April to November monthly index anomaly of 104.6±35.1.

Biological productivity is highly variable in the Gulf of the Farallones region and modulated to varying degrees by upwelling, advection, wind-driven and tidal circulation, and freshwater outflow. Primary productivity, estimated by chlorophyll *a* concentrations in May and June, was similar between the two years, but the distribution of phytoplankton differed. In 1998, phytoplankton were distributed within the gulf on the continental shelf whereas during the 1999 La Niña they were primarily off the shelf, seaward of the gulf. Greater nutrient-rich freshwater influx coupled with higher temperatures in 1998 may have accounted for greater primary productivity within the gulf during the El Niño event. Greater phytoplankton biomass within the Gulf of the Farallones in 1998 was accompanied by greater secondary production. Mean zooplankton biomass in the near-surface waters was 0.30±0.12 ml/m^3 in May and September 1998. In contrast, zooplankton mean settled volume was 0.13±0.03 ml/m^3 in August and October 1999.

In summary, during the 1997-98 El Niño, juvenile salmon in the Gulf of the Farallones grew at a greater rate, maintained higher TAG reserves, and were in better condition than those during the 1999 La Niña. This profile may be attributed to somewhat higher biological productivity in the gulf in 1998, due to increased nutrient input from freshwater inflow, and the protection afforded by Pt. Reyes and the Farallon Islands, which buffered the embayment from the full impacts of oceanic processes. But, for all measures of salmon development the differences were not great. The data do support the contention, however, that the 1997-98 El Niño was not detrimental to juvenile chinook salmon development in this region during the early stage of the ocean phase of their life cycle.

References

Bradford, M.J., and Geen, G.H. 1987. Size and growth of juvenile chinook salmon back-calculated from otolith growth increments, p. 453-461. *In* R.C. Summerfeldt and G.E. Hall [eds.] The age and growth of fish. Iowa State University Press, Ames, IA.

Kaeriyama, M., Nakamura, M., Ueda, H., Anma, G., Takagi, S., Aydin, K.Y., Walker, R.V., and Myers, K.W. 2000. Feeding ecology of sockeye and pink salmon in the Gulf of Alaska. NPAFC Bulletin 2: 55-63.

Lenarz, W.H., Ventresca, D.A., Graham, W.M., Schwing, F.W., and Chavez, F. 1995. Explorations of El Niño events and associated biological population dynamics off central California. CalCOFI Report 36: 106-119.

Lynn, R.J., Baumgartner, T., Garcia, J., Collins, C.A., Hayward, T.L., Hyrenbach, K.D., Mantyla, A.W., Murphree, T., Shankle, A., Schwing, F.B., Sakuma, K.M., and Tegner, M.J. 1998. The state of the California Current, 1997-1998: transition to El Niño conditions. CalCOFI Report 39: 25-49.

MacFarlane, R.B,. and Norton, E.C. 2002. Physiological ecology of juvenile chinook salmon (*Oncorhynchus tshawytscha*) at the southern end of their distribution, the San Francisco Estuary and Gulf of the Farallones, California. Fishery Bulletin 100 (2) (In press).

Mysak, L.A. 1986. El Niño, interannual variability and fisheries in the northeast Pacific Ocean. Can. J. Fish. Aquat. Sci. 43: 464-497.

Pearcy, W.G., and Schoener, A. 1987. Changes in the marine biota coincident with the 1982-1983 El Niño in the northeastern subarctic Pacific Ocean. J. Geophys. Res. 92: 14,417-14,428.

Simpson, J.J. 1992. Response of the Southern California current system to the mid-latitude North Pacific coastal warming events of 1982-1983 and 1940-1941. Fisheries Oceanogr. 1: 57-79.

Woodbury, D. 1999. Reduction of growth in otoliths of widow and yellowtail rockfish (*Sebastes entomelas* and *S. flavidus*) during the 1983 El Niño. Fishery Bulletin 97: 680-689.

Variability of the pink salmon sizes in relation with abundance of Okhotsk Sea stocks

Olga S. Temnykh[1] and Sergey L. Marchenko[2]

[1] Pacific Research Fisheries Center (TINRO-center), 4, Shevchenko Alley, Vladivostok, Russia, 690600. E-mail: tinro@tinro.ru

[2] MoTINRO, Magadan, Russia. E-mail: tinro@online.magadam.su

Beginning in the mid-1970s there was an increase in abundance of all Pacific salmon species. It was shown that global climatic factors may have caused changes in salmon abundance in the North Pacific (Beamish and Bouillon 1993, Klyashtorin and Sidorenkov 1996, Radchenko and Rassadnikov 1997, Shuntov *et al.* 1997). The rise in abundance of Asian and American stocks of salmon was accompanied by a decrease in the average size of fish, by an increase in age at maturity (due to the growth rate reduction during marine period of their life cycle), and by a reduction of the fecundity of females (Ishida *et al.* 1993, Welch and Morris 1994; Bigler *at.al.* 1996). Nevertheless, there are some exceptions to the general trend of Pacific salmon productivity in relation to stock abundance. For example, a decrease in abundance was observed for the Japan/East Sea pink salmon stocks (especially for the Primorye stock) while the average size of the Primorye pink salmon decreased during the 1970-1980s (Temnykh 1998). At the same time, abundant pink salmon from Sakhalin maintained a large size (Nagasawa 1998).

The main objectives of this research were to:

- Compare growth of pink salmon from "continental" (northern coast of the Okhotsk Sea) and "island" (Sakhalin, southern Kuril islands) regions during periods of high and low pink salmon abundance; and
- Determine those factors responsible for size differences among pink salmon stocks, particularly in the northern and southern Okhotsk Sea, during periods of low and high abundance from the 1970s-1990s.

Materials and methods

Statistical data on pink salmon catches collected by TINRO-Centre, SakhTINIRO, and MoTINRO, are used in this study. These include the average size of spawners from rivers on the Okhotsk Sea coast of Sakhalin (north and south Sakhalin as well as Terpenya and Aniva bays), from Iturup Is. (southern Kuriles), and from the mainland rivers of the northern coast of the Okhotsk Sea (Gizhiga, Kukhtuy, and Tauy rivers) (Fig. 5).

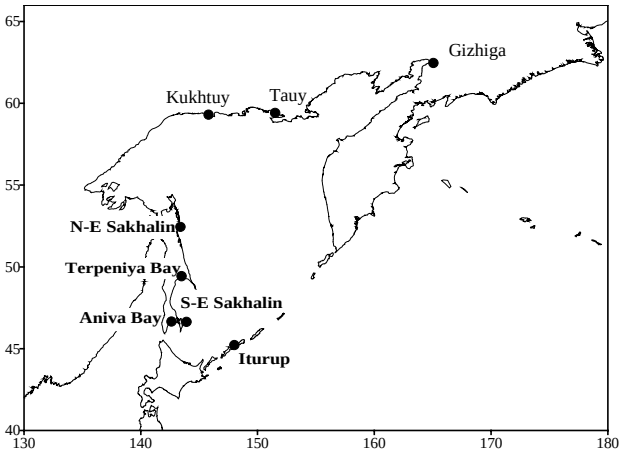

Fig. 5 Map of the location of Okhotsk Sea pink salmon regions studied.

Results

Catch dynamics for the Okhotsk Sea stocks of pink salmon

Eastern Sakhalin, western Kamchatka, southern Kurile, and northern Okhotsk Sea stocks of pink salmon are highly abundant stocks within the Okhotsk Sea. Following a period of low abundance in 1940-1960s, an increase in pink salmon number was observed in the Okhotsk Sea from the late 1970s. From the early 1990s, the total odd-year pink salmon catch increased 1.8 times when compared to the late 1970s and 1980s, and amounted to 62-133 thousand tons (Fig. 6). This was mainly due to a considerable rise of pink salmon abundance from the south-western Okhotsk Sea, particularly from eastern Sakhalin. During the last decade the share of those groups in the odd years reached 55-96% in the total number in the Okhotsk Sea.

Total even-year pink salmon catch increased 3.4 times when compared to the 1970-1980s, and amounted to 83-192 thousand tons (Fig. 6). On the Sakhalin and southern Kuriles, the number of pink salmon increased 2.2 times, while in the western Kamchatka and northern Okhotsk Sea regions it increased 4.6 and 4.3 times, respectively. Beginning in 1994, pink salmon from western Kamchatka was the most numerous among the odd-year generations (46-60% of the total number of the Okhotsk Sea stocks).

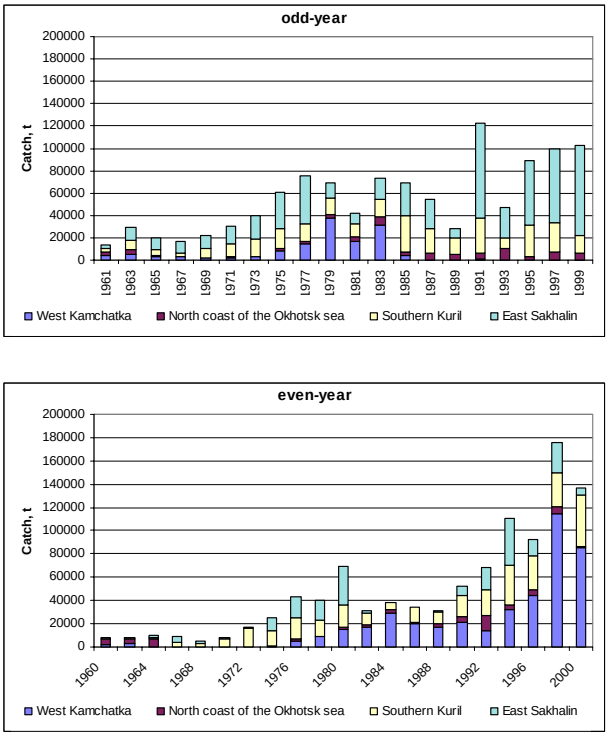

Fig. 6 Total annual catch of pink salmon in the main regions of coastal fisheries.

Changes of body weight of the Okhotsk Sea stocks of pink salmon

During the 1990s, both southern and northern pink salmon populations from the Okhotsk Sea were characterized by peculiar changes in mean size. Among the southern Okhotsk Sea stocks (eastern Sakhalin, southern Kuriles), there was a trend toward increasing body weight both in even-year, and especially in odd-year generations over the last decade (Fig. 7, Table 1).

As for the increased abundance of pink salmon from the northern Okhotsk Sea coast, the average weight was also growing in the odd-year broods, that were more abundant than even-year generations, though it was somewhat smaller in the even years. Average size changes within the "northern" and "southern" groups of pink salmon were synchronous. The increase in both abundance and average size of pink salmon from southern and northern Okhotsk Sea stocks is unequivocal evidence that favorable conditions prevailed for fish reproduction during the late 1980s - early 1990s.

Weakening of the Aleutian Low led to considerable warming of the northwestern Pacific after 1989. The carrying capacity for the Okhotsk Sea pink salmon increased. Unlike the North American pink salmon, the average size of the Okhotsk Sea pink salmon increased during a period of high abundance. We can only guess what was the main reason for that. It could be due to increased productivity as a consequence of general warming in the northwestern Pacific and/or improvements of forage reserves at the expense of significant decreases in abundance of other plankton consumers. In the 1980s, the total biomass of pelagic fishes amounted to

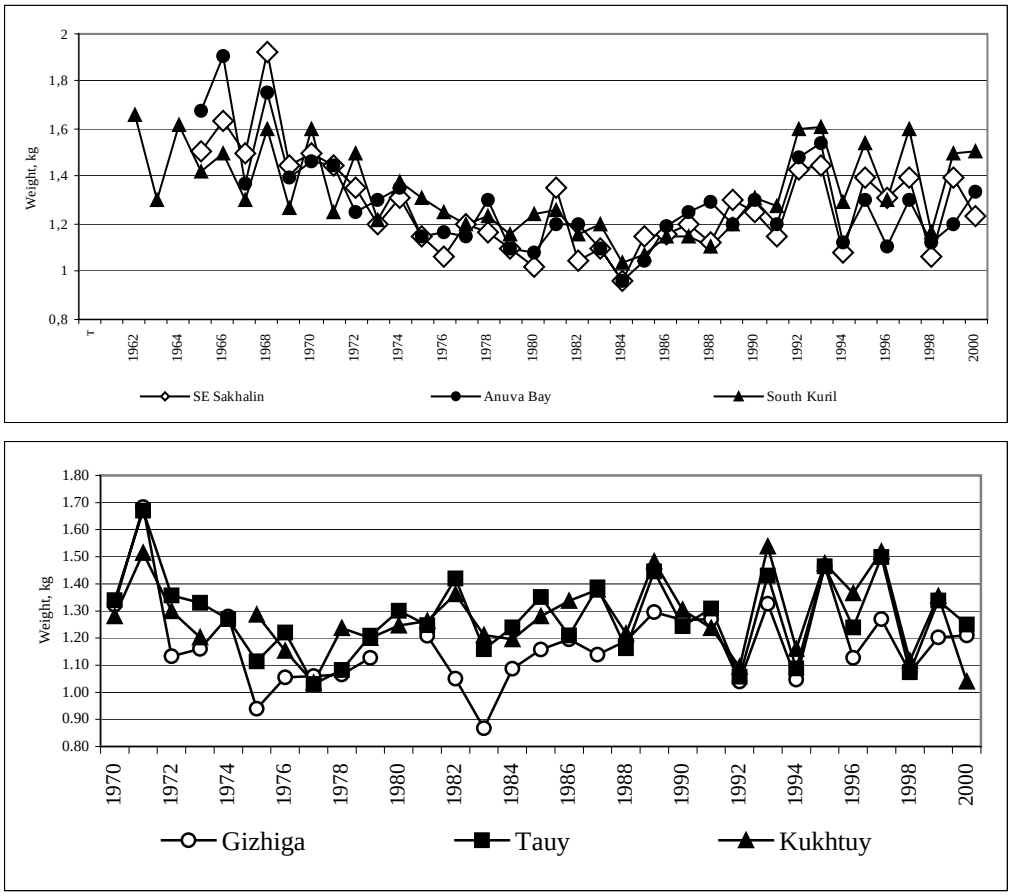

Fig. 7 Average pink salmon weight in Sakhalin-Kuril region (top panel) and northern coast of the Okhotsk Sea (bottom panel).

Table 1 Average Okhotsk Sea pink salmon catches and fish weight in the 1970-1980s and in the 1990s.

	Region		Average weight kg		Average catches ,000 t		Average total catches ,000 t	
			1978-1989	1990-2000	1978-1988	1990-2000	1978-1988	1990-2000
Even years	Northern coast of the Sea of Okhotsk	Gizhiga	1,12	1,13	1,72	5,58	43,1	123,3
		Tauy	1,12	1,13				
		Kukhtuy	1,27	1,18				
	Sakhalin Island	Aniva Bay	1,17	1,25	21,03	48,52		
		S-E Sakhalin	1,08	1,27				
		Terpeniya Bay*	1,02	1,14				
	South Kuril Islands	Iturup	1,16	1,36				
Odd years	Northern coast of the Sea of Okhotsk	Gizhiga	1,09	1,3	4,64	6,29	61,9	103,5
		Tauy	1,3	1,41				
		Kukhtuy	1,3	1,42				
	Sakhalin	Aniva Bay	1,15	1,31	39,52	85,64		
		S-E Sakhalin	1,2	1,36				
		Terpeniya Bay*	1,2	1,32				
	South Kuril Islands	Iturup	1,18	1,51				

million tons in the Kuroshio Current region. In the 1990s, the abundance of these fishes decreased by 7-8 times, mainly at the expense of Japanese sardine (Belyaev 2000). During this period, total plankton consumption by pelagic fishes decreased by up to 20 times compared to the 1980s in Pacific waters of Kuril islands (Naydenko, in press).

The increase in number and size of pink salmon from the southern Okhotsk Sea population took place together with the drop in abundance of Pacific sardine after the 1990s. The low abundance and small size of pink salmon took place together with decrease in abundance of Japanese sardine after 1989. The low abundance and small size of pink salmon were observed for stocks both in the southern Okhotsk Sea, and in Japan/East Sea during high abundance of Japanese sardine (Temnykh 1998). It is unlikely that sardine are a direct competitor with pink salmon. It appears that a high abundance of the predator results in enhanced pressure on planktonic organisms. A decrease in zooplankton abundance in the western North Pacific during the 1970 - 1980s (Odate 1994) could be due to both climate and oceanological changes, and predation of abundant nektonic species.

It is interesting to note that the average weight of pink salmon was larger in the northern Okhotsk Sea during the 1980s compared to the southern Okhotsk Sea stocks, in spite of the fact that the marine life period of northern stock fishes is 30-45 days shorter than southern Okhotsk Sea stocks. In winter, pink salmon from different Okhotsk Sea stocks dwell within the same region of the northwestern Pacific but these stocks are partly separated in time and space during migrations (Fig. 8). The range of the northern Okhotsk Sea pink salmon is less connected with feeding areas of subtropical migrants in the Subarctic Front Zone, especially at the beginning and at the end of marine period of pink salmon life.

During the last decade, there is some evidence that density-dependent factors caused the decrease in average weight of highly abundant pink salmon generations within the Okhotsk Sea. In the 1990s, a permanently high weight difference was observed between even- and odd-year generations of pink salmon from rivers of the northern Okhotsk Sea coast, Sakhalin and Iturup (Fig. 7, Table 1). In the Sakhalin-Kuril region, even-year pink salmon were 100-200 g lighter than odd-year. The average weight of eastern pink salmon is

lower at low stock abundance in even years, compared to fish size observed in odd years when Sakhalin population number was twice higher. Pink salmon sizes depend on the total abundance in the Okhotsk Sea, but not abundance of each stock.

We have suggested a hypothesis explaining the dynamics of fish size and stock abundance of pink salmon. To develop our knowledge in this field, it is of primary importance to look more carefully into the basic parameters of carrying capacity for pink salmon during marine period of the life cycle.

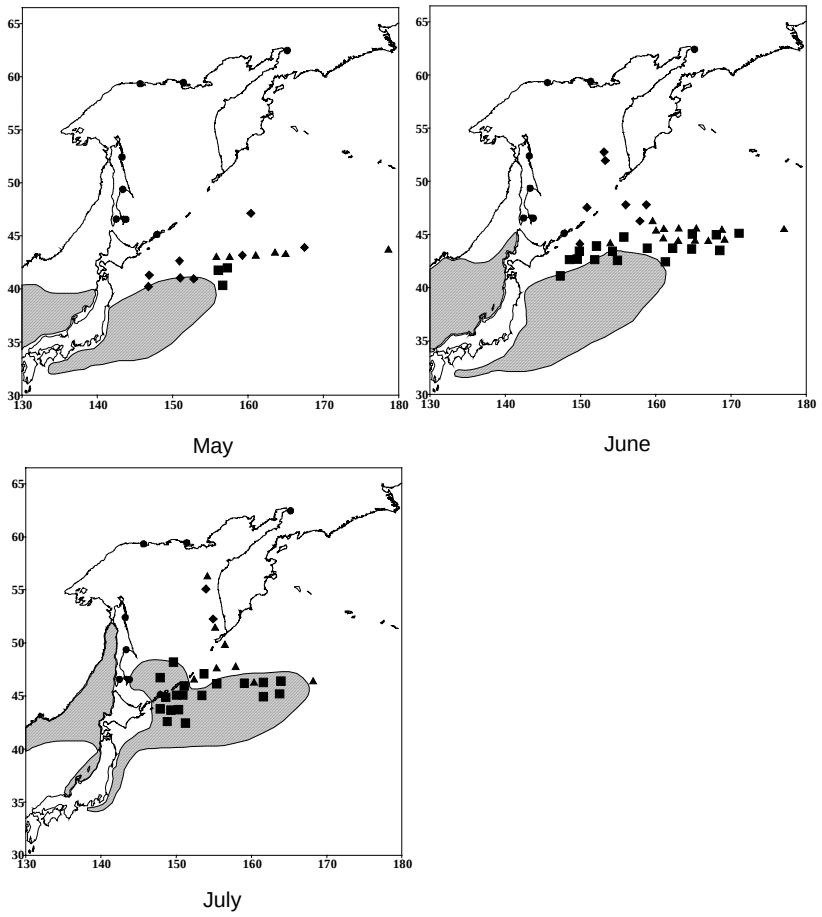

Fig. 8 Seasonal distribution of the Okhotsk Sea pink salmon and Japanese sardine in the northwestern Pacific. (■) pink salmon from Sakhalin-Kuril stocks, (▲) pink salmon from the northern Okhotsk Sea, (✡) pink salmon from western Kamchatka stocks (tagging data from Ogura 1994). The shaded area indicates Japanese sardine distribution during the period of high abundance in the 1970-1980s.

References

Beamish, R.J., and Bouillon, D.R. 1993. Pacific salmon production trends in relation to climate. Can. J. Fish. Aquat. Sci. 50: 1002-1016.

Bigler, B.S., Welch, D.W., and Helle, J.H. 1996. A review of size trends among North Pacific salmon (*Oncorhynchus* spp.). Can. J. Fish. Aquat. Sci. 53: 455-465.

Ishida, Y., Ito, S., Kaeriyama, M., McKinnell, S., and Nagasawa, K. 1993. Recent changes in age and size of chum salmon (*Oncorhynchus keta*) in the North Pacific Ocean and possible causes. Can. J. Fish. Aquat. Sci. 50: 290-295.

Klyashtorin, L.B., and Sidorenkov, N.S. 1996. The long-term climatic changes and pelagic fish stock fluctuations in the Pacific. Izv. TINRO. 119: 33-54 (in Russian).

Nagasawa, K. 1998. Long-term changes in climate, zooplankton biomass in the western North Pacific, and abundance and size of the East Sakhalin pink salmon. NPAFC Technical Report, Vancouver, Canada, pp. 35-36.

Ogura, M. 1994. Migratory behavior of Pacific salmon (*Oncorhynchu*s spp.) in the open sea. Bull. Nat. Res. Inst. Far Seas Fish. 31: 1-138.

Radchenko, V.I., and Rassadnikov, O.A. 1997. Long-term dynamics trends of Asian stocks of Pacific salmon and factors determing it. Izv. TINRO 122: 72-94 (in Russian).

Shuntov, V.P., Radchenko, V.I., Dulepova, E.P., and Temnykh, O.S. 1997. Biological resources of the Far Eastern Russian economic zone: structure of pelagic and bottom communities, up-to-data status, tendencies of long-term dynamics. Izv. TINRO 122: 3-15 (in Russian).

Temnykh O.S. 1998. Primorye pink salmon growth at high and low abundance. NPAFC Technical Report, Vancouver, Canada, pp. 20-22.

Welch, D.W., and Morris, J.F.T. 1994. Evidence for density-dependent marine growth in British Columbia pink salmon populations. NPAFC Doc. 97. 33 p.

The characteristic growth rate of herring in Peter the Great Bay (Japan/East Sea)

Ludmila A. Chernoivanova, Alexander N. Vdovin and D.V. Antonenko
Pacific Research Fisheries Center (TINRO-center), 4, Shevchenko Alley, Vladivostok, Russia, 690950. E-mail: tinro@tinro.ru

Pacific herring are subarctic species forming several local populations within its extensive natural habitat. The Peter the Great Bay herring form one of most southerly groups, and are typically characterized by a high growth rate. There is no uniform opinion about the hierarchical status of this group, but it has the highest biopotential among other herring groups of the Japan/East Sea (Posadova 1988, Gavrilov 1998, Rybnikova 1999).

The life cycle of Peter the Great Bay herring occurs within the Bay and in adjacent waters in the northwestern part of the Japan/East Sea. Considering its restricted distribution and spawning grounds, the potential level of biomass of this population does not exceed 150 thousand tons. From 1910 till now, three peaks of high abundance have been observed: in the mid 1920s, the mid 1950s, and the late 1970s/early 1980s. Each rise was associated with one or several dominant generations (Posadova 1988). In the 1990s, the abundance and productivity of Peter the Great Bay herring have come near to the historical minimum, and its biomass during these years varied from 5 - 10 thousand tons.

It is necessary to determine how the size-age characteristics and population structure changed in connection with the present depressed condition of Peter the Great Bay herring stocks. The biostatistical data from annual monitoring of the Peter the Great Bay herring stocks from 1971 to 2001 were analyzed. The data were collected from control catches by gill nets, seines and traps exposed directly on the spawning grounds. The data were processed using standard ichthyological techniques. The scales from a middle part of fish body under a dorsal fin were used for age interpretation. The following formula (Alimov 1989) was used for growth rate:

$$C_l = \frac{\lg(l_1) - \lg(l_0)}{0.4343(t_1 - t_0)} \times 100\%$$

where C_l is the average speed of linear growth, l_0 is length at the initial time, t_0, and l_1 is length at a later time, t_1.

The Peter the Great Bay herring are the fastest growing of all herring populations in the western Pacific (Posadova 1985). Growth is most rapid during the first and second years of life. At age

0+, herring in Peter the Great Bay have an average body length of 110 mm and weight of 9.9 g at the end of October. The average length and weight of age 1+ fish are 220 mm and 100.1 g, respectively at the end of October. After the second year of life the growth rate quickly decreases and, after the fifth year, does not exceed 10 % of the increase in the first year.

The relative daily linear growths of herring for the first year of life vary from 0.74 to 0.76% and appear to be constant during the periods of variable abundance (Table 2). The highest growth rate of herring during ontogenesis is 1.5% per day during the first six months of life (from May to October). The decreasing growth rate after the first year of life was associated with the process of sexual maturation.

Table 2 The relative daily linear growth (annual average, %) of Peter the Great Bay herring.

Period of observation	Age (years)							
	1	2	3	4	5	6	7	8
1999-2001	0.74	0.10	0.02	0.03	0.01	0.006	0.006	0.006
1971-1990	0.76	0.14	0.05	0.02	0.01	0.010	0.006	0.006

Table 3 Age structure (%) of herring catches in different parts of Peter the Great Bay in 1998-2001.

Period of observation	Age (years)										
	1	2	3	4	5	6	7	8	9	10	M
Amurskiy Bay											
1998			62.0	36.0		2.0					3.9
1999		6.4	68.3	19.1	3.5	2.2	0.5				3.8
2000		4.6	35.9	45.4	13.7	0.4					4.2
2001		8.3	20.5	27.1	35.8	7.1	0.7	0.5			4.2
Pos'et Bay											
1998			26.2	5.5	4.0	23.6	28.8	10.0	1.6	0.3	6.1
1999		1.8	14.1	14.3	27.6	29.0	11.1	2.1			5.6
2000		5.3	13.6	18.1	21.4	23.2	14.8	3.1	0.5		5.6
2001	0.7	13.8	24.8	6.9	37.2	8.3	1.4	3.4	1.4	2.1	4.9

A separate population of Pacific herring comprises 83% of genetic variability (Rybnikova 1999) which causes significant variability of the whole complex of its biological features.

The high interannual variability in mean body length among generations in Peter the Great Bay was connected with the annual cohort strength. In the period of high abundance during the 1970s and 1980s, high yield generations (*e.g.* 1974 and 1980) were distinguished by low growth rates (Gavrilov and Posadova 1982). That tendency was not shown during the last 15 years in Peter the Great Bay. First of all, the alternation of weak and strong cohorts was disrupted (during that period there were no strong cohorts). Secondly, all generations of herring consisted of a spawning part of the population on a background of a low reproduction level have been characterized by the low rate of growth from 1995 till now. The average body length of fish at age two and three years does not reach long-term value (Fig. 9).

Lower recruitment of Peter the Great Bay herring during the last decade has been accompanied by a reduction of the maximal age of spawners and variable age structure among sites. In the northwestern part of Peter the Great Bay (Amurskiy Bay) fish at age of 2-4 years comprised more than 80% of herring catches, whereas at the southwestern part (Pos'et Bay) the herring were from 2 to 10 years of age from 1998-2000 (Table 3).

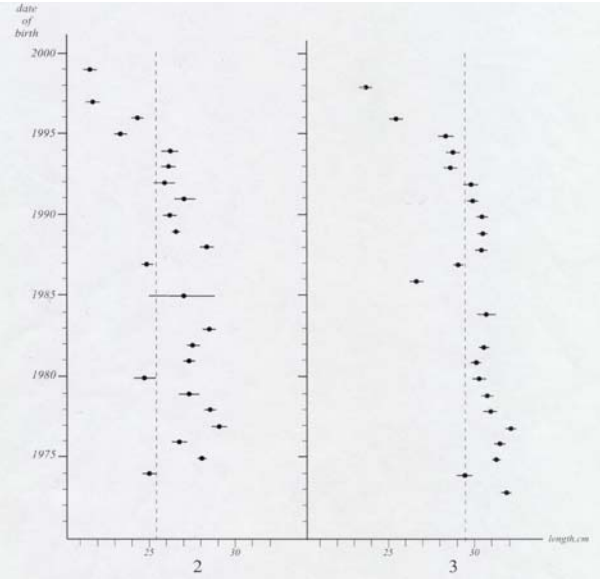

Fig. 9 Average length of Peter the Great Bay herring: generations at age 2 (left panel) and age 3 (right panel) years in 1974-1997. Dotted lines show long term average values (age 2: 25.2 cm, age 3: 29.5).

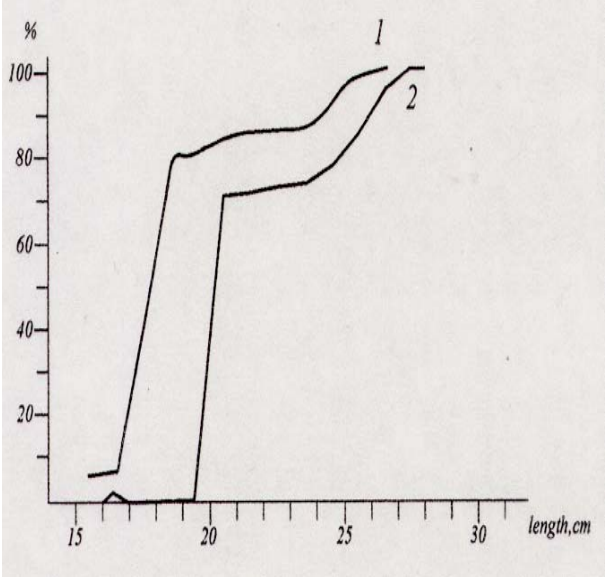

Fig. 10 The rate of maturation of herring in Peter the Great Bay in 1999-2001 (1) and 1978-1990 (2).

Evidently, the distortion of a complex age structure was consequence of the deterioration of reproduction conditions of Peter the Great Bay herring. It is quite probable that the decrease of growth rate in recent years is defined not only by any negative factors but also high rates of maturity. As was stated above, the sharp decrease of growth rate was caused by the maturation process. From 1999-2001, some herring (mainly males) began to mature at 14-17 cm body length, and 80% were mature by 18-19 cm. While in 1978-1990, the bulk of the population matured at 20-21 cm body length (Fig. 10). Accumulation of slow growing and early-maturing individuals in the spawning part of Peter the Great Bay herring population during low abundance contributes to increased reproductive potential and, probably, is one of mechanisms promoting the restoration of abundance.

References

Alimov, A.F. 1989. Introduction to the productional hydrobiology. Hydrometeoizdat, Leningrad, 152 pp.

Gavrilov, G. M. 1998. Seasonal and interannual variability of herring distribution in waters off the northern Prymorye. Izvestia TINRO-Centre 124: 758-764.

Gavrilov, G.M., and Posadova, V.P. 1982. Dynamics of Pacific herring *Clupea pallasi pallasi* Valenciennes (Clupeidae) abundance in Peter the Great Bay. J. Ichthyology 22(5): 760-772.

Posadova, V.P. 1985. Interannual variability in the spawning of herring in Peter the Great Bay. *In* Herring of the North Pacific Ocean. TINRO, Vladivostok, pp. 22-29.

Posadova, V.P. 1988. Stock assessment of herring in Peter the Great Bay. *In* Variability of ichthyofauna composition, yield year classes and forecasting techniques of fishes in the western Pacific. TINRO, Vladivostok, pp. 64-69.

Rybnikova, I.G. 1999. Population structure of Pacific herring *Clupea pallasi* (Valenciennes) in the Japan and Okhotsk seas. Abstract of the Ph.D thesis (marine biology). Vladivostok, 23 pp.

Temporal variations in size-at-age of the western Bering Sea herring

Nikolay I. Naumenko
Kamchatka Research Institute of Fisheries and Oceanography (KamchatNIRO), 18 Naberezhnaya Street., Petropavlovsk-Kamchatsky, 683600, Russia. E-mail: nnaumenko@kamniro.kamchatka.ru

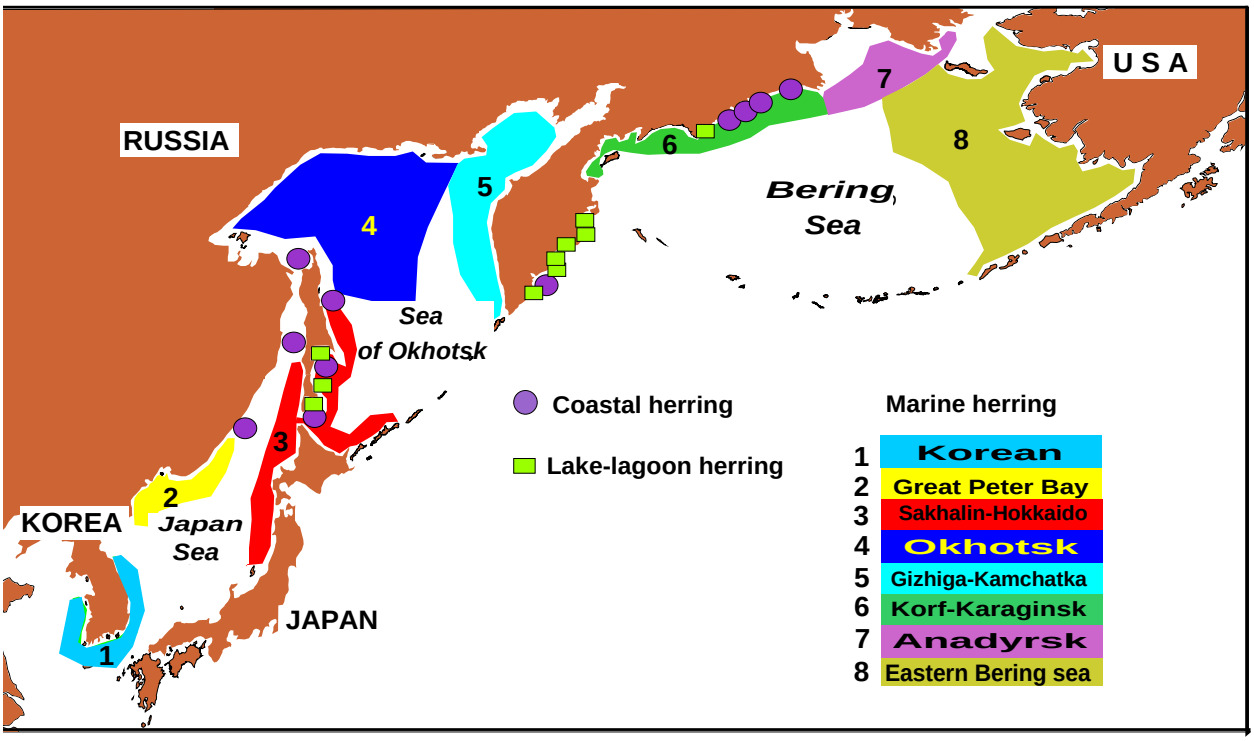

Fig. 11 Distribution of herring populations in the Far Eastern Seas.

Pacific herring inhabiting the Russian Far East Seas are represented by three ecological morphs: marine, offshore (coastal) and lagoon-lacustrine. Marine herring spend their whole life in higher salinity ocean waters where they undergo long migrations. The feeding area of this morph includes both shelf and bathypelagial waters. Off-shore herring inhabit only the shelf seas, particularly inlets and bays. This morph usually does not migrate long distances. Lagoon-lacustrine herring spend significant parts of their lives in brackish waters and migrate to feed in adjacent marine waters.

Russian waters in the northwest part of the Pacific Ocean are inhabited by 6 marine populations and by 22 off-shore and lagoon-lacustrine populations (Fig. 11). This ecological diversity provides maximum exploitation of forage resources for the species within the area and determines the extensive variability of size and growth parameters for this species.

Current information is based on many years of the author's personal observations of the growth in several herring populations inhabiting the Bering Sea and Pacific Ocean waters adjacent to Kamchatka: Korf-Karaginsky Bay, Eastern Bering Sea, Anadyr Bay, Yuzhnaya Lagoon, Nepichye Lake, Kalygyr Lake and Viluy Lake. The data on the growth of herring in the Sea of Japan and in the Sea of Okhotsk have been taken from literature. Forage base conditions are analyzed from annual standard surveys, each of them consisting of 7 stations sampled within Olyutorsky Bay in June.

The data on the size-at-age of herring taken from 19 areas within the northern part of the Pacific Ocean clearly indicate a significant difference in

the growth of fish (Tables 4 and 5). Off-shore and lagoon-lacustrine herring have been classified as moderate or slow growing (Fig. 12). Marine herring are the most divergent in the growth. For example, there are extremely fast-growing (Sakhalin-Hokkaido herring inhabiting the waters adjacent to Hokkaido Island and Peter the Great Bay herring), fast-growing (Sakhalin-Hokkaido herring inhabiting the waters adjacent to Sakhalin Island, Korf-Karaginsky Bay herring, Bristol Bay herring) and moderate-growing (Okhotsk Sea herring, Gijiga-Kamchatkan herring, Anadyr Bay herring, Nunivak Island herring and Norton Bay herring) herrings. In general, the marine morph has a higher growth rate (Fig. 13).

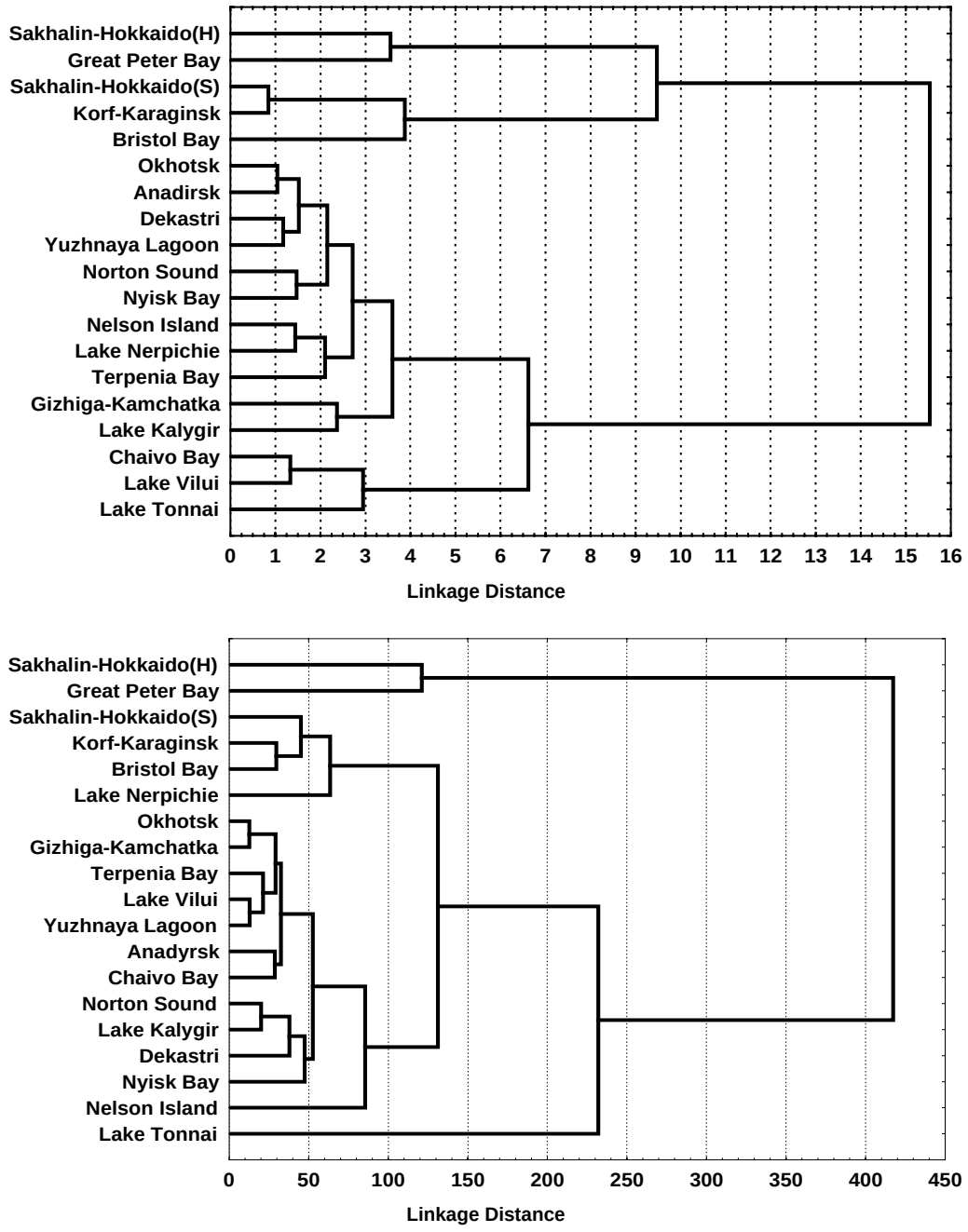

Fig. 12 Cluster analysis of length-at-age (upper panel) and weight-at-age (lower panel) of different Far East herring populations.

Table 4 Fork length-at-age (cm) of herring in different Far Eastern Seas.

Pupulation	Sea	Area	Age													Source
			1	2	3	4	5	6	7	8	9	10	11	12	13	
Marine herring																
Sakhalin-Hokkaido	Japan Sea	Hokkaido Island	15,0	22,0	26,0	29,0	30,5	32,0	33,0	34,0	34,5	35,0	35,3	35,6		1
Sakhalin-Hokkaido	Japan Sea	Sakhalin Island	12,3	19,4	23,8	26,1	28,3	29,7	31,0	32,0	32,5	33,0	33,3	34,0	34,5	2,3,4,5,6
The Great Piter Bay	Japan Sea	Western part	14,2	22,8	27,8	30,4	32,1	33,2	34,4	35,3	35,4	35,8	35,9	36,9	37,3	7,8,9
Okhotsk	Sea of Okhotsk	North West	7,9	15,0	20,4	23,4	25,5	27,1	28,2	29,1	29,9	30,4	31,1	31,3	31,4	6,10,11,12,13,14,15,16
Gizhiga-Kamchatka	Sea of Okhotsk	North East	7,5	13,5	19,2	22,6	24,8	26,6	27,8	27,9	29,7	29,8	30,1	30,4	31,3	6,17,18
Korf-Karaginsky	Bering Sea	Western part	12,2	19,6	24,1	26,8	28,5	30,0	31,1	32,1	32,9	33,5	34,4	35,1	35,5	19,20,21,22
Anadyrsky	Bering Sea	Gulg of Anadyr	8,2	15,6	20,7	23,3	25,0	26,6	27,9	28,9	29,7	30,8	31,4	31,8	32,2	19
Eeastern Bering Sea	Bering Sea	Norton Sound	9,8	17,2	20,5	23,0	24,7	26,4	27,9	28,8	29,6					19,23
Eeastern Bering Sea	Bering Sea	Nelson Island	9,1	16,2	20,9	23,6	25,9	27,5	28,7							19,23
Eeastern Bering Sea	Bering Sea	Bristol Bay	10,3	19,0	22,3	24,8	27,1	29,0	30,1	31,0	31,9	32,5	32,8			19,23
Coastal herring																
Dekastri	Japan Sea	Northern part	8,3	15,2	19,6	23,2	25,1	26,6	27,5	28,5	30,0	31,3	31,8	32,5		6,24,25,26
Nyisk Bay	Sea of Okhotsk	Sakhalin Island	8,9	15,7	20,2	22,5	24,5	26,6	27,9							7,27,28
Chaivo Bay	Sea of Okhotsk	Sakhalin Island	8,7	15,4	20,0	22,8	24,0	25,1	28,0							7,27
Terpenia Bay	Sea of Okhotsk	Sakhalin Island	9,0	15,6	20,6	22,5	24,4	25,3	27,1							27
Lake-lagoon herring																
Lake Vilui	N-W Pacific	Kamchatka	8,8	15	18,5	20,4	22,9	24	25,2	25,9	26,6	27	27,8	27,9	28,1	19
Lake Kalygir	N-W Pacific	Kamchatka	8,4	14,7	19,5	22,4	24,4	25,4	26,5	27,3	28,1	27,8	28,4	29,1	29,3	19
Lake Nerpichie	N-W Pacific	Kamchatka	9,1	15,4	21,4	24,5	26,3	27,3	28,2	29	29,9	30,5	31,1	31,5	32	19
Lake Tonnai	Sea of Okhotsk	Sakhalin Island	8,6	14,2	17,6	20,2	21,5	22,3	23,5							29
Yuzhnaya Lagoon	Bering Sea	North West	8,5	14,7	19,4	22,4	24,3	25,3	26,5	27,1	28,1	28,8	29,4	30,1	30,6	19,30

Sources: 1. Motoda, Hirano, 1963; 2. Kaganovsky, 1954; 3. Druzhinin, 1957; 4. Pushnikova, 1981; 5. Pushnikova, 1994; 6. Materials of Soviet-Japan Fisheries Commission, 1969-1976; 7. Ambroz, 1931; 8. Gavrilov, Posadova, 1982; 9. Posadova, 1985; 10. Kolesnik, Khmarov, 1970; 11. Labetsky, 1975; 12. Tyurnin, Yolkin, 1975; 13. Tyurnin, Yolkin, 1977; 14. Vyshegorodtsev, 1976; 15. Vyshegorodtsev, 1978; 16. Smirnov, 1994; 17. Piskunov, 1954; 18. Pravotorova, 1965; 19. Our data; 20. Kachina, 1967; 21. Kachina, 1969; 22. Kachina, 1981; 23. Wespestad, 1991; 24. Ambroz, 1930; 25. Kozlov, 1968; 26. Kozlov, Frolov, 1973; 27. Ivankova, Kozlov, 1968; 28. Gritsenko, Shilin, 1979; 29. Probatov, Frolov, 1951; 30. Prokhorov, 1965.

Table 5 Weight-at-age (g) of different populations of herring from Far Eastern Seas.

Pupulation	Sea	Area	Age													
			1	2	3	4	5	6	7	8	9	10	11	12	13	14
Marine herring																
Sakhalin-Hokkaido	Japan Sea	Sakhalin Island	24	72	140	191	242	279	317	360	375	398	416			
The Great Piter Bay	Japan Sea	Western part	28	135	250	308	371	399	432	465	484	525	547			
Okhotsk	Sea of Okhotsk	North West	8	30	84	119	155	186	213	237	266	285	303	315	364	
Gizhiga-Kamchatka	Sea of Okhotsk	North East	8	29	80	119	151	177	206	234	256	285	295	305	323	337
Korf-Karaginsk	Bering Sea	Western part	12	49	109	178	245	299	341	366	404	424	452	472	510	564
Anadyrsk	Bering Sea	Gulf of Anadyr	7	32	67	104	139	175	223	243	272	312				
Eeastern Bering Sea	Bering Sea	Norton Sound	8	46	79	134	166	210	234	281	313	348	357	373	391	405
Eeastern Bering Sea	Bering Sea	Nelson Island	9	38	84	129	187	227	280	306	337	376	410	429		
Eeastern Bering Sea	Bering Sea	Bristol Bay	12	62	118	174	229	283	331	376	414	445	470	492	508	523
Coastal herring																
Dekastri	Japan Sea	Northern part	8	44	102	125	153	194	215	242	274	304	305	323		
Nyisk Bay	Sea of Okhotsk	Sakhalin Island	8	42	70	100	182	198	224							
Chaivo Bay	Sea of Okhotsk	Sakhalin Island	7	39	83	121	141	160	221							
Terpenia Bay	Sea of Okhotsk	Sakhalin Island	8	40	90	117	148	164	201							
Lake-lagoon herring																
Lake Vilui	N-W Pacific	Kamchatka	8	42	80	107	145	162	184	201	218	228	248	252	255	257
Lake Kalygir	N-W Pacific	Kamchatka	8	39	90	140	179	205	232	258	274	287	295	320	328	359
Lake Nerpichie	N-W Pacific	Kamchatka	8	50	116	180	220	251	287	311	341	354	377	397	406	423
Lake Tonnai	Sea of Okhotsk	Sakhalin Island	7	30	57	85	102	114	132							
Yuzhnaya Lagoon	Bering Sea	North West	7	34	76	115	146	164	188	201	223	240	255	273	286	

Comment: sources as table 1

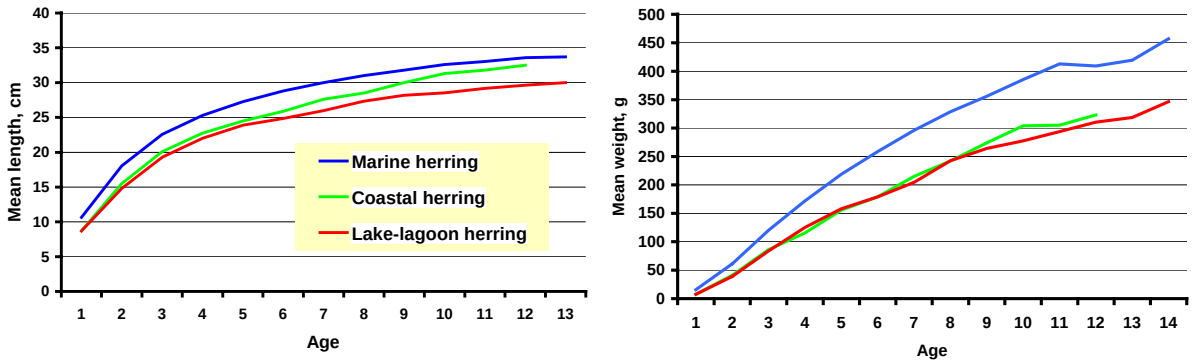

Fig. 13 Length-at-age (left) and weight-at-age (right) of different morphs of Far East herring.

The morphs differ in growth rate. By the character of the length growth the populations studied can be clearly divided into 3 types (Fig. 14A):

I. fast annual growth in the first year of life and rapid decrease of the growth in later years;
II. relatively fast annual growth in two initial years;
III slow growth in the first year of life and comparatively fast annual growth in later years.

Hokkaido Island herring have been classified to be of the first type. Most marine, all off-shore and some lagoon-lacustrine herring populations have been classified to be of second type. Most lacustrine and some marine herring populations are classified to be of the third type.

By the character of the mass growth, Far East herring populations have been divided into three types as well (Fig. 14B):

I. almost similar rich annual mass growth in second and third years of life (Sakhalin-Hokkaido herring inhabiting the waters adjacent to Hokkaido Island and Peter the Great Bay herring);
II. maximum annual mass growth in the third year of life cycle (majority of herring populations in the Sea of Japan and Okhotsk Sea);
III. maximum annual mass growth in the fourth year of life (all marine herring populations of Bering Sea).

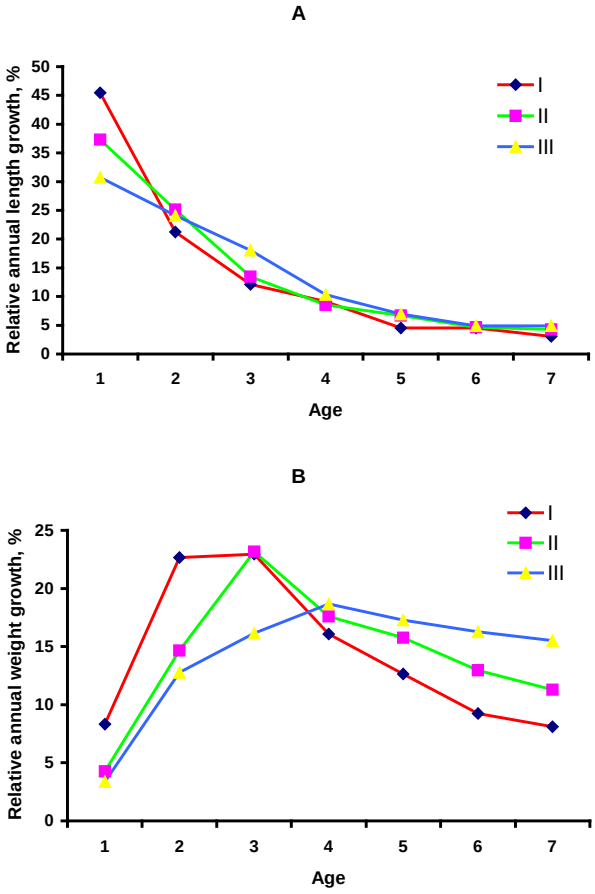

Fig. 14 Relative annual growth in length (A) and weight (B) in Far East herring morphs. See text for descriptions of each morph (I, II and III).

The most obvious trait of this species is significant year-to-year variations in size-at-age. For example, the range in the mean length of Korf-

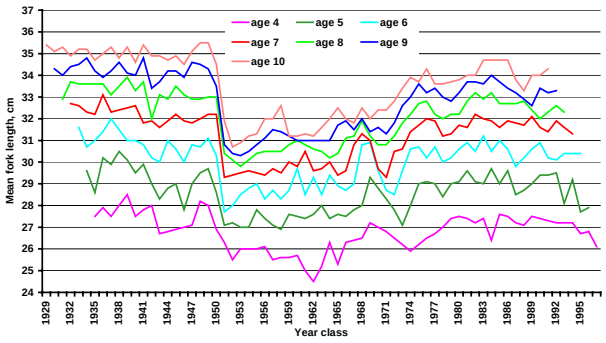

Fig. 15 Mean length-at-age of Korf-Karaginsky herring.

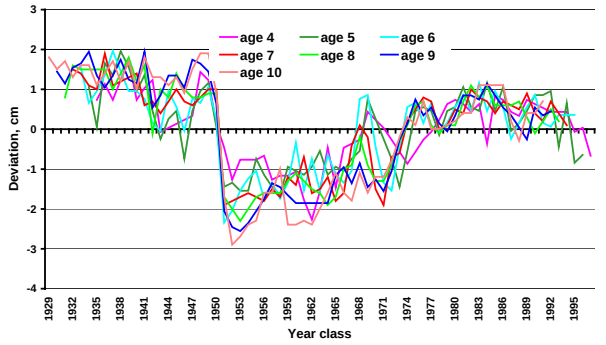

Fig. 16 Deviations from mean length-at-age.

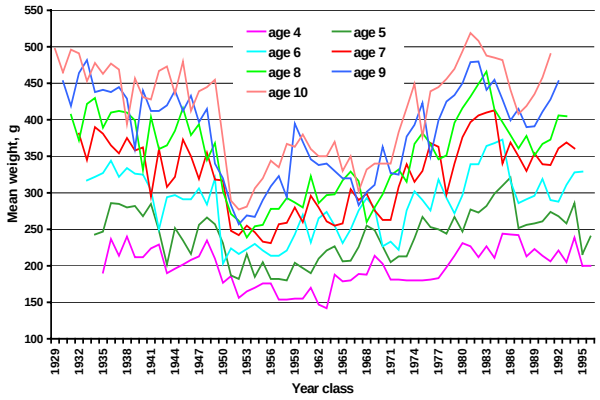

Fig. 17 Mean weight-at-age of Korf-Karaginsky herring.

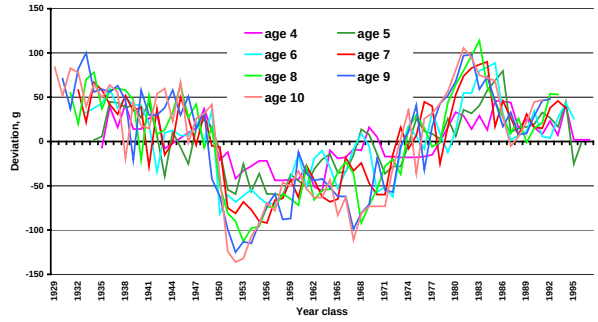

Fig. 18 Deviations in mean weight-at-age.

Karaginsky four-year-old fish is 4 cm (24.5-28.5 cm), of 10-years-old fish - 5.1 cm (30.4-35.5 cm), of 13-years-old fish - 5.9 cm (31.6-37.5 cm). The range in the mean mass of fish varies from 102 g in 4 year old fish to 227-255 g in 8-13 year old fish.

The variation in the biological patterns of Korf-Karaginsky herring demonstrates clear long-term cyclic dynamics (Figs. 15, 16, 17 and 18). The size (length and mass) of mature fish in generations for the 1930-40s was a maximum in all age groups for the whole observation period; the patterns were at a minimum for the 1950-70s and again relatively high for the 1980s. In the 1990s the size-at-age has been decreasing gradually, but being above the mean for many years, as early in the time series (Fig. 19).

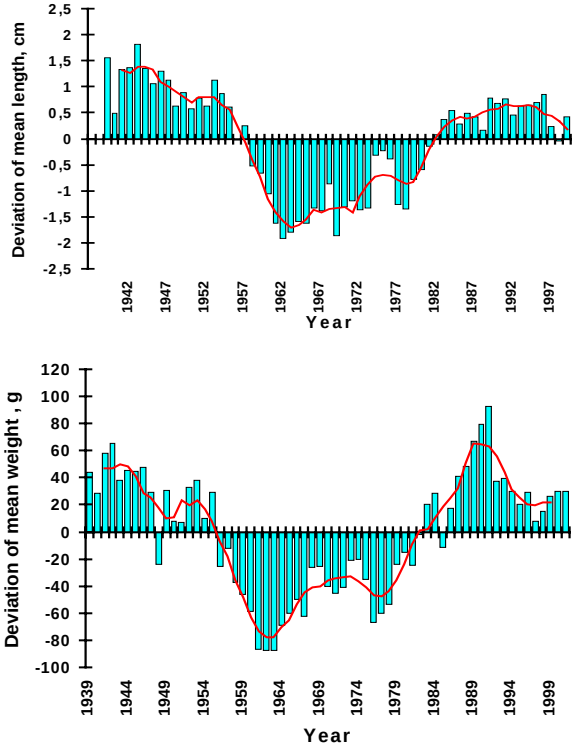

Fig. 19 Deviations of mean length (upper panel) and weight (lower panel) of age 4-10 Korf-Karaginsky herring from multi-year value.

For greater insight into the temporal pattern of the cycles of size variations in herring we used transformed data. We estimated deviations of the annual length and mass growth of 4-10-years-old

fish from the mean for many years (Figs. 20 and 21). There are three periods which could be seen clearly in the curve of the dynamics of the mean for 5-year periods of annual growth of mature herring.

The first period, bounded by generations of 1930 and 1951, was generally characterized by accelerated growth; the second period (1950-1970s) was characterized by slower growth, and 1970-1990s characterized by higher growth rates. Within the three twenty-year periods of high or low growth, there are two cycles of about 10 years. Thus, the growth of Korf-Karaginsky herring has cyclic dynamics, with the cycle consisting of 10 or 22-years approximately.

The growth of mature herring in the west part of Bering Sea has been regulated by several circumstances. The length of 5-10-year-old fish depends on the length of recruits *i.e.* maturating 4-year-old fishes (Fig. 22). The more definite length of recruits is, the greater is the length of mature fish in all older ages.

Beyond doubt the growth of herring has been influenced by stock abundance or density factor. Although a reliable correlation between abundance of a certain generation and annual growth has not been observed – very abundant generations demonstrate evidently slower growth as compared to that in other generations. The growth rate is very similar in generations of moderate and low abundance, also in general it is higher compared to that in abundant and highly abundant generations (Table 6). Actually, biological characteristics are influenced much more by population condition. The highest growth rates are observed in the 1940s and the early 1950s when the abundance of mature fish has been moderate (Table 7). After several abundant generations reproduced in 1951-1956 the abundance of mature fish increased quickly. To the late 1950s the abundance of mature fish reaches its' historical maximum. The size (length and mass) of 4-6 year-old fish for this period has been minimum for the whole period of observations. Slow growth has been observed in the fish of old age groups.

From the mid-1960s until mid-1970s the population underwent a depression. Despite the

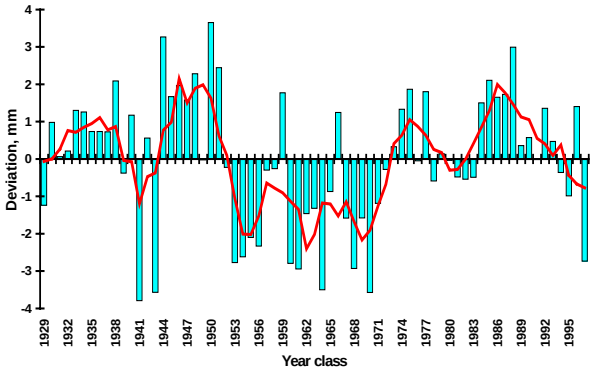

Fig. 20 Deviations of mean annual length growth of 4-10 age Korf-Karaginsky herring from multiyear value.

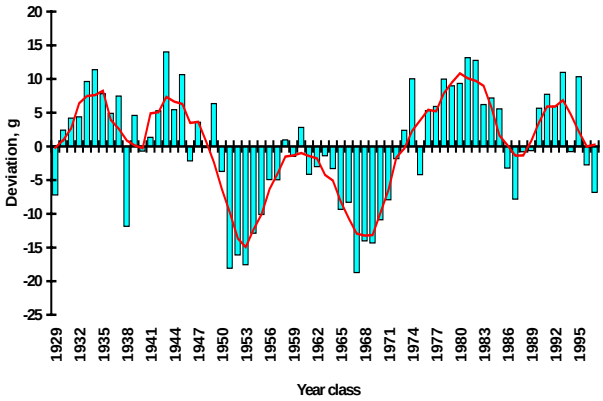

Fig. 21 Deviations of mean annual weight growth of 4-10 age Korf-Karaginsky herring from multiyear value.

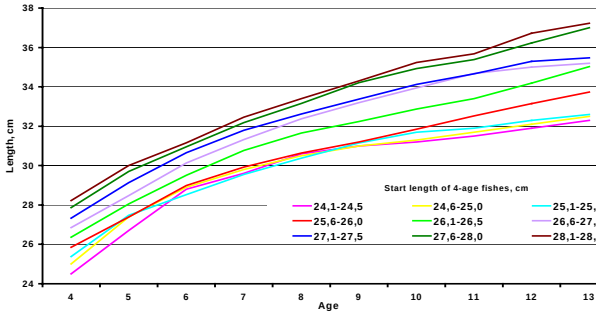

Fig. 22 Growth of Korf-Karaginsky herring in dependence on start length of 4-age fishes.

extremely low abundance of mature fish their growth stayed slow; also the individuals older than 6-years-old demonstrate the minimal growth for the whole historical period of the observations. In the late 1970s and in the 1980s the number of mature fish has increased a little, but remained

Table 6 Growth of Korf-Karaginsk herring in dependence from year-class strength.

Strength of year-class	Length/weight	Age									
		4	5	6	7	8	9	10	11	12	13
Very strong	Length, cm	26.3	27.4	28.6	29.9	30.8	31.2	31.5	31.8	32.0	32.4
	Weight, g	181	202	241	273	283	303	304	328	367	378
Strong	Length, cm	26.8	28.6	30.2	31.0	32.0	32.8	33.2	33.7	33.9	34.1
	Weight, g	192	239	273	313	355	379	401	412	414	416
Average	Length, cm	26.7	28.5	30.1	31.1	31.9	32.6	33.4	34.3	35.0	35.6
	Weight, g	198	245	284	324	348	385	414	444	475	506
Poor	Length, cm	27.0	28.8	30.2	31.6	32.6	33.4	34.2	35.1	36.0	36.2
	Weight, g	203	244	291	333	365	398	430	455	509	534

Table 7 Growth of Korf-Karaginsk herring in relation to stock abundance.

Level of stock-size	Length/weight	Age									
		4	5	6	7	8	9	10	11	12	13
High	Length, cm	25.8	27.3	28.6	30.3	31.3	32.3	33.4	33.9	34.2	-
	Weight, g	165	195	229	270	297	327	374	376	414	-
Average	Length, cm	27.3	29.1	30.7	32.0	33.0	34.0	34.6	35.3	36.1	36.4
	Weight, g	212	257	306	352	388	427	458	476	503	532
Low	Length, cm	26.9	28.8	30.2	31.3	32.1	32.7	33.1	33.7	34.4	34.9
	Weight, g	209	259	300	341	364	388	405	429	473	496
Depression	Length, cm	26.0	27.9	29.3	30.0	30.7	31.3	31.6	32.3	32.6	33.1
	Weight, g	180	220	261	277	300	335	345	352	358	365

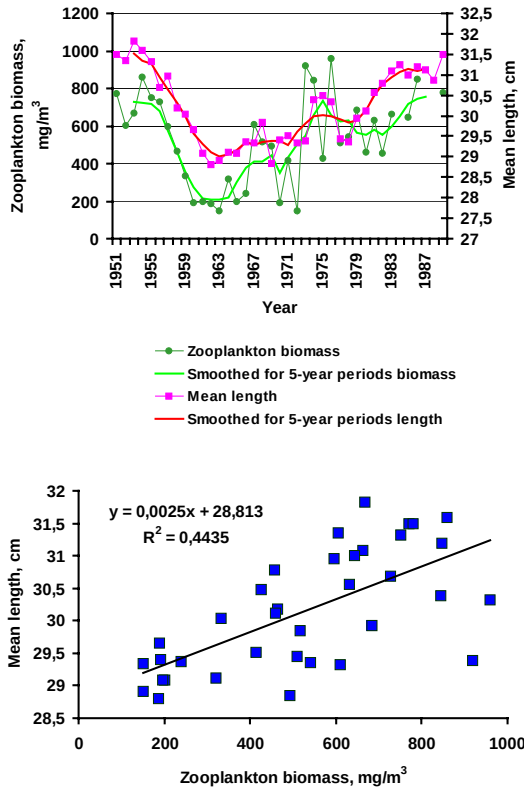

Fig. 23 Relationship between June zooplankton biomass in Olutorsk Bay and mean length of age 4-10 herring.

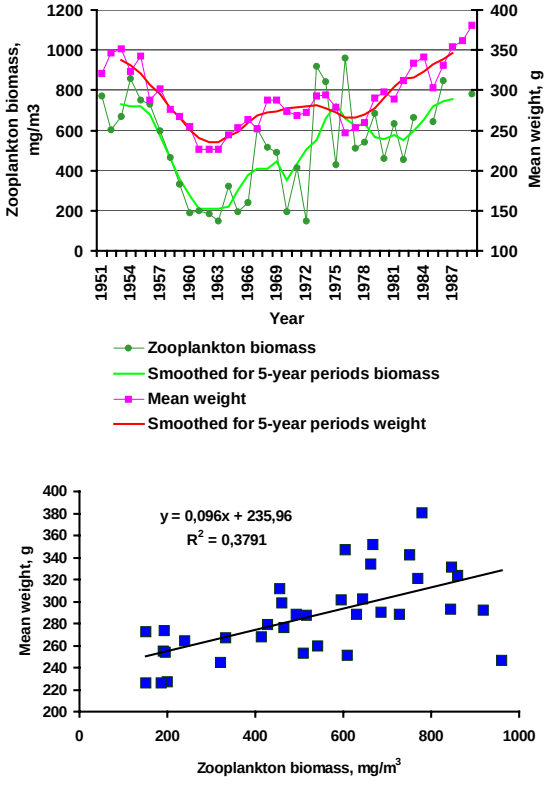

Fig. 24 Relationship between June zooplankton biomass in Olutorsk Bay and mean weight of age 4-10 herring.

low. In the 1990s the numbers have increased moderately. The size-at-age for 25 years (mid 1960s- late 1980s) has been increased gradually. To the early 1990s the size of herring has been similar to that for the 1940s. Thus, the most favorable conditions for growth of Korf-Karaginsky herring usually have been created at a moderate abundance of mature fish in the population. Under the extreme conditions (too high or too low stock abundance) individual growth has been slow.

The most important factor determining individual growth is food supply. In the 1950s - 1980s average zooplankton biomass in Olyutorsky Bay and average dimension (length and mass) of 4-10 years-old fish demonstrate synchronic variations (Fig. 23 and 24). In the periods when the biomass of zooplankton was increasing, the length and the mass of mature herring increased as well, and *vice versa*. A reliable direct correlation has been found between these patterns. The character of the correlation indicates that a zooplankton biomass increase of 100 mg/m^3 corresponds to a length increase of 2.5 mm and to the mass increase of 10 g in average in all age groups. Thus, the size-at-age variations of Korf-Karaginsky herring demonstrate cyclic dynamics. The stock abundance and forage base conditions influence the growth of fish considerably.

Effects of climate on Pacific herring, *Clupea pallasii*, in the northern Gulf of Alaska and Prince William Sound, Alaska

Evelyn D. Brown
University of Alaska Fairbanks, Institute of Marine Science, P.O. Box 757220, Fairbanks, AK 99775-7220, U.S.A. E-mail: ebrown@lms.uaf.edu

Introduction

Links between trends of North Pacific fish populations and climatic variations are well documented. One well-known example is the exceptional salmon production in the North Pacific that occurred during a period associated with an intensified Aleutian Low: high levels of salmon production are strongly correlated with the Pacific Decadal Oscillation (PDO) (Mantua *et al.* 1997), with Alaskan stocks responding positively to the positive phases of the PDO.

Pacific herring (*Clupea pallasii*) also appear to respond to climate. A negative correlation exists between southern British Columbia (BC) herring year-class strength and warm conditions; warm conditions appear to increase piscivory on herring and reduce zooplankton food resources (Ware 1992). The same negative correlation was later reported by Hollowed and Wooster (1995) with higher average recruitment for Vancouver Island herring during cool years associated with a weakened winter Aleutian Low (AL). However, the opposite effect occurred in northern BC and the Gulf of Alaska (GOA), with increased herring production during warm years associated with an intensified winter AL (Hollowed and Wooster 1995). Recruitment of Pacific herring in Southeast Alaska is positively associated with warm, wet climate conditions (Zebdi and Collie 1995). This indicates a north-south bifurcation in climate response by Pacific herring populations similar to that observed in Pacific salmon.

This study shows that the trend in abundance of northern GOA Pacific herring appears to be in phase with decadal-scale climate indices. Population parameters such as growth and spawn timing also appear to be related to climatic signals and may be in opposition to responses by Pacific herring from more southern locations.

Results

An index of GOA herring abundance was developed by combining historic fisheries catches with recent biomass estimate (Fig. 25). Herring abundances were compared to several climate indices and good, positive correlations were found for the Atmospheric Forcing Index (AFI) and Aleutian Low Pressure Index (ALPI) (Beamish

and Bouillon 1993), the Pacific Inter-Decadal Oscillation (PIDO) (Enfield and Mestas-Nunez 1999) and the winter time Pacific Decadal Oscillation (PDO) (Mantua et al. 1997). The abundance of herring in Prince William Sound over the period 1973-present was well-correlated with these indices (Fig. 26), as was the composite herring time series (from 1900-present) (Fig. 27). The common result was high population levels during the positive phases of the three indices. The positive phases correspond in general to intensification of the Aleutian Low, higher sea surface temperatures, and increased storms and wind stress in the GOA. A strong Aleutian Low causes above-average water column stability in the sub-arctic Pacific, creating conditions that optimize primary and secondary production and thus may be the mechanism involved in the positive response of zooplankton and Pacific herring, as previously hypothesized for salmon.

Herring size-at-age trends exhibited oscillatory behavior with a maximum spectral density at a period of 13 years for all ages (Fig. 28). There was no evidence of density-dependence as plots of size and biomass levels were flat for each age examined. The spectral peak was strongest in ages 3-5. The raw and smoothed (using the Hamming filter) size-at-age data was significantly correlated to peak zooplankton density lagged one year ($p < 0.05$; $r \geq 0.50$; Fig. 28). Peak and average zooplankton biomass was significantly correlated to the winter PDO lagged 3 yrs ($r = 0.52$ and 0.65

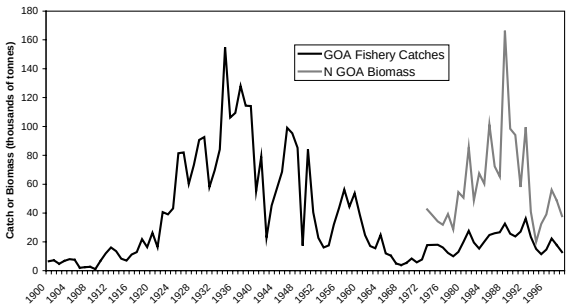

Fig. 25 The two types of fishery data used in this analysis. The solid black line is total annual Gulf of Alaska (GOA) fishery catches. The grey line represents the annual biomass estimates for Prince William Sound (see Brown and Funk for details).

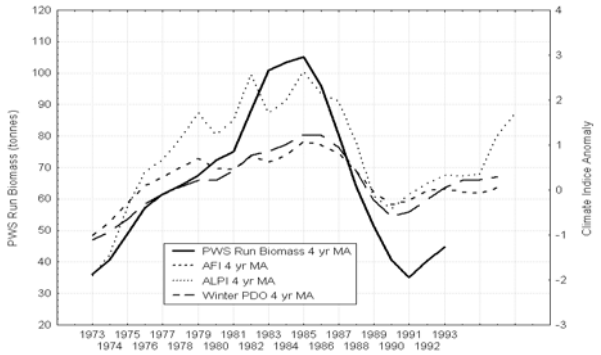

Fig. 26 A 4 year moving average (ma) transformation of the Prince William Sound (PWS) biomass index compared to the AFI, the ALPI and the winter PDO for the period of 1973 to 1993.

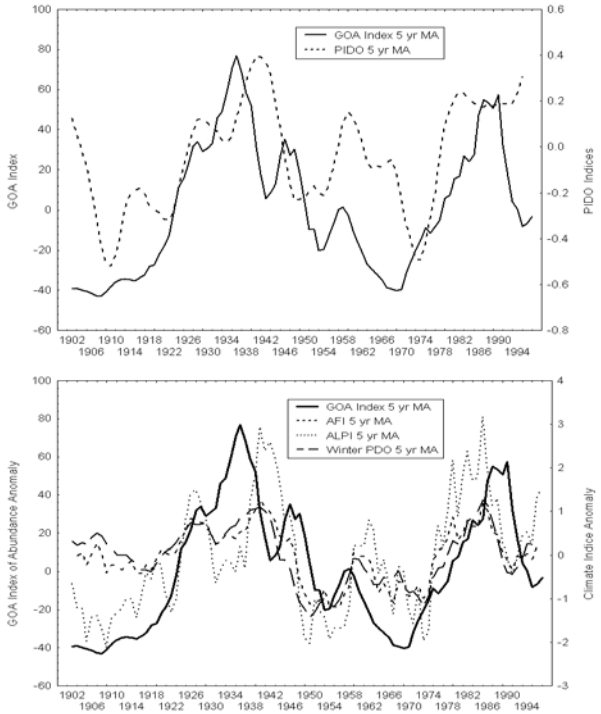

Fig. 27 A 5 year moving average (ma) transformation of the Gulf of Alaska (GOA) Index, created by combining catch and biomass, compared (upper panel) to a 5 year ma of the Pacific Inter-Decadal Oscillation and (lower panel), 5 year mas of the AFI, ALPI and winter PDO plotted for the period of 1902 to 1995.

respectively). Size-at-age for ages 7 and 8 were also significantly correlated to both the PDO lagged 3 years (r = 0.55) and the PIDO lagged 2 years (r = 0.61).

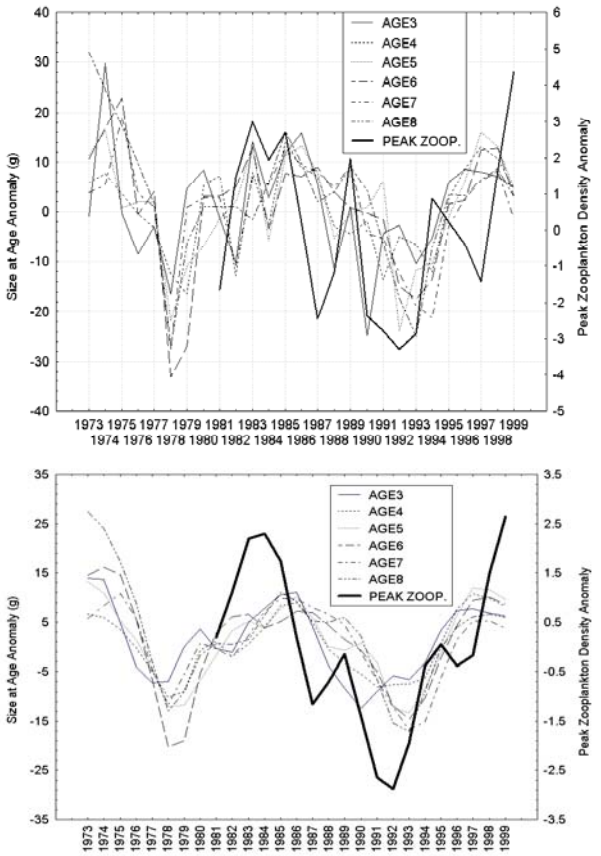

Fig. 28 Size-at-age by weight (g) of age 3-8 Pacific herring from PWS plotted with peak zooplankton density anomalies (from southwestern PWS) for the period of 1973 to 1999. The top figure are the raw values. The bottom figure shows a spectral transformation (type Hamming) of the size-at-age data plotted with a 4 year moving average transformation of the peak zooplankton anomalies.

There is an overall downward trend in spawn timing from 1973 to 1999 with mean spawn dates approximately 7 days earlier in the late 1990s than in the early 1970s (Fig. 29). Although not significantly correlated, there is a corresponding downward trend in PWS surface salinity during September and October, lagged 6 months from spawning, over the same period. There was no apparent relationship between spawn timing and either population size or climate trends. Spawn timing is affected by maturity rate that is in turn directly affected by ocean conditions, especially 6-9 months prior to spawning.

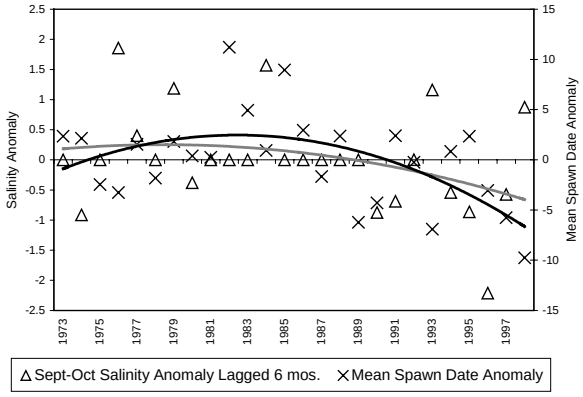

Fig. 29 Surface salinity (at 20 m) anomalies with a 6 month lag, for the combined months of September and October are plotted with the mean date of spawning anomaly for PWS for the period of 1973 to 1999. The solid lines represent 2nd order polynomial transformations of the mean spawn date (black) and salinity (grey). Note that black line is polynomial (2nd order) trend line for mean spawn date anomaly and the gray line is polynomial (2nd order) trend line for PWS Sept.-Oct. SSS anomaly

Spawning areas have also shifted over the same time period accompanied by a trend in reduced recruit per spawner rates. The implications of these observations are discussed more fully in Brown and Funk (unpublished manuscript).

References

Beamish, R.J., and Bouillon, D.R. 1993. Pacific salmon production trends in relation to climate. Can. J. Fish. Aquat. Sci. 50: 1002-1016.

Brown, E.D., and Funk, F. Effects of climate on Pacific herring, *Clupea pallasi*, in the northern Gulf of Alaska and Prince William Sound, Alaska. Unpublished manuscript available from the authors.

Enfield, D.B., and Mestas-Nuñez, A.M. 1999. Multiscale variabilities in global sea surface temperature and their relationships with tropospheric climate patterns. J. Climate 12: 2719-2733.

Hollowed, A.B., and Wooster, W.S. 1995. Decadal-scale variations in the eastern subarctic Pacific: II. Response of northeast Pacific fish stocks. Can. Spec. Publ. Fish. Aquat. Sci. 121: 373-385.

Mantua, N. J., Hare, S.R., Zhang, Y., Wallace, J.M., and Francis, R.C. 1997. A Pacific interdecadal climate oscillation with impacts on salmon production. ,Bull. Am. Meteorol. Soc. 78: 1069-1079.

Ware, D. M. 1992. Climate, predators and prey: behaviour of a linked oscillating system. *In* Kawasaki T., Tanaka S., Yoahiaki T., and Taniguchi A. (eds). Long-term variability of pelagic fish populations and their environment. Pergamon Press, Sendai, Japan, pp. 279-291.

Zebdi, A., and Collie, J. S. 1995. Effect of climate on herring (*Clupea pallasi*) population dynamics in the northeast Pacific Ocean. Can. Spec. Publ. Fish. Aquat. Sci. 121: 277-290.

Herring size-at-age variation in the North Pacific

Jake Schweigert[1], Fritz Funk[2], Ken Oda and Tom Moore[3]

[1] Fisheries and Oceans Canada, Pacific Biological Station, Nanaimo, BC, Canada. V9R 5K6 E-mail: schweigertj@pac.dfo-mpo.gc.ca

[2] Alaska Department of Fish and Game, P.O. Box 25526, Juneau, AK 99802-5526, U.S.A. E-mail: fritz_funk@fishgame.state.ak.us

[3] California Department of Fish and Game, Belmont and Bodega Bay, California, U.S.A.

Introduction

Herring have been one of the more important components of the marine fisheries on the west coast of North America over the past century. Dramatic population fluctuations are common in all stocks of herring but virtually all populations from Alaska to California declined dramatically and synchronously in the late 1960s and all have subsequently recovered. Despite the impacts of a significant harvest in most of these stocks, large scale environmental forcing appears to have been a significant factor in the observed population fluctuations. However, it is unclear what mechanisms were involved in affecting survival over such a broad geographical scale. Long time series of stock abundance estimates are not available for most of these populations. Instead, we investigated the available data on fish size and growth, reviewing trends in weight-at-age, condition factor, and growth increments of Pacific herring from Alaska to California in relation to environmental conditions or food supply to assess whether these factors may have affected herring survival in the North Pacific.

Methods

Pacific herring weight-at-age data were collated for a number of stocks in the North Pacific (Fig. 30) ranging from the Bering Sea [Togiak] through the Gulf of Alaska (Kodiak], Prince William Sound [PWS]), SE Alaska [Sitka], British Columbia (Queen Charlotte Islands [QCI], Prince Rupert [PRD], Central Coast [CC], Strait of Georgia [GS], west coast of Vancouver Island [WCVI]), and California (San Francisco Bay [SFB], Tomales Bay [TB]). Unfortunately, the available data is sparse in many cases and generally available for only limited time periods restricting the type and extent of statistical analyses possible. The time period investigated for this study ranges from 1940-2000. For some populations both length and weight at age data are available and for those we examined changes in condition factor. For all populations trends in weight at age 4 were examined as well as trends in the annual growth increment at age over time.

The condition factor was also calculated annually for each age-class in each stock following Tesch (1988), as:

$$CF_t = \frac{Weight_{at}}{Length_{at}^3}$$

Spratt (1987) has previously used similar methods to examine growth variation in San Francisco Bay herring following the strong 1982-83 El Niño.

The indices of environmental forcing that were examined included the Pacific decadal oscillation (PDO), atmospheric forcing index (AFI), the Aleutian low pressure index (ALPI), the Pacific circulation index (PCI) and the ENSO southern oscillation index (SOI). All but the last index are available from http://www.pac.dfo-mpo.gc.ca/sci/sa-mfpd/english/clm_indx1.htm. The SOI index was obtained from ftp://ftp.ncep.noaa.gov/pub/cpc/wd52dg/data/indices/soi. Information on plankton biomass is difficult to obtain since there have been few long-term efforts to collect these data. Recently, Hare and Mantua (2000) have consolidated a large number of data series for the period 1965-1997 and we have used their results in this study.

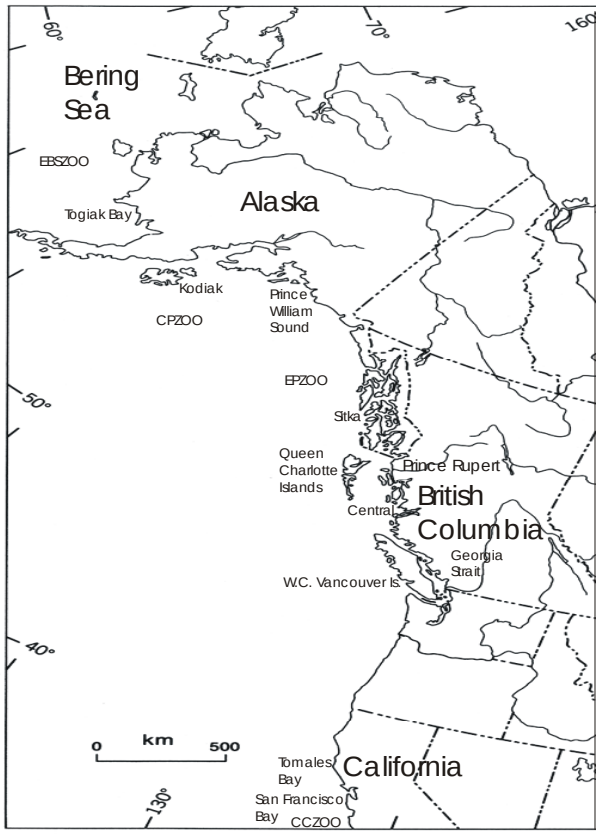

Fig. 30 Map of the study area illustrating the location of data sets for the analysis.

Results and discussion

Pacific herring generally exhibit a cline in size-at-age from south to north, with fish in the Bering Sea being far larger than fish from California. Herring also mature at later ages as one progresses from south to north. Therefore, comparison of size, condition, and growth increment becomes complicated as fish trade off growth for reproduction once they are mature. Consequently, we chose to examine trends in the average weight of fish at age 4 throughout the study area (Fig. 31). However, this is of limited utility as an index of growing conditions because it represents an integration by the fish of growing and feeding conditions over the preceding four years. Fish from the Bering Sea are much larger and demonstrate greater fluctuation in size at age 4 than herring from any of the other areas. Sitka and PWS indicate a long term decline in size since the 1940s. It should be noted that the pre-1970 data from all areas represent fall reduction fisheries whereas recent data are from spring roe fisheries and so may reflect some loss of weight by fish over the winter period. British Columbia stocks and those from Sitka show a marked increase in size at the time of the stock collapses in the early 1960s with a subsequent decline in the 1970s which may reflect a density-dependent response as the populations rebuilt. California stocks do not show evidence of any trends except for reductions in size during the 1982-83 and 1997-98 El Niño events.

The condition factor at age is presented in Figures 32 and 33. It represents an index of growing conditions for herring the previous year. However, it is possible that herring compensate for reduced food availability by growing more slowly in length while maintaining an average condition. Thus, it may not be a good indicator of growing conditions in the ocean except under extreme circumstances such as a severe El Niño which disrupted normal feeding patterns. British Columbia herring stocks do not show any marked trends in condition over time although the QCI, CC, and WCVI suggest a slight increase in condition from the 1950s through the 1990s.

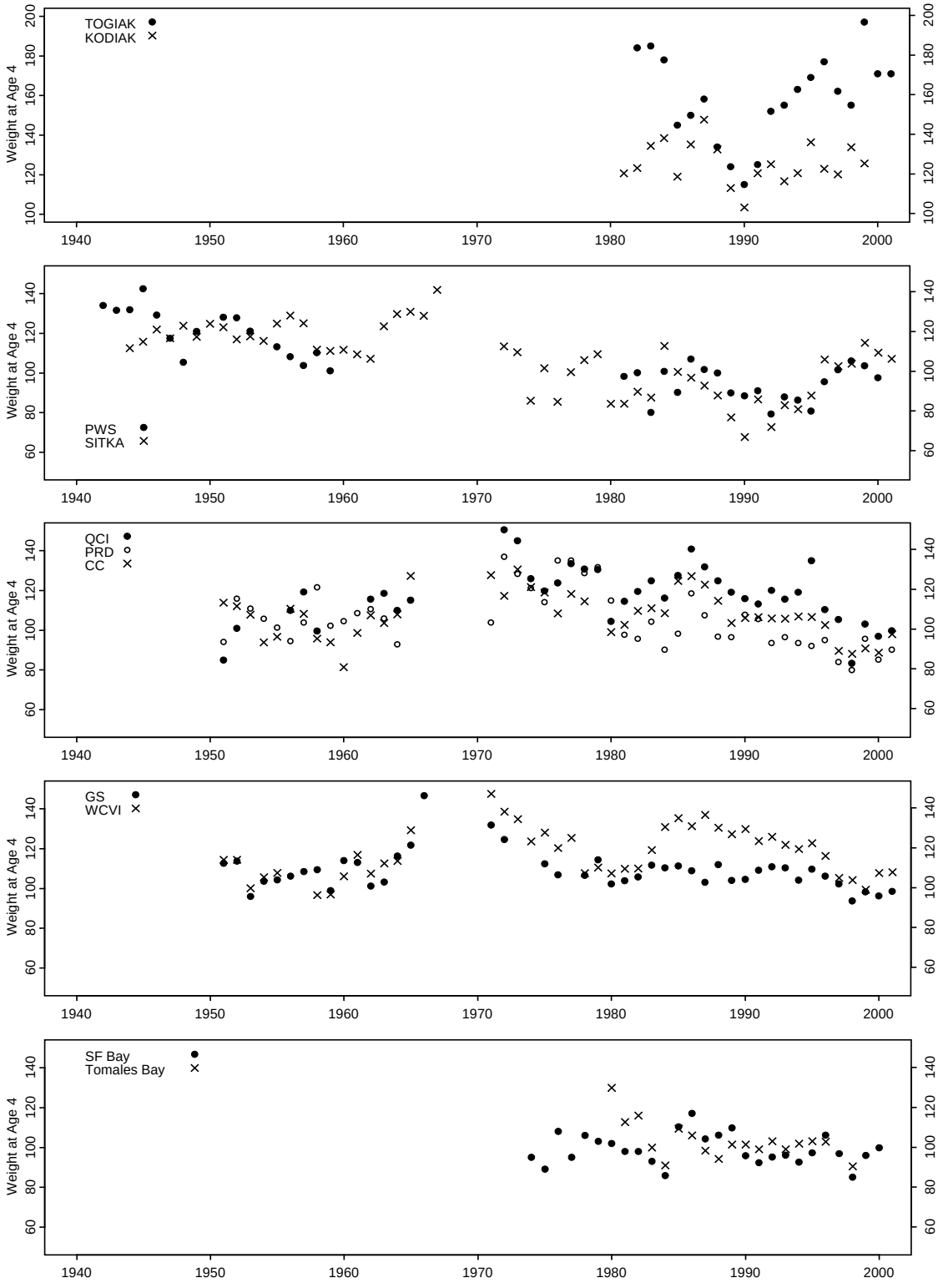

Fig. 31 Trends in weight-at-age 4 in Pacific herring from 1940-2000.

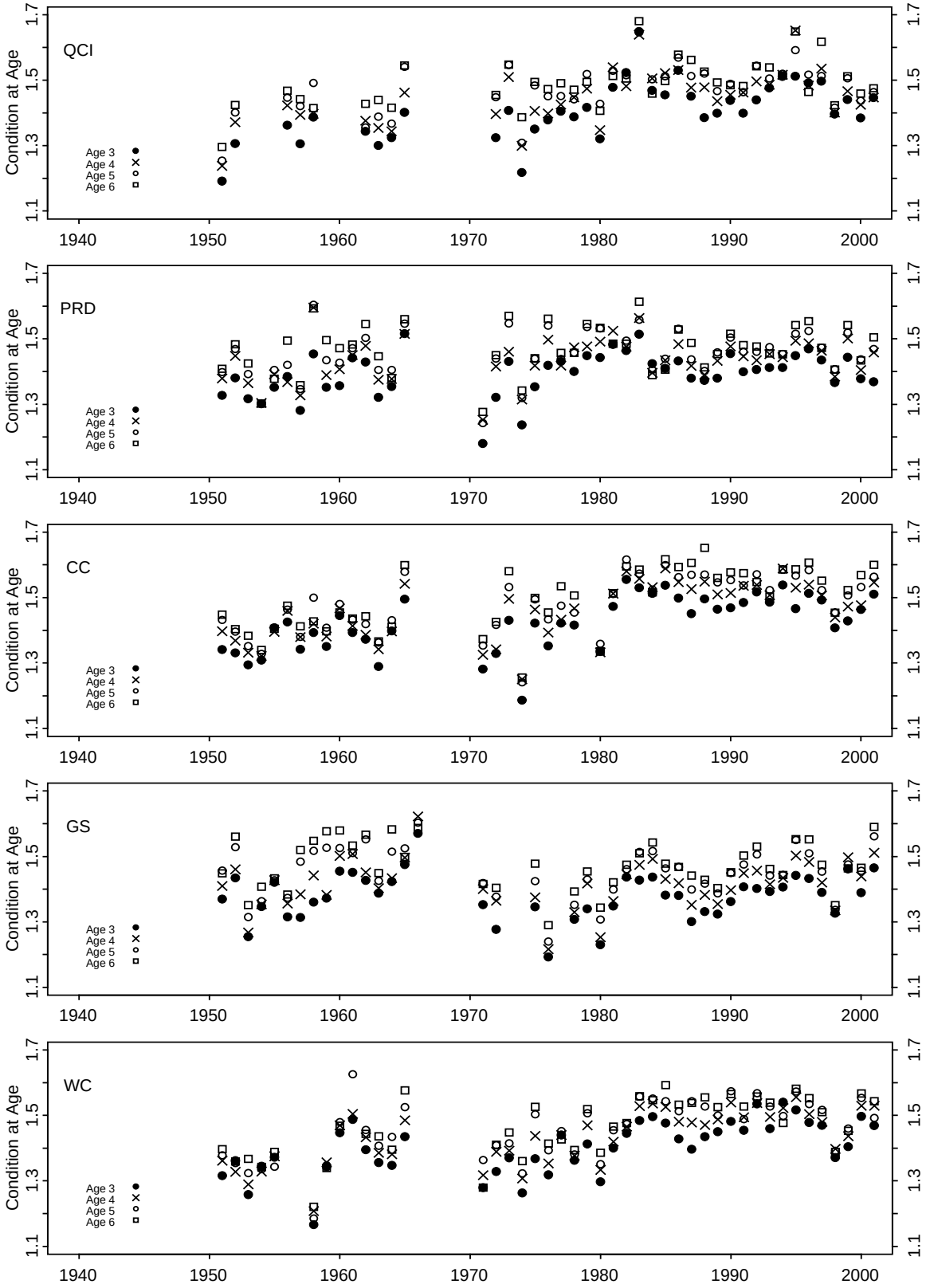

Fig. 32 Condition factor at age for British Columbia herring from 1940-2000.

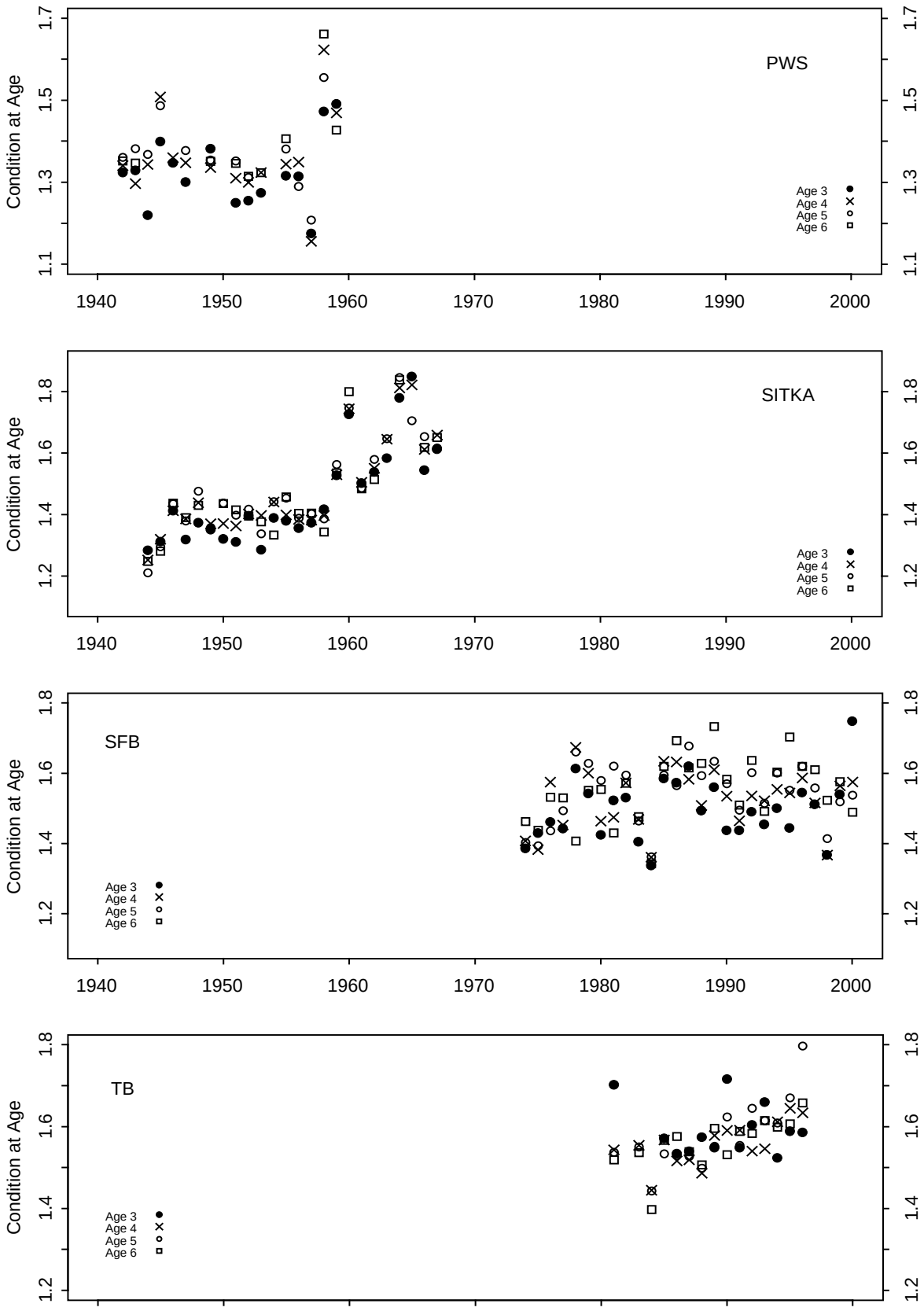

Fig. 33 Condition factor at age for Alaska and California herring from 1940-2000.

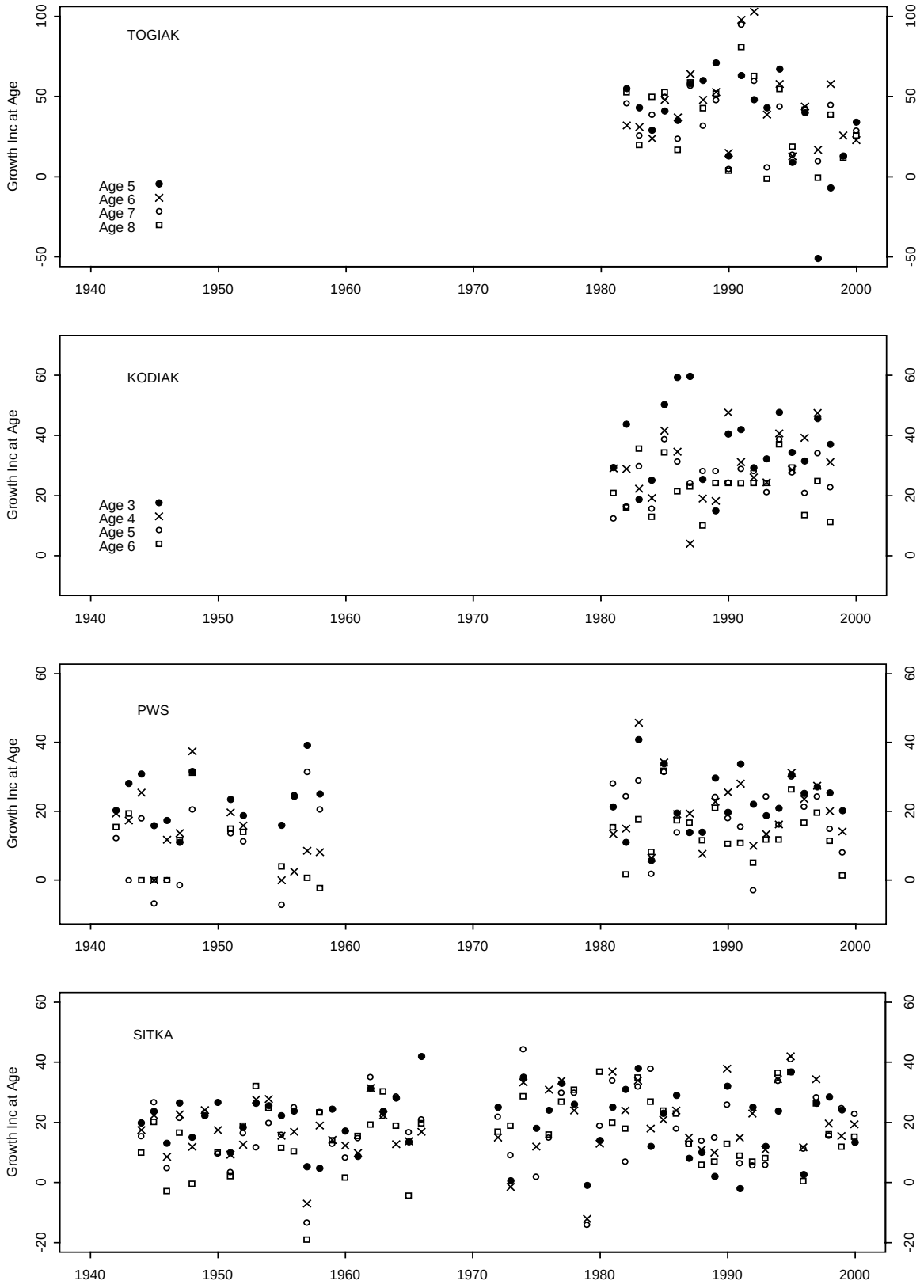

Fig. 34 Trends in the growth increment at age for Alaska herring stocks from 1940-2000.

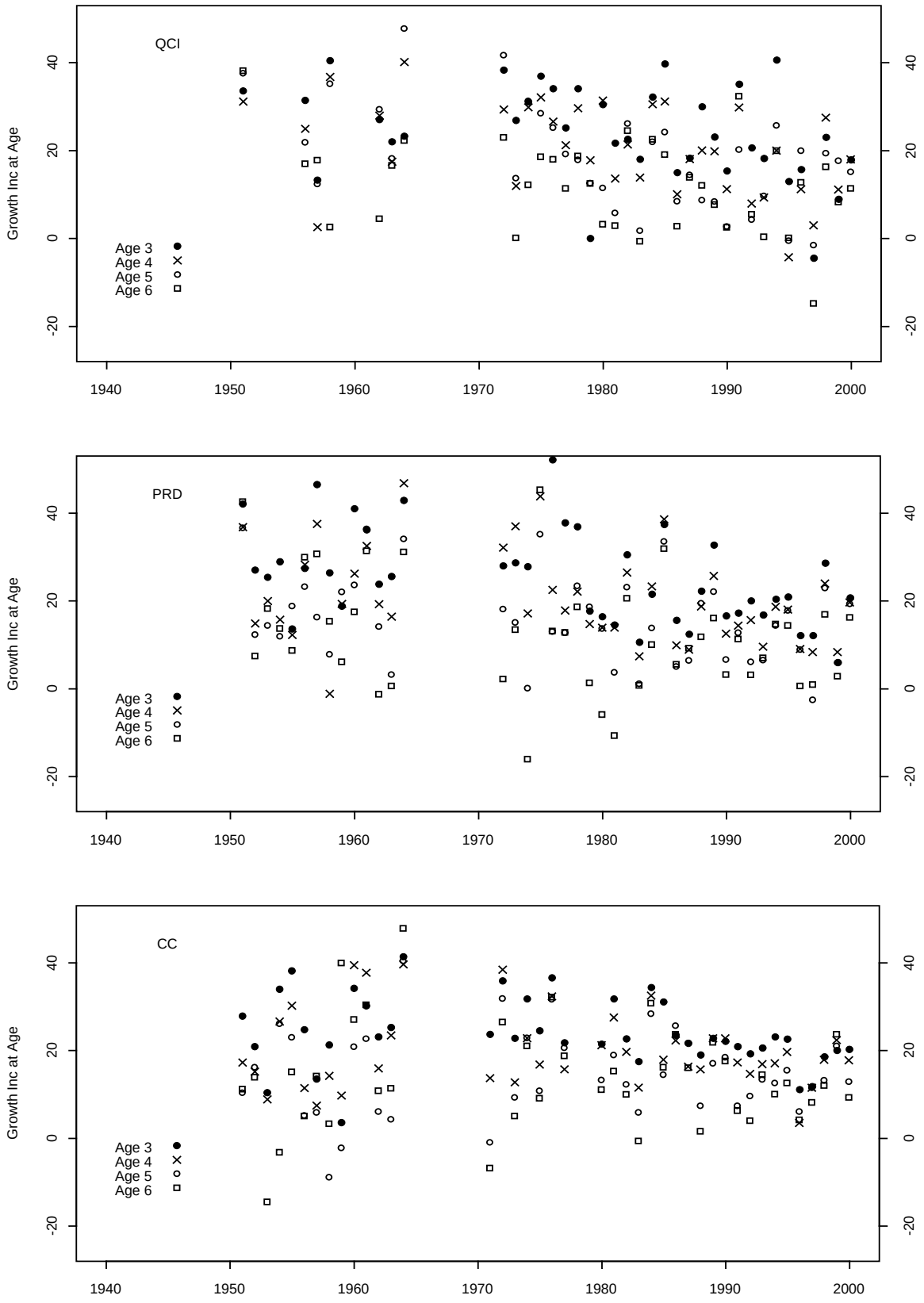

Fig. 35 Trends in growth increment at age for northern BC herring stocks from 1940-2000.

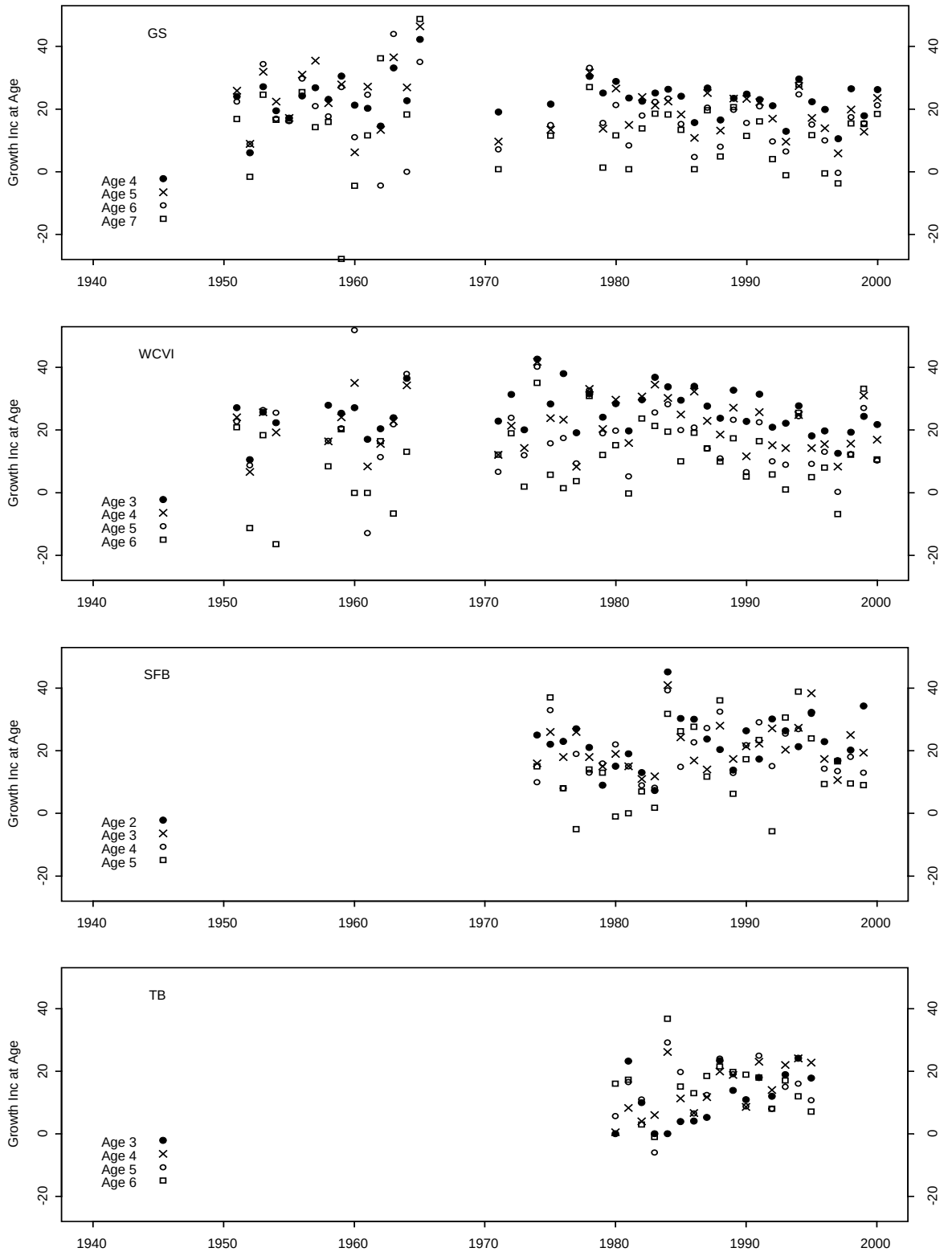

Fig. 36 Trends in the growth increment at age for southern BC and California herring stocks from 1940-2000.

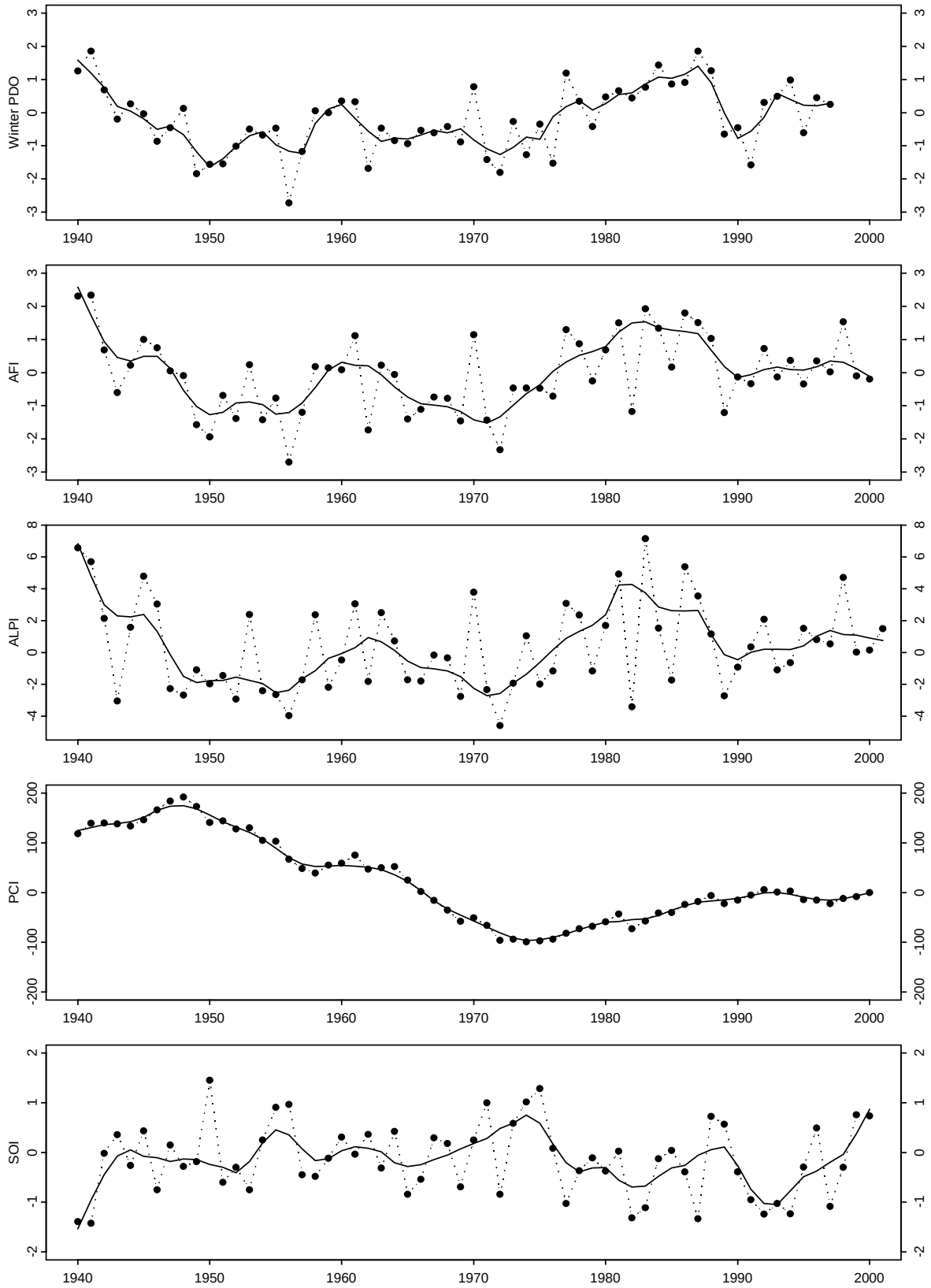

Fig. 37 Environmental indices for the North Pacific from 1940-2000.

All stocks also indicate a small decline in condition in the mid- to late 1980s and again in the late 1990s following the two strong ENSO events. Results for Alaska and California are quite variable with Sitka and PWS suggesting a marked increase in condition from the 1940s through the 1960s although this may be a function of changes in sampling locations. Both California stocks suggest a very slight increase in condition factor over time with sharp declines associated with the 1982-83 and 1997-98 ENSO events. Spratt (1987) has previously reported the strong negative effects of the 1982-83 El Niño on San Francisco Bay herring condition factor and growth.

The growth increments at age for Pacific herring stocks are presented in Figures 34-36 and are perhaps the best indicator of growing conditions in the previous year in each area. Togiak fish show the largest growth increment coastwide which includes a marked increase in the early 1990s followed by a recent decline. PWS and Sitka stocks do not demonstrate any long term trends in growth increment although there are declines in the mid-1980s and late 1990s which may correspond to El Niño effects. British Columbia stocks all show a decline in growth increment from the early 1970s through the late 1990s. They all show a marked decrease in 1997 and some in the mid-1980s. The California stocks do not indicate any clear trend in growth increment over time but both show the effects of the 1982-83 El Niño and SFB also the 1997-98 El Niño.

The environmental indices are presented in Figure 37 and demonstrate broadly similar patterns in winter PDO, AFI, and ALPI based on a lowess smoothed trend line. The PCI may be inversely related to these indices but at a different frequency since they are not quite in phase. The SOI index appears to be inversely related to the first three indices. A comparison of these indices with herring weight at age 4, condition factor, and growth increment does not indicate any strong correlation but there is the suggestion of a loose association between the trend in PDO and weight at age 4, condition, and perhaps growth increment since 1970.

Figure A9 from Hare and Mantua (2000) presents the available zooplankton data for the North Pacific and indicated a generally decreasing trend in zooplankton biomass since the 1977 regime shift (see Fig. A9 in their paper). This observation is consistent with the observed declining trend in herring growth increment in British Columbia but surprisingly not in California. It is also consistent with the trend of declining size at age 4 in British Columbia and parts of Alaska. Although not explicit in the plankton data, it is possible that changes in species composition during El Niño events are responsible for the marked decline in growth observed during these time periods so that overall plankton biomass remains relatively stable but the preferred prey items for herring decline markedly or are completely absent from the normal feeding areas.

Pacific herring populations in the eastern Pacific have experienced significant synchronous fluctuations in abundance that appear to be related to environmental forcing. We examined biological characteristics associated with changes in growth as a proxy for herring survival over the available data record. Results indicate a complex interaction between density dependent effects, food supply, and environmental variation. During the collapse of herring stocks throughout the Pacific in the late 1960s growth of herring increased dramatically, declining again as stock rebuilt. During the period from 1977 to present growth characteristics of many stocks in British Columbia and Alaska have shown a decline which is apparently a result of declining food availability. Plankton availability is most probably driven by changing environmental conditions that have at least recently not been favourable for herring growth in British Columbia and southern Alaska. Superimposed on these relationships are the recent strong ENSO episodes which have negatively impacted herring growth through the area of their effect. Overall, there appear to be threshold effects related to population density, ocean production and plankton availability, and sea surface temperature mediated by ENSO that affect the growth parameters of herring populations throughout the North Pacific. Future studies should be directed at defining the thresholds and their effects on long-term herring production.

References

Hare, S.R., and Mantua, N.J. 2000. Empirical evidence for North Pacific regime shifts in 1977 and 1989. Prog. Oceanography 47: 103-145.

Spratt, J.D. 1987. Variation in the growth rate of Pacific herring from San Francisco Bay, California. Calif. Fish and Game 73: 132-138.

Tesch, F.W. 1988. Age and Growth. *In* W.E. Ricker [ed.] Methods of assessment of fish production in fresh waters'. IBP Handbook No. 3. Blackwell Scientific Publications, Oxford, pp. 93-123.

Implications of variation in euphausiid productivity for the growth, production and resilience of Pacific herring (*Clupea pallasi*) from the southwest coast of Vancouver Island

Ron W. Tanasichuk
Pacific Biological Station, 3190 Hammond Bay Road, Nanaimo, B.C. Canada. V9R 5K6. E-mail: tanasichukr@pac.dfo-mpo.gc.ca

This presentation includes the results of a number of studies which collectively suggest that the recent order of magnitude reduction in euphausiid production along the southwest coast of Vancouver Island depressed the productivity and resilience of the West Coast Vancouver Island (WCVI) herring (*Clupea pallasi*) population.

We have been studying the oceanography of the southwest coast of Vancouver Island since 1985 to learn how the ocean affects fish productivity there. Results of diet analyses show that euphausiids are the dominant prey of the more abundant pelagic fish species and that herring feed on them exclusively. We have also been monitoring the species and size composition of prey. Tanasichuk (1999) showed that Pacific hake (*Merluccius productus*), the dominant planktivore, selects larger (>17 mm) euphausiids of one species (*Thysanoessa spinifera*) regardless of how euphausiid biomass varies. WCVI herring select the same prey. Euphausiid population biology and productivity along the WCVI have been monitored since 1991 (Tanasichuk 1998). Figure 38 shows that herring and hake prey biomass has varied by an order of magnitude over the last 10 years. The same degree of prey variation has also occurred for coho salmon (*Oncorhynchus kisutch*).

The effect on herring productivity and resilience appears to operate through influencing growth. Tanasichuk (1997) examined the effect of variations in year-class strength and oceanographic conditions on the size of recruit herring and the growth rates of adult fish. At that time, data were available to 1996 only. He suggested that the 1993 year-class was an outlier because this year-class was the first to be subjected to low *T. spinifera* biomass over its first three years of life. All subsequent year-classes have been outliers, over a period when *T. spinifera* biomass remained depressed (Fig. 39). This dataset suggests that the compensatory population-

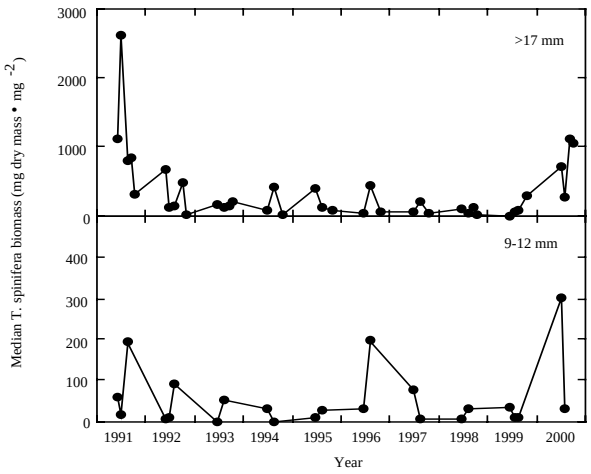

Fig. 38 Median biomass (mg dry mass/mg^2) of key prey for Pacific herring and Pacific hake (>17 mm *T. spinifera*) and coho salmon (9-12 mm *T. spinifera*) over the summer feeding period.

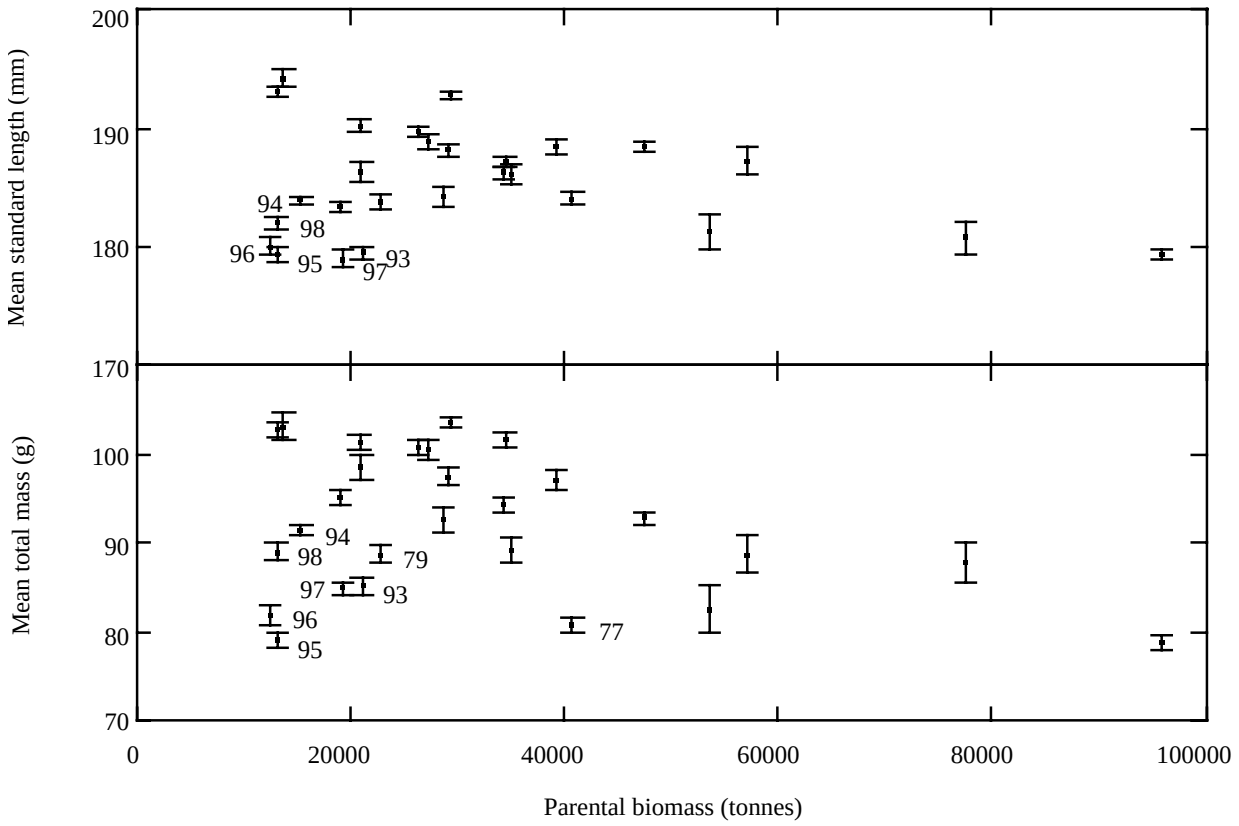

Fig. 39 Scatterplot of mean standard length- and total mass-at-age 3 for WCVI herring. Error bars are 95% confidence limits. Plot labels indicate year-class.

regulating mechanism of density-dependent recruit size has been disrupted by low euphausiid biomasses since 1993. Tanasichuk (1997) concluded that adult growth rates were influenced mainly by size at the beginning of the growth period. Because adult growth rates are affected mostly be initial size, the effect of low euphausiid biomass would persist over the entire life of the year-class. It appears that mortality and size-specific surplus energy allocation to ovarian production have not varied. Tanasichuk (2000) reported that age-specific natural mortality rates of adult herring vary as a function of age alone. Unpublished results showed that there has been no inter-annual variability in mass-specific ripe ovarian mass.

Growth suppression had a large effect on ovarian (=egg) production, and presumably resilience, that is the population's potential to increase or sustain biomass through recruitment. We calculated ovarian production for all ages for each year since 1982, when Fisheries and Oceans Canada started measuring ovarian mass. Annual estimates of observed mean mass-at-age were used to calculate ovarian production; this includes the observed mass-at-age over the time when growth appeared to be suppressed. "Non-suppressed" mass-at-age 3 was then estimated using the regression in Tanasichuk (1997) which describes recruit mass as a function of parental biomass. These estimates of recruit mass, and the regressions describing variations in adult growth rates in mass, were used to estimate what the mass of older fish of a year-class should have been in subsequent years. Figure 40 shows the effect of small recruit size on growth in subsequent years. Figure 41 demonstrates the effect on reduced growth on ovarian production. It would have been reduced by 20% as a consequence of growth suppression of recruit fish and its effect of subsequent adult size. However, after considering further that reduced egg production in 1996-98 could have reduced the number of spawners produced by these year-

classes, the suppression of reproduction could have become compounded. Calculations showed that egg production would have consequently been reduced by 40%, presumably a 40% reduction in resilience, in other words a 40% reduction in potential recruitment.

These results have implications for evaluating growth in herring and the concept of the pre-cautionary approach. Recruit size and subsequent adult growth are affected by year-class strength and food availability during the pre-recruit phase. We show an effect of food which complicates the interpretation of size-at-age trends. The precautionary approach (target- and limit reference points) implicitly assumes that fish population productivity and the ability to re-build are constant over time. These results show that assumption is invalid.

References

Tanasichuk, R. W. 1997. Influence of biomass and ocean climate on the growth of Pacific herring (*Clupea pallasi*) from the southwest coast of Vancouver Island. Can. J. Fish. Aquat. Sci. 54: 2782-2788.

Tanasichuk, R. W. 1998. Interannual variations in the population biology and productivity of the euphausiid *Thysanoessa spinifera* in Barkley Sound, Canada, with special reference to the 1992 and 1993 warm ocean years. Mar. Ecol. Prog. Ser. 173: 163-180.

Tanasichuk, R. W. 1999. Interannual variation in the availability of euphausiids as prey for Pacific hake (*Merluccius productus*) along the southwest coast of Vancouver Island. Fish. Oceanogr. 8: 150-156.

Tanasichuk, R. W. 2000. Age-specific natural mortality rates of adult Pacific herring (*Clupea pallasi*) from southern British Columbia. Can. J. Fish. Aquat. Sci. 57: 2258-2266.

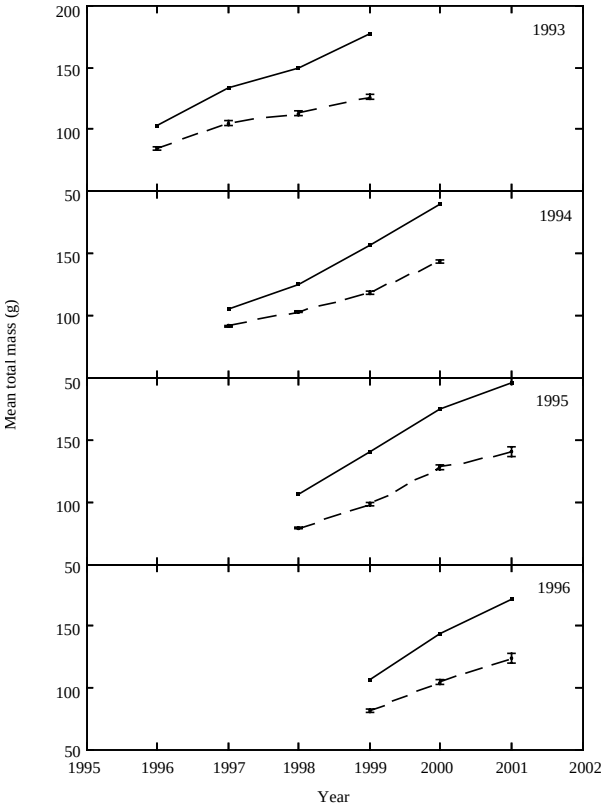

Fig. 40 Mass-at-age trajectories for WCVI herring. Dotted line – observed. Solid line - estimates from growth regressions in Tanasichuk (1997). Error bars are 95% confidence limits. Year-class is indicated in the upper right of each panel.

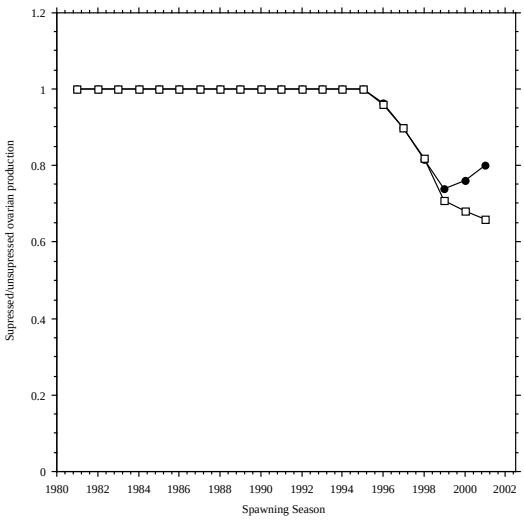

Fig. 41 Suppression of ovarian production due to growth (solid circle) and growth plus recruitment depression (open square).

Changes in growth with fluctuation of chub mackerel abundance in the Pacific waters off central Japan from 1970 to 1997

Chikako Watanabe[1], Akihiko Yatsu[1] and Yoshiro Watanabe[2]

[1] National Research Institute of Fisheries Science, 2-12-4 Fukuura, Kanazawa-ku, Yokohama, Japan 236-8648. E-mail: falconer@nrifs.affrc.go.jp; E-mail: yatsua@affrc.go.jp

[2] Ocean Research Institute, Tokyo University, 1-15-1Minamidai, Nakano-ku, Tokyo, Japan 164-8639. E-mail: ywatanab@ori.u-tokyo.ac.jp

Introduction

Changes in growth as stock size fluctuates have been found in many fish populations. Size-at-age of Japanese sardine (*Sardinops melanostictus*) has varied remarkably with the stock fluctuations from the late 1970s to the early 1990s (Wada 1989, Hiyama 1989, Wada *et al.* 1995); these have been considered to be density-dependent change in fish size.

Chub mackerel (*Scomber japonicus*) are one of the most important fish populations in Japanese waters. Two stocks are recognized, the Tsushima Current stock and the Pacific stock. The Tsushima Current stock is distributed in the East China Sea and the Sea of Japan, and the Pacific stock occurs along the Pacific coast of Japan. The biomass of the Pacific stock is larger and more variable than that of the Tsushima Current stock. Most of the catch of the Pacific stock is from the purse seine fishery in the waters off central and northern Japan. The Pacific stock spawns from March to June around the Izu islands off central Japan. Juveniles of about 6 months of age recruit to purse seine and set net fisheries from August or September in the coastal area off northeastern Japan.

The landings of the Pacific stock increased from the 1960s, to a maximum of 1.5 million tons in 1978, and then declined to 23 thousand tons in 1990 (Fig. 42). Recently, good year-classes occurred in 1992 and 1996 (Fig. 42), but most of these cohorts were exploited before first maturation, and therefore spawning stock did not recover and total biomass stayed low. With the drastic stock level fluctuations, size-at-age and maturity-at-age of the Pacific stock changed (Iizuka 1974, Chiba 1995). This study describes long-term changes in stock size and size-at-age of the Pacific chub mackerel stock and investigates the relationship between stock size and year-class abundance.

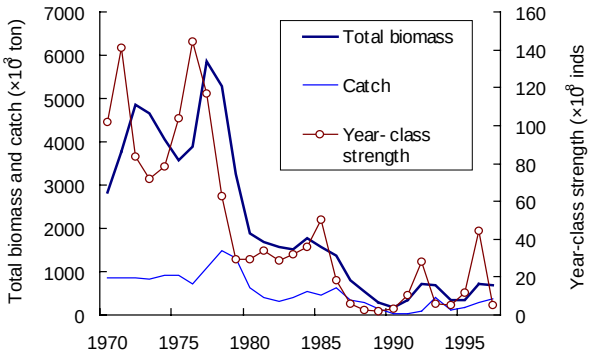

Fig. 42 Total biomass, catch and year-class strength of the Pacific stock of chub mackerel (*Scomber japonicus*). Total biomass and year-class strength were estimated by VPA.

Materials and methods

Data. Length composition and age-length keys for 1970-1997 were used to calculate mean length-at-age for each year. The length composition data of purse seine catches from September to December were used because total catches in these months were usually largest during the year. Scales were used for age determination. Length compositions of fish samples were applied to length compositions of total catches. Length compositions of total catches were divided into age groups from 0 (6 months old) to 5 years based on age-length keys. Mean fork length was calculated from length compositions of total catches for each age. Total biomass was represented by sum of VPA (virtual populations analysis) estimated biomass of chub mackerel from age 0 to age 6+. Year-class strength was represented by abundance in number at age 0.

Statistical analysis. ANOVA was used to determine if the mean length-at-ages 0 to 5 were significantly different among years. Regression analysis was applied to examine the relationships between mean length-at-age and total biomass and year-class strength.

Result and discussion

Mean length-at-age fluctuated greatly, especially at age 0 and 1, ranging from 164-259 mm at age 0 and 242-316 mm at age 1. While the biomass of chub mackerel decreased from the 1970s to the 1990s, mean lengths-at-age increased. Figure 43 shows the relationship between the total biomass and the mean length at age 0 among years. Regression analyses indicated significant negative relationships between the total biomass and the mean fork length-at-age of a year (Table 8, $p<0.05$). The biomass variations explained 19-36% of the inter-annual fluctuation of length-at-age.

Figure 44 demonstrates the relationship between the year-class strength and the mean length-at-age 0. Mean length-at-age of each year-class was negatively correlated with the year-class strength (Table 9, $p<0.01$). The variability in year-class strength explained 25-63% of the fluctuation of length-at-age.

The deviations of the mean fork length of a year-class from the mean of the 28-year time series (1970 to 1997) were calculated for several ages. Figure 45 shows the relationships between deviation at age 0 versus deviation at age 1 and the deviation at age 0 versus deviation at age 4. Regression analysis suggested significantly positive relationships between deviations at age 0 and ages 1 to 5, and between the deviations at age 1 and ages 2 to 5 (Table 10), indicating that the trend of length-at-age 0 is consistent through the life time (until 5 years old).

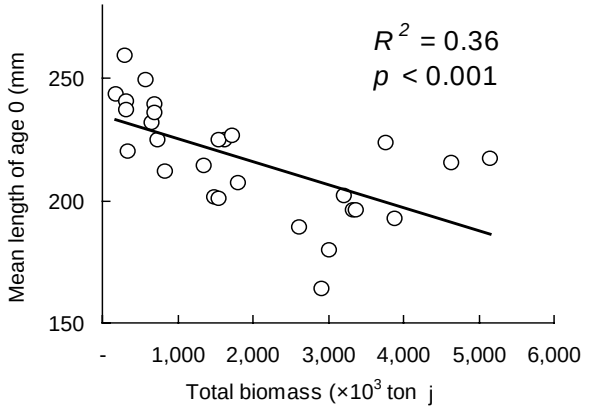

Fig. 43 Relationship between the total biomass and the length at age 0 of *Scomber japonicus*.

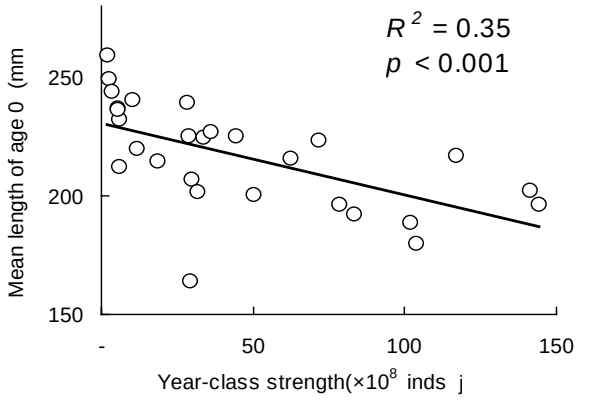

Fig. 44 Relationship between the year-class strength and the length-at-age 0 of *Scomber japonicus.*

Table 8 Statistics from regression of mean length-at-age of chub mackerel *vs*. biomass.

age	df	R	R^2	p
0	27	-0.60	0.36	0.001
1	27	-0.48	0.23	0.010
2	27	-0.53	0.28	0.004
3	27	-0.44	0.19	0.019
4	26	-0.47	0.22	0.013
5	26	-0.45	0.20	0.018

Table 9 Statistics from regression of mean length-at-age of each year-class *vs*. recruitment.

age	df	R	R^2	p
0	27	-0.59	0.35	0.001
1	27	-0.47	0.25	0.007
2	26	-0.60	0.34	0.001
3	25	-0.67	0.46	0.000
4	24	-0.80	0.63	0.000
5	23	-0.67	0.48	0.000

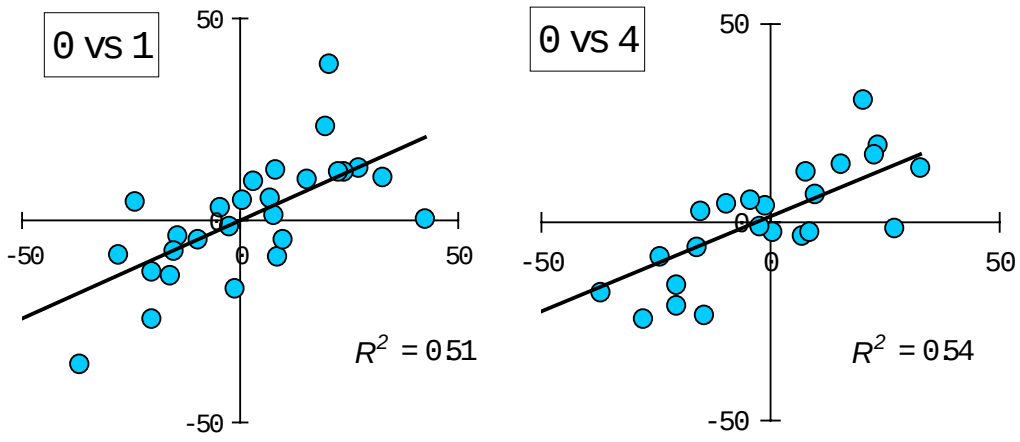

Fig. 45 Relationships between the annual mean length deviation at age 0 and age 1 (left), and between the annual mean length deviation at age 0 and age 4 (right).

Table 10 Statistics from regressions of annual mean length deviations at age 0 versus age 1 to 5 and deviations at age 1 versus age 2 to 5.

	age	R	R^2	p
0	1	0.71	0.52	0.001
	2	0.54	030	0.003
	3	0.54	0.29	0.005
	4	0.73	0.54	0.000
	5	0.53	0.28	0.009
1	2	0.67	0.44	0.000
	3	0.54	0.29	0.005
	4	0.71	0.50	0.000
	5	0.54	0.29	0.007

Our data confirmed that the trend in length of a year-class was determined during the first summer of life and maintained throughout the life span. These results are in agreement with Iizuka (1974), who reported on the growth of 1963-1973 year-classes of the Pacific stock of chub mackerel and found that the trend of growth at age 0 was maintained at least until age 2.

In this study, we investigated the effect of mackerel biomass and/or year-class strength on the mean length-at-age. Year-class strength significantly affected size-at-age of chub mackerel, but it only explained 25-63% of the fluctuations in the mean length-at-age. Other factors such as abiotic and/or biotic environment, sardine and spotted mackerel stocks may also influence the growth of chub mackerel.

References

Chiba. 1995. Shizuoka, Kanagawa Prefectural Fisheries Research Stations, Tokyo.

Hiyama, Y. 1998. Ecological changes in adults. 4. Migration range and growth rate in the Tsushima Current area. *In* Y. Watanabe and T. Wada [eds]. Stock fluctuations and ecological changes of the Japanese sardine. Tokyo, pp. 35-44.

Iizuka, K. 1974. The ecology of young mackerel in the north-eastern Sea of Japan: Estimation of the population size of the 0-age group and the tendencies of growth patterns on 0-age groups. Bull. Tohoku Reg. Fish. Res. Lab. 34: 1-16.

Overholts, W.J. 1989. Density-dependent growth in the Northwest Atlantic stock of Atlantic mackerel (*Scomber scomburus*). J. Northw. Atl. Fish. Sci. 9: 115-121.

Wada, T., Matsubara, Y., Matsumiya, Y., and Koizumi, N. 1995. Influence of environment on stock fluctuations of Japanese sardine, *Sardinops melanostictus*. Can. Spec. Publ. Fish. Aquat. Sci. 121: 387-394.

Wada, T. 1998. 3. Migration range and growth rate in the Oyashio area. *In* Y. Watanabe and T. Wada [eds]. Stock fluctuations and ecological changes of the Japanese sardine. Tokyo, pp. 27-34.

Inter-decadal fluctuations in length-at-age of Hokkaido-Sakhalin herring and Japanese sardine in the Sea of Japan

Yoshiro Watanabe[1], Yoshiaki Hiyama[2], Chikako Watanabe[3] and ShiroTakayana[4]

[1] Ocean Research Institute, Tokyo University, 1-15-1Minamidai, Nakano-ku, Tokyo, Japan 164-8639. E-mail: ywatanab@ori.u-tokyo.ac.jp

[2] Seikai National Fisheries Research Institute, Nagasaki 850-0951, Japan.

[3] National Research Institute of Fisheries Science, 2-12-4 Fukuura, Kanazawa-ku, Yokohama, Japan 236-8648. E-mail: falconer@nrifs.affrc.go.jp

[4] Hokkaido Prefectural Fisheries Experimental Station, Yoichi 012-3876, Japan.

Introduction

The total catch of Hokkaido spring herring (*Clupea pallasii*) in Japan peaked at 972 thousand tons in 1897 and tended to decline thereafter with steep peaks and deep troughs (Fig. 46). Spawning occurred from February to May along the coasts of northern Japan and southern Sakhalin, within the Sea of Japan and partly in the Sea of Okhotsk. With the decline of the population, spawning retreated to the north and finally disappeared from the coasts of Hokkaido in the middle 1950s (Morita 1985). After that the catches were from the local populations distributed in the coastal waters off northern Japan.

The Tsushima Current subpopulation of Japanese sardine (*Sardinops melanostictus*) in the East China Sea and the Sea of Japan experienced a peak in the late 1980s, similar to the Pacific subpopulation of these species (Watanabe *et al.* 1995). Total catch of the subpopulation first exceeded 1 million tons in 1984, maintained at this level until 1992, then rapidly declined to 33 thousand tons in 1998 (Fig. 47).

Size-at-age of these two clupeid fishes varied through the years of the large population fluctuations. In this paper we describe inter-decadal variability in size-at-age of both species and examine correlations between size-at-age and population size.

Materials and methods

Hokkaido spring herring mature at age 3 and start migrating to the spawning grounds along the west coast of Hokkaido (Hanamura 1963). Ages of about 4000 individual fishes per year caught in this area were determined from scales after 1910. Mean total length-at-age (TL) was calculated based on number of fish by ages and by 5 mm TL intervals (Kitahama, 1955). Time series of catch-at-age 3 and older fish from 1910-1960 reported by Hanamura (1963). We used this data for estimating total number of fish at age 3 and older from 1910-1950 by VPA (virtual population analysis).

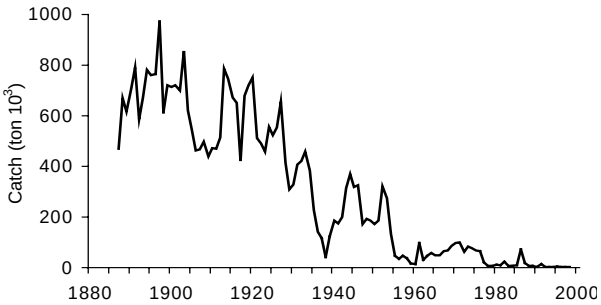

Fig. 46 Total catch of Hokkaido spring herring (*Clupea pallasii*) in Japan. Data for 1887-1911 are from Hanamura (1963); after 1911 - from Catch Statistics.

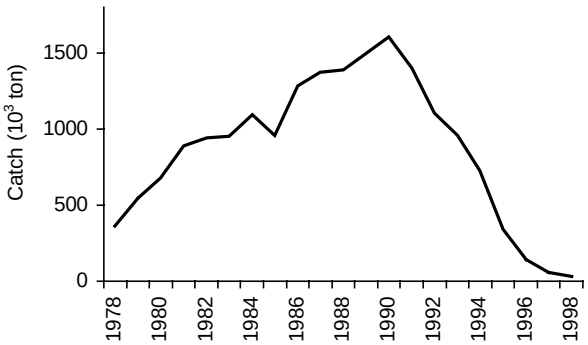

Fig. 47 Total catch of the Tsushima Current subpopulation of Japanese sardine (*Sardinops melanostictus*) from 1978-1998.

Data on catch-at-age and size-at-age of Japanese sardine caught by the Japanese purse seine fishery in the East China Sea and the Sea of Japan have been compiled since 1978. Total numbers of fish-at-age were estimated each year by VPA.

Results

Clupea pallasii. VPA estimates of spawner abundance (>3 years) of Hokkaido spring herring fluctuated greatly with a maximum of 19.6 billion fishes in 1924 and minimum of 0.4 billion in 1937. Total catch in number ranged from 3.0-0.04 billion fishes. The exploitation rate was estimated to be <30% with exceptions in the middle 1930s and the late 1940-early 1950s. Year-class population at age 4 varied greatly from 1907-1947 (Fig. 48). Dominant year-classes (>5.0 billion in number at age 4) occurred 6 times in 1909, 1911, 1915, 1921, 1926 and 1939. The maximum was 9.9 billion fishes in 1921, and minimum was 0.029 billion in 1933, about a 2.5 order of magnitude difference.

We calculated deviations (%) of the mean TL at age 3 year and older for each year-class from the 40-year mean (Fig. 49). The coefficients of determination (R^2) are summarized in Table 11. The deviations-at-age are positively correlated. The coefficients between age 3 *vs* 5 and 3 *vs* 7 were small compared with those between age 4 *vs* 6 or 4 *vs* 8. Correlations of 4 year and older ages with age 3 were not statistically significant, but those of 5 year and older ages with age 4 were highly significant. This implies that the TL trends of year-classes were fixed by age 4 at the latest. The mean TL at age 3 did not represent TL trend of a year-class. Total catches in number at age 3 accounted for about 60% of those at age 4 in the 40 year-classes. Only a limited proportion of age 3 fish migrated to the coastal spawning grounds.

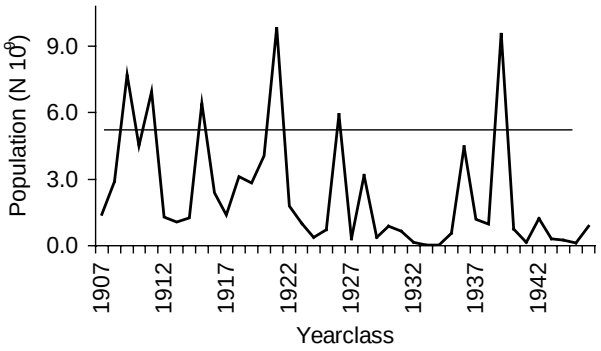

Fig. 48 Variability in year-class population at age 4 of Hokkaido spring herring.

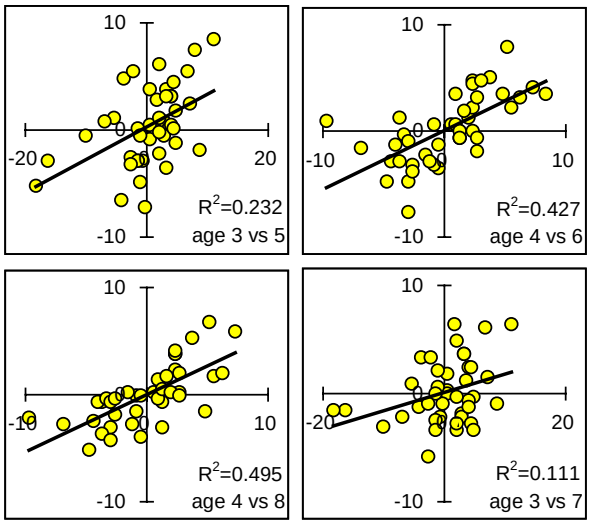

Fig. 49 Correlations of deviations (from the 40-year mean) of the mean TL-at-age in each year-class of Hokkaido spring herring.

Table 11 Coefficients of determination of TL deviations from the 40-year mean across ages (* P<0.01, ** P<0.001).

	Age 4	Age 5	Age 6	Age 7	Age 8	Age 9
Age 3	0.323	0.232	0.127	0.111	0.103	0.068
Age 4		**0.747	**0.427	**0.465	**0.495	**0.531
Age 5			**0.573	**0.431	**0.573	**0.533
Age 6				**0.509	**0.559	*0.505
Age 7					**0.601	*0.457

TL-at-age 4 varied from 25.5 in 1925 to 30.3 in 1944 with the average of 28.2±1.0 cm (Fig. 50). TL was not necessarily smaller than the long-term mean for the 6 dominant year-classes. It tended to be larger than the mean in the early 1910s, smaller in the 1920s, and recovered in the early 1930s. A similar TL trend was found at age 5 (40 year mean was 30.0 cm).

TL-at-age 4 was not correlated with the year-class size in number at age 4. The coefficient of determination was 0.068, indicating that only a small amount of the TL variability was explained by year-class strength (Fig. 51).

TL-at-age 4 was correlated significantly ($P < 0.05$) with the mean spawning population in years when a given year-class was at age 1 to 4. About 17% of the inter-annual variability in the mean TL of year-classes at age 4 could be explained by the size of the spawning population (R^2=0.165). The variability in size-at-age of the herring inhabiting the Sea of Japan and Sea of Okhotsk is considered to be determined in a density independent manner.

Sardinops melanostictus. For Japanese sardine, year-class abundance at age 2 varied greatly during the 20 year study from 1976-1996 (Fig. 52). The population was <20 billion fishes in the 1970s. Strong year-classes (>30 billion) occurred consecutively in 1980-82 and 1984-87. Abundance reduced dramatically in 1988 year-class and further declined to 1995. The maximum and minimum year-class strengths were 77.3 and 1.4 billion in number at age 2, about a 1.7 order of magnitude difference. Strong year-classes >50 billion occurred consecutively in the 1980s. Deviations (%) of the mean TL at age 3 of year-classes from the 20-year mean were correlated with those at age 2, but not with age 1 (Fig. 53). The inter-annual trend in TL-at-age of each were fixed by age 2 at the latest in sardine. Age 1 sardines of the Tsushima Current subpopulation are not fully recruited to the Japanese purse seine fishery and do not represent size-at-age or strength of the year-classes.

Body length (BL) at age 2 of the sardine was >180 mm in the 1970s. It remarkably declined to 169 mm in 1980 and remained smaller than 170 mm until 1988. Then BL recovered to the 1970s level of around 180 mm (Fig. 54). Similar BL trend was found in size-at-age 3. The interannual fluctuation in BL corresponded inversely with the fluctuation in year-class size (Fig. 54).

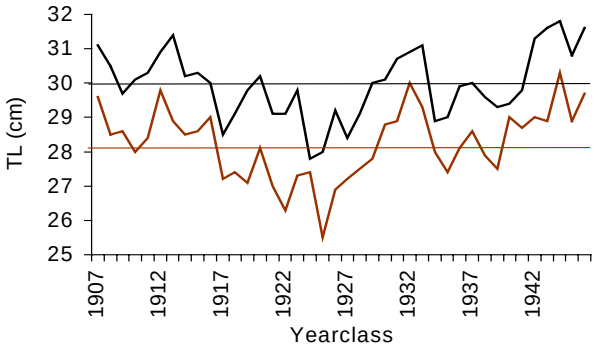

Fig. 50 Inter-decadal variations in TL-at-age 4 and age 5 of Hokkaido spring herring.

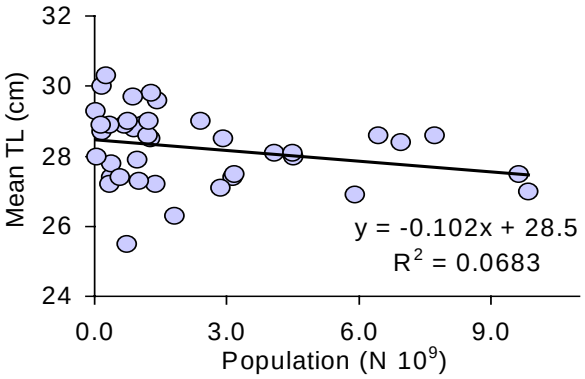

Fig. 51 Relationship between TL and year-classes size at age 4 of Hokkaido spring herring.

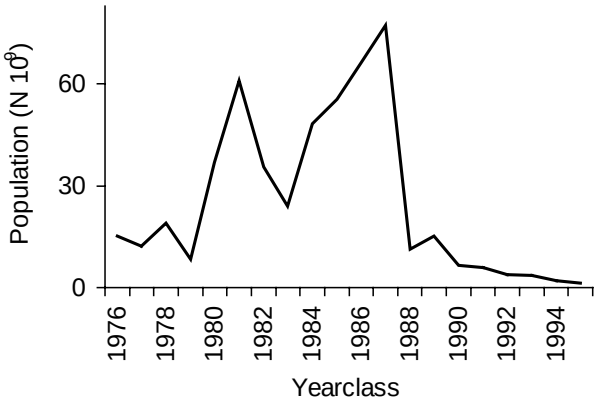

Fig. 52 Variability in year-class population at age 4 of Japanese sardine.

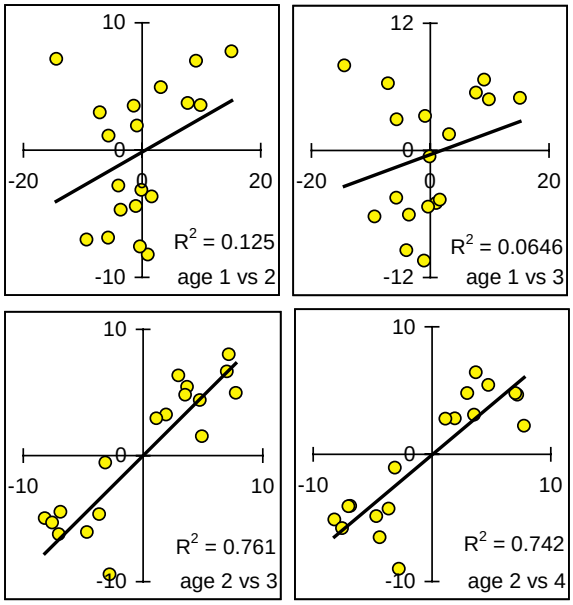

Fig. 53 Correlations of deviations from long term mean TL (20 years) among year-classes of Japanese sardine, by age.

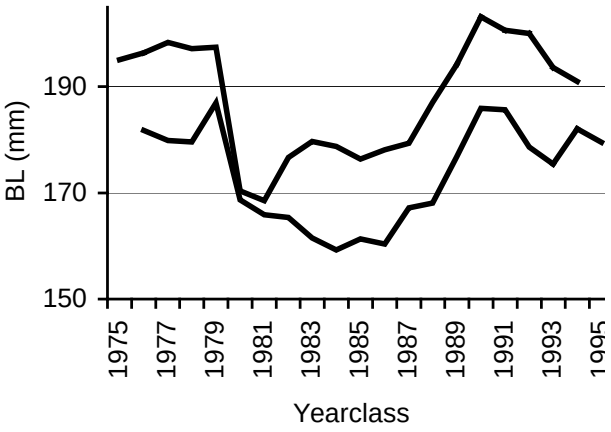

Fig. 54 Inter-decadal variations of BL-at-age 2 and 3 of Japanese sardine.

BL-at-age 2 was significantly ($P<0.001$) correlated with the year-class size in number at age 2 (Fig. 55). The coefficient of determination indicated that 60% of the BL variability can be explained by year-class strength. BL-at-age 2 was significantly ($P<0.001$) correlated with the total population at age 2. The coefficient of determination was 0.587. The variability in BL-at-age of the sardine inhabiting in the temperate Sea of Japan and the East China Sea is considered to be determined in a density-dependent manner.

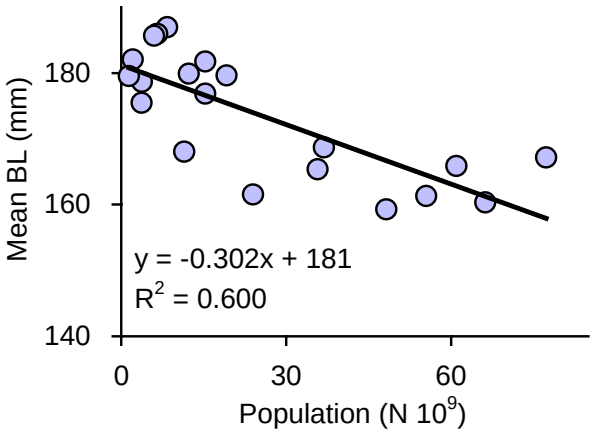

Fig. 55 Correlation of the mean BL with population of year-classes at age 2 of Japanese sardine.

Discussion

The fluctuations in year-class strengths were greater in the herring (2.5 orders) than in the sardine (1.7 orders) during the years studied. This may be related to the differences in the magnitude of inter-annual variability of ocean environment between the subarctic and temperate waters.

Size-at-age of herring and sardine varied about ±4 or 5% in the years studied. Growth of sardine up to 2 years old is considered to be largely determined through density-dependent processes such as competition for food, while that of the herring up to 4 years old was independent from the density of the population. Two factors may be responsible for the difference in the growth determining processes in herring and sardine.

The maximum year-class strength of the Tsushima Current subpopulation of the sardine was as large as 77.3 billion in 1987. The total population reached 370 billion in 1987. In the Hokkaido spring herring, the maximum year-class was 9.8 billion in 1921 and the total spawning population reached 19.6 billion in 1924. The population size of sardine was more than 10 times larger than herring. Comparison in migration ranges of sardine in the East China Sea and the Sea of Japan and of herring in the Sea of Japan and the Sea of Okhotsk are required, but the large population size of sardine seems to be a potential factor of density-dependent determination of size-at-age.

Another potential factor is the difference in biological productivity between the temperate and subarctic waters in the Sea of Japan and the Sea of Okhotsk. The Tsushima Current is derived from the warm Kuroshio Current and its productivity is considered to be lower than subarctic waters inhabited by the herring. Carrying capacity of the subarctic waters in the Sea of Japan and the Sea of Okhotsk may be sufficiently greater than the total food requirement of the herring population and competition for food may not be realized in these waters.

References

Hanamura, N. 1963. A study on the method of prediction of the Hokkaido spring herring resources. Bull Hokkaido Reg. Fish. Res. Lab. 26: 1-66.

Kitahama, H. 1955. Data on the total length compositions of Hokkaido spring herring. Hokkaido Pref. Fish. Exp. Stn., Yoichi, pp 46.

Morita, S. 1985. History of the herring fishery and review of artificial propagation techniques for herring in Japan. Can. J. Fish. Aquat. Sci. 42 (Suppl 1): 222-229.

Watanabe, Y., Zenitani, H., and Kimura, R. 1995. Population decline of the Japanese sardine *Sardinops melanostictus* owing to recruitment failures. Can. J. Fish. Aquat. Sci. 52: 1609-1616.

Long-term variability in length of walleye pollock in the western Bering Sea and east Kamchatka

Pavel A. Balykin and Alexander V. Buslov

Kamchatka Fisheries and Oceanography Research Institute (KamchatNIRO), 18 Naberezhnaya Street, Petropavlovsk-Kamchatsky, Russia 683600. E-mail: kamniro@mail.kamchatka.ru

The mean body length of walleye pollock yearlings from the western Bering Sea increases when the area of the ice cover is reduced. The average length of 2 to 6-year-old walleye pollock varies in relation to the dynamics of total stock biomass and environment. The biomass of walleye pollock is lower when the area of ice cover in the Bering Sea exceeds 700,000 km^2. When the area of ice cover is reduced, the total stock abundance of walleye pollock increases and the average length of 2 to 6-year-old fish decreases. A reliable relationship has been observed between condition factor and the growth of fish, indicating that the growth of walleye pollock is dependent on the forage base. Currently the biomass of walleye pollock in the western Bering Sea is very poor, therefore the growth in length is not dependent on the environment and total stock biomass.

The average length of 2 to 6-year-old walleye pollock in the Pacific Ocean waters adjacent to Kamchatka has changed in relation to the biomass of total stock and the abundance of generations. When the biomass has been high, the growth has been slow and *vice versa*. The environmental factors do not affect the growth of walleye pollock to the east of Kamchatka.

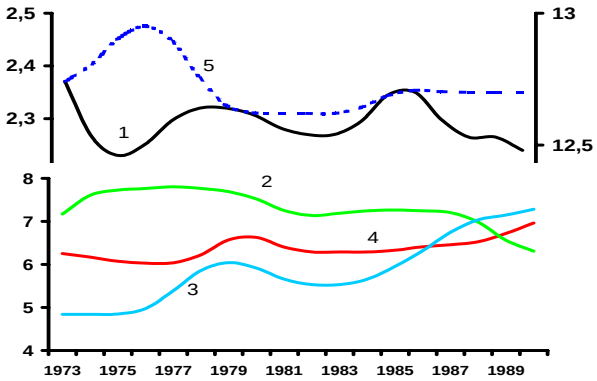

Fig. 56 Variation of natural logarithms of average length of walleye pollock yearlings (1), walleye pollock (2), Pacific herring (3), mesoplankton biomass (4), and area of ice cover (5) in the western Bering Sea.

Figure 56 shows changes in the length of walleye pollock yearlings, the biomass of mesoplankton and ice cover in the Bering Sea for the period from 1973-1990. The reduction of the ice cover area in the Bering Sea leads to the growth of total stock and an increase in average length of fish (Fig. 57).

Comparison of 2 to 6-year-old walleye pollock from the western Bering Sea and eastern Kamchatka waters indicates that variability in

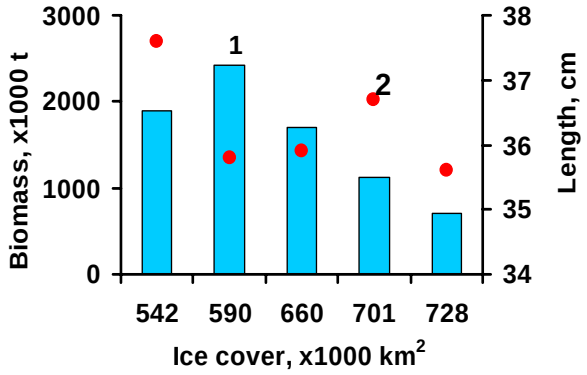

Fig. 57 Relationship between total biomass of walleye pollock (bars) and length of 4-year-old fish (dots) and ice conditions.

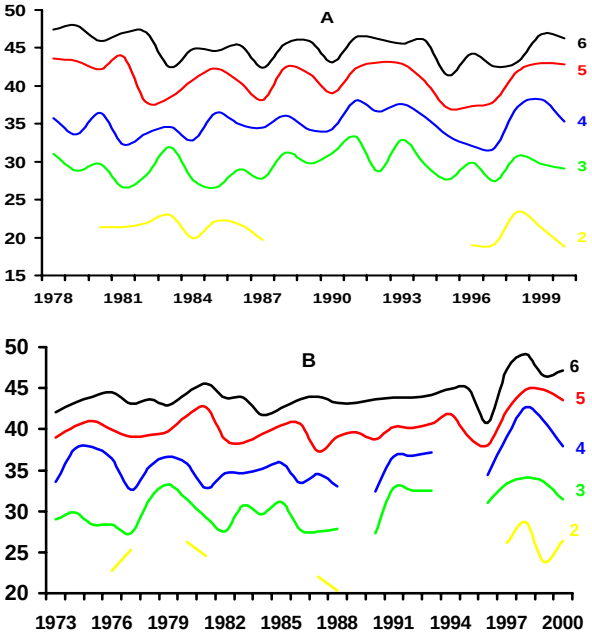

Fig. 58 Long-term dynamics of average length of 2 to 6-year-old walleye pollock: (A) western Bering Sea and (B) eastern Kamchatka.

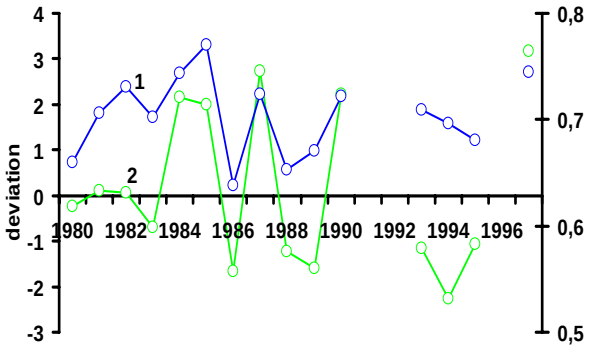

Fig. 59 Long-term dynamics of (1) average condition factor in 3 to 6-year-old walleye pollock and (2) averaged deviations in length from the long-term mean of these age groups.

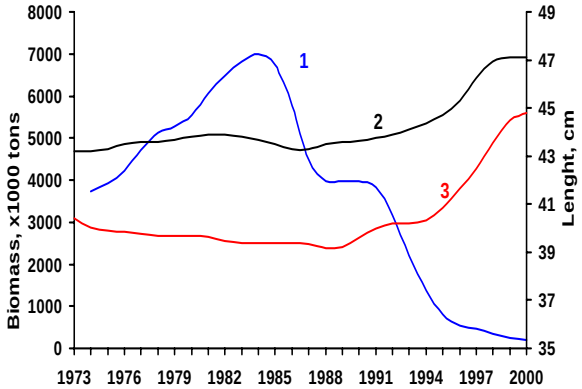

Fig. 60 Long-term dynamics of total biomass of east Kamchatka walleye pollock (1), average length of 6-year-old fish (2) and average length of 5-year-old fish (3).

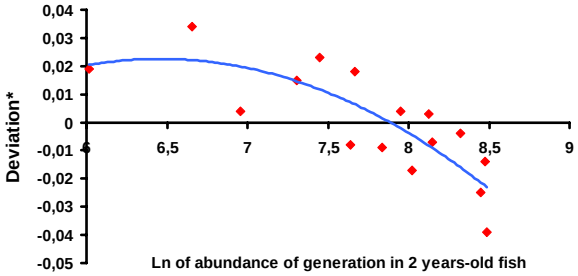

Fig. 61 Relationship between generation growth rate and abundance in the periods of high and intermediate stock abundance of the east Kamchatka walleye pollock, shown as the deviation from the average specific growth rate.

body length among nearby age groups is similar (Fig. 58). For the period 1980-1997, the condition factor is related to linear growth of fish (Fig. 59). For the east Kamchatka stock, changes in growth of 5-6-year-old walleye pollock are inversely related to the total biomass of species (Fig. 60). For the periods of high and intermediate stocks the growth rate of the east Kamchatka walleye pollock depends inversely on cohort abundance (Fig. 61).

Effect of population abundance increase on herring distribution in the western Bering Sea

Alexander A. Bonk
Kamchatka Fisheries and Oceanography Research Institute (KamchatNIRO), 18 Naberezhnaya Street, Petropavlovsk-Kamchatsky, Russia. 683600. E-mail: kamniro@mail.kamchatka.ru

The last two decades have been important for the development of the Korf-Karaginsky Pacific herring population. After a long period of low abundance in the 1980s, the population has been growing dynamically since 1990, reaching a maximum in 1997, and then started to decline again (Fig. 62).

The annual distribution and migratory behavior of the Pacific herring during are determined by hydrology and the stock abundance fluctuations. The time period and the distance of the Pacific herring feeding migration are now significantly different from those when stock abundance was low.

During periods of low abundance, the feeding migration of the mature part of the stock occurred in Anastasiya and Dezhneva bays (Fig. 63A). Herring returned to Olytorsky Bay for winter before October 10th. This period was characterized by relatively stable conditions providing sufficient feeding for the Korf-Karaginsky herring. From the 1980s until the mid-1990s positive changes were observed in the Bering Sea. These included: 1) warming of the upper 200 m which resulted in an increase of the forage zooplankton abundance, and 2) decrease in the stock abundance of walleye pollock, the nearest competitor of herring for food. Thus during the 1980s and early 1990s, when the herring abundance was low, the feeding conditions for the Pacific herring became favorable. In 1993, conditions were optimal for the production of an abundant generation (Fig. 64). In 1997, the

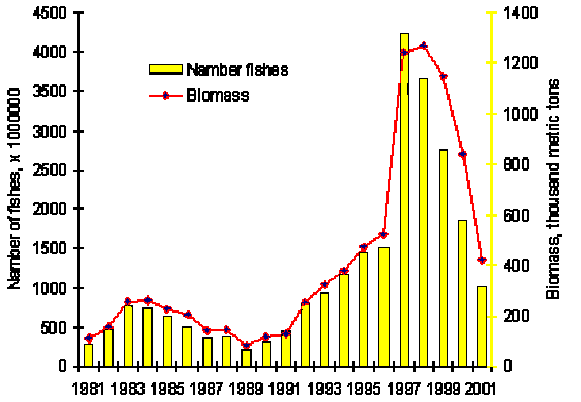

Fig. 62 The stock abundance dynamics of the Korf-Karaginsky herring in the western Bering Sea.

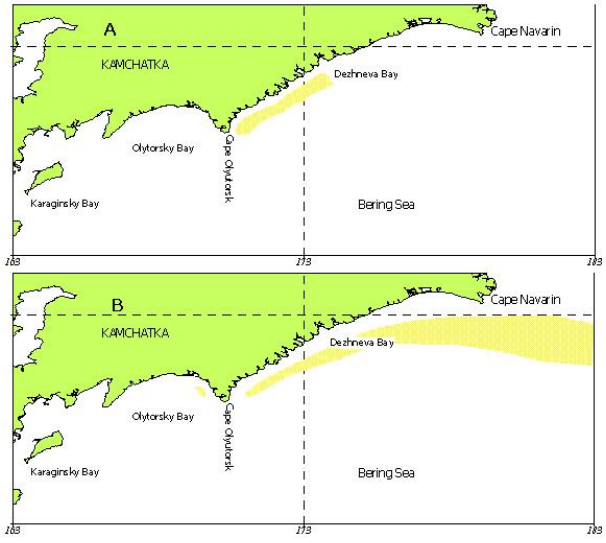

Fig. 63 The Korf-Kagarinsky herring distribution during the feeding migration: (A) low stock abundance and (B) high abundance.

4+ generation was the only one that recruited to the commercial fishery; in the last 40 years, it had the highest abundance and biomass, $4{,}230 \times 10^6$ fishes or $1{,}240 \times 10^3$ tons, respectively (Fig. 62).

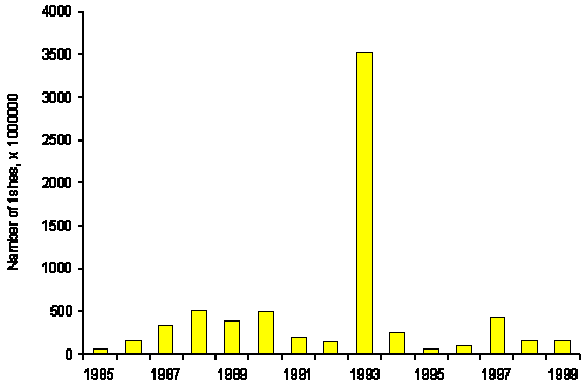

Fig. 64 Year-class abundance of age 4+ generations of the Korf-Kagarinsky herring in the western Bering Sea by brood year.

The increase in abundance of the fishery-size individuals in the Korf-Karaginsky herring population took place simultaneously with water cooling in the region. The indicators of that were: (1) a general decrease in the mixed water layer thermal capacity, and (2) extension of the ice cover in the Bering Sea since 1998. Cold water masses dominated on the shelf, providing poor conditions for the forage base. High abundance of the Korf-Karaginsky herring and poor food supply caused intensification of intra-specific competition for food. Unable to completely fulfil their food requirements, herring had to enlarge the area of feeding.

In 1998-2000, herring used marine bathypelagial in the Olytorsky-Navarinsky zone instead of the shelf zone for feeding until mid-October. In August and September, the echosounder tracks of herring shoals were discovered at the depth of 340-400 m. At the same time, local shoals of feeding herring were found in the eastern part of Olytorsky Bay (Fig. 63B). From the second half of October, fish shoals were distributed at depths of 80-150 m, on both sides of Olytorsky Cape (Fig. 65), however, these shoals were not stable. Herring migrated actively westward in small shoals, along the edge of the warmer and more saline Pacific waters, where trophic activity was high. During the daytime fish were distributed near the bottom, and at night they created thick shoals in the water column.

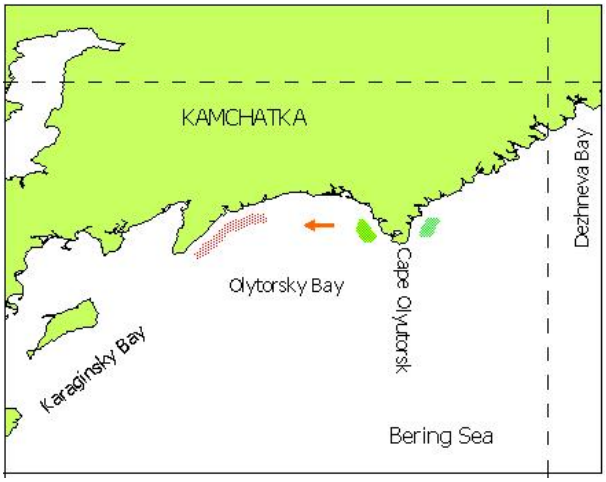

Fig. 65 Distribution of the Korf-Kagarinsky herring in the western Bering Sea, in October-November.

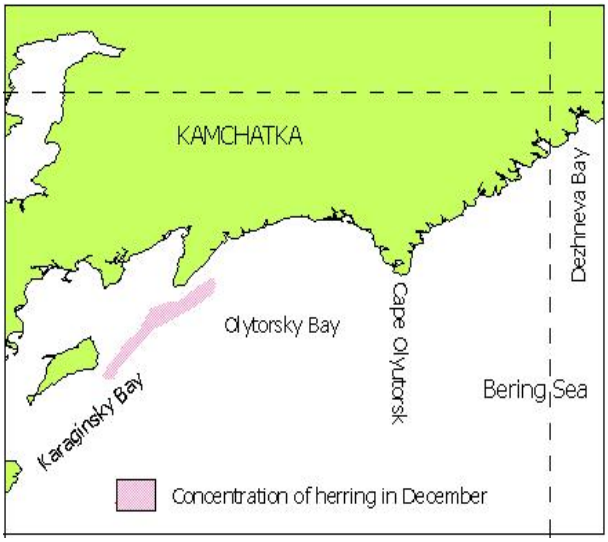

Fig. 66 The area of wintering of the the Korf-Kagarinsky herring in the western Bering Sea.

The transformation from summer to winter conditions in Olyorsky Bay has been normally completed in November. This transformation results in the quick cooling of the offshore waters. In 1998-2000, stable, favorable temperature conditions in November occurred at depths of 150-200 m, in the central and western parts of the bay. Therefore, the herring stocks formed at these depths. Their behavior at that time was similar to

their behavior in October. Following the arrival of cold water, herring migrated westward, forming non-mobile stocks at the depth of 180-250 m between the Cape of Goven and the Cape of Golenischev in December (Fig. 66).

Since 1993, there has been no single abundant cohort produced by the population. Due to natural mortality, and fishing, the stock abundance of the Korf-Karaginsky herring has decreased. Moreover, at the present time, hydrological conditions can hardly provide the required biomass of forage zooplankton. This should prolong the feeding period until mid October and expand the feeding area.

Survival of yellowfin sole (*Limanda aspera* Pallas) in the northern part of the Tatar Strait (Sea of Japan) during the second half of the 20th century

Sergey N. Tarasyuk
Sakhalin Research Institute of Fisheries and Oceanography, 196 Komsomolskaya Street, Yuzhno-Sakhalinsk, Russia 693023. E-mail: taras@sakhniro.ru

The northern part of the Tatar Strait is one of the traditional areas where yellowfin sole (*Limanda aspera* Pallas) dominate, averaging 60% of flounder abundance. The commercial fishery of flounder stocks began in 1943. In 1944, their catch reached the historical maximum – 10.1 thousand tons, but during the following year it reduced up to 7.4 thousand tons, and a catch per unit of effort (CPUE) decreased almost 2 times. Since 1945, the fishery ceased and until the beginning of the 1950s, the flounder catch did not exceed 0.1 – 1.0 thousand tons a year. Regular scientific research on this species was not conducted until 1956. Nevertheless, the data collected on the size composition of flounder catches during 1946, and some similar data since 1956, indicated overfishing in the mid-1940s (Tarasyuk, 1994A). After the 1950s, catch varied from 5.45 thousand tons in 1955 to 0.35 thousand tons in 1979. In the last ten years of the century, the catch constituted 0.4 – 2.0 thousand tons per year.

Age structure of the yellowfin sole population is characterized by an extended age distribution. Fish at age 4 to 18 occur in catches. Age-7 yellowfin sole are usually a modal age group, as their average long-term age value is 8.8. Body weights of yellowfin sole change according to the equation of allometric growth. A coefficient of allometry exponent in the equation is 3.1315, and the scale coefficient is 0.0073 when body weight is measured in grams and length (AC) in cm. Yellowfin sole from the shelf zone of western Sakhalin cease annual increments at age 8-9+. The instantaneous natural mortality rates vary by age decreasing from 0.22 to 0.12 beginning in age-4 to age-6-8 individuals, respectively, and then gradually increasing to 0.60 at age 15. The broods become fully available to the fishery beginning at age 8.

Methods

Data on the age structure of catches, annual catches, catch per unit of effort, natural mortality by age, rate of maturation, and average body weight by age during the period of 1956-2000 were processed using a method of virtual populations (VPA), with the help of program developed at the Fishery Laboratory Lowestoft (Darby and Flatman 1994). The Louric-Shepherd method was used for adjusting fishing mortality coefficients (Pope and Shepherd 1985).

Further processing of VPA results was done to reveal the causes determining brood year abundances. The abundance estimates of broods at age 4 were used as the index of recruitment. A cohort survival rate at age 4 was estimated as a quotient between the number of age 4 fish obtained from the VPA method, and the number at age 0. The spawning stock was calculated as the total number of the age groups taking into account the rate of maturation, less a year catch, since the fishery in this region is the most intensive before

the beginning of spawning. The number at age 0, or a start number of generation was determined from the number of spawners in the year of reproduction, considering the fecundity and age, and assuming under equal sex ratio from the catches.

Results

The biomass of the commercial part of the stock calculated by VPA changed significantly during the period of observation. In 1956, it constituted 13.9 thousand tons, reduced to the minimum 2.8 – 3.1 thousand tons in 1971 – 1975, and then began to increase to the maximum 19.2 thousand tons in 1991 – 1992. At the end of the century yellowfin sole stock reduced a little (Fig. 67). The commercial stock varied by 6.9 from 1956-2000. Spawning stock also varied within the wide limits: from the minimum 11.7 million fish in 1970 to 68.8 million fish in 1996, a factor of 5.8. The cohort size at age 4 varied from 6.09 million to 30.62 million fish in the 1962 and 1989 brood years, respectively, a factor of 5.0.

A potential population fecundity or cohort strength at age 0 varied from 4.0 to 25.4 trillion eggs according to changes in spawning stock and its age structure. Survival from age 0 to 4 averaged one individual from 3,000 eggs. This index ranged widely, up to 7.5.

Figure 68 shows the stock recruitment relationship and the estimated Ricker's model. A correlation coefficient with the amount of spawning stock was significant (0.79, $p<0.05$) for abundance of broods. The portion of the explained dispersion after calculating the coefficients of non-linear regression for the Ricker's model was 63.08%.

The survival rate for generations was well-correlated with the numbers of age group 0; the correlation coefficient was 0.61 ($p < 0.05$). Use of the equation of exponential growth approximated the relationship between those indices, with 37.16% dispersion explained. Based on the estimated curve, survival practically does not change at the initial number of brood more than 7 million individuals, and keeps at a stable level providing a minimum survival for population. Reduction in the number of eggs laid brings about a sharp increase in survival, varying about twofold (Fig. 69). This suggests a density dependent mortality.

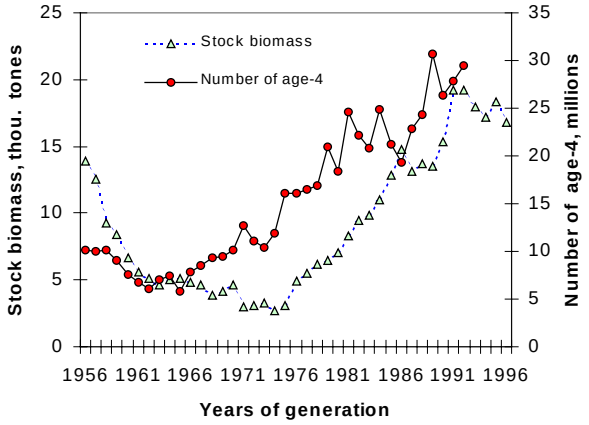

Fig. 67 Dynamics of biomass of the spawning stock and number of broods at age 4 from this stock generation for the Tatar Strait yellowfin sole population.

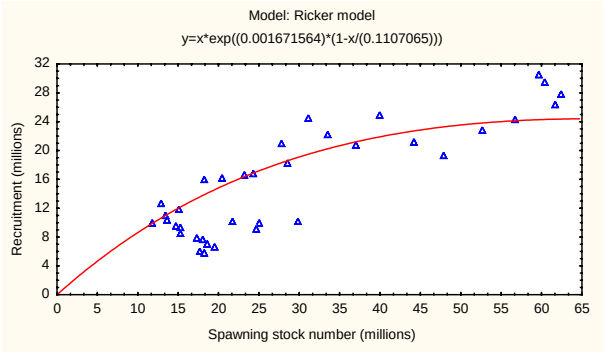

Fig. 68 Ricker's "stock-recruitment" model fit to the 1956-1992 observed data.

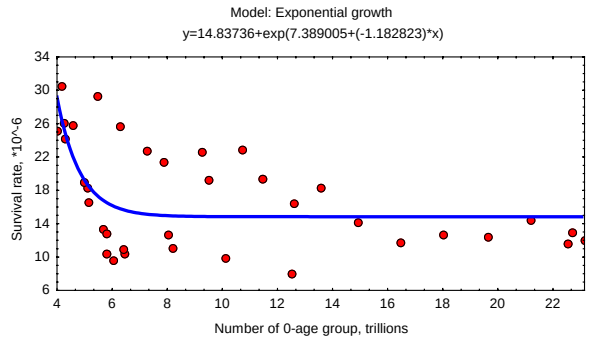

Fig. 69 Exponential model of the relation between survival rate and number of broods at age 0.

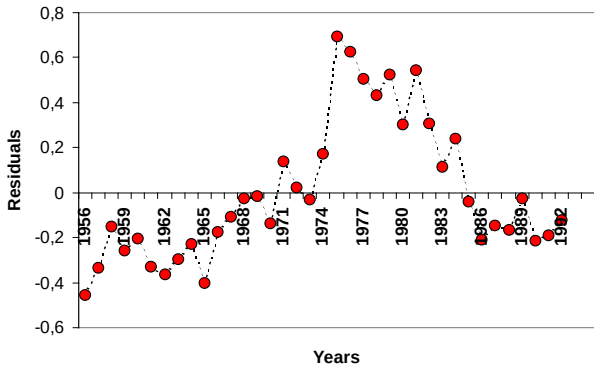

Fig. 70 Dynamics of standardized residuals of the survival rate regression by the birth years of broods.

The observed deviations from the exponential growth curve have causes other than the initial density of a population. The standardized residuals indicated a maximum of survival appears from 1974 to 1984, and low survival from the mid-1950s through the mid-1960s, 1985 through 1992 is characterized as slightly less than average.

A temporal series of the regression residuals on fish density demonstrates the potential climatic causes affecting a survival. According to the data of coastal hydrometeorological stations (Kholmsk GMS), a maximum heating of the surface water in the northern part of the Sea of Japan occurred in the early to mid 1970s, whereas the 1980s were characterized as cold years. Nevertheless, temperature conditions in the coastal zone may non-adequately characterize biota during early stages of the yellowfin sole ontogenesis when a brood abundance is formed. The longest oceanographic time-series observations in Tatar Strait are standard transects: Antonovsky and Cape Slepikovsky. The temperature regime in this region strongly depends upon the Tsushima Current. Its strengthening during the autumn in a warm year forms a stable water column until the beginning of winter. This is evident in the dynamics of May temperature in the layer 50-100 m (Kantakov 2000; Fig. 71). The layer temperature, smoothed by a 5 point moving averages, has decreased from the mid-1970s to the late 1980s, whereas the mid-1950s to the mid-1970s was characterized by higher temperatures. A correlation of initial estimates of the layer temperature with the regression residuals, the index of survival, appeared to be significant with a correlation coefficient of -0.48. A reconstructed zooplankton biomass time series for the southwestern Sakhalin coast has shown that maximum zooplankton biomass observed in cold years, and low plankton biomass occurred in warm years (Kantakov 2000; Fig. 71).

Maximum of atmospheric activity also occurred in the 1950s, when the greatest number of tropical typhoons moved through the region, whereas in the 1970s, the number of typhoons was minimum (Fig. 72). The correlation coefficient was -0.50 (Tarasyuk 1994 B).

Discussion

The noted relationships demonstrate the influence of climatic factors on the abundance of yellowfin sole generations. To understand the mechanism of these relationships, we review the ecology of yellowfin sole spawning. They spawn in the northern part of the Sea of Japan in July-August, at the depths less than 50 m. Eggs are spawned in batches (Fadeev 1957, Ivankov *et al*. 1972). Spawned eggs are relatively small, their diameter is 0.8 – 0.9 mm. Embryos and larvae develop in the upper 50-m of water column at temperatures from 8 to 19ºC (Pertseva- Ostroumova 1961). At the length of 16 - 27 mm, larvae settle on the bottom (Nikolotova 1975). The planktonic stage is about a one month, and on the whole, taking into account the duration of spawning, may continue up to 4 months (Tarasyuk 1994B). The peculiarity of yellowfin sole reproduction is the timing of their aggregations at plankton stages of development to small areas with circulation that prevents the larvae from flowing out of favorable sites (Moiseev 1952). Plankton and nektobenthic crustaceans at juvenile stages of development form the basic food for planktotrophic larvae (Nikolotova 1975). Evidently, a long stay in the upper water column, their peculiarities of feeding, and concentration in a limited area create a special vulnerability of yellowfin sole at early stages of ontogenesis to the negative affects of environment, and also a high mortality as a result of intra-population competition.

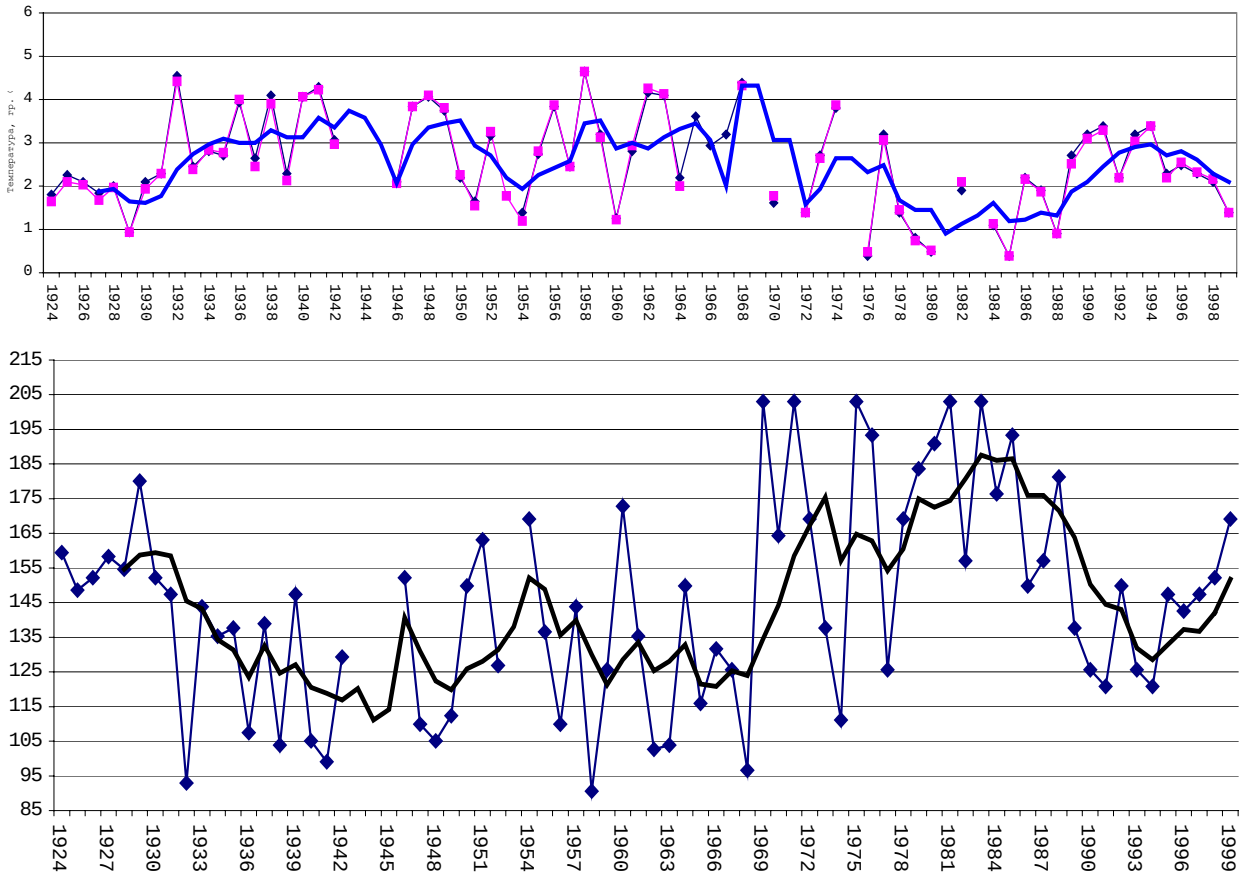

Fig. 71 Dynamics of the May temperature in the 50-100 m layer along the transects Antonovsky and Cape Slepikovsky (top panel) and autumn biomass of the net zooplankton (bottom panel). Zooplankton biomass is in units of mg wet weight per cubic meter. (Source: Kantakov 2000).

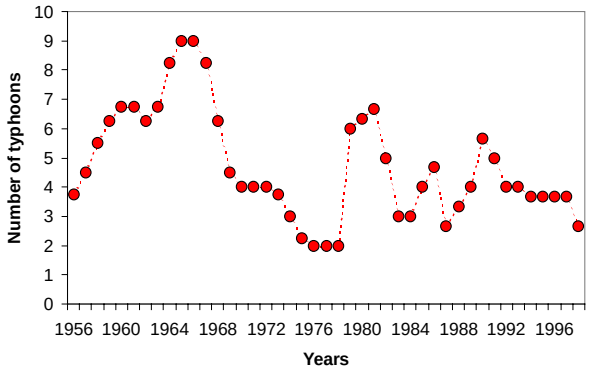

Fig. 72 Frequency of tropic typhoons moving through the area of Sakhalin Island.

Comparing these relationships with the peculiarities of reproduction of yellowfin sole, we conclude that the negative influence of the initial cohort abundance upon their survival is realized through the deterioration of feeding conditions under the increased density of larval aggregations, diet selectivity, and limited resources of food fields. The influence of tropical typhoons (more than 80 % of them occur in June-August) (Eremin and Tretyakova 1980) may result both in the negative impact of hydrodynamic wave on the embryos survival at the sensitive stages of development, and in their impact on the small-scale circulation systems, causing the appearance of cold deep water masses on the surface and carrying eggs and larvae out of zones favorable for inhabitation. In the cold year periods, zooplankton biomass in the northern Sea of Japan increases, and that reduces the level of intra-population competition for food. In turn, this favorably affects the larval survival.

References

Darby, C.D. and Flatman, S. 1994. Virtual Population Analysis: Version 3.1 (Windows/DOS) User Guide. Info. Tech. Ser., MAFF Direct, Fish. Res., Lowestoft, (1): 85 pp.

Eremin, P.G. and Tretyakova, E.I. 1980. To a question about the cyclicity of typhoons above Sakhalin Region. Information Letter No. 1/90. Yuzhno-Sakhalinsk, SakhUGCS, pp. 31– 45 (in Russian).

Fadeev, N.S. 1957. On the type of spawning and fecundity for some commercial Sakhalin flounders. Zoological Journal 36(12): 18-41 (in Russian).

Ivankov, V.I., Ivankova, Z.G., and Volkova, T.D. 1972. Types and terms of spawning for flounders from Peter the Great Bay. Scientific Notes of DVGU 60: 49-61 (in Russian).

Kantakov, G.A. 2000. Oceanographic Retrospective Analysis of the Zooplankton Population Inhabitation Conditions at the Southwest Sakhalin in 20th Century. *In* 15th International Symposium on Okhotsk Sea & Sea Ice. Okhotsk Sea & Cold Ocean Research, pp. 384-390.

Moiseev, P.A. 1952. Some specific features of the bottom and near-bottom fish distribution in the Far East seas. Izv. TINRO 27: 129 – 137 (in Russian).

Nikolotova, L.A. 1975. Larval feeding of the west Kamchatka flounders. Izv. TINRO 97: 51-61 (in Russian).

Pertseva-Ostroumova, T.A. 1961. A spawning and developing patterns of the Far East flounders. M.: AS USSR Publishers. 484 pp. (in Russian).

Pope, J.G. and Shepherd, J.G. 1985. A comparison of the performance of various methods for tuning VPA's using effort data. J. Cons. Int. Explor. Mer. 42: 129-151.

Tarasyuk, S.N. 1994A. Results of modeling biological indices of the yellowfin flounder from the western Sakhalin waters during the initial period of fishery. *In* "Fishery researches in Sakhalin-Kuril region and adjoining areas". Yuzhno-Sakhalinsk, Sakhalin Region Book Publishers, pp. 33-38 (in Russian).

Tarasyuk S.N. 1994B. On the possible causes providing the abundant broods of yllowfin flounder. *In* "Fishery researches in Sakhalin-Kuril region and adjoining areas". Yuzhno-Sakhalinsk, Sakhalin Region Book Publishers, pp. 23-32 (in Russian).

MODEL/REX WORKSHOP TO DEVELOP A MARINE ECOSYSTEM MODEL OF THE NORTH PACIFIC OCEAN INCLUDING PELAGIC FISHES

(Co-conveners: Bernard A. Megrey and Michio J. Kishi)

Summary

A 4-day MODEL/REX workshop made several significant achievements:

1. Assembled an international team of marine biologists, fisheries biologists, and physical oceanographers who collectively achieved a consensus on the structure and function of a PICES Climate Change and Carrying Capacity (CCCC) prototype lower trophic level (LTL) ecosystem model for the North Pacific Ocean that included pelagic fishes, and named it "*NEMURO.FISH*";
2. Developed a computer simulation model of fish bioenergetics and growth;
3. Coupled the fish model to the NEMURO lower trophic level model;
4. Adapted the fish bioenergetics model to Pacific herring (*Clupea harengus pallasi*) in the eastern North Pacific, and Pacific saury (*Cololabis saira*) in the western North Pacific;
5. Made recommendations for future modeling activities.

The significance of these achievements will ultimately be evaluated by how well the CCCC Program effectively utilizes and embraces these models as a basis of future modeling activity.

1.0 Workshop overview

Introduction

The North Pacific Marine Science Organization (PICES) organizes and promotes an international science program, CCCC, in the temperate and subarctic regions of the North Pacific Ocean. Ecosystem modeling is one of five key research activities defined by the CCCC Implementation Panel. The PICES CCCC MODEL Task Team is given the role to encourage, facilitate and coordinate modeling activities within the member nations with respect to the goals and objectives of the PICES-CCCC Program. At the 2000 Nemuro Workshop, the MODEL Task Team developed NEMURO, a lower trophic level marine ecosystem model. NEMURO has been internationally recognized, and recently, the Max Planck Institute has adopted the use of NEMURO.

At PICES IX in Hokkodate, the REX and MODEL Task Teams met and agreed it would be useful to extend NEMURO to include higher trophic level components. Based on some presentations there, we agreed to try Pacific herring as a candidate higher trophic level species and plans began for a joint workshop. Dr. Michio Kishi prepared a proposal to the Heiwa-Nakajima foundation of Japan to help fund attendance to the workshop. The proposal was successful and planning began to hold the next workshop in Nemuro, Japan in 2002.

Goals and objectives of the Workshop

The goals of the 2002 Nemuro PICES workshop were to (1) develop a bioenergetics-based fish model for Pacific herring (*Clupea harengus pallasi*) and Pacific saury (*Cololabis saira*) and (2) to couple this model with output from the NEMURO lower trophic level model developed at the 2000 Nemuro PICES workshop.

Organizing Committee, participants, sponsors and venue

Drs. Michio J. Kishi, Bernard A. Megrey and Francisco E. Werner organized the meeting. Drs. Megrey and. Kishi served as workshop co-chairmen. The Heiwa-Nakajima foundation of Japan, PICES, and the city of Nemuro provided financial support and access to excellent meeting rooms in the City Hall. The Nemuro Support Committee supplied local logistical support.

The venue was set at the Multi Purpose Hall, a large octagon-shaped room, in the Nemuro City Cultural Center. The hall had a local area network which included a server workstation, laser and color printers, and another personal computer connected to the Internet. A classroom style table was arranged in the center of the room for the plenary session. A set of LCD projectors and screens and AC power outlets for participants' laptop computers were available and were arranged in each work area to make group work more effective.

Twenty six scientists from China, Korea, Russia, Japan, Canada and the United States (Fig. 1) convened in Nemuro, Japan, between January 25 and January 27, 2002, to participate in a modeling workshop focused on developing a coupled lower trophic level-higher trophic level model of the marine ecosystem. Most scientists arrived with their own laptop computers. Participants (Appendix 1) consisted of plankton scientists, modelers, and individuals with biological knowledge of herring and saury. Key regional data sets were also provided by many workshop participants. The workshop was continued at the Frontier Research System for Global Change (FRSGC) facilities in Yokohama on January 29, 2002.

Fig. 1 Nemuro Workshop participants. Left to right –Top Row: Douglas Hay, Tomokazu Aiki, Masakatsu Inada, Daiki Mukai, Lan S. Smith, Vadim V. Navrotsky, Alexander V. Leonov, Francisco E. Werner, Robert A. Klumb, Bernard A. Megrey, Toshio Katsukawa, Takeshi Okunishi, Yasuhiro Yamanaka, Tomonori Azumaya. Bottom Row: Chul-hoon Hong, Sanae Chiba, Yuri I. Zuenko, Daji Huang, Masahiko Fujii, Kazuaki Tadokoro, Shin-ichi Ito, Shoichi Hamaya (Nemuro City Supporter), Michio J. Kishi, Makoto B. Kashiwai.

Workshop schedule

Date: January 25th-29th, 2002

Venue: Nemuro City Culture Center* (25-27 Jan. 2002), FRSGC (28,29 Jan. 2002)

Conveners: Michio J. Kishi (Hokkaido University), Bernard A. Megrey (NOAA), Francisco E. Werner (University of North Carolina)

Workshop Co-Chairmen: M. Kishi and B. Megrey

Agenda

January 25th, Friday

18:00	Opening ceremony
19:00	Welcome reception

January 26th, Saturday

09:00-09:10	Remarks by M. J. Kishi
09:10-09:30	Review of NEMURO (North Pacific Ecosystem Model for Understanding Regional Oceanography) developed by PICES MODEL Task Team in 2000 (Michio Kishi)
09:30-10:30	Review of NEMURO FORTRAN code (Yasuhiro Yamanaka)
10:30-11:00	Fish bioenergetics/biomass modeling: an application to Pacific herring (Bernard Megrey)
10:30-11:00	Review of NEMURO FORTRAN code (Yasuhiro Yamanaka)
11:00-11:30	Review of Clupeid biology with emphasis on energetics (Robert Klumb)
11:30-12:00	Analysis of change in Pacific herring distributions (Douglas Hay)
12:00-13:00	Lunch
13:00-13:30	Review of Pacific saury (*Cololabis saira*) study under VENFISH (Shin-ichi Ito)
13:30-17:00	Grouping of scientists ("team herring" and "team saury")

January 27th, Sunday

09:00-12:00	Continue working in teams
12:00-13:00	Lunch
13:00-15:30	Discussion on the results and modification of model
15:40-16:00	Closing ceremony
16:30-	Press conference (Megrey, Kishi, Werner)
18:30-20:30	Farewell party by Nemuro city (at hotel)

January 28th, Monday

Move to Frontier Research System for Global Climate Change

January 29th, Tuesday

09:00-12:00	Discussion on the results of new model and future strategy
12:00-13:00	Lunch
13:00-17:00	Seminar at FRSGC
13:00-13:30	Zuenko
13:30-14:00	Navrotsky
14:00-14:30	Huang
14:30-15:00	Klumb
15:00-15:30	Hong
15:30-16:00	Tea break
16:00-16:30	5-minute speech of Japanese participants
16:30-17:00	Discussion of future work

Workshop activity

After an opening ceremony with the people of Nemuro and a welcome party held the day before, the participants convened at the venue to start the workshop.

On the first day, the workshop officially opened with a welcome to all who had endured a long journey to come back to Nemuro. In the morning session, individual presentations were made on the NEMURO LTL model, a review of the FORTRAN program to execute NEMURO, the proposed fish bioenergetics model, and presentations on herring and saury biology as outlined in the agenda. During the afternoon session, the workshop participants split into two groups, to adapt the generalized fish bioenergetics model for Pacific herring ("team herring") and Pacific saury ("team saury").

The second day was taken up primarily with the two working groups dealing with their specific tasks. Results of the Pacific herring and saury

applications were presented for discussion in the afternoon. Also on the second day the coupled lower trophic level-higher trophic level model was named NEMURO.FISH (North Pacific Ecosystem Model for Understanding Regional Oceanography.For Including Saury and Herring). Robert Klumb suggested the name.

The participants received closing remarks from the vice-chairman of the Nemuro Supporting Committee where appreciation was extended to have brought into being such a productive workshop. These feelings were amplified during a Sayonara Party, which was full of warm hospitality by the people of Nemuro city.

The third session was held at the Frontier Research System for Global Change in Yokohama. The group discussed the structure and organization of the final report, made writing assignments, generated a list of workshop recommendations, discussed where the MODEL Task Team should be going next, and the possibility of holding future workshops. Several individual seminars were presented by workshop participants dealing with their personal research topics.

2.0 Workshop presentations

This section contains abstracts, extended abstracts, or fully prepared reports and workshop summaries given at the workshop. The reports that follow are organized by authors, according to the schedule provided in the agenda. The authors whose last name is in underline and bold font made the presentation. Model versions referenced in these reports are described in Megrey *et al.* (2000).

2.1 A generalized fish bioenergetics/biomass model with an application to Pacific herring

Bernard A. Megrey[1], Kenny Rose[2], Francisco E. Werner[3], Robert A. Klumb[4] and Douglas Hay[5]

1 National Marine Fisheries Service, Alaska Fisheries Science Center, 7600 Sand Point Way NE, Seattle, WA 98115, U.S.A. E-mail: bern.megrey@noaa.gov

2 Coastal Fisheries Institute and Departm ent of Oceanography and Coastal Sciences, Wetlands Resources Building, Louisiana State University, Baton Rouge, LA 70803, U.S.A. E-mail: karose@lsu.edu

3 Marine Sciences Department, CB # 3300, University of North Carolina, Chapel Hill, NC 27599-3300, U.S.A. E-mail: cisco@unc.edu

4 Department of Natural Resource, Cornell Biological Field Station, Cornell University, 900 Shackelton Point Road, Bridgeport, NY 13030, U.S.A. E-mail: rak11@cornell.edu

5 Pacific Biological Station, Fisheries and Oceans Canada, 3190 Hammond Bay Rd, Pacific Biological Station, Nanaimo, British Columbia, Canada V9R 5K6. E-mail: hayd@pac.dfo-mpo.gc.ca

We chose to use bioenergetics/biomass modeling to represent fish growth because (1) the theory is based on the Law of Thermodynamics, (2) outputs must equal inputs, *ie.*, the energetic budget must balance (Law of Conservation of Mass), (3) terms in the equations are simple to biologically interpret, (4) fish physiological terms are well known and in general can be directly measured, and (5) this modeling approach allows users to focus on important external regulators such as temperature and diet composition. Model formulation and parameters for Pacific herring followed the approach used by Rudstam (1988) for Atlantic herring (*Clupea harengus*).

The growth rate of an individual Pacific herring (non reproductive) is calculated as weight increment per unit of weight per time and is defined by:

(2.1.1) $$\frac{dW}{dt} = \left[C - (R + S + F + E)\right] \cdot \frac{CAL_z}{CAL_f} \cdot W$$

where C is consumption (g prey·g fish^{-1}·d^{-1}), E is excretion or losses of nitrogenous excretory wastes (g prey·g fish^{-1}·d^{-1}), F is egestion or losses due to feces (g prey·g fish^{-1}·d^{-1}), R is respiration or losses through metabolism (g prey·g fish^{-1}·d^{-1}), S is specific dynamic action or losses due to energy costs of digesting food (g prey·g fish^{-1}·d^{-1}), W is the weight of the fish (g wet weight), t is time (days) CAL_z is the caloric equivalent of zooplankton (cal·g zooplankton^{-1}), and CAL_f is the caloric equivalent of fish (cal·g fish^{-1}). Note that (2.1.1) does not include energetic costs of reproduction (spawning).

If we define CAL_z as calories·g zooplankton^{-1}

$$CAL_z = \frac{2580\, joules}{gram\ \ zoop} \cdot \frac{1\ \ cal}{4.18\, joules} = 617.22$$

and CAL_f as calories·g fish^{-1}

$$CAL_f = \frac{5533\, joules}{gram\ \ fish} \cdot \frac{1\ \ cal}{4.18\, joules} = 1323.68$$

then once the change in weight from 2.1.1 is computed in terms of g zooplankton·g fish^{-1}·d^{-1}, we can multiply it by the weight of the fish (W, g) to get g zooplankton·d^{-1}, and finally convert g zooplankton·d^{-1} to g fish·d^{-1} by multiplying the change in weight (dW/dt) by the ratio CAL_z/CAL_f.

In the simulations described in this report, equation 2.1.1 was solved using an Euler numerical integration routine using a dt=0.01.

The formulation of the individual processes represented by the terms in equation 2.1.1 is described individually below. Consumption and respiration are nonlinear functions of fish weight and water temperature.

In addition to the physiological parameters, the model requires information about caloric content of herring (which can change seasonally), caloric content of the prey, diet composition, prey densities, and water temperatures.

Consumption

Consumption is estimated as the proportion of maximum daily ration for herring at a particular mass and temperature. Maximum daily consumption rate (g of prey per g body mass of herring per day) is estimated using an allometric function of mass from *ad libitum* feeding experiments conducted at the optimum temperature.

The basic form of the consumption function is

(2.1.2) $$C = C_{MAX} \cdot p \cdot f_C(T)$$

(2.1.3) $$C_{MAX} = a_C \cdot W^{b_C}$$

where C is the specific consumption rate (g prey·g fish^{-1}·d^{-1}), C_{MAX} is the maximum specific feeding rate (g prey·g fish^{-1}·d^{-1}), p is the proportion of maximum consumption, $f_C(T)$ is a temperature dependence function for consumption, T is water temperature (ºC), W is herring mass (g wet weight), a_c is the intercept of the allometric mass function (for a 1 g fish at 0°C), and b_c is the slope of the allometric mass function. The subscript C on the parameters refers to the consumption process.

In equation (2.1.2), the maximum specific feeding rate is modified by a water temperature dependence function described below and an additional proportionality constant that accounts for ecological constraints on the maximum feeding rate. The p can range from 0 to 1, with 0 representing no feeding and 1 indicating the fish is feeding at its maximum rate, based on its body mass and water temperature. The lower panel of figure 2.1.1 shows the relationship between fish weight and consumption from equation 2.1.3.

Temperature dependence for cool and cold water species (Thornton and Lessem 1978)

The Thornton and Lessem description of temperature dependence is essentially the product

of two sigmoid curves: one curve is fit to the increasing portion of the temperature dependence function (*gcta*), and the other to the decreasing portion (*gctb*). Four temperatures and percentages are needed. We used two sets of parameters, one for herring ages ≤1 year old, and one set for herring > 1 years old.

As an example, parameters for the second set are *xk1*=0.1, *xk2*=0.98, *xk3*=0.98, *xk4*=0.01, *te1*=1.0, *te2*=13.0, *te3*=15.0, and *te4*=23.0. For the increasing part of the curve, *te1* is the lower temperature at which the temperature dependence is a small fraction (*xk1)* of the maximum rate, and *te2* is the water temperature corresponding to a large fraction (*xk2)* of the maximum consumption rate. For the decreasing portion of the curve, *te3* is the water temperature (≥ *te2*) at which dependence is a fraction (*xk3)* of the maximum, and *te4* is the temperature at which dependence is some reduced fraction (*xk4)* of the maximum rate.

The temperature dependence model is given by

(2.1.4) $f_C(T) = gcta \cdot gctb$

where T is water temperature (°C)

$$tt5 = \frac{1}{(te2 - te1)}$$

$$t5 = tt5 \cdot \ln\left[xk2 \cdot \frac{(1.0 - xk1)}{(0.02 \cdot xk1)} \right]$$

$$t4 = e^{[t5 \cdot (T - te1)]}$$

$$tt7 = \frac{1}{(te4 - te3)}$$

$$t7 = tt7 \cdot \ln\left[xk3 \cdot \frac{(1.0 - xk4)}{(0.02 \cdot xk4)} \right]$$

$$t6 = e^{[t7 \cdot (te4 - T)]}$$

$$gcta = \frac{(xk1 \cdot t4)}{(1.0 + xk1 \cdot (t4 - 1.0))}$$

$$gctb = \frac{(xk4 \cdot t6)}{(1.0 + xk4 \cdot (t6 - 1.0))}$$

Figure 2.1.2 shows an example of the Thornton and Lessem (1978) temperature adjustment function for a theoretical set of parameters. The upper panel of Figure 2.1.1 shows the Thornton and Lessem temperature adjustment function over a typical temperature range, and Figure 2.1.3 shows the flexibility of this curve by adjusting *te2* for a range of temperatures. Finally, Figure 2.1.4 shows the multi-dimensional relationship between consumption, body mass and water temperature from equation 2.1.2.

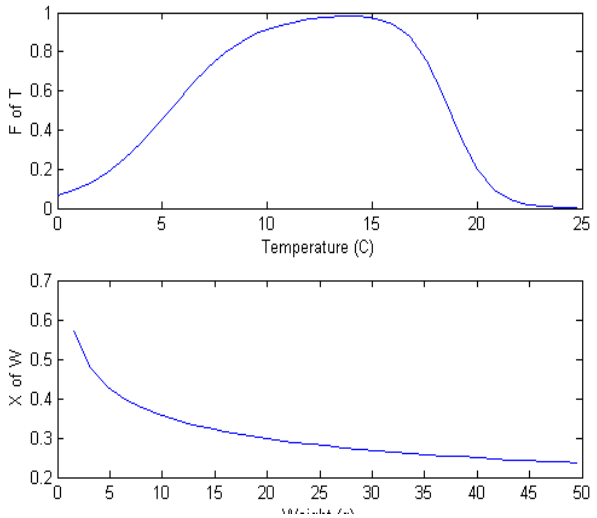

Fig. 2.1.1 Relationship between consumption and temperature from equation 2.1.4 (upper panel) and consumption and weight from equation 2.1.3 (lower panel).

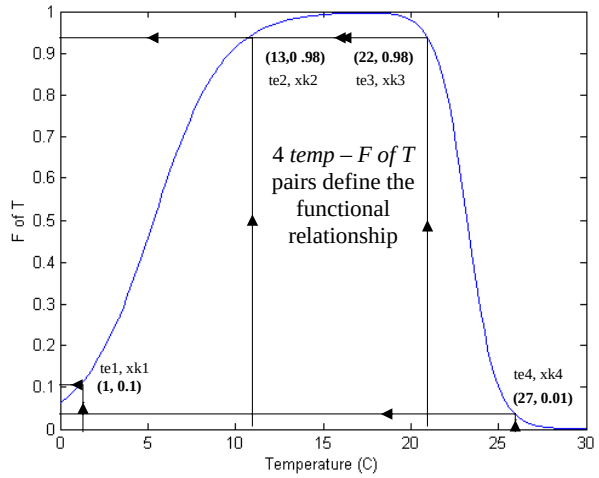

Fig. 2.1.2 Example of the Thornton and Lessem (1978) temperature adjustment curve for a theoretical set of parameters.

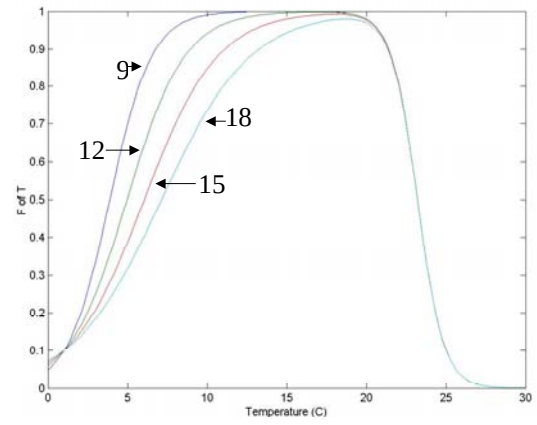

Fig. 2.1.3 Example of the Thornton and Lessem (1978) temperature adjustment curve from Figure 2.1.2 as a result of changing te2 from 9, 12, 15, 18.

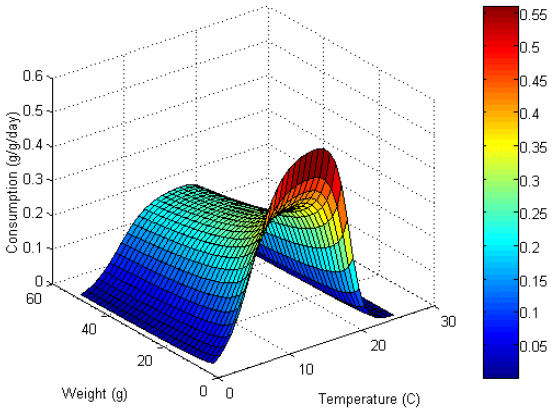

Fig. 2.1.4 Plot of the consumption, temperature and weight relationships from equation 2.1.2.

Respiration

The respiration or metabolic rate is dependent on body weight, ambient temperature and activity (swimming speed). Total metabolic rate is estimated by adding the costs of respiration to the costs of digestion, specific dynamic action (SDA).

Metabolism is modeled as

(2.1.5) $R = a_R \cdot W^{b_R} \cdot f_R(T) \cdot activity \cdot 5.258$

(2.1.6) $S = SDA \cdot (C - F)$

where R is resting respiration (*i.e.* standard metabolism) in (g O_2·g $fish^{-1}$·d^{-1}), W is wet weight in g, $f_R(T)$ is the temperature dependence function for respiration, T is temperature in ºC, a_R is the intercept of the allometric mass function and represents the weight specific oxygen consumption rate of a 1 g fish (g O_2·g $fish^{-1}$·d^{-1}) at 0ºC and no activity, b_R is the slope of the allometric mass function for standard metabolism, *activity* is the activity multiplier, S is the specific dynamic action, SDA is the proportion of assimilated energy lost to specific dynamic action, C is the specific consumption rate (g prey·g $fish^{-1}$·d^{-1}) and F is the specific egestion rate (g prey·g $fish^{-1}$·d^{-1}). The subscript R on the parameters refers to the respiration process. The coefficient 5.258 converts g O_2·g $fish^{-1}$·d^{-1} into g prey·g $fish^{-1}$·d^{-1} using the conversion

(2.1.7)

$$\left(\frac{13560\ joules}{gO_2}\cdot\frac{1\ cal}{4.18\ joules}\right)\div\left(\frac{2580\ joules}{g\ \ zoop}\cdot\frac{1\ cal}{4.18\ joules}\right)=5.258g\ \ zoop/g(O_2)$$

The temperature dependence function for respiration is a simple exponential relationship given by

(2.1.8) $f_R(T) = e^{(c_R \cdot T)}$

where c_R approximates the Q_{10} (the rate at which the function increases over relatively low water temperatures).

Activity is a power function of body weight conditioned on water temperature and is given by

(2.1.9) $activity = e^{(d_R \cdot U)}$

where U is swimming speed in cm·s^{-1} and d_R is a coefficient relating swimming speed to metabolism. Swimming speed is calculated as a function of body weight and temperature using

(2.1.10) $U = a_A \cdot W^{b_A} \cdot e^{(c_A \cdot T)}$

where $a_{A=}$ 3.9, b_A = 0.13 and c_A=0.149 if T <9.0 °C and $a_{A=}$ 15.0, b_A = 0.13 and c_A=0.0. if T ≥9.0 °C

Figure 2.1.5 shows the three dimensional relationship between respiration, water temperature and fish weight.

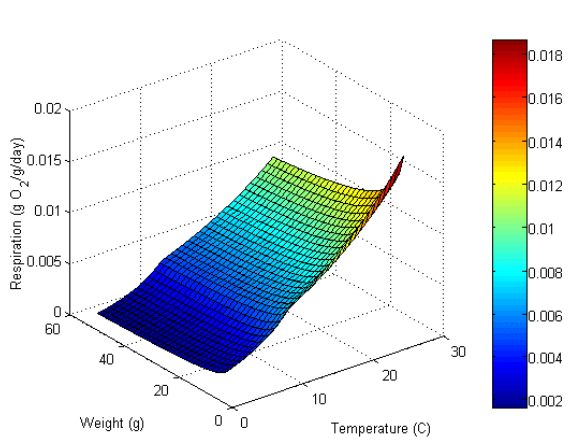

Fig. 2.1.5 Relationship between standard respiration, weight and temperature from equation 2.1.5.

Egestion and excretion

Egestion (*F*, fecal waste) and excretion (*E*, nitrogenous waste) can be computed as a constant proportion of consumption.

(2.1.11) $F = a_F \cdot C$

(2.1.12) $E = a_E \cdot (C - F)$

where a_F and a_E are constant proportions of consumption for egestion and excretion respectively. The subscript F and E on the parameters refers to the egestion and excretion process.

Multispecies feeding functional response

In most cases realized consumption is calculated by adjusting C_{MAX} from equation 2.1.2 by *p*, and this would be sufficient if there were only one prey type by using a Type II functional response equation (Fig. 2.1.6). When there are multiple prey types, realized consumption depends on prey densities, vulnerability of each prey item to herring (the predator), and half-saturation constants governing the rate of herring saturation. A Type II functional response equation for multiple prey types (after Rose *et al.* 1999) is used to compute realized daily consumption of each herring *i* (C_r, g prey·g fish^{-1}·d^{-1}) and the consumption of each prey type *j* (C_j, g prey·g fish^{-1}·d^{-1}) using

(2.1.13) $C_r = \sum_{j=1}^{n} C_j$

(2.1.14) $C_j = \dfrac{C_{MAX} \cdot \dfrac{PD_{ij} \cdot v_{ij}}{K_{ij}}}{1 + \sum_{k=1}^{n} \dfrac{PD_{ik} \cdot v_{ik}}{K_{ik}}}$

where C_{MAX} , which is dependent on the weight of an individual fish and water temperature, is the consumption rate (g prey·g fish^{-1}·d^{-1}) of individual herring *i* from equation 2.1.3, PD_{ij} is the density of prey type j (g wet weight/m^3), v_{ij} is the vulnerability of prey type *j* to herring *i* (dimensionless), and K_{ij} is the half saturation constant (g wet weight/m^3) for individual herring *i* feeding on prey type *k* (*k=1, 2, … j, … n*). Because the herring model is tracking one fish, there is only one predator.

A total of three prey types are represented in the current fish model, microzooplankton, copepods and euphausids. The prey densities are read in from the NEMURO model (µmole N/liter) and converted to g wet weight/m^3 using the conversion

$$\frac{14\mu g\ N}{\mu mole\ N} \cdot \frac{1.0e^{-6} g}{\mu g} \cdot \frac{1g\ dry\ weight}{0.07 g\ N\ dry\ weight} \cdot \frac{1g\ wet\ weight}{0.2 g\ dry\ weight} \cdot \frac{1.0e^{3} liters}{m^3}$$

In Figure 2.1.7, the time-dependent solution to the NEMURO model for the three prey groups at the Station P location is shown. These data were used to drive herring consumption using the multiple species functional response model.

In the situation when there are multiple prey types, Figure 2.1.6 becomes more difficult to graphically represent. Figures 2.1.8 to 2.1.11 represent equations 2.1.13 and 2.1.14 for various parameter values.

In Figure 2.1.8, we represent fish consumption of three prey types from the NEMURO LTL model (small zooplankton, large zooplankton and predatory zooplankton) as stacked bars, where the height of the bar is cumulative consumption from equation 2.1.13, and the colored segments within a bar represent the consumption of each prey type.

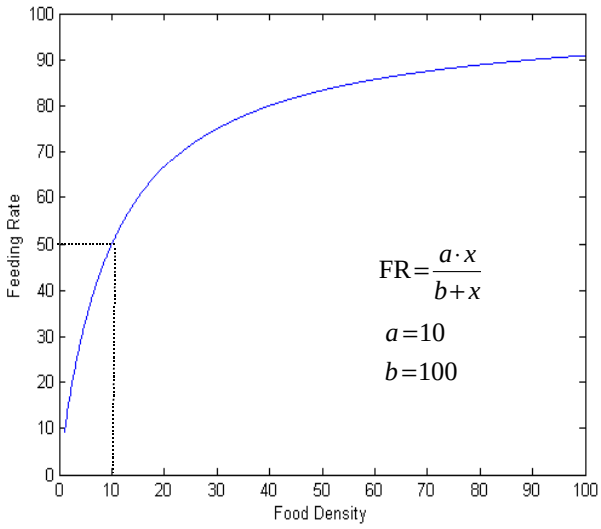

Fig. 2.1.6 Type II functional response describing the theoretical relationship between available food density and feeding rate when there is just one prey type.

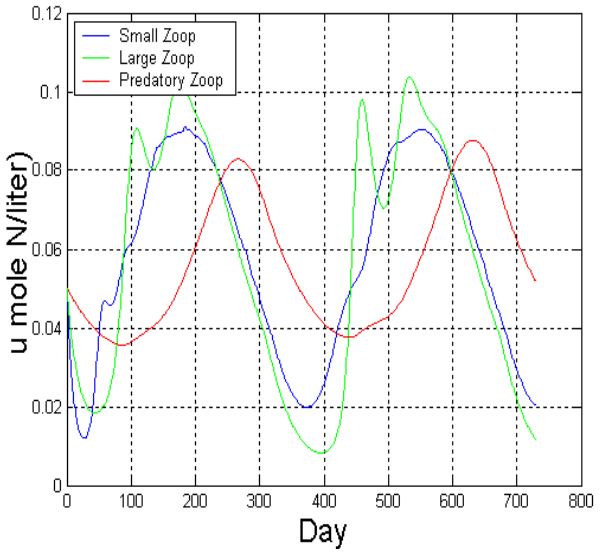

Fig. 2.1.7 NEMURO model output showing time-dependent dynamics of small, large and predatory zooplankton.

The parameters at the left of the figure were used in equations 2.1.13 and 2.1.14. For each panel within a figure, the vulnerability of one prey type was changed from 0 to 1, while keeping all other parameters the same and assigning the vulnerability parameter for the remaining two prey type to 1.0. For example, in the top panel of Figure 2.1.8, the vulnerability parameter for small zooplankton was varied from 0.0 to 1.0, while keeping the vulnerability parameter for large zooplankton and predatory zooplankton equal to 1.0 and using the parameters at the left of the figure in equations 2.1.13 and 2.1.14. In the middle panel, just the vulnerability for large zooplankton was varied from 0.0 to 1.0, while holding the vulnerabilities for small zooplankton and predatory zooplankton at 1.0. In the bottom panel, only the vulnerability for predatory zooplankton was varied from 0.0 to 1.0.

These results show that, for the prey whose vulnerability is changing (let us call it the target prey type), the contribution of the target prey type to total consumption ranges from 0.0 at 0.0 vulnerability, gradually increases as vulnerability increases, until a vulnerability of 1.0, where its contribution to total consumption is exactly one third. Also total consumption gradually increases as the proportion of the target prey type increases with increasing vulnerability to the predator.

Also note that the right-most bar in each panel is the same (height and contribution of each prey type) when vulnerability is 1.0 for all prey types.

Using Figure 2.1.8 as a base case, Figure 2.1.9 shows the change when the half saturation constant for large zooplankton (K_2) is changed from 100.0 to 10.0. Now each panel in Figure 2.1.9 is similar to the corresponding panel in Figure 2.1.8 (the base case), except that large zooplankton make up the bulk of total consumption regardless of which prey types vulnerability is changed.

Now using Figure 2.1.9 as a base case, Figure 2.1.10 shows the change when the density of predatory zooplankton (PD_3) is changed from 2.0 to 4.8. Now each panel in Figure 2.1.10 is similar to the corresponding panel in Figure 2.1.9, except that the contribution of predatory zooplankton to total consumption is higher in each case. Also, the height of each bar (total consumption) is higher in Figure 2.1.10 compared to Figure 2.1.19.

Figure 2.1.11 shows the results of the mutispecies feeding functional response for the parameter values used in the herring application.

PD_1=2.0
PD_2=2.0
PD_3=2.0
C_{MAX}=2.5

K_1=100.0
K_2=100.0
K_3=100.0

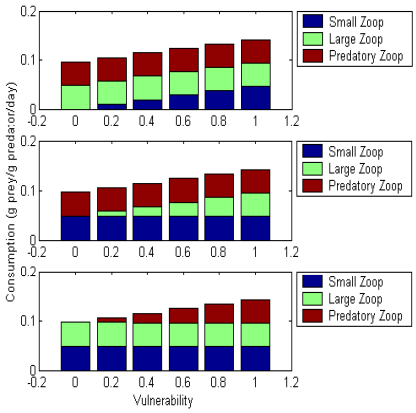

Fig. 2.1.8 An example of the mutispecies functional response formulation (equations 2.1.13 and 2.1.14) for three prey groups, varying the vulnerability of the target prey group one at a time.

PD_1=2.0
PD_2=2.0
PD_3=2.0
C_{MAX}=2.5

K_1=100.0
K_2=10.0
K_3=100.0

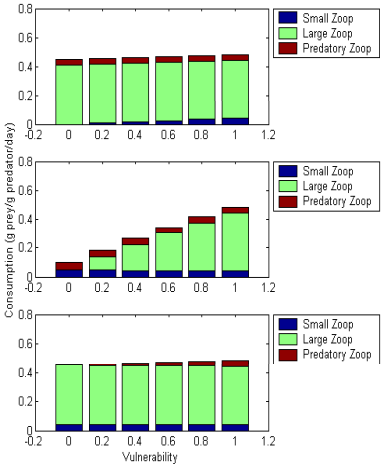

Fig. 2.1.9 An example of the multispecies functional response formulation (equations 2.1.13 and 2.1.14) for three prey groups, varying the vulnerability of the target prey group one at a time, and changing the half saturation constant for prey group 2 (K_2) from 100.0 to 10.0.

PD_1=2.0
PD_2=2.0
PD_3=4.8
C_{MAX}=2.5

K_1=100.0
K_2=10.0
K_3=100.0

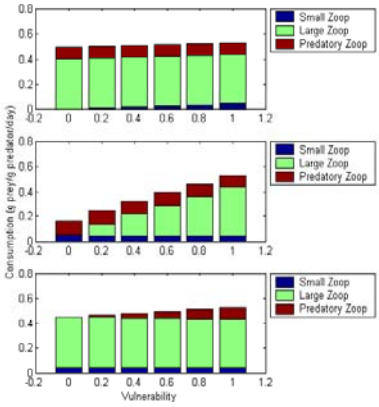

Fig.2.1.10 An example of the multispecies functional response formulation (equations 2.1.13 and 2.1.14) for three prey groups, varying the vulnerability of the target prey group one at a time, changing the half saturation constant for prey group 2 (K_2) from 100.0 to 10.0, and changing the density of prey group 3 (PD_3) from 2.0 to 4.8.

PD_1=1.8
PD_2=0.8
PD_3=4.8
C_{MAX}=2.5

K_1=100.0
K_2=10.0
K_3=100.0

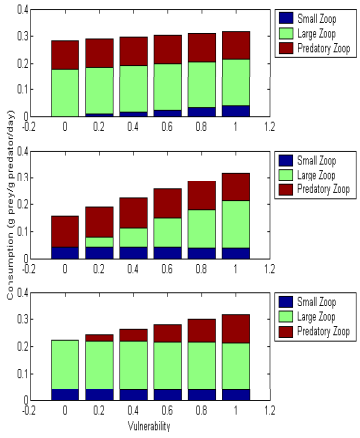

Fig. 2.1.11 An example of the multispecies functional response formulation (equations 2.1.13 and 2.1.14) for three prey groups, varying the vulnerability of the target prey group one at a time using the parameters in the herring model.

Linking a fish bioenergetics model to the NEMURO LTL model

The NEMURO LTL model and the fish bioenergetics model were developed independently. Linking the two models involves paying close attention and reconciling two important differences: 1) the way the two models account for time, and 2) the way NEMURO generates phytoplankton and zooplankton densities (mole N/liter), and the way the fish bioenergeticsmodel expects phytoplankton and zooplankton densities (µmole N/liter). These differences are presented in Table 2.1.1. Reconciling these differences requires the use of several conversion coefficients, which can be seen in the code presented in Appendices 4 and 5.

Table 2.1.1 Ways in which NEMURO and the fish bioenergetics model account for time and LTL densities.

Model	Time	LTL Density
NEMURO	seconds	mole N/liter
Fish Bioenergetics	day	µ mole N/liter

Linking the fish bioenergetics model to NEMURO can be done in two ways. In a static linkage (Fig 2.1.12), the NEMURO model is run and a time series of small, large and predatory zooplankton abundances are stored in an output file and used as an input file for the fish bioenergetics model where they influence the consumption term of the bioenergetics governing equation 2.1.1. The models are run sequentially and there is no feedback between the two models.

In the dynamic linkage (Fig 2.1.13), the models are run simultaneously, the zooplankton prey groups contribute to the consumption term of the fish bioenergetics governing equation 2.1.1, the ZOOS, ZOOL, and ZOOP state variables of NEMURO are reduced by the amount eaten by herring, fish excretion waste is added to the nitrogen pool of NEMURO, and fish egestion waste is added to the DOM pool of NEMURO.

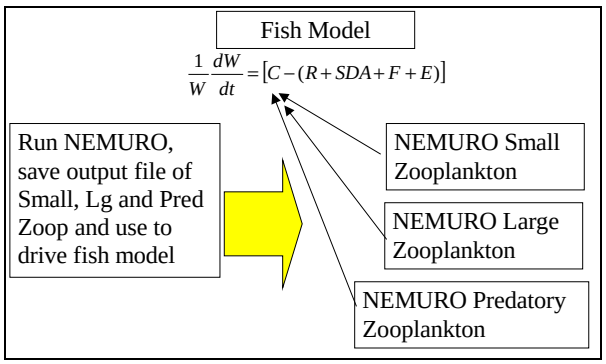

Fig. 2.1.12 Example of a static linkage between NEMURO and the bioenergetics fish model.

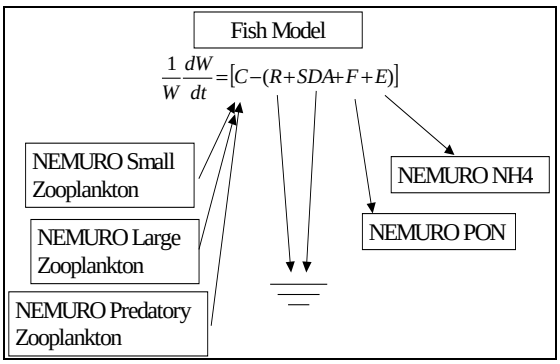

Fig. 2.1.13 Example of a dynamic linkage between NEMURO and the bioenergetics fish model..

Table 2.1.2 Summary of parameter values used in the generalized herring bioenergetics model from Rudstam (1988).

Symbol	Parameter description	Value	
Consumption, C_{MAX}			
a_C	Intercept for C_{MAX} at (te1+te3)/2		0.642
b_C	coefficient for C_{MAX} versus weight	-0.256	
te1	Temperature for xk1 (in ºC)		1[a] 1[b]
te2	Temperature for xk2 (in ºC)		15[a] 13[b]
te3	Temperature for xk3 (in ºC)		17[a] 15[a]
te4	Temperature for xk4 (in ºC)		25[a] 23[b]
xk1	Proportion of C_{MAX} at te1	0.10	
xk2	Proportion of C_{MAX} at te2	0.98	
xk3	Proportion of C_{MAX} at te3	0.98	
xk4	Proportion of C_{MAX} at te4	0.01	
Metabolism, R			
a_R	Intercept for R		0.0033
b_R	Coefficient for R versus weight		-0.227
c_R	Coefficient for R versus temperature		0.0548
d_R	Coefficient for R versus swimming speed	0.03	
S	Coefficient for Specific Dynamic Action		0.175

Table 2.1.2 (cont.)

Symbol	Parameter description	Value	
Swimming Speed, U			
a_A	Intercept U (< 9 ºC) (in cm/s)		3.9
a_A	Intercept U (≥ 9 ºC) (in cm/s)		15.0
b_A	Coefficient U versus weight		0.13
c_A	Coefficient U versus temperature (< 9 ºC)	0.149	
c_A	Coefficient U versus temperature (≥ 9 ºC)	0.0	
Egestion and Excretion, F and E			
a_F	Proportion of consumed food egested		0.16
a_E	Proportion of consumed food excreted		0.10

a - values for age 0 and 1herring
b - values for age 2 and older herring

2.2 Review of Clupeid biology with emphasis on energetics

Robert A. Klumb
Department of Natural Resources, Cornell Biological Field Station, Cornell University, 900 Shackelton Point Road, Bridgeport, NY 13030, U.S.A. E-mail: rak11@cornell.edu

The general bioenergetics model based on the Law of Thermodynamics balances all consumed energy as follows: G = C – R – F – U, where G=growth, C=consumption, R=metabolism (respiration), F=egestion, and U=excretion. Consumed energy is first allocated to costs of metabolism and waste losses with the remainder available for somatic growth. Energy lost by the gametes released during spawning can also be included. Formulas and parameters provided below for the individual components in the bioenergetics model follow the terminology and symbols used in Hansen *et al.* (1997). Energy equivalent conversion factors for oxygen consumption, carbohydrates, fats, and protein can be found in Elliott and Davison (1975), with additional comments on the oxycalorific coefficient found in Brett (1985).

Consumption

Consumption (C) = C_{max}*P-value*f(T) and $C_{max}=CA*W^{CB}$

Consumption (g prey·g^{-1}·d^{-1}), is generally modeled as an allometric (power) function of weight. Maximum consumption rates are determined in laboratory experiments by feeding fish a known (by weight) *ad libitum* ration and then subtracting uneaten food after a specified time interval. For adult alewife *Alosa pseudoharengus*, the specific slope for weight dependence on maximum consumption was -0.3 (Stewart and Binkowski 1986), a value intermediate to that found in studies of larval and juvenile clupeids (De Silva and Balbontin 1974; Theilacker 1987). The specific weight-dependent slope (CB) for maximum consumption of northern anchovy *Engraulis mordax* larvae (wet weight < 0.001 g) re-calculated from data in Theilacker (1987) was -0.367, while the slope for Atlantic herring (wet weight 8 – 15 g) was -0.256 (De Silva and Balbontin 1974). Rudstam (1988) used the slope and intercept derived by De Silva and Balbontin (1974) in the bioenergetics model for adult Atlantic herring *Clupea harengus* consumption. Due to a lack of data for larval and juvenile fishes, the same relations for maximum consumption of adult herring and alewives were applied to age-0 fish by Arrhenius (1998a) and Klumb *et al.* (in review), respectively.

The "P-value" in the bioenergetics model refers to the proportion of maximum consumption. This value is used to fit the bioenergetics model to observed growth or can be set constant to check resultant growth potential in varied environments.

Temperature dependence of consumption is usually modeled as simple or modified exponential functions (Hansen *et al.* 1997). For cool- and cold-water species, the temperature dependence of consumption is generally modeled using a curve proposed by Thorton and Lessem (1978), which modified the logistic equation. This function is the product of two intersecting sigmoid curves (one ascending and one descending) forming a "humped" curve across the entire temperature range inhabited by a given species.

Required parameters include the approximate temperatures for optimum consumption, and the high and low temperatures where consumption is dramatically reduced (~98%) compared to maximum consumption. Any temperatures derived from laboratory or field data showing maximum or reduced consumption levels can be used. If specific data relating consumption and temperature are lacking, the optimum of consumption is generally equated to the fish's thermal optimum for growth (Beitinger and Magnuson 1979), and the temperatures where consumption is dramatically reduced are derived from the thermal tolerances (survival limits) of a species.

Metabolism/respiration

Total metabolism = Respiration + specific dynamic action (SDA)

where

Respiration (R) = $RA*W^{RB}$ * f(T)*Activity and $f(T) = e^{RQ*T}$

Metabolism of fishes is determined by measuring oxygen consumption at various temperatures over a known time period, and generally modeled as an allometric function of weight and an exponential function of temperature. Brett and Groves (1979) distinguished three types of metabolism in fishes: standard, routine and active. By definition, standard metabolism is the minimum energy requirements needed by a fish at rest (also known as basal metabolism), and it is this metabolic state that is used in bioenergetics models. Measuring standard metabolism is difficult and requires use of anesthetized fish or fish with movements confined by small respirometers. Routine metabolism includes normal spontaneous activity, while active metabolism includes the cost for activity above the spontaneous activity level. Winberg (1956) stated that active metabolism was approximately twice standard metabolism (*i.e.* the "Winberg multiplier" of 2). However, Ware (1975) indicated active metabolism could range from 2 to 3 times standard rates. Bioenergetics models generally use allometric function parameters derived for standard metabolism multiplied by a temperature function and an activity factor to estimate total respiration costs.

Respiration (g oxygen$\cdot g^{-1}\cdot d^{-1}$) of adult fishes generally scales negatively with weight (*i.e.* negative slope), and ranges from -0.25 to -0.15 on a weight specific basis (Winberg 1956). For clupeids, slopes of the metabolism-weight relations ranged from -0.19 to -0.28 for Atlantic menhaden *Brevoortia tyrannus* (Hettler 1976), -0.215 for alewife (Stewart and Binkowski 1986), and -0.227 for Atlantic herring (De Silva and Balbontin 1974). Rudstam (1988) used -0.227 in the adult Atlantic herring bioenergetics model, and this value was also applied to age-0 herring (Kerr and Dickie 1985; Arrhenius 1998a). The slope for the metabolism-weight relation of *Maurolicus muelleri*, a mesopelagic planktivore, was -0.15 (Ikeda 1996).

The relation of respiration to weight of fishes has been found to change ontogentically, with isometric (mass independent) relations for larvae switching to negative allometries in adults (Post and Lee 1996). However, the variability of slopes found in the review of 31 species by Post and Lee (1996) highlighted the need to derive weight-metabolism relations for the larvae of individual species. The final weight-metabolism relation derived likely depends on the range of fish sizes used. Studies of larval fishes encompassing greater than three orders of magnitude in weight documented isometric relations between metabolism and weight for Clupeidae (Klumb *et*

al., in review), Cyprinidae (Kamler 1972), and Scombridae (Giguère *et al.* 1988).

Specific dynamic action (SDA)

SDA = SDA*(C – F)

Specific dynamic action, or more appropriately termed "apparent specific dynamic action" and also known as the "heat increment", is the energy allocated to the digestive processes of food, principally deamination of proteins but also includes energy costs of absorption, transportation and deposition of food (Beamish 1974). Oxygen consumption by fasting and fed fish in flow-through respirometers (where the fish is subjected to a known level of activity, *i.e.*, forced to swim against a known current) is required to measure SDA (Beamish and Trippel 1990). Beamish and Trippel (1990) found that SDA increased with meal size and body weight but declined with weight at fixed rations. However, in most bioenergetic models, SDA is considered a constant proportion of ingested energy with values for adult fish ranging from 10-29% (reviewed by Beamish and Trippel 1990). The SDA parameter in bioenergetics models is generally borrowed from non-related species because proper measurement requires strict laboratory experiments using specialized equipment. For adult alewife (Stewart and Binkowski 1986) and adult Atlantic herring (Rudstam 1988), SDA was assumed to be 17.5% based on data for aholehole *Kuhlia sandvicensis* (Muir and Niimi 1972). Arrhenius (1998a) lowered SDA to 15% for age-0 Atlantic herring. Larval clupeids have been found to assimilate food more efficiently than adults (Kiørboe *et al.* 1987). In energetic terms, Kiørboe *et al.* (1987) estimated SDA for larval Atlantic herring to be 10% of assimilated rations, and Limburg (1994) calculated the mean SDA for American shad *Alosa sapidissima* juveniles to be 13%.

Activity

$Activity = e^{RTO*VEL}$,
where $VEL = RK1*W^{RK4}$ for $T \geq RTL$
or $VEL = ACT*W^{RK4}*e^{BACT*T}$ when $T < RTL$

The energetic cost of activity is generally considered a multiple of standard metabolism. A simple constant, *i.e.* the "activity multiplier = 2" of Winberg (1956), can be used to accord increased (aerobic) metabolic costs due to swimming. Exponential functions have been used to model activity costs of adult alewife (Stewart and Binkowski 1986) and Atlantic herring (Rudstam 1988). The exponential model is composed of three components: 1) VEL which is the weight dependence of swimming speed (cm/s), 2) the temperature (T) dependence of swimming speed (BACT), and 3) the relation of respiration to swimming speed (RTO). The parameter ACT is the intercept (cm/s) for a 1-g fish at 0°C. Swimming speed can change from temperature dependence to independence (at T = RTL). Swimming speeds of Atlantic herring were only dependent on weight at temperatures > 9°C (Rudstam 1988), and alewife swimming speeds were independent at > 15°C. (Stewart and Binkowski 1986)

The coefficient for swimming speed dependence of metabolism (RTO) used in the adult alewife model was assumed constant (RTO = 0.03) and based on data in Muir and Niimi (1972). Data for Cape anchovy *E. capensis* found that coefficients before, during, and after feeding ranged from 0.01 to 0.04 (James and Probyn 1989). A coefficient relating respiration and swimming speed of 0.03 has also been reported for adult menhaden (Durbin *et al.* 1981), and the coefficient for adult coregonids was 0.02 (Dabrowski 1985). However, the coefficient relating respiration rate to swimming speed increased substantially in larval coregonids (Dabrowski 1986) and cyprinids (Kaufmann 1990); therefore, a constant relating metabolic cost to swimming speed is inappropriate for early life stages. Using an exponential activity function and a constant relating swimming speed to oxygen consumption resulted in essentially no energetic costs for the activity of YOY alewife (Klumb *et al.*, in review).

How to best model the activity costs of larval fish is uncertain since existing data from the few studies relating metabolism and swimming speeds at early life stages are equivocal. Because the slope of metabolism versus swimming speed varied with body size, Dabrowski *et al.* (1988) found active metabolic rates of coregonids to be 5 - 50 times standard metabolism. A size-effect on

the slope for the metabolism-swimming speed relation also existed for larvae of two cyprinid species (Kaufmann 1990); however, ratios of routine metabolism to standard metabolism were low (< 1.5) and essentially flat from 0.005 - 0.300 g (wet weight). In Kaufmann's (1990) study, ratios of active to routine metabolism (*i.e.*, the factorial scope) ranged from 2 - 4. These contrasting results may lie in the function chosen to describe the metabolism-swimming speed relation, *i.e.*, exponential (Dabrowski 1986; Dabrowski *et al.* 1988) or allometric (Kaufmann 1990). However, using an exponential model, Wieser and Forstner (1986) found the ratios of active to routine metabolism for larvae of three cyprinid species ranged from 1 - 4 and were independent of weight (0.01 - 0.3 g wet) and temperature (12 - 24°C). Activity rates of fishes can also vary widely with growth rate and food density (Ware 1975), while laboratory measurements of metabolism during activity may be higher than actual costs in the wild, since larvae are also passively moved by water currents. Klumb *et al.* (in review) used routine metabolism parameters without an activity multiplier in a bioenergetics model for age-0 alewife.

Clupeids have pronounced changes in activity patterns possibly due to circadian rhythms (Katz 1978; Batty 1987). Clupeids do not swim in schools during darkness (Limburg 1994). Accuracy of bioenergetic estimates of herring consumption were improved when including diel feeding cycles (Arrhenius 1998a).

Egestion

Egestion (F) = FA*C

Egestion is modeled as a constant proportion of consumption. Assimilation efficiency (in terms of energy) of adult menhaden ranged from 86 to 92% (Durbin and Durbin 1981). In the adult alewife (Stewart and Binkowski 1986) and Atlantic herring models (Rudstam 1988), egestion was assumed to be 16% of consumption.

Data for egestion processes and models are not common; most extensive studies have been done for brown trout *Salmo trutta* (Elliot 1976a, 1976b). Egestion has been found to be a function of temperature and ration (Elliott 1976a). However, Stewart and Binkowski (1986) found small changes in estimated consumption when making the simplified assumption of egestion being a constant proportion of consumption in the bioenergetics model for alewife.

The proportion of consumption egested has been found to be low in larval and juvenile clupeids (Kiørboe *et al.* 1987; Limburg 1994). Arrhenius (1998) used 16%, the value from the adult Atlantic herring (Rudstam 1988) and alewife (Stewart and Binkowski 1986) models for the proportion of assimilated ration egested by larval Atlantic herring. Both Kiørboe *et al.* (1987) and Limburg (1994) found the percentage of food egested was 10% (by mass). However, Klumpp and von Westernhagen (1996) found egestion for Atlantic herring larvae age 8 - 33 days averaged 17.6% (range 13.4 - 25.6%) of ration (*Artemia* sp. nauplii) energy content.

Based on the above three studies on larval and juvenile clupeids (Kiørboe *et al.* 1987; Limburg 1994; Klumpp and von Westernhagen 1996), Klumb *et al.* (in review) chose 0.125 as a first approximation for the proportion of consumption egested by larval and juvenile alewife.

Excretion

Excretion (U) = UA*(C – F)

Excretion is modeled as a constant proportion of assimilation (consumption minus egestion). In the adult alewife (Stewart and Binkowski 1986) and Atlantic herring models (Rudstam 1988), excretion was assumed to be 10% of assimilation based on rates measured for brown trout (Elliott 1976b).

Few studies on larval fish excretion have been conducted. For three species, *Blennius pavo*, plaice *Pleuronectes platesssa*, and Atlantic herring, Klumpp and von Westernhagen (1996) found the mean percent of the assimilated ration excreted was 6.0, 6.6 and 10.7%, respectively. Due to high mortality for Atlantic herring larvae in Klumpp and von Westernhagen's study, Klumb *et al.* (in review) used the average value of 7.8% for all three species as a first approximation of the

percent of assimilation excreted by larval and juvenile alewife.

Data requirements

There are four data requirements for the bioenergetics model: 1) diet (in proportions of prey types), 2) energy density of the predator fish, 3) energy density of the prey, and 4) water temperatures. The bioenergetics model is an individual based model but can incorporate populations by multiplying mean weight by population number.

Diet

Diet information was summarized by Douglas E. Hay (Pacific Biological Station, Fisheries and Oceans Canada) based on recent observations (Hay and McCarter 2001, and older literature such as Wailes 1936). Depending on the population, herring diets can be simple or complicated. The simple story is that herring eat mainly copepod eggs and nauplii as larvae, copepod adults and nauplii as juveniles and euphausiids as adults. This over-simplified` story gets messy when the smaller, non-migratory marginal populations are examined because they appear to eat a wider variety of taxa. Herring feed intensely in the summer months but they also eat during winter. In all areas, winter diets, although small in relation to total annual consumption, may be more variable than summer diets. Perhaps the main point to emphasize, however, is that in southern British Columbia, most herring feed in shelf waters where the main food items are euphausiids. Atlantic herring and sprat *Sprattus sprattus* diets consisted of 70 - 73% copepods, 12 - 14% *Oikopleura*, and 9 - 12% cladocerans (De Silva 1973).

Adult clupeids feed by filtering or particulate feeding (Blaxter and Hunter 1982; Janssen 1976). Janssen (1976) found for alewives that the filter feeding mode displayed by large alewives (total lengths > 170 mm) was not size-selective, while particulate feeders (total lengths 50 - 115 mm) selected zooplankton > 1.0 mm. Transition of larvae to adult body morphology and feeding modes occurs at metamorphosis (~35 mm) after gill rakers and the upper and lower jaws become developed (Blaxter and Hunter 1982). Although activity of clupeids may be lower at night (Katz 1978), filter feeders can still feed in darkness (Hettler 1976; Janssen and Brandt 1980; Grabe 1996).

Feeding activity of larval herring has been found to be dependent on densities of copepod nauplii (Munk and Kiorboe 1985) with success a function of prey size (Hunter and Blaxter 1982). Atlantic herring (length 25 mm) larvae were able to consume prey sizes ≥ 1.0 mm (Sherman and Honey 1971, cited in Hunter and Blaxter 1982). Foraging behavior of Altantic herring larvae changed with prey size and was related to larval length by the equation: prey length = 0.027*larval length (Munk 1992), and attack success was directly related to relative prey size. Fiksen and Folkford (1999) included the mouth size of herring larvae, perception (visual field and reaction distance), light intensity, and the length, width and density of plankton prey when modeling encounter rates and probabilities of successful strikes.

Energy density of predator and prey

Energy density, also called caloric content and energy content, in bioenergetics models is used in terms of wet weight. Dry-weight data are customarily converted (approximated) to wet weight assuming dry weight is 10 - 20% of total weight. Hartman and Brandt (1995) provided many equations for estimating energy density from the percent dry weight of various marine and freshwater fish species. Assuming constant energy densities or using values that are too high or low can greatly affect bioenergetics model consumption estimates (Stewart and Binkowski 1986).

Energy density (ED) of clupeids has been found to vary seasonally, peaking in fall and declining through winter (Arrhenius and Hansson 1996; Flath and Diana 1985; Paul *et al.* 1998). Age-0 EDs are lower than older fish (Arrhenius and Hansson 1996; Flath and Diana 1985; Paul *et al.* 1998). For age-1 alewife in Lake Michigan, ED in June and July was 4520 $J \cdot g^{-1}$, increased in August and September to 4729 and 5440, respectively, then declined to 4729 in April, and 4436 by May (Flath and Diana 1985). For age-0 Atlantic herring, Arrhenius and Hansson (1996) found ED

increased from 2600 $J \cdot g^{-1}$ in mid-July to 4500 $J \cdot g^{-1}$ in October. The ED of age-0 Baltic Sea sprat increased from 4000 $J \cdot g^{-1}$ in August to approximately 5250 $J \cdot g^{-1}$ by December (Arrhenius 1998b). October ED of alewife was 5020 $J \cdot g^{-1}$ (Flath and Diana 1985).

Higher energy densities were found for Pacific herring off Alaska (Paul *et al.* 1998; Foy and Paul 1999) compared to Great Lakes alewives and Baltic Sea clupeids. Age 2+ Pacific herring had EDs in fall that ranged from 9400 to 10200 $J \cdot g^{-1}$ and declined over winter to 5200 to 6300 $J \cdot g^{-1}$ by spring. Females had higher energy densities in both seasons than males by 200 - 400 $J \cdot g^{-1}$. Age-0 herring had EDs of 5700 $J \cdot g^{-1}$ in fall which declined to 4400 $J \cdot g^{-1}$ by the following spring (Paul *et al.* 1998). Equations to predict ED from standard length of juveniles by month are provided in Paul and Paul (1998a). The ED for age-0 captive fasting herring declined 23 $J \cdot g^{-1} \cdot d^{-1}$ from December to the end of January (Paul and Paul 1998b).

Energy densities of freshwater and marine invertebrates can be found in Cummins and Wuycheck (1971), while good tables of the caloric content of marine invertebrates (with references) are presented in Foy and Norcross (1999) and Foy and Paul (1999). Laurence (1976) provides energy densities for marine calanoid copepods in the Atlantic. Like fish, the energy density for invertebrates has been found to vary seasonally.

Table 2.2.1 Energy densities (jouls/gram) for main food items of Pacific herring.

Food Item	**$J \cdot g^{-1}$**
Copepoda	2580
Euphausiids (per gram wet weight)	5020
Fish eggs (per gram wet weight)	4520

Table 2.2.2 Existing bioenergetic models.

Reference	Comments
General models	
Winberg 1956	extensive early work but reference not that accessible
Kitchell *et al.* 1974	results of International Biological Program (IBP) workshops and first paper of the "Wisconsin" bioenergetics model – applied to bluegill sunfish (*Lepomis macrochirus*) in terms of mass balance
Elliott 1976b; 1979	general review of energetics resulting from his extensive work with brown trout (*Salmo trutta*)
Stewart *et al.* 1983	changed the Kitchell *et al.* 1974 model from mass to energy balance, for lake trout (*Salvelinus namaycush*)
Clupeid bioenergetics models	
Rudstam 1988	Adult Atlantic herring (*Clupea harengus*)
Kerr and Dickie 1985	Age-0 Atlantic herring
Arrhenius 1998	Age-0 Atlantic herring
Fiksen and Folkford 1999	Larval Atlantic herring– Individual based model, which includes metabolism, ingestion, prey encounter success, and multiple prey functional response
Stewart and Binkowski 1986	Adult alewife (*Alosa pseudoharengus*)
Hewett and Stewart 1989	Age-0 alewife: (only temperatures for the consumption component differed from the adult model)
Klumb *et al.* In review	Age-0 alewife
Durbin and Durbin 1983	Adult menhaden (*Breoortia tyrannus*):– in terms of energy and Nitrogen

2.3 Reflections of factors affecting size-at-age and strong year classes of herring in the North Pacific

Douglas E. Hay
Pacific Biological Station, Fisheries and Oceans Canada, 3190 Hammond Bay Road, Nanaimo, British Columbia, Canada V9R 5K6. E-mail: hayd@pac.dfo-mpo.gc.ca

One approach to the investigation of linkages between oceanographic process and subsequent impacts on marine fish populations, is retrospective analyses of age-specific growth rates (size-at-age) from archive collections of scales or otoliths. This approach can be linked to independent observations on (1) temporal variation in abundance, (2) synchrony or asynchrony of year-class strength among different populations, or different species, and (3) habitat requirements of life history stages (eggs, larvae, juveniles, adults) that have different spatial and trophic characteristics.

Widespread geographic synchrony sometimes occurs in Pacific herring (Hollowed and Wooster 1995, Hay *et al.* 2001). An exceptionally strong year-class occurred in 1977 over a broad and geographic range (Fig. 2.3.1). It was strong in northern BC, parts of south-eastern and central Alaska and the Bering Sea (Hollowed and Wooster 1995). This 1977 year-class developed in different populations with different spawning times, with a range of about 3 months from the earliest to the latest mean spawning time. Pacific herring spawn in shallow, inshore inter-and subtidal waters. In many areas of the Pacific coast of North America, spawn deposition is monitored and quantified annually. Spawn deposition was not exceptional in 1977. Therefore, it follows that in 1977, survival from eggs to the juvenile and recruit stage, between 1977 and 1980, was relatively higher (or mortality was lower) than most other years. It also follows that the factor(s) that promoted the strong year-class were widely distributed in space and time.

Retrospective analysis of archived herring scales (Fig. 2.3.2) from northern BC populations, indicates that individuals of the 1977 year-class were of normal size, or slightly larger than normal, relative to samples from other years (Fig. 2.3.3).

After age 4, the relative size-at-age of individuals in the 1977 year-class declined, and was smaller than normal, which indicates that growth rate declined in older individuals. This retrospective analysis of growth from scale analysis was corroborated by analyses of catch-sampling data, collected routinely for the last 70 years. The size-at-age of 3-year-old members of the 1977 year-class was normal in most areas in 1980, but size-at-age of older individuals (*e.g.* age 6 fish collected in 1983) was smaller than normal (Fig. 2.3.4).

A strong 1977 year-class also occurred in several other species, including blackcod and lingcod (Hollowed and Wooster 1995). Climate-related changes, but not necessarily increases in abundance, also occurred in other marine species including salmonids (Beamish *et al.* 1999) and pollock *Theragra chalcogrammus* (Ohtani and Azumaya 1995). Further, there are periods when there has been synchrony of strong year-classes among different species in the North Pacific (Hollowed *et al.* 1987), which is evidence of environmental influence on the production of year-class strength.

The habitats occupied by age 1 and 2 herring are mainly inshore (Haegele 1997), whereas most of the older age groups (age 3 and older) tend to occupy shelf waters. During intensive summer feeding periods, juvenile herring are found mainly in shallow, nearshore waters of less that 50 m. In general, age 1 juveniles occur in shallower waters, closer to shore, than age 2 herring. In general, herring form shoals of similar-sized individuals so the two larger age groups do not mix, although both age groups of juveniles occur in the same vicinities, herring juveniles are widely dispersed through all BC coastal waters.

Over the last 70 years in British Columbia (BC), herring stomachs have been examined by different

people, in different years, at different places and at different herring life history stages. Wailes (1936) summarized the food of young herring mainly in the first summer of life. At very young stages, eggs (ova) and nauplii from various invertebrates are most important. Copepod nauplii seem to dominate the food but food composition varied with location. The youngest juveniles (age 1) fed mainly on copepods. Older, larger juveniles took various zooplankton, with euphausiids being common. More recent work examined gut data from herring juveniles in Georgia Strait, BC, Hecate Strait and Prince William Sound Alaska (Haegele 1997, Foy and Norcross 1999, Hay and McCarter 2001). In general the main food for herring at ages 1 and 2 is copepods. Therefore if the abundant 1977 year-class ate mainly copepods at ages 1 and 2, then copepods must have been abundant in nearshore northern waters, both in 1977 and 1978. From our present understanding of herring life history, there is little opportunity for trophic interaction (*i.e.* direct density-dependent competition for food) between age-classes: either among juveniles (ages 1 versus age 2) or between juveniles versus adults (age 3+ and older). In BC waters, probably the first opportunity for direct interaction occurs during the third winter of life, at age 2+, when (BC) herring start to mature sexually and join the adult stock. At this time, however, winter feeding is minimal and growth is slight.

The observations above can be summarized as follows. In 1977, and some other years, we see that strong year-classes can develop over broad areas of time and space. They develop in years when spawn deposition is normal, and sometimes even lower than normal. Further, sometimes they can be synchronous over broad areas of time and space. Synchrony may develop in other species. Retrospective analysis of herring scales indicates superior juvenile growth among strong cohorts, but decreased growth during older adult stages (in 1977). Strong year-classes can arise in years of normal or modest spawn deposition. These observations indicate that survival, between the egg and recruit stages, is enhanced. Such enhanced survival must occur during the juvenile stages that consume mainly copepods in nearshore habitats. Therefore strong year-classes may develop as a consequence of changes in these habitats.

If lower mortality of early life history stages is part of the explanation for the formation of the 1977 year-class - or other year classes, why did this happen? Presumably it must reflect decreases in mortality by starvation, disease or predation? In 1977, starvation seems unlikely, because juvenile growth was enhanced compared to other years. We have no evidence to suggest that disease routinely limits survival. Rather, outbreaks seem episodic, and this could explain years with exceptionally bad year-classes, but not the reverse. A decrease in predation, between the egg/larval stages and pre-recruit stage could occur if there were (i) fewer predators, or (ii) if the predators 'switched' or decreased predation on herring for a different prey species. Were predation rates on juvenile herring lower in 1977 and 1978? We have no data on this, but we observe that some common herring predators (lingcod and blackcod and some piscivorous salmon) also had strong 1977 year-classes. Therefore it seems improbable that there was a decrease in the potential community of herring predators between 1977 and 1980.

From the observations and reasoning above, we conclude that the most parsimonious explanation for the development of the strong 1977 year-class was a general decrease in predation of juveniles because the main herring predators had alternate prey. Such a reduction in predation could occur through predator switching during early life history stages - specifically, predators of herring chose to feed on an alternate food source. If this alternate food source was an unusually abundant supply of copepods, available both to the juveniles of herring and their predators, this could explain our observations. Specifically if predators preferentially switched to copepods, instead of herring juveniles, the consequence of a substantial increase in copepod availability would be both enhance survival and growth of juvenile herring.

If the cause(s) of the strong 1977 year-class was similar in all geographic areas where it occurred, from northern BC to the Bering Sea, and if the cause was from decreased predation associated with availability of an alternate food source, then clearly the factors which promoted this alternate food source were widespread. There have been

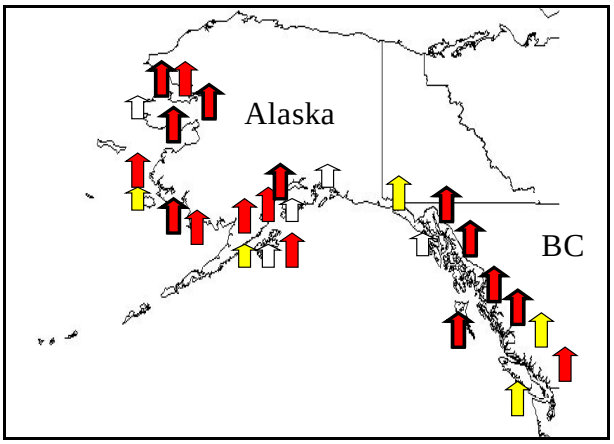

Fig. 2.3.1 Approximate locations of the strong 1977 year-class, indicated by arrows. Red arrows with dark outlines show locations where the 1977 year-class made up 70% or more of the spawning population as age 3 in 1980, or age 4 in 1981. Plain red and yellow arrows show populations where the 1977 year-class represented over 50% and 40% of the populations, respectively.

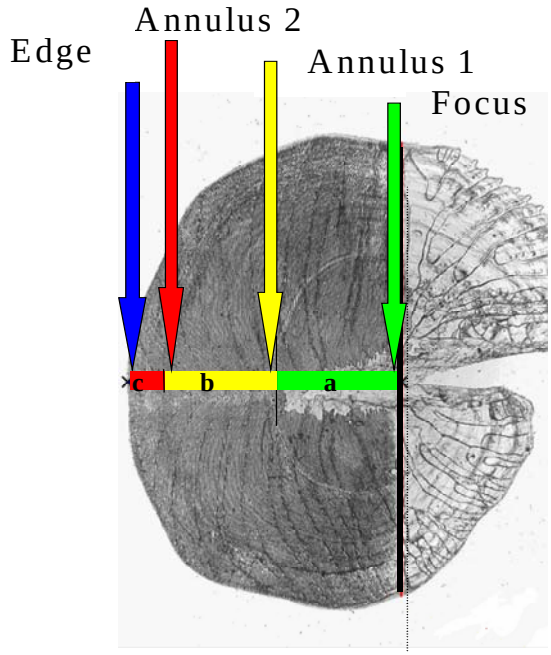

Fig. 2.3.2 A herring scale, showing the focus (start of growth) and the first and second annuli. Retrospective indices of age-specific growth rates during the first year (green bar a) and second year (yellow bar b) was determined by direct measurement of scales.

some suggestions (Hollowed and Wooster 1992; Polovina *et al.* 1995) that there can be such linkages between offshore oceanographic changes and changes in productivity or food abundance on shelf and inshore waters, resulting from mid-gyre changes, but these are not well understood. If there were such a relationship, the impact of an

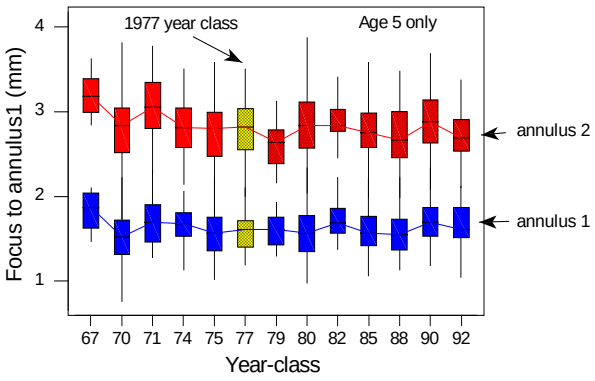

Fig. 2.3.3 Retrospective analyses of scale growth of 5-year-old-herring from archived collections of scales from northern BC. Scale growth, corresponding to juveniles at age 1 (blue rectangles) and age 2 (red rectangles), as estimated from comparison of focus: annuli distances, was normal in the 1977 year-class. The 1977 year-class is shown in yellow. The boxes and vertical lines represent the range and 95% confidence limits about the mean.

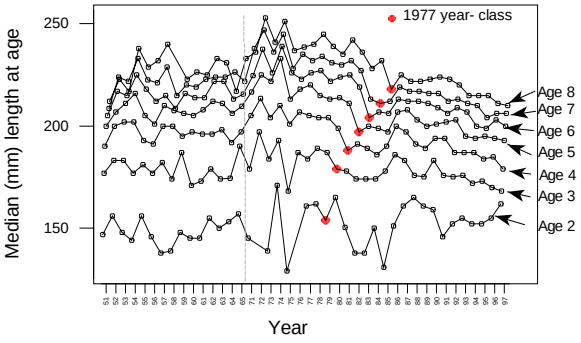

Fig. 2.3.4 Comparison of the size-at-age of the 1977 year-class with those of other years from catch sampling data collected in northern BC. The 1977 year-class (large dark circles) was normal (or slightly larger than normal at age 2). Thereafter, the relative size-at-age, relative to previous year-classes, decreased until age 8.

abundant production of zooplantion, specifically copepods, could explain both enhanced growth and year-class survival in herring and other species. There is a precedent for assuming that an abundant source of an alternate zooplankton prey species can reduce predation on herring. Ware and McFarlane (1995) showed that increased euphausiid production resulted in a decreased hake predation on adult herring off the west coast of Vancouver Island. Similar mechanisms mightoperate at the juvenile stages, so factors promoting a strong year-class of herring might also support strong year-classes of other species, leading to synchrony between unrelated species such as such as blackcod and lingcod. Again, the answer is a tentative yes. Both of these species have early life stages (first several years of life) in nearshore waters.

2.4 Review for Pacific saury (*Cololabis saira*) study under the VENFISH project

Shin-ichi Ito[1], Yutaka Kurita[1], Yoshioki Oozeki[2], Satoshi Suyama[3], Hiroya Sugisaki[1], Yongjun Tian[2]

[1] Tohoku National Fisheries Research Institute, 3-27-5 Shinhamacho, Shiogama, Miyagi 985-0001, Japan. E-mail: goito@affrc.go.jp, sugisaki@mgy.affrc.go.jp

[2] National Research Institute of Fisheries Science, 2-12-4 Fukuura, Kanazawa-ku, Yokohama, Kanagawa 236-8648, Japan. E-mail: oozeki@affrc.go.jp

[3] Hachinohe Branch, Tohoku National Fisheries Research Institute, Same, Hachinohe, Aomori 031-0841, Japan. E-mail: suyama@myg.affrc.go.jp

VENFISH (Comprehensive study of the Variation of the oceanic ENvironment and FISH populations in the northwestern Pacific) project was started in April 1997 and will end in March 2002. This project has been supported by Japan Agriculture Forest Fisheries Agency. The aim of this project is clarification of bottom-up control process for Pacific saury and walleye pollock in the Northwestern Pacific. More than 20 scientists from National Fisheries Research Centers at Hokkaido, Tohoku, Yokohama and Shimizu, and Hokkaido University and Tohoku University joined this project.

The VENFISH team is composed of 5 teams and there are primary production, zooplankton and fish teams. The fish team is composed of Pacific saury and walleye pollock groups. Between these three teams there is a plankton ecosystem model team and a fish population model team. In this report we will note our studies of saury, which is only one portion of this project.

The main target area of the VENFISH project is east of 160ºE in the northwestern Pacific, and in that region there is a warm Kuroshio current and a cold Oyashio current. Between these two western boundary currents, there is a mixed water region, and in that area many eddies are detached from the Kuroshio and Oyashio and make very complicated environments. The saury spawning starts in the mixed water region in autumn, moves to the Kuroshio area in winter, and moves back to the mixed water region in spring (Fig. 2.4.1) (Odate 1977; Watanabe and Lo 1989; Watanabe *et al.* 1997). Juveniles are advected to the Kuroshio extension region, then grow and migrate to the Oyashio region through the mixed water region for feeding. After sufficient feeding they migrate back to the Kuroshio region for spawning. On the southward migration, they are fished in the Japanese coastal zone. We will briefly report the new findings for Pacific saury in the later sections.

Feeding habitat

The feeding habitat of Pacific saury (*Cololabis saira*) changes according to the life stage and the location. Larvae smaller than 15 mm mainly feeds on *Oncea* and *Oitona* sp. (Nakata and Koyama 2002), whereas larvae and juvenile larger than 15 mm prefer *Calanus* sp. Young saury which migrate to the mixed water region mainly feed on *Euphausia pacifica*. In the Oyashio region they feed mainly on *Euphausia pacifica* and *Neocalanus cristatus* and the ration becomes the

maximum in this season. On the way of their backward migration, they feed *Euphausia pacifica* and *Sagitta elegans*, but the ration decreases to the minimum. In the spawning area they feed on calanoid copepods and the ration is higher than in autumn (Sugisaki and Kurita, in preparation; Kurita and Sugisaki, in preparation).

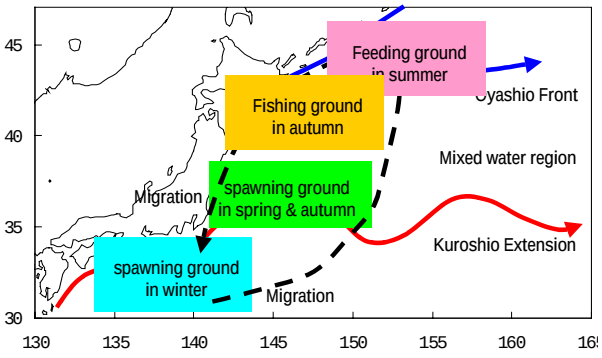

Fig. 2.4.1 Schematic picture of Pacific saury (*Cololabis saira*) life history. Spawning starts in September and continues until June, shifting location from the mixed water region and Kuroshio region. The main spawning season is winter. Juveniles are advected to the Kuroshio extension region and migrate to the Oyashio region through the mixed region for feeding. After sufficient feeding they migrate back to the Kuroshio region for spawning. On the southward migration, they are fished in the Japanese coastal zone.

Spawning density

Kurita and Sugisaki (in preparation) surveyed the seasonal change of the saury distribution and the ratio of mature stage in the three regions. In early autumn, half of the saury occur in the Oyashio region and they are immature. In winter almost all of the saury are in the Kuroshio and they are mature. In spring, half of the saury exist in the Kuroshio and most of them are mature. But the other half occurs in the mixed water region and only about 70% of them are mature. These results show that the most important area is the Kuroshio region and the most important season is winter for the saury spawning.

Kurita and Sugisaki (in preparation) estimated the spawning interval and batch fecundity. Using these values and ratio of mature saury to the total, they estimated the spawning density for each season. Their result showed that the most important season for spawning is winter.

Larvae and juvenile

Many studies have been done about larval and juvenile saury (Watanabe *et al.* 1997; Oozeki and Watanabe 2000; Oozeki and Watanabe, in preparation). Using widely sampled field data, Watanabe *et al.* (1997) and Oozeki and Watanabe (2000) estimated the production of hatched larvae in each season since 1990 to 1997. The average value for 8 years showed the highest value in autumn and the lowest value in spring. They also estimated the growth rate and mortality of larvae and production of juveniles. Growth rate showed a maximum in autumn and a minimum in spring. Mortality was highest in autumn and lowest in spring. As a result, the production of surviving juveniles showed a maximum in spring and a minimum in autumn. But the fluctuation of juvenile production in spring is very high and stable in winter. Watanabe *et al.* (1997) suggested that the stable winter juvenile might contribute to stable recruitment and middle size saury landings in autumn. Also Watanabe and Lo (1989) pointed out that winter was the most active spawning season using larval catch data during 1973-1986.

Oozeki and Watanabe (2000) conducted laboratory incubation experiments on saury eggs. They reared same age larvae at three different temperatures and observed growth rate. This was done for three different age larvae (9, 20, 30 days) and the dependency of growth rate on age was also tested. The result showed that the growth rate increased linearly with temperature and also increased with age. Analysis of the otolith increment and the knob length of the larvae showed the possibility of the estimation of growth rate of saury juveniles from the otolith field data. Then, they estimated the instantaneous growth rate from otolith field data and analyzed the relationship between the recent growth rate and oceanic environments (Oozeki and Watanabe: in preparation). Their result showed that the SST and food density affected larval growth during the early stages, and SST and chlorophyll become more important in the later stage.

Growth rate of adults

Suyama *et al.* (in preparation) analyzed the presence of a hyaline zone in the otoliths of Pacific saury. Usually the size decomposition is done by knob length, but sometimes it is difficult to divide them only from body length information. On the other hand, the otoliths of large size saury have the hyaline zone whereas the small and middle sizes do not. They analyzed the existence the hyaline zone and found out that the large and middle size cohort can be decomposed by the boundary of 50% existence ration of hyaline zone. Using this definition they decomposed the large and middle cohort and analyzed the inter-annual variability in the growth of each cohort. The middle size fluctuated between 264 and 286 mm, and the large size fluctuated between 303 and 314 mm, and the fluctuation was larger in the middle size.

For example, the growth increment of the large and middle cohort from July to November 1999, was 11.3 and 19.3 mm respectively. On the other hand, they increased to 12.5 and 31.3 mm respectively in 2000. This result suggests that the growth rate of the large size cohort is more stably estimated compared to the middle size cohort.

Growth rate between juvenile and large size

Using the hyaline zone information from the otolith it is possible to estimate the growth rate of young and adult saury, but the growth rate between juvenile and young saury is very difficult to estimate because of the existence of the hyaline zone. We cannot count the increment of the otolith because the increment is unclear in the hyaline zone. So, we cannot determine the age of adult saury.

For this problem, Kurita (personal communication) developed a new method to estimate the hatch date from the age at which the otolith increment width reached a second maximum. It became possible to estimate the age of saury using this method even if there is a hyaline zone. He estimated the hatch date of the large size saury and developed a new scenario of the life history of Pacific saury combined with the information of the growth of the saury with no hyaline zone. According to his scenario, saury which are born in the earlier season spawn in the first winter and also in the second winter. But the later spawned saury do not spawn in the first year and spawn in the second year.

Energy for migration and spawning

Kurita (personal communication) analyzed seasonal variation of lipid and protein content in 30 cm knob length saury. The protein content did not vary much but lipid variation showed very large variability. The average lipid content is about 40 g in summer. In winter, which is the active spawning season, mature saury contained little neutral lipid. Moreover, protein seemed to be utilized as energy sources because the sum of protein and water content was constant. From this result he concluded that saury need to feed in order to spawn eggs in the Kuroshio region.

Thus, the environment may be very important for the saury reproduction in the Kuroshio region. From the energy balance between the food nutrient and egg production, he estimated that about 35.6% of total assimilated energy was used for winter egg production in the Kuroshio.

Population dynamics model for Pacific saury

Tian *et al.* (2002b) analyzed the interannual variability of the saury stock using a population dynamics model. In his model there are two cohorts. One is a cohort spawned during autumn - winter and the other is spawned during winter - spring. The life span of the saury was assumed to be two years, and as a result the large size saury included both cohorts. The governing equations were growth rate, population, fishing effort and reproduction equations. In the population dynamics the mortality included environmental effects. As environment factors they adapted SST in the Kuroshio Extension zone (KE SST) and SOI (Southern Oscillation Index) according to the result of Tian *et al.* (2000a).

The results showed that the effect of KE SST was important to the longer-period variability, and the SOI effect was important to both the longer-period and inter-annual variability.

Conclusion

Under the VENFISH project, much has been learned about Pacific saury and a new life history of the saury was proposed. But information about the time between the juvenile and small saury stages are still limited. In the future more study is needed on these stages.

A population dynamics model was constructed under VENFISH and the effect of KE SST and SOI was tested. But in that model the environment influenced only mortality. In the future we should include the environmental influence on production and clarify the bottom-up control mechanism of Pacific saury.

2.5 Formalization of interactions between chemical and biological compartments in the mathematical model describing the transformation of nitrogen, phosphorus, silicon and carbon compounds

Alexander V. Leonov[1] and Gennady A. Kantakov[2]

[1] Institute of Oceanology, Russian Academy of Sciences, 36 Nakhimovsky Ave., Moscow, 117851, Russia. E-mail: leonov@sio.rssi.ru

[2] Sakhalin Research Institute of Fisheries and Oceanography, 196 Komsomolskaya St., Yuzhno-Sakhalinsk, 693023, Russia. E-mail: okhotsk@sakhniro.ru

In the significant part of the ecological models used for studying the joint dynamics of the microorganism biomasses and biogenic substance concentrations in the natural waters, several most important biological functions are formalized.

They are connected with the consumption of biogenic substances (UP) by microorganisms, excretion of the metabolic products (L) by them, the microorganism mortality (S) and grazing (G) by microorganisms of higher trophic levels. The change of the microorganism biomass in the course of time (dB/dt) in the ecological models, as a rule, is represented by the following structural equation:

$$(2.5.1) \quad dB / dt = (UP - L - S) * B - G * B^{*}$$

here B* is the biomass of microorganisms from the higher trophic level, and due to grazing they have an influence on the development and activity of the considered microorganism group B; UP, L, S, and G are specific rates of the biogenic substance consumption, the metabolic product excretion, the mortality of microorganisms B and their grazing by B*, respectively (day^{-1}).

Biomasses B and B* are calculated in the units of biogenic elements (N, P, C or Si).

The simulation of processes of the substrate consumption by microorganisms

For the simulation of processes of the substrate consumption by microorganisms (bacterio-, phyto- and zooplankton), the equation of Michaelis-Menten-Monod is traditionally used:

$$(2.5.2) \quad UP = K (T, L) * C_i / (K_m + C_i)$$

where UP is the growth rate of the microorganism biomass (or the substrate uptake), day^{-1}; C_i is the concentration of concrete substratum, mg/l; K_m is the Michaelis constant, mg/l; K (T, L) is the maximum growth rate of the microorganism biomass (or the substrate uptake) corrected to the temperature (T) and radiation (L) conditions in the water environment, mg/(l day). Thus, for description of the process of the substrate uptake by one group of microorganism (by bacterio-, phyto- or zooplankton) it is necessary to estimate the values of two coefficients - K (T, L) and K_m. Using this equation form for the description of the consumption of several substrata by microorganisms, means that the process of the substrate uptake is described independently of each other for any substrate, and in this case, the values of the rate constants for the consumption of each substrata should be evaluated. If the number of such substrata reaches five (ammonia, nitrites,

nitrates, phosphates, silicates) then the number of evaluated coefficients should be equal to ten.

The form of equation (2.5.2) with some modifications is used for describing the processes of the substrate consumption by microorganisms in the models developed by PICES MODEL Task Team for the studying of chemical and biological compartment dynamics in the marine environment. However, in the marine environment, the substrate concentrations are always little and therefore it is very difficult to describe the dynamics of the biomasses and substrate concentrations even for one season. Frequently the very task of the simulation of the chemical and biological compartment dynamics in the marine systems is a rather difficult labor-consuming or even insurmountable problem.

Here we present the logic of the simulation of the substrate consumption process by the microorganisms that is used for development of the model describing the transformation of N, P, C and Si compounds in the polysubstrate environment (Leonov and Saposhnikov 1997). First we shall transform the equation (2.5.2) subdividing the terms of equation in the numerator and the denominator on C_i. As a result, we obtain the following equation:

(2.5.3) $UP = K(T, L) / (1 + K_m / C_i)$

The analysis of literature shows that the value of K_m in different examples of using equation (2.5.2) for describing of processes in the natural waters changes by 2-3 orders. Consequently, the convincing arguments of the application of the equation (2.5.2) for describing the substrate consumption processes in the marine ecosystems is clearly insufficient (large number of coefficients for the polysubstratal environment and the large variability of the coefficient K_m). The value of the coefficient K_m for the marine ecosystems may be compared with the values of the microorganism biomasses. Therefore we have all reasons to use, instead of the coefficient K_m, the value of the biomass in the units of biogenic element (N, P, C or Si) from which biomass can be evaluated. If the biomass is considered in N, then the equation (2.5.3) can be written as:

(2.5.4) $UP = K(T, L) / (1 + B_N / C_N)$

where B_N is the biomass of the studied group of microorganisms, in units of N, mg N/l; C_N is the concentration of N fractions consumed by these microorganisms, mg N/l.

If there are several N-containing substrata in the water environment (for example, ammonia NH_4, nitrites NO_2, and nitrates NO_3) and these substrates are interchangeable and may be consumed by the microorganism (let us mark it as F and taking into account that the biomass is expressed in units of N, it may be written as F_N), then the expression for C_N can be represented in the form of the pool on N ($PoolF_N$) for the studied group of microorganism:

(2.5.5) $PoolF_N = d(1) * NH4 + d(2) * NO2 + d(3) * NO3$

Here the coefficients d(i) show preferences in the consumption of each substrate by the microorganism for this N-substrates (NH_4, NO_2, and NO_3). Value of the coefficients d(i) for each substrate can change from 0 to 1, and their sum for the selected set of substrata is 1.

How are the values of coefficients d(i) evaluated? It is known from literature that the phytoplankton consumes more preferably ammonium N than other mineral forms. The nitrate N is in second place. So, in the first approximation, we can assign the values of the preference coefficients in the uptake of indicated substrates by the studied group of phytoplankton: d(1) = 0.5; d(2) = 0.2; d(3) = 0.3. Inserting the equation (2.5.5) into the equation (2.5.4), we obtain:

(2.5.6) $UP_{FN} = K(T, L) / (1 + B_N / PoolF_N)$

or

(2.5.6a) $UP_{FN} = K(T, L) / (1 + B_N / (d(1)*NH4 + d(2)*NO2 + d(3)*NO3))$

The general rate of the N-containing substrata consumption, UP_{FN}, is composed of the rates of the consumption of the individual substrates:

(2.5.7) $UP_{FN} = UP_{NH4} + UP_{NO2} + UP_{NO3}$

Let us write down the equations, which describe the consumptions of individual substrates (NH_4, NO_2 and NO_3) by phytoplankton taking into account that in the water environment several substrates are interchangeable on N, as indicated by the equation (2.5.6a). Making elementary algebraic conversions, we shall obtain the equations, which describe the consumption of each studied substrates by the phytoplankton:

(2.5.8) $UP_{NH4} = K (T, L) * d(1) * NH4 / (PoolF_N + B_N)$

(2.5.9) $UP_{NO2} = K (T, L) * d(2) * NO2 / (PoolF_N + B_N)$

(2.5.10) $UP_{NO3} = K (T, L) * d(3) * NO3 / (PoolF_N + B_N)$

The suggested form of the description of the interchangeable substrates by the microorganism assumes that the rates of the consumption of each substrate will be compared only in such a case, when the product of substrate concentrations to their preference coefficient will be close. With the maximum rate will be consumed that substratum, for which the product of its preference coefficient to the concentration will be the greatest (in this case, from of three given substrates). This form of the equations for the consumption of the interchangeable substrates by microogranism (in particular, by phytoplankton) gives the possibility of switching for the intensive consumption by the hydrobionts only of those substrata whose concentrations to these are greatest in the comparison with other substrata. It gives a possibility for the water environment to restore the pool of those substrata, which in the process of the biomass growth descend to the smallest (sometimes critically small) values. This phenomenon in the description of the processes of increasing of the biomass and substrate consumption is impossible by equations the traditionally used for the simulation of marine ecosystems, in which the substrate consumption by different groups of microorganism is assigned independently of each other.

Let us consider the case, when there are several substrates as the interchangeable (as it was examined above), so also not interchangeable, in the water environment for the phytoplankton. If we want correctly describe in the model the substrate uptake processes then we should remember the basic Odum's postulate that everything is interrelated in the natural water environment. The requirements of phytoplankton in P cannot be compensated by N or Si compounds, and vice versa. Therefore the compounds of different biogenic elements cannot be considered as interchangeable for the formation of the microorganism biomass and the kinetics of the uptake substrate processes should be formulated with point of view their mutual influence on each other and not their interchangeability.

Taking into account these reasons, let us write down the equation (2.5.6) for the rate of biomass growth (or the different substrate uptake) for the conditions of the combined influence of N and P compounds on the biomass of the considered microorganism group (for example, the phytoplankton) keeping the logic of all foregoing reasons. Then we obtain, that

(2.5.11) $UP_F = K (T, L) /(1 + B_N / PoolF_N + B_P / PoolF_P)$

Here B_P is the biomass in units of P, mg P/l; $PoolF_p$ - the pool of the P substrates, mg P/l, that may be consumed by the phytoplankton, and these substrates are the dissolved mineral (DIP) and organic (DOP) forms of P:

(2.5.12) $PoolF_p = d(4)*DIP + d(5)*DOP$

In this case the total rates of the uptake of N and P compounds by the given group of microorganisms are represented as:

(2.5.13) $UP_{FN} = UP_{NH4} + UP_{NO2} + UP_{NO3}$

(2.5.14) $UP_{FP} = UP_{DIP} + UP_{DOP}$

Accordingly to the same logic, let us formulate equations for describing the individual substrates taking into account the influence of each of them on the kinetics of the formation of biomass and the substrate uptake being oriented toward general equation (2.5.11):

(2.5.15) $UP_{NH4} = K(T, L) * d(1) * NH4 / MF$

(2.5.16) $UP_{NO2} = K(T, L) * d(2) * NO2 / MF$

(2.5.17) $UP_{NO3} = K(T, L) * d(3) * NO3 / MF$

(2.5.18) $UP_{DIP} = K(T, L) * d(4) * DIP / MF$

(2.5.19) $UP_{DOP} = K(T, L) * d(5) * DOP / MF$

where

(2.5.20) $MF=PoolF_N * PoolF_P + B_N * PoolF_P + B_P * PoolF_N$.

When the joint consumption of N, P, and SI compounds is considered for the same group of microorganism, the equation (2.5.11) takes the form:

(2.5.21) $UP_F = K(T, L) /(1 + B_N / PoolF_N + B_P / PoolF_P + B_{si} / PoolF_{Si})$

where

(2.5.22) $PoolF_{Si} = d(6) * DISi$

and DISI is the content of dissolved inorganic silicon, mg Si/l.

In accordance to the accepted logic for the formulations of kinetic dependences, the equations describing the individual substrate uptake and their mutual influence on each other are written in the following form:

(2.5.23) $UP_{NH4} = K(T, L) * d(1) * NH4 / MF1$

(2.5.24) $UP_{NO2} = K(T, L) * d(2) * NO2 / MF1$

(2.5.25) $UP_{NO3} = K(T, L) * d(3) * NO3 / MF1$

(2.5.26) $UP_{DIP} = K(T, L) * d(4) * DIP / MF1$

(2.5.27) $UP_{DOP} = K(T, L) * d(5) * DOP / MF1$

(2.5.28) $UP_{DISi} = K(T, L) * d(6) * DISi / MF1$

where

(2.5.29) $MF1 = PoolF_N * PoolF_P * PoolF_{Si} + B_N * PoolF_P * PoolF_{Si} + B_P * PoolF_N * PoolF_{Si} + B_{Si} * PoolF_N * PoolF_P$

A similar form of equations may be used for any functional group of microorganism taking into account any the variety of the substrate assortment including the components of the water environment pollution (for example, oil products). The substrate assortment for the organisms of higher trophic levels is higher than for the organisms of lowest trophic status. In this assortment fall the dissolved and particulated organic compounds of biogenic elements, including biomasses of certain microorganisms and detritus.

The equation for the term G (the specific grazing rate of the microorganism from the lowest trophic levels by the organisms of higher levels) is constructed, on the basis of the presented above principles considering the high-constituent nature of water environment and the mutual influence of the uptake of individual substrates on each other in the process of the microorganism biomass growth.

The value of the maximum growth rate of the microorganism biomass (or the substrate consumption), K (T, L) should be corrected to the conditions on the temperature and for light (for the planktonic organisms) in the water environment. The analysis of ecological models existing at present shows that there are many methods of carrying out a similar correction.

In the model of the transformation of nitrogen, phosphorus, silicon and carbon compounds the temperature dependence is considered by the exponential function, which differs for the different groups of microorganisms in the slope and the optimum values of temperature. The dependence of the plankton biomass growth as a function of light conditions in water environment is considered by the traditional functions that are used at the simulation of the processes of phytoplankton photosynthesis and daily vertical migration of zooplankton.

Formalization of the excretion processes of metabolic products by microorganisms

At first stages of mathematical simulation model development as the independent scientific direction in the studies of the natural aquasystems state, this important biological function of

microorganisms was not considered at all. At present time, in the majority of the cases the specific rate of the metabolic excretion by microorganisms (L) is formulated in the ecological models by the simplest method and, as a rule, it is represented in the form of a constant quotas (α) from the UP function:

(2.5.30) $L = \alpha * UP$

The experience of the experimental research of the microorganism population dynamics and the simulation of the conditions for the biomass growth shows that the excretion fraction of the products of metabolic exchange in different microorganisms differs very substantially, and it can change considerably in the process of the biomass growth in each group of microorganisms.

This fact was taken into account, and during the development of the mathematical model of the transformation of nitrogen, phosphorus, silicon, and carbon compounds the different forms of the expression of the excretion fraction of metabolic products changing in the time were checked. It was found the form of equation for α that most completely consider the special features of the microorganism biomass growth, and it is formulated as the dependence from the specific rate of the substrate uptake, UP:

(2.5.31) $\alpha = a * UP / (1 + b * UP) + (1 - a / b)$

where a and b are constants (moreover $a < b$) whose values determine the nature of change in the excretion fraction in the dependence on the values of the total substrate uptake by considered group of microorganisms.

The first term of the equation (2.5.31) shows the forming quota of the metabolic excretion of substance in the favorable on the nutrient conditions of the water environment, when values of UP are significant.

The second term of the equation (2.5.31) shows the quota of the metabolic excretion at the substrate deficite when values of UP become minimum.

With the values of coefficients a and b can be reproduced the significant spectrum of the conditions for the microorganism biomass growth which can be evaluated in the units of different biogenic elements (N, P, C or Si).

Formalization of the processes of the microorganism mortality

The processes of development and growth of the microorganism biomass are continuous with the processes of the internal losses of biomasses (S). It is possible to assume that the natural physiological losses of the biomasses of any group of microorganisms compose 5-10% of the total biomass although this problem remains insufficiently studied experimentally for all microorganism groups. In the process of the microorganism mortality, the detritus (or the dead suspended matter) is formed in the water environment. The biogenic substances containing in it are actively included in turnover by bacteria and zooplankton which transform detritus into the labile nutrients well assimilated by other microorganisms. Under the conditions of reduced temperatures, the detrital links become the most important in the nutrition and growth of the populations of fishes.

At the first ecological models, the microorganism mortality S is not taken into account at all or only natural physiological biomass losses are considered. The modern ecological models include the natural internal biomass losses and take into account losses inevitable at the stimulation of the biomass growth processes. It may be differently formulated. In the mathematical model of the transformation of N, P, Si, and C compounds this important biological function is described by the equation:

(2.5.32) $S_N = g(1) + g(2) * B_N / UP_{FN}$

where g (1) and g (2) are constants describing the processes of the natural biomass losses and mortality depending on the conditions of activating the growth, respectively. If the biomass of the microorganism group is evaluated in the units of different biogenic elements (N, P, C or Si) then respectively for each case their specific rates of the internal losses of biomasses are evaluated

with the use of specific values of coefficients g (i), values of biomasses B and rates of the substrate consumption UP.

The set of model coefficients applied in two case studies (for the Okhotsk Sea (Leonov and Sapozhnikov 1997) and Caspian Sea (Leonov and Srygar 1999) for the simulation of microorganism dynamics is presented in Table 2.5.1.

Thus, in the mathematical model of the transformation of N, P, Si, and C compounds, the interactions between chemical (concentrations of biogenic substances) and biological (biomasses the microorganisms - bacteria, phyto- and zooplankton) compartments are considered and reproduced the most important biological processes of the substrate uptake, excretion of the metabolic products and mortality of the microorganisms. As a result of these processes, the turnover of chemical substances (organic and mineral) are performed in natural marine ecosystems. The special feature of this model is the formalization of the important biological functions (the excretion of the metabolic products and mortality of microorganisms) in a dependence on the consumption of different biogenic substances by microorganism. These biogenic substrates are subdivided on interchangeable (on one biogenic element) and not interchangeable (on the different biogenic elements). The used form of equations for the description in this model of the most important biological functions serves as the example for the formalization of the processes of the internal regulation (self regulation) of the microorganism activity within the ecosystems. The account of a similar internal regulation mechanism of the microorganism activity makes this model sufficiently resistant and allow us to apply it without the significant correction of the parameters in the study the aqueous ecosystems which essentially differ in the environmental conditions (temperature, radiation, water regime, transparency). There are several positive experiences in the application of this model to study the special features of the ecosystem functioning of the Sea of Okhotsk (Leonov and Sapozhnikov 1997) and Caspian Sea (Leonov and Stygar 1999). The first results are also obtained on the simulation of the intraannual dynamics of biogenic substances in the ecosystem in La Perouse Strait and Aniva Bay (Sea of Okhotsk) (Pischalnik and Leonov 2002).

Table 2.5.1 Values of model parameters used for description of biological compartment dynamics in the Sea of Okhotsk and the Caspian Sea.

Case study 1 - The Sea of Okhotsk	**Case study 2 - The Caspian Sea**
Heterotrophic bacteria (B)	**Heterotrophic bacteria (B)**
Maximum growth rate: K=1.0	Maximum growth rate: K=0.75
Preference coefficients for substrate uptake:	*Preference coefficients for substrate uptake:*
for C-containing substrate: d_{DOC}=1;	for C-containing substrate: d_{DOC}=1;
for Si-containing substrate: d_{DOSi}=0.6; d_{DISi}=0.01 d_{SID}=0.39;	for Si-containing substrate: d_{DOSi}=0.6; d_{DISi}=0.01 d_{SID}=0.39;
for N-containing substrate: d_{DON}=0.6; d_{ND}=0.4	for N-containing substrate: d_{DON}=0.6; d_{ND}=0.4
for P-containing substrate: d_{DOP}=0.4; d_{PD}=0.6	for P-containing substrate: d_{DOP}=0.4; d_{PD}=0.6
Excretion activity:	*Excretion activity:*
for C substrate: a_C=0.05; b_C=0.09	for C substrate: a_C=0.05; b_C=0.088
for Si substrate: a_{Si}=0.05; b_{Si}=0.088’	for Si substrate: a_{Si}=0.05; b_{Si}=0.088
for N substrate: a_N=0.05; b_N=0.087	for N substrate: a_N=0.05; b_N=0.1
for P substrate: a_P=0.05; b_P=0.09	for P substrate: a_P=0.05; b_P=0.086
Mortality coefficients:	*Mortality coefficients:*
for C substrate: $g(1)_C$=0.04; $g(2)_C$=0.04	for C substrate: $g(1)_C$=0.03; $g(2)_C$=0.025
for Si substrate: $g(1)_{Si}$=0.045; $g(2)_{Si}$=0.05	for Si substrate: $g(1)_{Si}$=0.045; $g(2)_{Si}$=0.05
for N substrate: $g(1)_N$=0.035; $g(2)_N$=0.035	for N substrate: $g(1)_N$=0.028; $g(2)_N$=0.03
for P substrate: $g(1)_P$=0.055; $g(2)_P$=0.055	for P substrate: $g(1)_P$=0.045; $g(2)_P$=0.05

First phytoplankton group (F1-diatom algae) Maximum growth rate: K=2.5 *Preference coefficients for substrate uptake:* for Si-containing substrate: d_{DOSi}=0.3; d_{DISi}=0.7 for N-containing substrate:d_{NH4}=0.025; $_{NO2}$=0.025 d_{NO3}=0.9; d_{UR}=0.05 for P-containing substrate: d_{DOP}=0.3; d_{DIP}=0.7 *Excretion activity:* for Si substrate: a_{Si}=0.051; b_{Si}=0.052 for N substrate: a_N=0.05; b_N=0.053 for P substrate: a_P=0.05; b_P=0.065 *Mortality coefficients:* for Si substrate: $g(1)_{Si}$=0.0; $g(2)_{Si}$=0.08 for N substrate: $g(1)_N$=0.0; $g(2)_N$=0.02 for P substrate: $g(1)_P$=0.0; $g(2)_P$=0.02	**First phytoplankton group (F1-diatom algae)** Maximum growth rate: K=2.5 *Preference coefficients for substrate uptake:* for Si-containing substrate: d_{DOSi}=0.3; d_{DISi}=0.7 for N-containing substrate: d_{NH4}=0.2; d_{NO2}=0.05 d_{NO3}=0.7; d_{UR}=0.05 for P-containing substrate: d_{DOP}=0.05; d_{DIP}=0.95 *Excretion activity:* for Si substrate: a_{Si}=0.051; b_{Si}=0.052 for N substrate: a_N=0.05; b_N=0.052 for P substrate: a_P=0.05; b_P=0.055 *Mortality coefficients:* for Si substrate: $g(1)_{Si}$=0.04; $g(2)_{Si}$=0.03 for N substrate: $g(1)_N$=0.05; $g(2)_N$=0.049 for P substrate: $g(1)_P$=0.05; $g(2)_P$=0.07
Second phytoplankton group (F2-peridinium algae) Maximum growth rate: K=1.8 *Preference coefficients for substrate uptake:* for N-containing substrate: d_{NH4}=0.15; d_{NO2}=0.05 d_{NO3}=0.2; d_{UR}=0.6 for P-containing substrate: d_{DOP}=0.4; d_{DIP}=0.6 *Excretion activity:* for N substrate: a_N=0.049; b_N=0.0495 for P substrate: a_P=0.049; b_P=0.053 *Mortality coefficients:* for N substrate: $g(1)_N$=0.0; $g(2)_N$=0.05 for P substrate: $g(1)_P$=0.0; $g(2)_P$=0.1	**Second phytoplankton group (F2-green algae)** Maximum growth rate: K=2.5 *Preference coefficients for substrate uptake:* for N-containing substrate: d_{NH4}=0.2; d_{NO2}=0.05 d_{NO3}=0.7; d_{UR}=0.05 for P-containing substrate: d_{DOP}=0.05; d_{DIP}=0.95 *Excretion activity:* for N substrate: a_N=0.049; b_N=0.0495 for P substrate: a_P=0.049; b_P=0.052 *Mortality coefficients:* for N substrate: $g(1)_N$=0.04; $g(2)_N$=0.03 for P substrate: $g(1)_P$=0.04; $g(2)_P$=0.06
Third phytoplankton group (F3-green algae) Maximum growth rate: K=1.8 *Preference coefficients for substrate uptake:* for N-containing substrate: d_{NH4}=0.15; d_{NO2}=0.05 d_{NO3}=0.2; d_{UR}=0.6 for P-containing substrate: d_{DOP}=0.4; d_{DIP}=0.6 *Excretion activity:* for N substrate: a_N=0.049; b_N=0.0495 for P substrate: a_P=0.049; b_P=0.0523 *Mortality coefficients:* for N substrate: $g(1)_N$=0.0; $g(2)_N$=0.05 for P substrate: $g(1)_P$=0.0; $g(2)_P$=0.1	**Third phytoplankton group (F3-blue-green algae)** Maximum growth rate: K=2.5 *Preference coefficients for substrate uptake:* for N-containing substrate: d_{NH4}=0.2; d_{NO2}=0.05 d_{NO3}=0.7; d_{UR}=0.05 for P-containing substrate: d_{DOP}=0.05; d_{DIP}=0.95 *Excretion activity:* for N substrate: a_N=0.049; b_N=0.0495 for P substrate: a_P=0.049; b_P=0.052 *Mortality coefficients:* for N substrate: $g(1)_N$=0.04; $g(2)_N$=0.03 for P substrate: $g(1)_P$=0.04; $g(2)_P$=0.06
First zooplankton group (Z1-herbivorous) Maximum growth rate: K=1.5 *Preference coefficients for substrate uptake:* for Si-containing substrate: d_{DOSi}=0.15; d_{DISi}=0.02 d_{SiD}=0.77; d_{BSi}=0.01 d_{F1Si}=0.05 for N-containing substrate: d_{ND}=0.48; d_{F1N}=0.34 d_{F2N}=0.05; d_{F3N}=0.02	**First zooplankton group (Z1-herbivorous)** Maximum growth rate: K=0.75 *Preference coefficients for substrate uptake:* for Si-containing substrate: d_{DOSi}=0.15; d_{DISi}=0.02 d_{SiD}=0.77; d_{BSi}=0.01 d_{F1Si}=0.05 for N-containing substrate: d_{ND}=0.5; d_{F1N}=0.05 d_{F2N}=0.25; d_{F3N}=0.1

d_{BN}=0.11; for P-containing substrate: d_{PD}=0.78; d_{F1P}=0.15 d_{F2P}=0.025; d_{F3P}=0.025 d_{BP}=0.02; *Excretion activity:* for Si substrate: a_{Si}=0.048; b_{Si}=0.052 for N substrate: a_N=0.041; b_N=0.05 for P substrate: a_P=0.035; b_P=0.05 *Mortality coefficients:* for Si substrate: $g(1)_{Si}$=0.0; $g(2)_{Si}$=0.2 for N substrate: $g(1)_N$=0.0; $g(2)_N$=0.4 for P substrate: $g(1)_P$=0.0; $g(2)_P$=0.8	d_{BN}=0.1; for P-containing substrate: d_{PD}=0.73; d_{F1P}=0.1 d_{F2P}=0.025; d_{F3P}=0.025 d_{BP}=0.02; d_{DOP}=0.1 *Excretion activity:* for Si substrate: a_{Si}=0.035; b_{Si}=0.052 for N substrate: a_N=0.041; b_N=0.05 for P substrate: a_P=0.035; b_P=0.052 *Mortality coefficients:* for Si substrate: $g(1)_{Si}$=0.05; $g(2)_{Si}$=0.2 for N substrate: $g(1)_N$=0.05; $g(2)_N$=0.4 for P substrate: $g(1)_P$=0.035; $g(2)_P$=0.5
Second zooplankton group (Z2-predatory) Maximum growth rate: K=0.5 *Preference coefficients for substrate uptake:* for N-containing substrate: d_{ND}=0.55; d_{F1N}=0.31 d_{Z1N}=0.1; d_{BN}=0.04 for P-containing substrate: d_{PD}=0.8; d_{F1P}=0.1 d_{BP}=0.05; d_{Z1P}=0.05 *Excretion activity:* for N substrate: a_N=0.0276; b_N=0.0287 for P substrate: a_P=0.0276; b_P=0.0287 *Mortality coefficients:* for N substrate: $g(1)_N$=0.0; $g(2)_N$=0.5 for P substrate: $g(1)_P$=0.0; $g(2)_P$=1.0	**Second zooplankton group (Z2-predatory)** Maximum growth rate: K=0.75 *Preference coefficients for substrate uptake:* for N-containing substrate: d_{ND}=0.55; d_{F1N}=0.2 d_{F2N}=0.02; d_{F3N}=0.02; d_{Z1N}=0.15; d_{BN}=0.06 for P-containing substrate: d_{PD}=0.75; d_{F1P}=0.05 d_{BP}=0.05; d_{Z1P}=0.05; d_{DOP}=0.1 *Excretion activity:* for N substrate: a_N=0.0276; b_N=0.03 for P substrate: a_P=0.0276; b_P=0.032 *Mortality coefficients:* for N substrate: $g(1)_N$=0.05; $g(2)_N$=0.4 for P substrate: $g(1)_P$=0.035; $g(2)_P$=0.6

Note: the dimension of parameters: K - day^{-1}, d_i, a_i, b_i - (undimension), $g(1)$ - day^{-1}, $g(2)_i$ - $[(mg\ Element/l)^{-1}\ (day^{-2})]$.

3.0 Herring group report and model results

Douglas E. Hay[1], Robert A. Klumb[2], Bernard A. Megrey[3], S. Lan Smith[4] and Francisco E. Werner[5] (authors listed alphabetically)

[1] Pacific Biological Station, Fisheries and Oceans Canada, 3190 Hammond Bay Road, Nanaimo, B. C., Canada, V9R 5K6. E-mail: hayd@pac.dfo-mpo.gc.ca

[2] Department of Natural Resources, Cornell Biological Field Station, Cornell University, 900 Shackelton Point Road, Bridgeport, NY 13030, U.S.A. E-mail: rak11@cornell.edu

[3] National Marine Fisheries Service, Alaska Fisheries Science Center, 7600 Sand Point Way NE, Seattle, WA 98115, U.S.A. E-mail: bern.megrey@noaa.gov

[4] Frontier Research System for Global Change, Showa-machi 3173-25, Kanazawa-ku, Yokohama, Kanagawa, 236-001, Japan. E-mail: lanimal@jamstec.go.jp

[5] Marine Sciences Department, CB# 3300, University of North Carolina, Chapel Hill, NC 27599-3300, U.S.A. E-mail: cisco@unc.edu

Summary report from the herring group

Specific data for most physiological parameters of Pacific herring are lacking. The first task of "Team Herring" towards linking the LTL NEMURO model to pelagic fish required modifications of the existing Atlantic herring bioenergetics model of Rudstam (1988). Three main areas focused on at the workshop included: 1) modifying the temperature dependence function

for consumption and cutoff temperature values, where swimming speed changes in the Rudstam model to describe the actual temperatures inhabited by Pacific herring, 2) accounting for known differences in larval and juvenile fish physiology (age-0) compared to adults, and 3) incorporating known seasonal changes in energy density of adult Pacific herring. Trends in size-at-age were discussed and potential hypotheses to be tested after completion of the model were proposed. In the application to Pacific herring our objectives were to model one fish, generate data to compare to observed size-at-age, follow one cohort through time, and provide a means to perform regional comparisons.

Temperature-dependence of consumption and swimming speed

Douglas Hay provided diet data for Pacific herring from near Vancouver, British Columbia, from which he and Robert Klumb tried to extract the temperature-dependence terms for the herring consumption equation. The original herring bioenergetics model was formulated for the Baltic Sea, but the Vancouver site has lower temperatures and less seasonal variation of temperature. Because temperature is one of the main process-mediating functions in the bioenergetics model, we had to modify the parameters for temperature dependence on consumption function to agree with the temperature ranges inhabited by Pacific herring off the coast of Vancouver. Vadim Navrotsky suggested that we formulate this temperature dependence in terms of DT = T - T_{opt} , where T_{opt} is the optimal temperature for consumption (depending upon location). One could also use the temperature of the waters in which the growth of herring is maximized as a proxy for the temperature at which their consumption rate is maximum (*e.g.*, 12°C, based on the data for peak growth versus abundance and temperature in Haist and Stocker (1985)).

As a preliminary approximation, Bernard Megrey normalized the Baltic Sea temperatures to a zero-one scale, based on the maximum and minimum temperatures observed for a location off the west coast of Vancouver Island, Amphitrite lighthouse (Fig. 3.1).

Fig. 3.1 Location of B.C. Lighthouse stations including Amphitrite Point Lighthouse, the source of the temperature data used in the model.

Values for the two temperature series were rescaled using the formula:

(3.1)

$$TA = \frac{(TB - TB_{\min}) \cdot (TA_{\max} - TA_{\min})}{(TB_{\max} - TB_{\min})} + TA_{\min}$$

where TB_{max}=30.0, TB_{min}=1.0, TA_{max}=14.0, TA_{min}=8.0, TA refers to temperatures from Amphitrite lighthouse, and TB refers to temperatures from the Baltic Sea.

The re-scaled temperatures used for the Thornton and Lessem (1978) temperature dependence function for consumption were as follows:

Age 0		**Age 1**		**Age > 1**	
Amphitrite	Baltic	Amphitrite	Baltic	Amphitrite	Baltic
8.0	1	8.0	1	8.0	1
10.897	15	10.897	15	10.483	13
11.31	17	11.31	17	10.897	15
12.552	23	12.552	23	12.553	23

Temperatures in the respiration model, where activity changed needed to be re-computed for age-0 and age-1 herring:

Old	▶	New
15°C		10.897°C
9°C		9.655°C

Finally the equation describing the annual temperature signal needed to be re-computed based on observed mean monthly sea surface temperature (SST) data from Amphitrite lighthouse. The following equation

(3.2)

$$T = 7.717 + \left(5.6796 \cdot 0.5 \cdot \left(1 - \cos\left(\frac{2 \cdot \pi \cdot (JDAY - 30)}{365} \right) \right) \right)$$

was fit to the observed data (Fig 3.2) where JDAY is Julian day and T is water temperature.

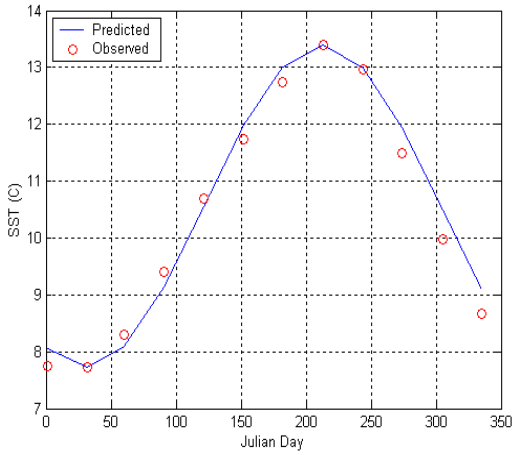

Fig. 3.2 Observed and predicted mean SST at Amphitrite Lighthouse.

Validation to Pacific herring

To validate the bioenergetics model to herring, we used model structure and parameters after Rudstam (1988) for Baltic Sea herring, but included no young-of-the-year (YOY) dynamics, no multispecies functional response, and no spawning (Rudstam model has spawning).

Results of the model (Fig 3.4) can be compared to the Rudstam results (Fig. 3.3) and good agreement in dynamical behavior can be noted.

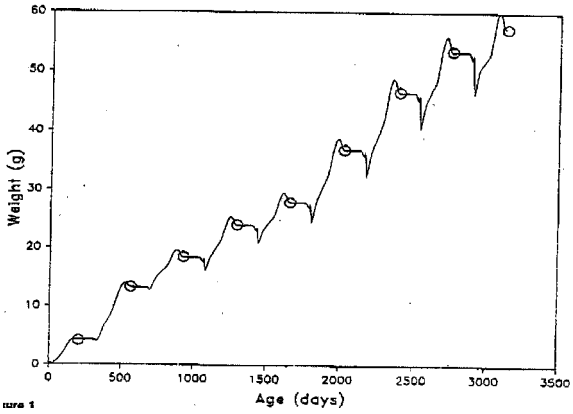

Fig. 3.3 Results of the Baltic Sea herring model from Rudstam (1988). The solid line represents model output and the open circles are weight-at-age values from field observations.

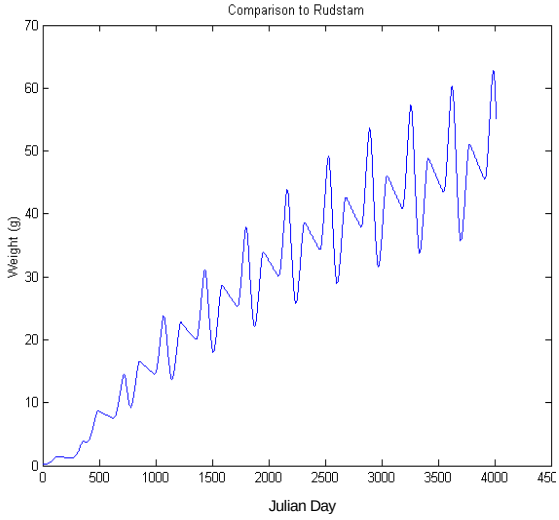

Fig. 3.4 Simulated growth from the herring bioenergetics model.

Separate age 0 and adult formulations

Describing the growth of a YOY fish involves more than just rescaling process equations derived for adult fishes. Often the process rates differ substantially between different life stages (Post and Lee 1996). Cisco Werner and Rob Klumb modified the Atlantic herring bioenergetics model for age-0 herring. Rob's parameters for respiration were based on his laboratory measurements from age-0 alewife, another clupeid, which used routine metabolism without an activity multiplier. Literature values for larval and juvenile clupeids

were also used that lowered SDA, egestion, and excretion parameters compared to the adult Atlantic herring parameters.

The YOY formulation for herring respiration proposed by Arrhenius (1998) along with our conversion factor from wet weight (g) to energy (J) was:

(3.5) $R = a_R \cdot W^{b_R} \cdot f_R(T) \cdot activity \cdot 5.258$

where the units are the same as in equation 2.1.5 and $a_{R=}$ 0.0033, b_R = -0.227.

The temperature dependence function for respiration

(3.6) $f_R(T) = e^{(c_R \cdot T)}$

for a age-0 herring was similar to equation 2.1.8.

Activity is a power function of body weight conditioned on water temperature and is given by

(3.7) $activity = e^{(d_R \cdot U)}$

where U is swimming speed in cm·s^{-1} and d_R is a coefficient relating swimming speed to metabolism. Swimming speed is calculated as a function of body weight and temperature using

(3.8) $U = a_A \cdot W^{b_A} \cdot e^{(c_A \cdot T)}$

Swimming speeds have been observed to switch from temperature dependence (at low temperatures) to temperature independence (at high temperatures). Formulations by life stage for changes in swimming speeds versus the adjusted temperatures from temperature-dependence of consumption and swimming speed section (given earlier) were:

if age=0 and T ≤10.897 °C then
$a_{R=}$ 0.0033, b_R = -0.227, $c_{R=}$ 0.0548,
$a_{A=}$ 5.76, b_A = 0.386, c_A=0.238 and d_R=0.03

if age=0 and T >10.897 °C then
$a_{R=}$ 0.0033, b_R = -0.227, $c_{R=}$ 0.0548, $a_{A=}$ 8.6,
b_A = 0.386, c_A=0.0 and d_R=0.03

if age≥=1 and T ≤9.655 °C then
$a_{R=}$ 0.0033, b_R = -0.227, $c_{R=}$ 0.0548, $a_{A=}$ 3.9,
b_A = 0.13, c_A=0.149 and d_R=0.03

if age≥=1 and T >9.655 °C then
$a_{R=}$ 0.0033, b_R = -0.227 $c_{R=}$ 0.0548, $a_{A=}$ 15.0,
b_A = 0.13, c_A=0.0 and d_R=0.03

In the final set of simulations, the Arrhenius (1998) equations 3.5 and 3.6 were modified after Klumb *et al.* (in press) to use the parameters.

if age=0 then
$a_{R=}$ 0.00528, b_R = -0.007, $c_{R=}$ 0.0548, $a_{A=}$ 1.0,
b_A = 0.0, c_A=0.0 and d_R=0.0.

In all simulations, equations for age 1 and older Pacific herring were the same as described in Arrhenius (1998).

The coefficients of SDA, egestion, and excretion in equations 2.1.6, 2.1.11, and 2.1.12 were made age dependent with the parameters given in Table 3.1.

Formulation for energy density

The energy density of clupeids varies seasonally. Instead of using constant conversion factors, as in equation 2.1.1, we incorporated a simple energy cycle based on data in Paul *et al.* (1998) for age-2 and greater herring. Paul *et al.* (1998) found energy density peaked at 9800 J/g wet wt. (range 9400 - 10200) in fall (October 1), and in spring (March 1) dropped to 5750 J/g wet wt. (range 5200 - 6300). For age-0 and age-1 herring we assumed a constant energy density of 4460 J/g wet wt. (Foy and Paul 1999). Age-0 herring do exhibit a seasonal energy cycle from 5000 J/g wet wt. in November to 3900 J/g wet wt. in March, and could be included in future modifications of the model.

The following code was used to implement a straight-line approximation to a sinusoid that described seasonal changes in energy density. The period between March 1 and October 1 consisted of 214 days. The period prior to March 1 and the period after October 1, together summed to 151 days.

Table 3.1 Summary of final parameter values used in the herring bioenergetics model.

Symbol	Parameter description		Value	
Consumption, C_{MAX}				
a_C	Intercept for C_{MAX} at		0.642	
b_C	coefficient for C_{MAX} versus weight	-0.256		
te1	Temperature for xk1 (in ºC)		8.0[a]	8.0[b] 8.0[c]
te2	Temperature for xk2 (in ºC)		10.897[a]	10.897[b] 10.483[c]
te3	Temperature for xk3 (in ºC)		11.310[a]	11.310[b] 10.897[c]
te4	Temperature for xk4 (in ºC)		12.552[a]	12.966[b] 12.552[c]
xk1	Proportion of C_{MAX} at te1	0.10		
xk2	Proportion of C_{MAX} at te2	0.98		
xk3	Proportion of C_{MAX} at te3	0.98		
xk4	Proportion of C_{MAX} at te4	0.01		
Metabolism, R				
a_R	Intercept for R		0.00528[a]	0.0033[bc]
b_R	Coefficient for R versus weight		-0.007[a]	-0.227[bc]
c_R	Coefficient for R versus temperature		0.083[a]	0.0548[bc]
d_R	Coefficient for R versus swimming speed	0.0[a]	0.03[bc]	
S	Coefficient for Specific Dynamic Action	0.125[a]	0.175[b]	0.175[c]
Swimming Speed, U				
a_A	Intercept U (< 9.655 ºC) (in cm/s)	3.9[bc]		
a_A	Intercept U (≥9.655 ºC) (in cm/s)	15.0[bc]		
b_A	Coefficient U versus weight		0.13[bc]	
c_A	Coefficient U versus temperature (<9.655 ºC)		0.149[bc]	
c_A	Coefficient U versus temperature (≥9.655 ºC)	0.0[bc]		
Egestion and Excretion, F and E				
a_F	Proportion of consumed food egested		0.125[a]	0.16[bc]
a_E	Proportion of consumed food excreted		0.078[a]	0.10[bc]
Multispecies Functional Response				
V_{11}	Vulnerability of prey group 1 to predator 1	1.0		
V_{12}	Vulnerability of prey group 2 to predator 1	1.0		
V_{13}	Vulnerability of prey group 3 to predator 1	1.0		
K_{11}	Half saturation constant for prey group 1 to predator 1 (g wet weight/m^3)		750.0	
K_{12}	Half saturation constant for prey group 2 to predator 1 (g wet weight/m^3)		75.0	
K_{13}	Half saturation constant for prey group 3 to predator 1 (g wet weight/m^3)		750.0	

a - values for age-0 herring, b - values for age-1 herring, c - values for age-2 and older herring

```
if(iage.ge.2)then
      enMar1=5750.
      jdMar1=60
      enOct1=9800.
      jdOct1=274
if(jjday.lt.60)then
      delen=(enMar1-enOct1)/151
      en=enOct1+(90+jjday)*delen
end if
if(jjday.ge.60.and.jjday.lt.274)then
      delen=(enOct1-enMar1)/(jdOct1-jdMar1)
      en=enMar1+(jjday-jdMar1)*delen
end if
if(jjday.ge.274)then
      delen=(enMar1-enOct1)/151
      en=enOct1+(jjday-jdOct1)*delen
end if
else
      en=4460.
end if
```

Figure 3.9 shows the straight line approximation to seasonal energy density. Forcing prey fields are given in Figure 2.1.7.

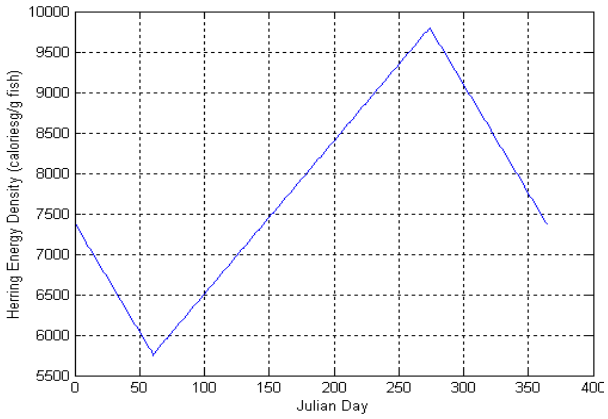

Fig. 3.9 Straight line approximation to a seasonal energy density curve.

Simulation results and final modifications to the herring model

The base model included YOY processes, included no multi-species functional response and provided a comparison of observed and predicted size-at-age, and included no spawning (observed data were taken after feeding but before spawning). Figures 3.10 to 3.12 show the fit of observed size (weight)-at-age compared to size-at-age predicted by the herring bioenergetics model by adjusting the "p" parameter of equation 2.1.2.

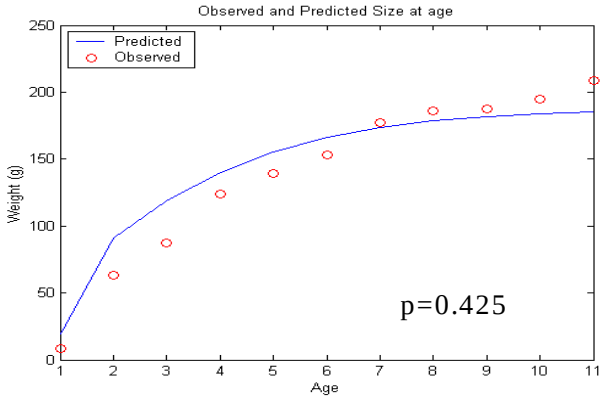

Fig. 3.10 Observed size-at-age of the 1973 herring year-class and size-at-age predicted from the herring bioenergetics model using p=0.425.

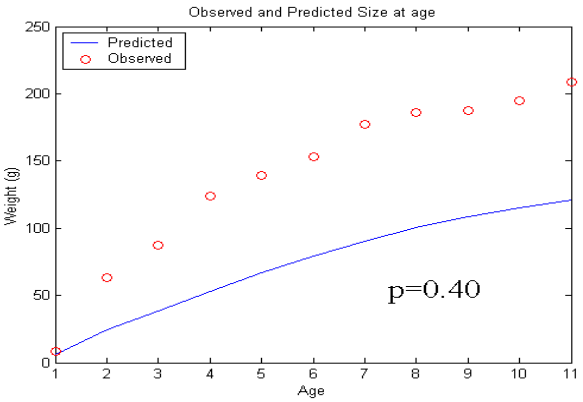

Fig. 3.11 Observed size-at-age of the 1973 herring year-class and size-at-age predicted from the herring bioenergetics model using p=0.40.

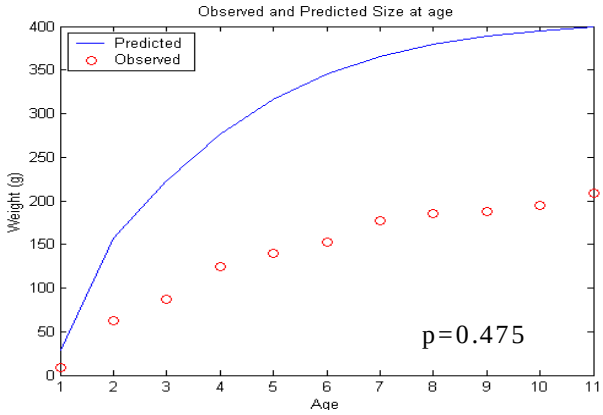

Fig. 3.12 Observed size-at-age of the 1973 herring year-class and size-at-age predicted from the herring bioenergetics model using p=0.475.

Observed herring size-at-age data were taken from the Straight of Georgia herring data using the 1973 age class, seen as age-1 in 1973 and present in the fishery until age 12 in 1984. As can be seen from these figures the model predictions of size-at-age were extremely sensitive to changing this parameter, the best fit being when p=0.425. A long-term simulation with these parameters is shown in Figure 3.13.

The base case was modified to include YOY improvements, age specific rates, multispecies functional response, location specific temperature description and change of temperature curve parameters, re-adjustment of p and k's to temperature change, and seasonal and age dependent energy density for fish.

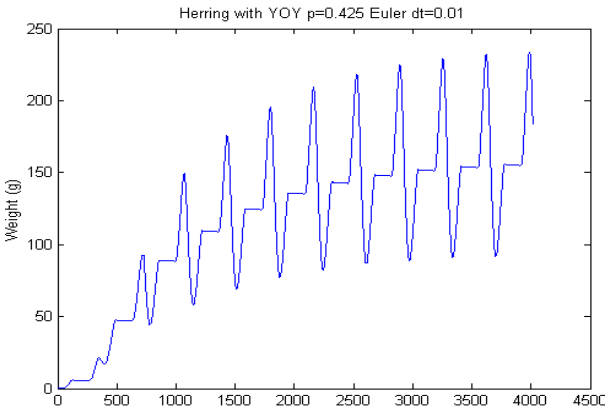

Fig. 3.13 Example of a long-term simulation of herring growth using tuned model parameters.

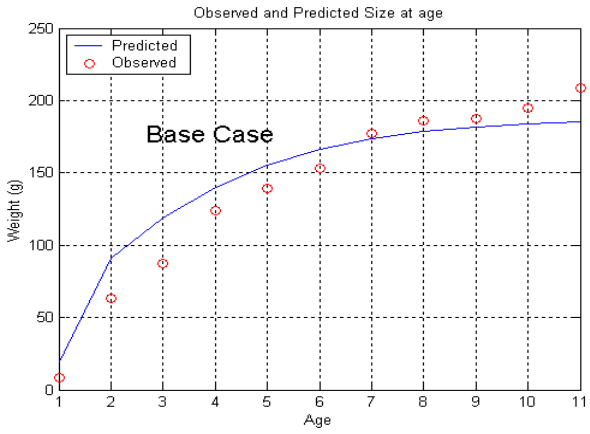

Fig. 3.14 Comparison of observed and predicted size-at-age, base case.

Figure 3.14 shows the base case. Figure 3.15 shows the base curve plotted against a run where the SDA, E and F equations were made age dependent. Age dependent parameters are given in Table 3.1. Also plotted in Figure 3.15 are model predictions when modifying the respiration equation to more accurately reflect the metabolic requirements of an age-0 herring (R) (Klumb *et al.* In review). The final curve in Figure 3.15 (All) demonstrates model output when all of these features were activated.

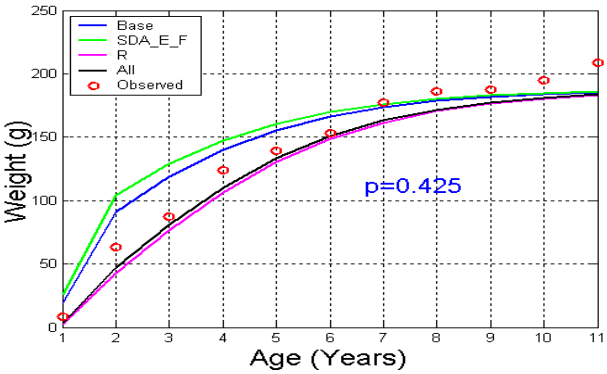

Fig. 3.15 YOY sensitivity. Observed and predicted size-at-age due to implementing age specific formulation for Specific Dynamic Action, egestion, excretion, respiration one at a time. The "all" line represents the run where all processes are age dependent and compared to the base run.

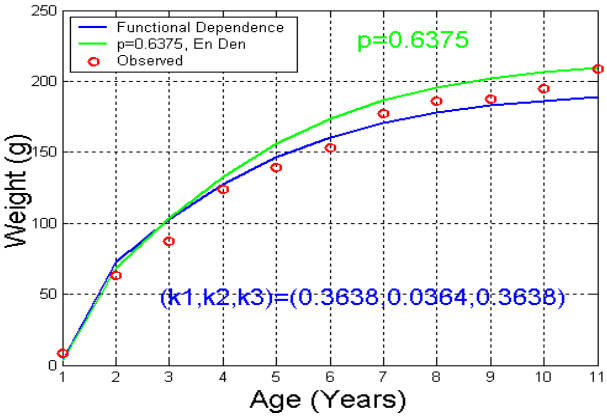

Fig. 3.16 Simulation run incorporating new temperature dependent values (seasonal range 8-14ºC) and the seasonal herring energy density algorithm. Comparisons are made of observed size-at-age between adjusting little "p" in equation 2.1.2 and using the multispecies functional dependence function (equations 2.1.13 and 2.1.14) with the k values as described above.

Finally, Figure 3.16 demonstrates results of the customized herring model for a p value of 0.6375, and for a run where the multispecies functional response to three prey types was activated using the parameters (k1, k2 and k3) shown in Figure 3.16, as well as the seasonal energy density algoritm. Note that to implement the multispecies functional response feature the line "con=0.75*gcmax" in the FORTRAN code needs to be commented out.

Trends in size-at-age: some ideas for hypothesis testing

Douglas Hay has data for size-at-age of Pacific herring over several decades. Over the last 20 years, the mean size-at-age has decreased at several locations for fish aged greater than 3 years. However, the mean size-at-age for ages 1–3 years did not show a significant decrease which may result from difficulties in sampling small fish (*i.e.* gear selectivity). In agreement to the observed size-at-age data, measurements from scale annuli collected over the same period from larger herring also showed no consistent decrease in growth for fish during the first 3 years of life. This decrease in size-at-age first appears when herring can begin to eat euphausiids in addition to copepods (age 3+). Generally, when euphausiids are abundant, the predation on herring by other piscivores that also eat euphausiids is reduced. Given this double benefit of more available food and less predation, the growth of herring should be highly sensitive to euphausiid production. The predatory zooplankton (ZP) compartment in the NEMURO model was designed to represent euphausiids.

Thus the coupled NEMURO-herring bioenergetics model could be used to examine the effects of temperature and other physical forcings (*e.g.*, Pacific Decadal Oscillation) on the production of euphausiids and thereby on the size-at-age of herring.

4.0 Saury group report and model results

Shin-ichi Ito[1], Michio J. Kishi[2], Yasuhiro Yamanaka[3] and Masahiko Fujii[4]

[1] Tohoku National Fisheries Research Institute, 3-27-5 Shinhamacho, Shiogama, Miyagi 985-0001, Japan. E-mail: goito@affrc.go.jp

[2] Hokkaido University, Minato-cho 3-1-1, Hakodate, Hokkaido 041-8611, Japan. E-mail: kishi@salmon.fish.hokudai.ac.jp

[3] Graduate School of Environmental Earth Science, Hokkaido University, North 10, West 5 Kita-ku, Sapporo, Hokkaido 060-0810, Japan. E-mail: galapen.ees.hokudai.ac.jp

[4] National Institute for Environmental Studies, 16-2 Onogawa, Tsukuba, 305-8506, Japan. E-mail: fujii.masahiko@nies.go.jp

The members of "team saury" were D. Huang, C. Hong, Y. I. Zuenko, T. Katukawa, T. Azumaya, S. Chiba, M. Fujii, M. J. Kishi, K. Tadokoro, M. B. Kashiwai, Y. Yamanaka, T. Okunishi, A. Tsuda, D. Mukai, M. Inada, T. Aiki and S. Ito.

According to the life history of Pacific saury, S. Ito proposed to have saury bioenergetics model coupled with the ecosystem model composed of a three- ocean-box model which corresponds to Kuroshio, Oyashio, and the mixed water region. But the three-box model is a little complicated to start with. As a first step we started from a coupled saury bioenergetics-ecosystem model with one box, and adapted the same type of governing equations for bioenergetics model as the ones for Pacific herring.

Model parameters are discussed for applying the model to Pacific saury. Here we report the discussion summary and model results.

Life history stages

Pacific saury are spawned in the Kuroshio and the mixed water region from autumn to spring. The larvae are advected to the Kuroshio extension region and juveniles migrate to the Oyashio region

through the mixed water region. After sufficient feeding in the Oyashio region, they migrate back to the spawning region. The swimming activity, feeding habitat and metabolism are different according to the life history stages. Odate (1977) and Kosaka (2000) divided the Pacific saury life history stages according to knob length (KL) (Table 4.1).

Table 4.1 Life stages of Pacific saury after Odate (1977).

Stage	Knob length
larvae	< 2.5 cm
juvenile	2.5 - 5.9 cm
earlier young	6.0 - 9.9 cm
later young	10.0 - 14.9 cm
small	15.0 - 19.9 cm
adult	> 20.0 cm

About the earlier stage growth, Watanabe and Kuji (1991) reared the saury larvae from hatching and they showed that it takes 60 days to grow to 79 mm KL. Watanabe *et al.* (1988) analyzed the growth rate of Pacific saury and they showed that it takes about 100 days to grow to 100 mm KL. According to their result, it takes about 180 days to become adult saury. Suyama *et al.* (1996) showed lower growth rate and it takes about 200 days to become an adult. For simplicity, only three life stages are assumed in the saury bioenergetics model (Table 4.2).

Table 4.2 Life stages of Pacific saury in the saruy bioenergetics model.

Stage	Age
larvae and juvenile	< 60 days
young and premature	60-180 days
adult	> 180 days

Maximum consumption rate C_{MAX}

Because adult Pacific saury are too difficult to rear in laboratories, there is no experimental estimation of consumption rate. Field data showed the average ration of the Pacific saury are 5.0 gww/day/individual for 20 cm, 7.2 gww/day/individual for 26 cm, and 10.2 gww/day/individual for 30 cm saury (Kurita and Sugisaki; in preparation). These data were estimated in the Oyashio region. Comparing this with observational data, we adapted 0.6 for a_c and -0.256 for b_c parameters. Figure 4.1 shows the C_{MAX} curve and observational value of ration per unit wet weight of the Pacific saury.

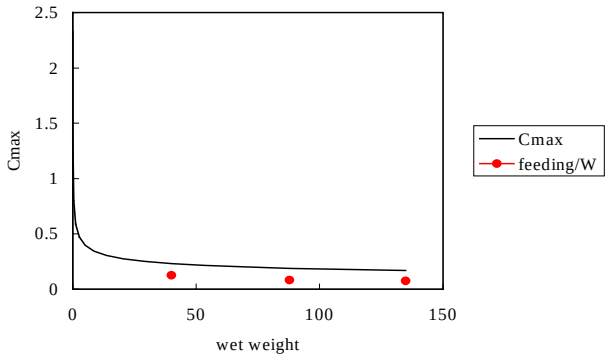

Fig. 4.1 C_{MAX} curve and observational value of ration per unit wet weight of the Pacific saury.

Temperature dependency for C_{MAX}

Oozeki (in preparation) analyzed the relationship between saury growth rate and environmental factors using the same field data reported in Watanabe *et al.* (1997). His result showed positive contributions from surface temperature and food density to growth rate. The SST range was between 16-22°C. Oozeki and Watanabe (2000) reared Pacific saury in the laboratory with different water temperatures and found a strong dependence of growth rate on temperature. The temperature range was between 12-24°C.

For adult saury we have no measures of growth rate at different temperatures. But the habitat temperature is between 16 and 20°C. We adapted the following values for the temperature dependency parameters for C_{MAX} of Pacific saury (Table 4.3). Figure 4.2 shows the temperature dependence function for each stage.

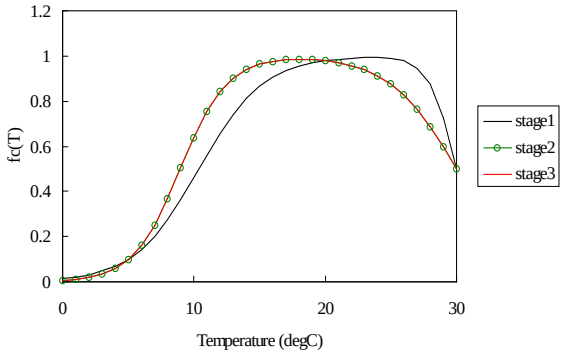

Fig. 4.2 Temperature dependence function of consumption rate of Pacific saury for each life stage.

Table 4.3 Temperature dependency parameters for $C_{MAX.}$

		Stage 1	Stage 2	Stage 3
te1	Temperature for xk1 (in ºC)	5	5	5
te2	Temperature for xk2 (in ºC)	20	16	16
te3	Temperature for xk3 (in ºC)	26	20	20
te4	Temperature for xk4 (in ºC)	30	30	30
xk1	Proportion of C_{MAX} at te1		0.10	
xk2	Proportion of C_{MAX} at te2		0.98	
xk3	Proportion of C_{MAX} at te3		0.98	
xk4	Proportion of C_{MAX} at te4		0.5	

Swimming speed

Although we do not have actual data on swimming speed of Pacific saury, other small pelagic fish swim at speeds of several times their body length per second. We assumed the normal swimming speed is two times of the knob length (nearly same as body length) per weight (Fig. 4.3).

$$U = 2.0\ KL$$

On the other hand, the wet weight (g)-knob length (cm) relation was proposed by Kosaka (2000) as:

larvae and juvenile
$\log W = -2.069 + 2.42439 \log L$
earlier young
$\log W = -2.483 + 3.06174 \log L$
later young
$\log W = -2.335 + 2.93760 \log L$
small
$\log W = -2.688 + 3.22526 \log L$
adult
$\log W = -2.685 + 3.21229 \log L$

Figure 4.4 shows the wet weight-knob length relation curves of Kosaka (2000). If we adapt the simple one curve for all stages, it becomes

$$W = (KL / 6.13)^{3}$$

and the curve will look like Figure 4.4. The broken line in Figure 4.3 shows the same curve.

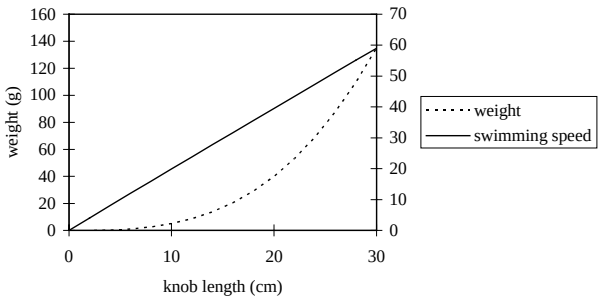

Fig. 4.3 Swimming speed (cm/s) and wet weight (g) as a function of body length (cm).

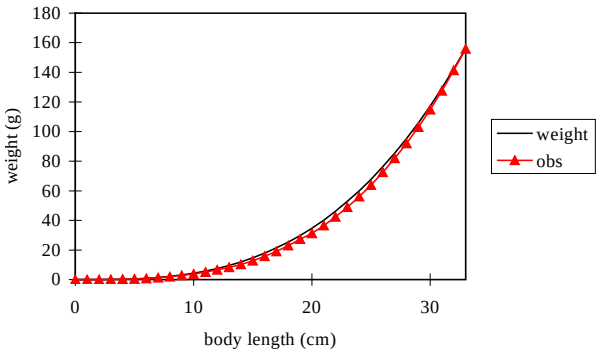

Fig. 4.4 Wet weight (g)-knob length (cm) relation curves of Kosaka (2000) (red) and fitting curve (black).

The last equation could be rewritten as

$$KL = 6.13\ W^{0.33}$$

and the swimming speed becomes

$$U = 12.3\ W^{0.33}$$

and we adapted 12.3 as a_A parameter when the temperature is higher than 12°C and 0.33 for b_A value. For temperatures less than 12°C we adapted 2.0 as a_A. The weight - swimming speed relation looks like Figure 4.5 when the temperature is higher than 12°C.

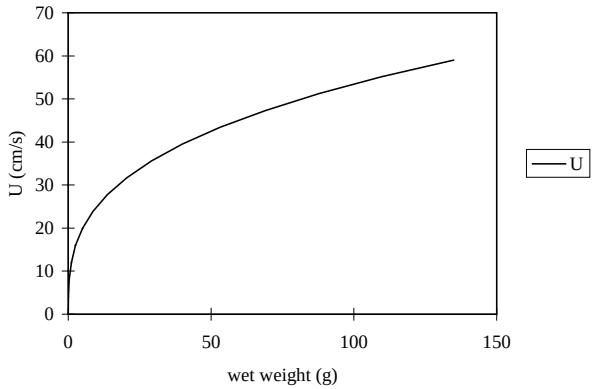

Fig. 4.5 Wet weight (g)-swimming speed (U-cm/s) relation curve for higher temperature.

The parameters we adapted for Pacific saury bioenergetics model are summarized on Table 4.4.

Table 4.4 Summary of parameter values used in the saury bioenergetics model.

Symbol	Parameter description	Value
Consumption, C_{MAX}		
a_C	Intercept for C_{MAX} at (te1+te3)/2	0.6
b_C	coefficient for C_{MAX} versus weight	-0.256
te1	Temperature for xk1 (in ºC)	5, 5, 5
te2	Temperature for xk2 (in ºC)	20, 16, 16
te3	Temperature for xk3 (in ºC)	26, 20, 20
te4	Temperature for xk4 (in ºC)	30, 30, 30
xk1	Proportion of C_{MAX} at te1	0.10
xk2	Proportion of C_{MAX} at te2	0.98
xk3	Proportion of C_{MAX} at te3	0.98
xk4	Proportion of C_{MAX} at te4	0.5
Metabolism, R		
a_R	Intercept for R	0.0033
b_R	Coefficient for R versus weight	-0.227
c_R	Coefficient for R versus temperature	0.0548
d_R	Coefficient for R versus swimming speed	0.03
S	Coefficient for Specific Dynamic Action	0.175
Swimming speed, U		
a_A	Intercept U (< 12 ºC) (in cm/s)	2.0
a_A	Intercept U (≥ 12 ºC) (in cm/s)	12.3
b_A	Coefficient U versus weight	0.33
c_A	Coefficient U versus temperature (< 12 ºC)	0.149
c_A	Coefficient U versus temperature (≥ 12 ºC)	0.0
Egestion and excretion, F and E		
a_F	Proportion of consumed food egested	0.16
a_E	Proportion of consumed food excreted	0.10
Multispecies functional response (by saury size groups)		

V_{11}	Vulnerability of prey group 1 to predator 1	1.0
V_{12}	Vulnerability of prey group 2 to predator 1	0.0
V_{13}	Vulnerability of prey group 3 to predator 1	0.0
K_{11}	Half saturation constant for prey group 1 to predator 1 (g wet weight/m^3)	100.0
K_{12}	Half saturation constant for prey group 2 to predator 1 (g wet weight/m^3)	100.0
K_{13}	Half saturation constant for prey group 3 to predator 1 (g wet weight/m^3)	100.0
V_{21}	Vulnerability of prey group 1 to predator 2	1.0
V_{22}	Vulnerability of prey group 2 to predator 2	1.0
V_{23}	Vulnerability of prey group 3 to predator 2	0.0
K_{21}	Half saturation constant for prey group 1 to predator 2 (g wet weight/m^3)	100.0
K_{22}	Half saturation constant for prey group 2 to predator 2 (g wet weight/m^3)	100.0
K_{23}	Half saturation constant for prey group 3 to predator 2 (g wet weight/m^3)	100.0
V_{31}	Vulnerability of prey group 1 to predator 3	0.0
V_{32}	Vulnerability of prey group 2 to predator 3	1.0
V_{33}	Vulnerability of prey group 3 to predator 3	1.0
K_{31}	Half saturation constant for prey group 1 to predator 3 (g wet weight/m^3)	100.0
K_{32}	Half saturation constant for prey group 2 to predator 3 (g wet weight/m^3)	100.0
K_{33}	Half saturation constant for prey group 3 to predator 3 (g wet weight/m^3)	100.0

start day is February 1st

stage 1	0-50mm	0-30days
stage 2	50-200mm	30-150days
stage 3	>200mm	150day-720days

Model result

The parameters which are revised for the Pacific saury were used to integrate the bioenergetics model coupled with the ecosystem model. Figure 4.6 shows the result of the integration, and shows that the weight of saury reached 120 g after one year. This seems reasonable for Pacific saury. The model shows a high growth rate around 13ºC water temperature. This corresponds to the habitat temperature in the Oyashio region during the feeding season.

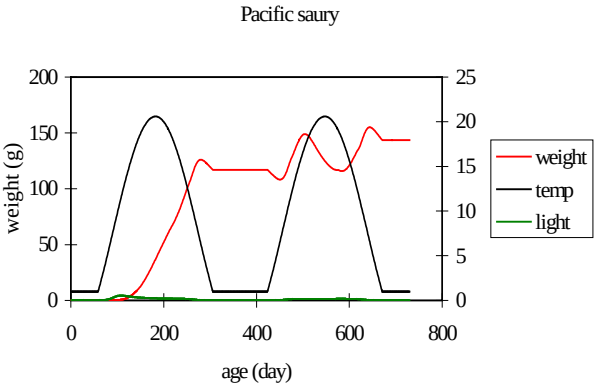

Fig. 4.6 Result of Pacific saury bioenergetics model. Light is in units of ly/min.

Figure 4.7 shows the interannual experiment of ecosystem-saury coupled model with realistic

forcing of A7 (Akkeshi line St 7 off Hokkaido, Japan). The model results show low growth rate in the third and fourth year cohort. The result strongly depends on water temperature.

Future work

This model is not perfect and needs improvements in several respects.

- The weight of the earliest stage is not reproduced well. We should re-parameterize values for this stage.
- More than half of the Pacific saury spawn in the first year and all of them spawn in the second year (Kurita and Sugisaki; in preparation). We should include the effect of spawning in this model.
- In this model only one ocean region is included. But the saury migrate from the subtropical to the subarctic region through the mixed water region, each with its own seasonal cycle of temperature and prey. We should include at least three ocean regions in the ecosystem-saury coupled model. We suggest Figure 4.8 as a prototype three ocean region model. This kind of model is very useful for the analysis of interannual variability of saury growth.

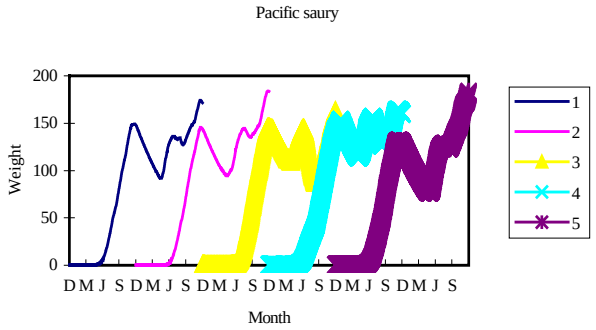

Fig. 4.7 Result of Pacific saury bioenergetics model with realistic forcing.

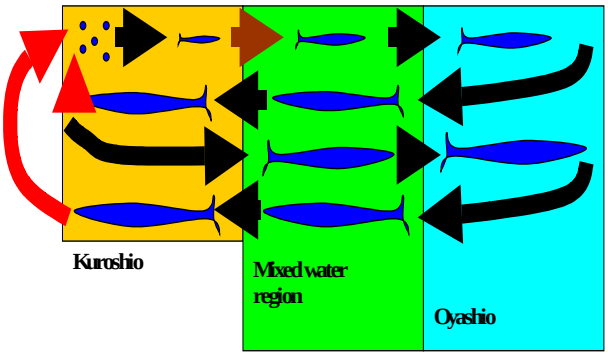

Fig. 4.8 Schematic picture of a three-ocean-box model. This model includes three ocean regions but only one saury bioenergetic model.

5.0 Model experiments and hypotheses

Several model experiments were discussed to test hypotheses regarding the effects of climate change. The details of the experiments and hypotheses are described below.

Space hypothesis

Geographic variation in fish growth: Differences in environmental conditions, and resulting differences in lower trophic conditions, can account for the differences in herring growth rates among selected sites in the North Pacific ecosystem. There exist long-term data sets on size-at-age of herring from many locations in the North Pacific. These data sets show that herring growth rates over the past decades have varied consistently among the different locations. Understanding the extent to which environmental conditions account for these temperature differences in herring growth is important for predicting climate change effects and for effective management of these fisheries in the future.

Key regions contributing to fish growth and biomass variations: Pacific saury are spawned in the subtropical and transition zone from autumn to spring, and migrate from the subtropical to the subarctic ocean through a transition zone. The environments of these three regions show different interannual variability, and it is very difficult to distinguish which location (or season) is most important to the interannual variability of fish growth and biomass. We will tune up the NPZ model coupled to the fish growth model with long-

term climate and weather records by comparing the model results of fish growth with interannual variability in observed size composition. To understand which region contributes most to the interannual variability in fish growth and biomass, sensitivity tests of this model will be very useful. Understanding key regions in fish growth and biomass variation is also important for predicting climate change effects and for effective management of these fisheries in the future.

Time hypothesis

Understanding regime shifts: Synchronous changes in herring growth rates across locations may be accounted for by basin-wide decadal-scale changes in environmental conditions. Preliminary examination of herring growth rates at several locations showed sudden shifts in growth rates occurring in the same years across all locations. We will combine the long-term datasets on herring growth, where possible, with regional and local long-term climate and weather records, and use the NPZ model coupled to the fish growth model to examine possible environmental regime changes.

Understanding how regime shifts cascade up the food web may be our best chance for using past conditions to infer future effects of climate change.

Change of dominant species: Changes in the dominant small pelagic fish species seems to coincide with basin-wide decadal-scale changes in environmental conditions. For example, the dominant species changed from sardine to saury across the regime shift in 1987.

Comparing different fish bioenergetics models with the same NPZ model is very useful to understand the climate change effects on ocean ecosystems through bottom-up processes.

Climate change hypothesis

Global climate change effects on energy pathways and fish production: Climate change may result in energy being diverted from the pelagic pathway and shunted through the microbial pathway, resulting in less food for pelagic fish and consequently slower fish growth rates. We will use the coupled NPZ and fish models, the long-term datasets, and defined climate change scenarios to predict how climate change might affect energy cycling, shift the dominance among different phytoplankton and zooplankton groups, and affect fish growth and production in the North Pacific ecosystem. Model simulations will be performed under present-day (baseline) environmental conditions, and for a suite of realistic climate change scenarios. Comparing these linkages and pathways under baseline and climate change scenarios for a variety of locations that have different environmental conditions (*e.g.*, shallow coastal versus deep blue water) will aid in the interpretation and generalization of our results.

6.0 Recommendations

Results of the model work accomplished at the workshop resulted in several recommendations. They are listed here in priority. A description of workplan scheduling is indicated after each item in parentheses and in italics:

1. Develop site-specific applications (*to be scheduled*);
2. Perform herring comparison between the Sea of Okhotsk and Vancouver Island (*to be scheduled*);
3. Incorporate data observations into NEMURO (*to be programmed*);
   a. Obtain physical parameters (radiation, cloud cover, wind stress);
   b. Obtain realistic time series of SST and photosynthetically active light;
   c. Obtain physical observed time series;
   d. Obtain observed zooplankton time series;
4. Execute a dynamics linkage in NEMURO.FISH (*to be scheduled*);

5. Revise physiological parameters (fish and LTL) (*to be scheduled*);
6. Public web distribution (PICES to support) (*to be scheduled*);
7. Meet in Qingdao with (1) and (2) finished (*to be scheduled*);
8. Consider explicit spatial (x, y, z) and temporal structure (*to be programmed*);
9. Dissemination of NEMURO.FISH results in GLOBEC newsletter and scientific publications (*to be scheduled*);
10. Develop a project home page (*to be scheduled*);
11. Incorporate age structure, reproduction and early life history into NEMURO.FISH (*to be programmed*).

The last recommendation was discussed at length because of a perceived need to provide a tool for the management of fisheries.

It was noted that fish biomass at any time can be represented as the product of fish weight (W) and fish numbers (N).

(6.1) $B_t = N_t \cdot W_t$

The rate of change of fish biomass can be written as

(6.2) $$\frac{dB}{dt} = N\frac{dW}{dt} + W\frac{dN}{dt}$$

where we know from the fish bioenergetics model that

(6.3) $$\frac{dW}{dt} = C - (R + SDA + E + F)\cdot W$$

and from fish population dynamics we know that

(6.4) $$\frac{dN}{dt} = e^{-(F+M)} \cdot N$$

where F is the instantaneous fishing mortality rate and M is the instantaneous natural mortality rate. Thus all of the components of equation 6.2 are known or can be estimated.

Also note that with this approach we can compare observed growth to von Bertalanffy growth, a growth model very commonly used in fisheries science.

The von Bertalanffy empirical growth model (von Bertalanffy 1938) is written

(6.5) $W(t) = W_\infty \cdot (1 - e^{-k\cdot(t-t_0)})^3$

where W_∞ is the asymptotic weight, W is the weight at time t, k is the growth parameter with units t^{-1}, and t_0 is the theoretical age the fish would have zero weight had they always grown as described by (6.5).

The differential form of (6.5) is

(6.6) $$\frac{dW}{dt} = 3k \cdot (W^{2/3} \cdot W_\infty^{1/3} - W)$$

We know that the change in weight formulation from the fish bioenergetics model (6.3) can be collapsed into a simpler form because most terms are dependent on consumption thus they are proportional to C and the C and R terms are weight dependent. So (6.3) can be simplified to

(6.7) $$\frac{dW}{dt} = p3 \cdot C - p1 \cdot W^{p2}$$

Equating (6.7) and (6.6) we can calculate the rate of consumption required for von Bertalanffy growth, C*, as

(6.8)
$$C^* = \frac{1}{p3} \cdot \left[3k \cdot W^{2/3} \cdot W_\infty^{1/3} - 3k \cdot W + p1 \cdot W^{p2} \right]$$

So it seems the theoretical foundation of extending NEMURO.FISH to a population level model useful for fisheries management is possible with a few minor modifications.

7.0 Achievements and future steps

The achievements of the Workshop can be listed as follows:

1. Developed the prototype model, *NEMURO.FISH*. This was an extremely important step because it translates our science into something tangible and economically relevant to human populations that rely on fishes for food - obtaining food from the seas on a sustainable basis;
2. Assembled an international team of marine biologists, fisheries biologists, and physical oceanographers who collectively achieved a consensus on the structure and function of a PICES Climate Change and Carrying Capacity (CCCC) prototype lower trophic level (LTL) ecosystem model for the North Pacific Ocean that included pelagic fishes, and named it "*NEMURO.FISH*";
3. Developed a computer simulation model of fish bioenergetics and growth;
4. Coupled the fish model to the NEMURO lower trophic level model;
5. Adapted the fish bioenergetics model to Pacific herring (*Clupea harengus pallasi*) in the eastern North Pacific and Pacific saury (*Cololabis saira*) in the western North Pacific;
6. Made recommendations for future modeling activities.

The significance of these achievements will ultimately be evaluated by how well the CCCC Program effectively utilizes and embraces these models as a basis of future modeling activity.

8.0 Acknowledgements

This workshop was proposed and convened by PICES, more precisely the PICES/CCCC-IP/MODEL and REX Task Teams. On behalf of the workshop participants, the co-conveners would like to express sincere thanks for giving us a timely and valuable opportunity to participate in the development of a linked higher trophic level - lower trophic level marine ecosystem model common among component programs of the PICES GLOBEC Program. The Heiwa-Nakajima Foundation of Japan contributed the major part of financial support for this workshop. We note this valuable support, for without it, the workshop would not have been possible. Nemuro was selected as the venue due in large part to the invitation from the Nemuro Supporting Committee. The conveners express their very deep appreciation for the warm welcome and perfect support arranged and given by the Nemuro Supporting Committee, their staff, and the people of Nemuro.

9.0 References

Arrhenius, F. 1998a. Variable length of daily feeding period in bioenergetics modelling: a test with 0-group Baltic herring. Journal of Fish Biology 52:855-860.

Arrhenius, F. 1998b. Food intake and seasonal changes in energy content of young Baltic Sea sprat (*Sprattus sprattus L.*). ICES Journal of Marine Science 55:319-324.

Arrhenius, F. and Hansson, S. 1996. Growth and seasonal changes in energy content of young Baltic Sea herring (*Clupea harengus* L.). ICES Journal of Marine Science 53:792-801.

Batty, R. S. 1987. Effect of light intensity on activity and food-searching of larval herring, *Clupea harengus*: a laboratory study. Marine Biology 94:323-327.

Beamish, R.J., Noakes, D.J., Mcfarlane, G.A., Klyashtorin, L., Ivanov, V.V., and Kurashov, R. 1999. The regime concept and natural trends in the production of Pacific salmon. Can. J. Fish. Aquat. Sci. 56: 516-526.

Beamish, F. W. H. 1974. Apparent specific dynamic action of largemouth bass, *Micropterus salmoides*. Journal of the Fisheries Research Board of Canada 31:1763-1769.

Beamish, F. W. H. and Trippel, E. A. 1990. Heat increment: A static or dynamic dimension in bioenergetic models? Transactions of the American Fisheries Society 119:649-661.

Beitinger, T. L. and Magnuson, J. J. 1979. Growth rates and temperature selection of bluegill, *Lepomis macrochirus*. Transactions of the American Fisheries Society 108:378-382.

Bertalanffy, L. von. 1938. A quantitative theory of organic growth (Inquiries on growth laws II). Human Biology, 10(2): 181-213.

Blaxter, J. H. S. and Hunter, J. R. 1982. The biology of clupeoid fishes. *In* J. H. S. Blaxter, F. S. Russell, and M. Yonge (eds.) Advances in Marine Biology Volume 20. Academic Press, London, UK.

Brett, J. R. 1985. Correction in use of oxycalorific equivalent. Canadian Journal of Fisheries and Aquatic Sciences 42:1326-1327.

Brett, J. R. and Groves, T. D. D. 1979. Physiological energetics. *In* W. S. Hoar, D. J. Randall, and J.R. Brett (eds.) Fish physiology Vol. VIII bioenergetics and growth. Academic Press, Inc., New York, pp. 279 – 352.

Cummins, K. W. and Wuycheck, J. C. 1971. Caloric equivalents for investigations in ecological energetics. Mitteilungen Internationale Vereinigung fur Theoretische und Angewandte Limnologie 18.

Dabrowski, K. 1985. Energy budget of coregonid (*Coregonus* spp.) fish growth, metabolism and reproduction. Oikos 45:358-364.

Dabrowski, K. 1986. Energy utilization during swimming and cost of locomotion in larval and juvenile fish. Sonderdruck aus Journal of Applied Ichthyology 2:110-117.

Dabrowski, K., Takashima, F. and Law, Y. K. 1988. Bioenergetic model of planktivorous fish feeding, growth and metabolism: theoretical optimum swimming speed of fish larvae. Journal of Fish Biology 32:443-458.

De Silva, S. S. 1973. Food and feeding habits of the herring *Clupea harengus* and the sprat *C. sprattus* in inshore waters of the west coast of Scotland. Marine Biology 20:282-290.

De Silva, C. D. and Tytler, P. 1973. The influence of reduced environmental oxygen on the metabolism and survival of herring and plaice larvae. Netherlands Journal of Sea Research 7:345-362.

De Silva, S. S. and Balbontin, F. 1974. Laboratory studies on food intake, growth and food conversion of young herring, *Clupea harengus* (L.). Journal of Fish Biology 6:645-658.

Durbin, E. G. and Durbin, A. G. 1981. Assimilation efficiency and nitrogen excretion of a filter-feeding planktivore, the Atlantic menhaden, *Brevoortia tyrannus* (Pisces: Clupeidae). Fishery Bulletin U.S. 79:601-616.

Durbin, E. G. and Durbin, A. G. 1983. Energy and nitrogen budgets for the Atlantic menhaden, *Brevoortia tyrannus* (Pisces: Clupeidae), a filter-feeding planktivore. Fishery Bulletin U.S. 81:177-199.

Durbin, A. G., Durbin, E. G., Verity, P. G., and Smayda, T. J. 1981. Voluntary swimming speeds and respiration rates of a filter-feeding planktivore, the Atlantic menhaden, *Brevoortia tyrannus* (Pisces: Clupeidae). Fishery Bulletin U.S. 78:877-886.

Elliott, J. M. 1976a. Energy losses in the waste products of brown trout (*Salmo trutta* L.). Journal of Animal Ecology 45:561-580.

Elliott, J. M. 1976b. The energetics of feeding, metabolism, and growth of brown trout (*Salmo trutta* L.) in relation to body weight, water temperature, and ration size. Journal of Animal Ecology 45:923-948.

Elliott, J. M. 1979. Energetics of freshwater teleosts. Symposium Zoological Society of London 44:29-61.

Elliott, J. M. and Davison, W. 1975. Energy equivalents of oxygen consumption in animal energetics. Oecologia 19:195-201.

Flath, L. E. and Diana, J. S. 1985. Seasonal energy dynamics of the alewife in southeastern Lake Michigan. Transactions of the American Fisheries Society 114:328-337.

Fiksen, O. and Folkvord, A. 1999. Modelling growth and ingestion processes in herring *Clupea harengus* larvae. Marine Ecology Progress Series 184:273-289.

Foy, R. J. and Norcross, B. L. 1999. Spatial and temporal variability in the diet of juvenile Pacific herring (*Clupea pallasi*) in Prince William Sound, Alaska. Canadian Journal of Zoology 77:697-706.

Foy, R. J. and Paul, A. J. 1999. Winter feeding and changes in somatic energy content of age-0 Pacific herring in Prince William Sound, Alaska. Transactions of the American Fisheries Society 128:1193-1200.

Grabe, S. A. 1996. Feeding chronology and habits of *Alosa* spp. (Clupeidae) juveniles from the lower Hudson River estuary, New York. Environmental Biology of Fishes 47:321-326.

Giguère, L. A., Côté, B., and St-Pierre, J.-F. 1988. Metabolic rates scale isometrically in larval fishes. Marine Ecology Progress Series 50:13-19.

Haegele, C.W. 1997. The occurrence, abundance and food of juvenile herring and salmon in the Strait of Georgia, British Columbia in 1990 to 1994. Can. Man. Rep. Fish. Aquat. Sci. 2390: 124 pp.

Haist, V. and Stocker, M. 1985. Growth and maturation of Pacific herring (*Clupea harengus pallasi*) in the Strait of Georgia. Proceedings of The Symposium on the Biological Characteristics of Herring and Their Implication for Management. Can. J. Aquat. Sci., vol. 42(l), pp. 138-146.

Hanson, P. C., Johnson, T. B., Schindler, D. E., Kitchell, J. F. 1997. Fish bioenergetics 3.0 for Windows. University of Wisconsin Sea Grant Institute. Technical Report WISCU-T-97-001, Madison, Wisconsin, USA.

Hartman, K. J. and Brandt, S. B. 1995. Estimating energy density of fish. Transactions of the American Fisheries Society 124:347-355.

Hay, D.E. and McCarter, P.B. 2001. Spatial, temporal and life-stage variation in herring diets in British Columbia. PICES Workshop Reports. PICES Sci. Report 15: 95-98.

Hay, D.E., Thompson, M.J., and McCarter, P.B. 2001. Anatomy of a strong year class: Analysis of the 1977 year class of Pacific herring in British Columbia and Alaska. Herring: Expectations for a new millennium. University of Alaska Sea Grant, AK-SG-01-04, Fairbanks, pp. 171-198.

Hettler, W. F. 1976. Influence of temperature and salinity on routine metabolic rate and growth of young Atlantic menhaden. Journal of Fish Biology 8:55-65.

Hollowed, A.B. and Wooster, W.S. 1992. Variability of winter ocean conditions and strong year-classes of Northeast Pacific groundfish. ICES Mar. Sci. Symp. 195: 433-444.

Hollowed, A.B. and Wooster, W.S. 1995. Decadal scale variations in the eastern subarctic Pacific: II. Response of Northeast Pacific fish stocks. *In* R.J. Beamish. (ed.) Climate change and northern fish populations. Canadian Special Publication of Fisheries and Aquatic Sciences 121: 375-386.

Ikeda, T. 1996. Metabolism, body composition, and energy budget of the mesopelagic fish *Maurolicus muelleri* in the Sea of Japan. Fishery Bulletin U.S. 94:49-58.

James, A. G. and Probyn, T. 1989. The relationship between respiration rate, swimming speed and feeding behaviour in the Cape anchovy *Engraulis capensis* Gilchrist. Journal of Experimental Marine Biology and Ecology 131:81-100.

Janssen, J. 1976. Feeding modes and prey size selection in the alewife (*Alosa pseudoharengus*). Journal of the Fisheries Research Board of Canada 33:1972-1975.

Janssen, J. and Brandt, S. B. 1980. Feeding ecology and vertical migration of adult alewives (*Alosa pseudoharengus*) in Lake Michigan. Canadian Journal of Fisheries and Aquatic Sciences 37:177-184.

Kamler, E. 1972. Respiration of carp in relation to body size and temperature. Polskie Archiwum Hydrobiologii 19: 325-331.

Katz, H. M. 1978. Circadian rhythms in juvenile American shad, *Alosa sapidissima*. Journal of Fish Biology 12:609-614.

Kaufmann, R. 1990. Respiratory cost of swimming in larval and juvenile cyprinids. Journal of Experimental Biology 150:343-366.

Kerr, S. R. and Dickie, L. M. 1985. Bioenergetics of 0+ Atlantic herring (*Clupea harengus*

harengus). Canadian Journal of Fisheries and Aquatic Sciences 42 (1):105-110.

Kiørboe, T., Munk, P. and Støttrup, J. G. 1985. First feeding by larval herring *Clupea harengus* L. Dana 5:95-107.

Kiørboe, T., Munk, P. and Richardson, K. 1987. Respiration and growth of larval herring *Clupea harengus*: relation between specific dynamic action and growth efficiency. Marine Ecological Progress Series 40:1-10.

Kitchell, J. F., Koonce, J. F., O'Neill, R. V., Shugart, H. H., Jr., Magnuson, J. J. and Booth, R. S. 1974. Model of fish biomass dynamics. Transactions of the American Fisheries Society 103:786-798.

Klumb, R. A., Rudstam, L. G., and Mills, E. L. Respiration rates and swimming speeds of larval and juvenile alewives *Alosa pseudoharengus*: implications for bioenergetics models. Transactions of the American Fisheries Society (in review).

Klumpp, D. W. and Westernhagen, H. von. 1986. Nitrogen balance in marine fish larvae: influence of developmental stage and prey density. Marine Biology 93:189-199.

Kosaka S. 2000. Life history of the Pacific saury *Cololabis saira* in the northwest Pacific and considerations on resources fluctuations based on it. Bull. Tohoku Natl. Fish. Res. Inst. 63: 1-96.

Kurita Y. and Sugisaki, H. 2002. Seasonal changes in daily ration of Pacific saury, *Cololabis saria*. to be submitted to Fish. Oceanogr.

Laurence, G. C. 1976. Caloric content of some north Atlantic calanoid copepods. Fishery Bulletin U.S. 78: 218-220.

Leonov A.V and Sapozhnikov V.V. 1997. Biohydrochemical model of organic substance transformations and its applying for the calculation of primary production in the Okhots Sea ecosystem. *In* Complex studies of the Okhotsk Sea ecosystem. Publ. House VNIRO, Moscow, pp. 143-166. (In Russian).

Leonov A.V. and Stygar O.V. 1999. Seasonal variations of biogenic substance concentrations and bioproductivity of waters in northern part of the Caspian Sea. Vodnye Resoursy V. 26 (6), pp. 743-756. (In Russian).

Limburg, K. E. 1994. Ecological constraints on growth and migration of juvenile American shad (*Alosa sapidissima* Wilson) in the Hudson River Estuary, New York. Doctoral dissertation. Cornell University, Ithaca, New York.

Muir, B. S. and Niimi, A. J. 1972. Oxygen consumption of the euryhaline fish aholehole (*Kuhlia sandvicensis*) with reference to salinity, swimming, and food consumption. Journal of the Fisheries Research Board of Canada 29:67-77.

Munk, P. 1992. Foraging behaviour and prey size spectra of larval herring *Clupea harengus*. Marine Ecology Progress Series 80:149-158.

Munk, P. and Kiorboe, T. 1985. Feeding behaviour and swimming activity of larval herring (*Clupea harengus*) in relation to density of copepod nauplii. Marine Ecology - Progress Series 24:15-21.

Nakata, K., Ito, H., Ichikawa, T., and Sasaki, K. 2002. Reproduction of three Oncaea speices in the Kuroshio Extention in spring. Fish. Oceanogr. (submitted).

Odate, S. 1977. On distribution of Pacific saury in the North Pacific Ocean. Res. Inst. North Pac. Fish. Sp. Vol. 10 Faculty of Fisheries, Hokkaido University, Hakodate, Japan, pp. 353-382.

Ohtani, K. and Azumaya, T. 1995. Influence of interannual changes in ocean conditions on the abundance of walleye pollock (*Theragra chalcogramma*) in the eastern Bering Sea. *In* R.J. Beamish. (ed.) Climate change and northern fish populations. Canadian Special Publication of Fisheries and Aquat. Sci. 121: 87-95.

Oozeki, Y. and Watanabe, Y. 2000. Comparison of somatic growth and otolith increment growth in laboratory-reared larvae of Pacific saury, *Cololabis saira*, under different temperature conditions. Marine Biology 136: 349-359.

Oozeki, Y. and Watanabe, Y. 2002. Environment factor affecting the larval growth of Pacific saury, *Cololabis saira*, in the northwestern Pacific Ocean. Fish. Oceanogr. (submitted).

Paul, A. J. and Paul, J. M. 1998a. Spring and summer whole-body energy content of Alaskan juvenile Pacific herring. Alaska Fishery Research Bulletin 5:131-136.

Paul, A. J. and Paul, J. M. 1998b. Comparisons of whole body energy content of captive

fasting age zero Alaskan Pacific herring (*Clupea pallasi Valenciennes*) and cohorts over-wintering in nature. Journal of Experimental Marine Biology and Ecology 226:75-86.

Paul, A. J., Paul, J. M., and Brown, E. D. 1998. Fall and spring somatic energy content for Alaskan Pacific herring (*Clupea pallasi Valenciennes* 1847) relative to age, size and sex. Journal of Experimental Marine Biology and Ecology 223:133-142.

Pischalnik V.M. and Leonov A.V. 2001. Experience of combined application of electronic atlas of oceanographical data for shelf zone of Sakhalin Island and simulation mathematical model for the study of biotransformation processes in marine environment (examples for La Perouse Strait and Aniva Bay). (in press, in Russian).

Polovina, J.J., Mitchum, G.T. and Evans, G.T. 1995. Decadal and basin-scale variation in mixed layer depth and the impact on biological production in the Central and North Pacific 1960-1988. Deep Sea Research 42:1701-1716.

Post, J. R. and Lee, J. A. 1996. Metabolic ontogeny of teleost fishes. Canadian Journal of Fisheries and Aquatic Sciences 53:910-923.

Rose, K.A., Rutherford, E.S., McDermot, D.S., Forney, J.L., and Miles, E.L. 1999. Individual-based model of yellow perch and walleye populations in Oneida Lake. Ecological Monographs 69(2): 127-154.

Rudstam, L. G. 1988. Exploring the dynamics of herring consumption in the Baltic: applications of an energetic model of fish growth. Kieler Meeresforschung Sonderheft 6:312-322.

Sherman, K. and Honey, K. A. 1971. Seasonal variations in the food of larval herring in coastal waters of central Maine. Rapports et Proces-Verbaux des Reunions. Conseil International pour l'Exploration de la Mer 160:121-124.

Stewart, D. J. and Binkowski, F. P. 1986. Dynamics of consumption and food conversion by Lake Michigan alewives: an energetics-modeling synthesis. Transactions of the American Fisheries Society 115:643-661.

Stewart, D. J., Weininger, D., Rottiers, D. V., and Edsall, T. A. 1983. An energetics model for lake trout, *Salvelinus namaycush*: application to the Lake Michigan population. Canadian Journal of Fisheries and Aquatic Sciences 40: 681-698.

Sugisaki H. and Kurita, Y. 2002. Daily rhythm and seasonal variation of feeding habit of saury. Fish. Oceanogr. (submitted).

Suyama S., Sakurai, Y., and Shimazaki, K. 1996 Age and growth of pacific saury *Cololabis saira* (Brevoort) in the Western North Pacific Ocean estimated from daily otolith growth increments. Fish. Science 62: 1-7.

Suyama S., Kurita, Y., Kamei, Y., Kajiwara, Y., and Ueno, Y. 2002. Annual change of the size in each year class of Pacific saury (*Cololabis saira*) estimated based on the hyaline zone in the otolith. Fish. Oceanogr. (submitted).

Theilacker, G. H. 1987. Feeding ecology and growth energetics of larval northern anchovy, *Engraulis mordax*. Fishery Bulletin U.S. 85:213-228.

Thornton, K. W. and Lessem, A. S. 1978. A temperature algorithm for modifying biological rates. Transactions of the American Fisheries Society 107:284-287.

Tian Y., Akamine, T., and Suda, M. 2002a. Long-term variability in the abundance of Pacific saury in the northwestern Pacific ocean and climate changes during the last century. Bull. Jpn. Soc. Fish. Oceanogr. 66; 16-25.

Tian Y., Ueno, Y., Akamine, T., and Suda, M. 2002b. Climate-ocean variability and the response of Pacific saury (*Cololabis saira*) in the northwestern Pacific during the last century. Fish. Sci. (submitted).

Wailes, G. H. 1936. Food of *Clupea pallasii* in southern British Columbia waters. Journal of the Biology Board of Canada 1:477-?

Watanabe. Y., and Butler, J. L., and Mori, T. 1988. Growth of Pacific saury, *Cololabis saira*, in the northeastern and northwestern Pacific Ocean. Fish. Bull. U.S. 86: 489-498.

Watanabe. Y., and Kuji, Y. 1991. Verification of daily growth increment formation in saury otolith by rearing larvae from hatching. J. Ichthyol. 38: 11-15.

Watanabe, Y., Oozeki, Y., and Kitagawa, D. 1997. Larval parameters determining preschooling juvenile production of Pacific saury (*Cololabis Saira*) in the northwestern

Pacific. Can. J. Fish. Aquat. Sci., 54: 1067-1076.

Watanabe. Y., and Lo, N. C. H. 1989. Larval production and mortality of Pacific saury, *Cololabis saira*, in the northwestern Pacific Ocean. Fish. Bull. U.S. 86: 601-613.

Ware, D.M.and McFarlane, G.A. 1995. Climate-induced changes in Pacific hake *(Merluccius productus*) abundance in the Vancouver Island upwelling system. *In* R.J. Beamish. (ed.) Climate change and northern fish populations. Canadian Special Publication of Fisheries and Aquat. Sci. 121: 509-521.

Ware, D. M. 1975. Growth, metabolism, and optimal swimming speed of a pelagic fish. Journal of the Fisheries Research Board of Canada 32:33-41.

Wieser, W. and Forstner, H. 1986. Effects of temperature and size on the routine rate of oxygen consumption and on the relative scope for activity in larval cyprinids. Journal of Comparative Physiology B 156:791-796.

Winberg, G.G. 1956. Rate of metabolism and food requirements of fishes. Belorussian University, Minsk. Translated from Russian: Fisheries Research Board of Canada Translation Service 194, 1960, Ottawa.

Appendix 1 List of Nemuro 2002 workshop participants.

Canada

HAY, Douglas E.
Fisheries and Oceans Canada
Pacific Biological Station
3190 Hammond Bay Road
Nanaimo, BC.
Canada. V9R 5K6
hayd@pac.dfo-mpo.gc.ca

Japan

AZUMAYA, Tomomori
Hokkaido National Fisheries Research Institute
Katsurakoi-116,
Kushiro, 085-0802
Japan
azumaya@fra.affrc.go.jp

CHIBA, Sanae
Frontier Research System for Global Change
Showa-machi 3173-25, Kanazawaku, Yokohama
Kanagawa, 236-001
Japan
chibas@jamstec.go.jp

FUJII, Masahiko
National Institute for Environmental Studies
16-2 Onogawa, Tsukuba
Japan
fujii.masahiko@nies.go.jp.ac.jp

INADA, Masakatsu
Hokkaido University
Minato-cho 3-1-1
Hakodate, 041-8611
Japan
f990061@ec.hokudai.ac.jp

ITO, Shin-ichi
Tohoku National Fisheries Research Institute
Shinhama-cho 3-27-5, Shiogama
Miyagi, 985-0001
Japan
goito@affrc.go.jp

KATUKAWA, Toshio
Ocean Research Institute, University of Tokyo
Minamidai-1-15-1, Shinjuku-ku
Tokyo, 164-8639
Japan
katukawa@ori.u-tokyo.ac.jp

KASHIWAI, Makoto B.
Hokkaido National Fisheries Research Institute
Katsurakoi-116,
Kushiro, 085-0802
Japan
kashiwai@fra.affrc.go.jp

KISHI, Michio J.
Hokkaido University
Minato-cho 3-1-1
Hakodate, 041-8611
Japan
kishi@salmon.fish.hokudai.ac.jp

KOBAYASHI, Tokimasa
Tohoku National Fisheries Research Institute
Samemachi Shimomekurakubo
Hachinohe, Aomori, 031-0841
Japan
tokikoba@fra.affrc.go.jp

MUKAI, Daiki
Hokkaido University
Minato-cho 3-1-1
Hakodate, 041-8611
Japan
f980102@ec.hokidai.ac.jp

OKUNISHI, Takeshi
Hokkaido University
Techo-park 1-2-14 Shinonoppro Atshetsu-ku
Sapporo, Hokkaido, 005-8601
Japan
t-okunishi@econixe.co.jp

SMITH, Lan S.
Frontier Research System for Global Change
Showa-machi 3173-25, Kanazawaku, Yokohama
Kanagawa, 236-001
Japan
lanimal@jamstec.go.jp

TADOKORO, Kazuaki
Frontier Research System for Global Change
Showa-machi 3173-25, Kanazawaku, Yokohama
Kanagawa, 236-001
Japan
denden@jamstec.go.jp

TOMOKAZU, Aiki
Hokkaido University
Minato-cho 3-1-1
Hakodate, 041-8611
Japan
f990001@ec.hokudai.ac.jp

TSUDA, Atsushi
Hokkaido National Fisheries Research Institute
Katsurakoi-116,
Kushiro, 085-0802
Japan
tsuda@fra.affrc.go.jp

YAMANAKA, Yasuhiro
Graduate School of Environmental Earth Science
Hokkaido University
North 10, West 5 Kita-ku
Sapporo, 060-0810
Japan
galapen@ees.hokudai.ac.jp

YOSHIE, Naoki
Graduate School of Environmental Earth Science
Hokkaido University
North 10, West 5 Kita-ku
Sapporo, 060-0810
Japan
naoki@ees.hokudai.ac.jp

People`s Republic of China

HUANG, Daji
2nd Institute of Oceanography
P. O. Box 1207, Hangzhou
Zhejiang, 310012
People`s Republic of China
dajih2001@yahoo.com

Republic of Korea

HONG, Chul-Hoon
Pukyong National University
599-1 Daeyeon3-Dong Nam-Gu
Pusan, 608-737
Republic of Korea
hongch@pknu.ac.kr

Russian Federation

ZUENKO, Yury I.
Pacific Fisheries Research Center
4 Shevchenko Alley
Vladivostok, 690950
Russia
kheng@tinro.ru

LEONOV, Alexander
Shirshov Institute of Oceanology
36 Nakhimovsky Prospekt
Moscow, 117997
Russia
leonov@sio.rssi.ru

NAVROTSKY, Vadim V.
Pacific Oceanological Institute
43 Baltiyskaya Street
Vladivostok, 690041
Russia
navr@online.vladivostok.ru

U.S.A.

KLUMB, Robert A.
Cornell University
Cornell Biological Field Station
900 Shackelton Point Road
Bridgeport, NY 13030
U.S.A.
rak11@cornell.edu

MEGREY, Bernard A.
National Marine Fisheries Service
Alaska Fisheries Science Center
7600 Sand Point Way N.E.
Seattle, WA 98115-0070
U.S.A.
bern.megrey@noaa.gov

WERNER, Francisco E.
Department of Marine Science
University of North Carolina
Chapel Hill
NC 27599-3300
U.S.A.
cisco@marine.unc.edu

Appendix 2 Herring bioenergetic model FORTRAN code for the base case.

```
C ---------------------------------------------------------------------
C Bioenergetic herring model based on the paper of Rudstam (1988).
C Exploring the dynamics of herring consumption in the Baltic:
C Aplications of an energetic model of fish growth.
C Kieler Meeresforsch Sonderth 6:312-322.
C
C Originally coded as difference equation in FORTRAN by Kenny Rose 26 Dec 01
C
C Corrected and changed to differential equation with Euler and
C Runge Kutta numerical integration scheme
C
C                       01/03/02 Bernard A. Megrey
C
C Added observed and predicted size at age data
C                       01/12/02 Bernard A. Megrey
C
C Added YOY formulations per Arrhenius (1998)
C                       01/22/02 Bernard A. Megrey
C
C All relic code removed for general distribution at
C Nemuro 2002 workshop
C                       01/25/02 Bernard A. Megrey
C
C
C ---------------------------------------------------------------------
      program NemuroHerring

          include 'stuff.cmn'
          include 'state.cmn'
          include 'sizeaa.cmn'
          REAL NYEARS, NSTEPS, NSTEP

      OPEN(UNIT=11,FILE='nemuro.txt',STATUS='unknown')
      OPEN(UNIT=8,FILE='compareEuler.out',STATUS='unknown')
      OPEN(UNIT=9,FILE='sizeatage.out',STATUS='unknown')
C
C-----read in the 3 zoop groups from Nemuro output (7th, 9th and 11th columns)
C
      do 45 ii=1,731
      READ(11,999)id(ii),zop1(ii),zop2(ii),zop3(ii)
  999   FORMAT(1x,i3,1x,5(13x,1x),2(e13.6,1x,13x,1x),e13.6)
C
C-----   take the first year for now
C
      IF(ii.le.365)then
        zoop1(ii)=zop1(ii)
        zoop2(ii)=zop2(ii)
        zoop3(ii)=zop3(ii)
      endif
```

```
45    continue

C------convert Nemuro zoop in uM N/L to g ww/m3
C------  tt1 is conversion from uM N/liter to g ww/m3
C------  14 ug N/uM * 1.0e-6 g/ug * 1 g dw/0.07 g N dw
C------   * 1 g ww/0.2 g dw *
C------   1.e3 liters/m3
      do 55 i=1,365
        tt1=14.0*1.0e-6*(1.0/0.07)*(1.0/0.2)*1.0e3
        zoop1(i)=zoop1(i)*tt1
        zoop2(i)=zoop2(i)*tt1
        zoop3(i)=zoop3(i)*tt1

C----initial weight and age of newly metamphosed herring
             x(1)=0.2
        iage=0
        maxage=0
 55       continue
C
C --- number of state variables
C
      nstate=1
C
C - time initialization
C
        TZERO = 0.0
        NYEARS = 11.0
        NSTEPS = 100.0
        TEND = 365.0*NYEARS
        dt= 1/NSTEPS
        TPRINT = 1.0
        TEPS = 1.0E-05

C
C --- MAIN TIME LOOP
C
      NSTEP=0.0
      DO WHILE (time .LT. TEND)
        NSTEP=NSTEP+1.0
        time= TZERO + NSTEP*dt
        CALL EULER(x,xdot,nstate,dt,time)
C       CALL KUTTA(x,xdot,nstate,dt,time)
        iday=int(amod(time,365.0))+1
        iyr=int(time/365.)+1
C
C-----   update age every time iday 365 goes by and
C-----   after NSTEP have gone by
C-----   the NSTEPS test is to avoid incrementing iage
C-----   every dt
C
        IF(iday.eq.365 .and. amod(NSTEP,NSTEPS).eq.0) then
```

```
        iage=iage+1
            jpage(iage)=iage
        psizeaa(iage)=x(1)
        if(iage .gt. maxpage) maxpage=iage
       endif
C
C --- check for time to print
C
      IF(ABS(AMOD(time,TPRINT)) .LT. TEPS) THEN
      write(8,1001) time, x(1), wtemp, gcmax
1001   format(1x,4(f9.3,1x))
C      ENDIF
     ENDIF
     END DO
     kage=min(maxoage,maxpage)
C
C --- write predicted and observed size-at-age output
C
     do 73 i=1,kage
          write(9,1002) i, psizeaa(i), osizeaa(i)
73    continue
1002  format(1x,i4,2(1x,f9.3))

     close(8)
     close(9)
     STOP
     END
    SUBROUTINE DER(x,xdot,time)

C-------------------------------------------------------
C
C Herring bioenergetics differential equation process.
C Prey base are in units of micromoles N /m^3 and are
C converted
C via converson factors
C
C    programmed by BAM 01/05/02
C
C Added YOY formulations per Arrhenius (1998)
C                    01/22/02 Bernard A. Megrey
C
C-------------------------------------------------------

   include 'stuff.cmn'
   include 'state.cmn'

C          WRITE(*,*) 'IN DER', time


   iday=int(amod(time,365.0))+1
   iyr=int(time/365.)+1
```

```
C
C zero out xdot
C
          DO 15 i=1,nstate
          xdot(i)=0.0
  15 CONTINUE
C----  start age-0 on day 200
C----  jday is julian day (1,..., 400) but goes past 365
C----  iday is counter for day in model simulation
C----- jjday is julian day (i.e., jday reset for >365)
C----  I start on day 200; i you want different then change 200
C---   below and 165, which 365 minus the start day.
         jday=iday+200
         IF(jday.le.365)then
           jjday=jday
         else
           jjday=iday-165
         endif

C
C-----  generate daily temperatures for a year -- made up
C
       t1=float(jjday)
       t2=12.75-10.99*cos(0.0172*t1)-6.63*sin(0.0172*t1)
       wtemp=t2-5.0
       IF(wtemp.le.1.0)wtemp=1.0
C          write(*,*) "wtemp",wtemp
C50    continue

C
C Herring = x(1)
C

C
C----- set vulnerabilities and k values for 3 zoop groups
C
     vul(1)=1.0
     vul(2)=1.0
     vul(3)=1.0

     k(1)=100.0
     k(2)=10.0
     k(3)=100.0
C
C-----if using constant p rather than functional response, set p
C-----here
C      p=0.6


C-----  loop over years
C      do 100 iyr=1,9
```

```
C----   loop over days for each year
C       do 200 iday=1,365
C         write(*,*) 'iday jday jjday', iday,jday,jjday

C-----iiday is running value of days in simulation (1,...., 2000)
C          iiday=(iyr-1)*365+iday

          tt1=1.0/x(1)
          t1=0.0033*tt1**0.227
C         write(*,*) 't1 tt1', x(1), t1, tt1

c----***this is the new stuff from Arrhenius (1998) for YOY only***
c-----   The 5.258 puts resp is in units of g zoop/g fish/day
c----- [13560 joules/gram oxygen]/4.18 joules/cal = 3244 cal/gO2
c------[2580 joules/gram zoop]/4.18 joules/cal = 617 cal/g zoop
c------ 3244/617 = 5.258

          IF(iage.eq.0)then
            IF(wtemp.le.15.0)then
              v=5.76*EXP(0.0238*wtemp)*x(1)**0.386
            endif
            IF(wtemp.gt.15.0)then
              v=8.6*x(1)**0.386
            endif
            a=EXP((0.03-0.0*wtemp)*v)
            resp=t1*EXP(0.0548*wtemp)*a*5.258
          endif
c------***back to the old equations for respiration for age-1 and
C------older ***
          IF(iage.ge.1)then
            IF(wtemp.le.9.0)then
             u=3.9*x(1)**0.13*EXP(0.149*wtemp)
            else
             u=15.0*x(1)**0.13
            endif
            resp=t1*EXP(0.0548*wtemp)*EXP(0.03*u)*5.258
          endif
C         write(*,*) 'after new stuff'
C                   IF(wtemp.lt.9.0)then
C            u=3.9*x(1)**0.13* exp(0.149*wtemp)
C          else
C            u=15.0*x(1)**0.13
C          endif
c--   ---  13,560 joules/g O2  1 cal/4.18 joules  1 g ww/5533 cal
C        resp=t1*EXP(0.0548*wtemp)*EXP(0.03*u)*0.59

C
C-----     Thornton and Lessem (1978)temperature effect
c----**Arrhenius (1998) for age-0  changed te4 from 25 to 23 degrees***
          IF(iage.eq.0)then
            xk1=0.1
```

```
          xk2=0.98
          xk3=0.98
          xk4=0.01

          te1=1.0
          te2=15.0
          te3=17.0
          te4=23.0
        endif
C
        IF(iage.eq.1)then
          xk1=0.1
          xk2=0.98
          xk3=0.98
          xk4=0.01

          te1=1.0
          te2=15.0
          te3=17.0
          te4=25.0
        endif
        IF(iage.gt.1)then
          xk1=0.1
          xk2=0.98
          xk3=0.98
          xk4=0.01

          te1=1.0
          te2=13.0
          te3=15.0
          te4=23.0
        endif
C
C- non age dependent temperature effect on consumption
C           xk1=0.1
C           xk2=0.98
C           xk3=0.98
C           xk4=0.01
C           te1=1.0
C           te2=13.0
C           te3=15.0
C           te4=23.0

        tt5=(1.0/(te2-te1))
        t5=tt5 * alog(0.98*(1.0-xk1)/(0.02*xk1))
        t4=exp(t5*(wtemp-te1))

        tt7 = 1.0/(te4-te3)
        t7=tt7*alog(0.98*(1.0-xk4)/(0.02*xk4))
        t6=exp(t7*(te4-wtemp))
```

```
          gcta=(xk1*t4)/(1.0+xk1*(t4-1.0))
          gctb=xk4*t6/(1.0+xk4*(t6-1.0))
          gctemp=gcta * gctb
          gcmax=0.642*tt1**0.256*gctemp
C
C----- no tempeature effect
C           gcmax=0.642*tt1**0.256*1.0

C-----  either use fixed p or call functional response
C       con=p*gcmax
C       write(*,*) 'der time iday iyr jjday zoop123',time,iday,
C       iyr,
C       jjday, zoop1(jjday),zoop2(jjday), zoop3(jjday)
      cnum=zoop1(jjday)*vul(1)/k(1)+zoop2(jjday)*vul(2)/k(2)
     $      +zoop3(jjday)*vul(3)/k(3)
          c1=gcmax*zoop1(jjday)*vul(1)/k(1)
          c2=gcmax*zoop2(jjday)*vul(2)/k(2)
          c3=gcmax*zoop3(jjday)*vul(3)/k(3)
          con1=c1/(1.0+cnum)
          con2=c2/(1.0+cnum)
          con3=c3/(1.0+cnum)
          con=con1+con2+con3
C
C --- for comparison to Kenny's version
C
C           con=0.75*gcmax
C
C --- to tune to observed size at age data
          con=0.48*gcmax
C
C --- egestion
C
          f=0.16*con
C
C --- excretion
          e=0.1*(con-f)
C
C --- Specific Dynamic Action
C
c------   ********Arrhenius (1998)  changed SDA from 17.5% to 15% ****
          IF(iage.eq.0)sda=0.15*(con-f)
          IF(iage.ge.1)sda=0.175*(con-f)


c-----   J/g ww 1 cal=4.18 J
C                     con1=con*2580.0/5533.0
C           write(*,*) 'der',con1,resp,xdot(1)
C
C --- bioenergetics differential equation
C
         xdot(1)=(con-resp-f-e-sda)*x(1)*2580./5533.
```

```
        IF(wtemp.le.1.0)xdot(1)=0.0
              t1=float(jjday)
                    if(amod(t1,365.0).ge.152.0.and.amod(t1,365.0).le.156.0) then
        write(*,*) 'in spawn'
                     xdot(1)=(con-resp-f-e-sda-0.20)*x(1)*2580./5533.
        endif


c-----   update age every time day 365 goes by
c        IF(iday.eq.365) then
c                     iage=iage+1
c           jage(iage)=iage
c          psizeaa(iage)=x(1)
c           write(*,*)'iday, iyr, jjday, iage, maxage',iday, iyr,
c     $      jjday, iage, maxage
c          if(iage .gt. maxage) maxage=iagec
c             endif

C          WRITE(*,*) 'OUT OF DER'
      RETURN
      END
           SUBROUTINE EULER(x,xdot,nstate,dt,time)
C-----------------------------------------------------
C
C USE THE EULER METHOD TO SOLVE A SYSTEM OF NONLINEAR
C DIFFERENTIAL EQUATIONS. A SUBROUTINE DER IS NEEDED
C TO COMPUTE THE DERIVATIVS OF THE STATE VARIBALES
C
C X - STATE VARIABLE ARRAY
C XDOT - ARRAY OF DERIVATIVES OF STATE ARIABLES
C NSTATE - NUMBER OF STATE VARIABLES
C DT - TIME STEP
C TIME - CURRENT TIME
C
C-----------------------------------------------------
           include 'stuff.cmn'
           include 'state.cmn'


      INTEGER I

       CALL DER(x,xdot,time)

        DO 10 i=1, nstate
             x(i) =x(i) + dt * xdot(i)
  10  CONTINUE

      RETURN
      END
           SUBROUTINE KUTTA(x,xdot,nstate,dt,time)
```

```
C-------------------------------------------------------
C
C USE THE 4TH ORDER RUNGE KUTTA METHOD TO SOLVE A SYSTEM OF NONLINEAR
C DIFFERENTIAL EQUATIONS. A SUBROUTINE DER IS NEEDED
C TO COMPUTE THE DERIVATIVS OF THE STATE VARIBALES
C
C X - STATE VARIABLE ARRAY
C XDOT - ARRAY OF DERVATIVES OF STATE VARIABLES
C NSTATE - NUMBER OF STATE VARIABLES
C DT - TIME STEP
C TIME - CURRENT TIME
C
C programmed by Bernard A. Megrey 01/06/02
C
C
C-------------------------------------------------------
      include 'stuff.cmn'
            include 'state.cmn'

      INTEGER I
      REAL SUMDX(16), DTO2, XPLUS(16)
C           WRITE(*,*) 'IN KUTTA'

      DTO2 = dt/2.0

      CALL DER(x,xdot,time)

      DO 10 I=1, nstate
             XPLUS(I) = x(I) + DT02 * xdot(I)
             SUMDX(I)= xdot(I)
  10  CONTINUE

      CALL DER(XPLUS,xdot,time)

      DO 20 I=1, nstate
            XPLUS(I) = x(I) + DTO2 * xdot(I)
            SUMDX(I) = SUMDX(I) + 2.0 * xdot(I)
  20  CONTINUE

      CALL DER(XPLUS,xdot,time)

      DO 30 I=1, nstate
            XPLUS(I) = x(I) + dt * xdot(I)
            SUMDX(I) = SUMDX(I) + 2.0 * xdot(I)
   30 CONTINUE

      CALL DER(XPLUS,xdot,time)

      DO 40 I=1, nstate
            SUMDX(I) = SUMDX(I) + xdot(I)
            x(I) = x(I) + dt * SUMDX(I) / 6.0
```

```
   40 CONTINUE
C      WRITE(*,*) 'OUT OF KUTTA'
       RETURN
       END


C=======================================================
C
C Include file: state.cmn
C state variable declarations
C
C  BAM 1/02/02
C-------------------------------------------------------
       REAL*4 dt, time, x(1), xdot(1)
       INTEGER*4 nstate


C=======================================================
C
C Include file: stuff.cmn
C miscellaneous common block variables
C
C  BAM 1/2/02
C-------------------------------------------------------
       COMMON /ZOO/ zoop1(365), zoop2(365), zoop3(365)
       COMMON /ISV/ wtemp, con, gcmax,f, e ,sda, con1, resp
             COMMON /TIMER/ iday, jday, iyr, iage
             REAL*4 zoop1,zoop2,zoop3,k(3),vul(3)
       REAL*4 zop1(731),zop2(731),zop3(731)
             INTEGER*4 id(731)


C=======================================================
C
C Include file: sizeaa.cmn
C Size at age common block
C
C   BAM 1/06/02
C
C-------------------------------------------------------
       COMMON /SIZEAA/joage(25),jpage(25),psizeaa(25),osizeaa(25),
      $               maxoage,maxpage
C --- joage Observed age
C --- jpage Predicted age
C --- psizeaa Predicted size at age
C --- osizeaa Observed size at age

       INTEGER*4 joage, jpage, maxoage, maxpage
       REAL*4 psizeaa, osizeaa
       DATA maxoage /11/
       DATA joage /1,2,3,4,5,6,7,8,9,10,11,14*0/
```

```
C
C --- observed size at age Pacific herring  data (wt) from the C
C --- 1973 year class
C --- as supplied by Doug Hay
C
     DATA osizeaa /8.75,63.0,87.66,124.13,139.26,152.98,177.43,
    $             185.78,187.64,195.0,208.73,14*0.0/
```

Appendix 3 Fully customized herring subroutine. See Appendix 2 for main program and common block including files.

```
SUBROUTINE DER(x,xdot,time)

C-------------------------------------------------------
C
C Herring bioenergetics differential equation process.
C Prey base are in units of micromoles N /m^3 and are converted
C via converson factors
C
C    programmed by B.A. Megrey 01/05/02
C
C Added YOY formulations per Arrhenius 1998
C                    01/22/02 B.A. Megrey

C modifications and customizations by F.E.Werner and R.A.Klumb 1/26/02
C while at the Nemuro workshop
C
C-------------------------------------------------------

      include 'stuff.cmn'
      include 'state.cmn'

C
C- calculate date and year
C
      iday=int(amod(time,365.0))+1
           iyr=int(time/365.)+1
C
C zeroout xdot
C
           DO 15 i=1,nstate
           xdot(i)=0.0
   15 CONTINUE
c
c----  start age-0 on day 200
c----       jday is julian day (1,..., 400) but goes past 365
c----       iday is counter for day in model simulation
c----       jjday is julian day (i.e., jday reset for >365)
c----      I start on day 200; i you want different then change 200
c----       below and 165, which 365 minus the start day.
          jday=iday+200
          IF(jday.le.365)then
            jjday=jday
          else
            jjday=iday-165
          endif
C
C-----  generate daily temperatures for a year -- made up
C
```

```
      t1=float(jjday)                                  ! BaseCase T
      t2=12.75-10.99*cos(0.0172*t1)-6.63*sin(0.0172*t1)        ! BaseCase T
      wtemp=t2-5.0                                     ! BaseCase T
      IF(wtemp.le.1.0)wtemp=1.0                        ! BaseCase T
          pi=acos(-1.)
          wtemp=7.717+(5.6796*0.5*(1.-cos(2.*pi*(t1-30.)/365.)))
C
C--- Herring weight state variable = x(1)
C--- weight affect on respiration
C
          tt1=1.0/x(1)
          t1=0.0033*tt1**0.227
C
C --- *********this is the new stuff from Arrhenius (1998) for YOY only*********
C --- The 5.258 puts resp (g oxygen/fish) into units of g zoop/g fish/day
C --- [13560 joules/gram oxygen]/4.18 joules/cal = 3244 cal/gO2
C --- [2580 joules/gram zoop]/4.18 joules/cal = 617 cal/g zoop
C --- so respiration in grams/oxygen/g fish/day is multiplied
C --- by 3244/617 = 5.258
C --- to get food energy equivalents of a gram of oxygen respired
C
c          IF(iage.eq.0)then                                ! BASE
c            IF(wtemp.le.15.0)then                                ! BASE
c              v=5.76*EXP(0.0238*wtemp)*x(1)**0.386                       ! BASE
c            endif                                          ! BASE
c            IF(wtemp.gt.15.0)then                                ! BASE
c              v=8.6*x(1)**0.386                                  ! BASE
c            endif                                          ! BASE
c            a=EXP((0.03-0.0*wtemp)*v)                            ! BASE
c            resp=t1*EXP(0.0548*wtemp)*a*5.258                          ! BASE
c          endif                                            ! BASE
C
          IF(iage.eq.0)then                    !  R.A. Klumb (26 Jan 2002)
               t1=0.00528*tt1**0.007                !  R.A. Klumb (26 Jan 2002)
               resp=t1*EXP(0.083*wtemp)*5.258       !  R.A. Klumb (26 Jan 2002)
             end if                             !  R.A. Klumb (26 Jan 2002)
C
C --- *********back to the old equations for respiration for age-1 and
C --- older********
C
          IF(iage.ge.1)then
C Base            IF(wtemp.le.9.0)then
            IF(wtemp.le.9.655)then
             u=3.9*x(1)**0.13*EXP(0.149*wtemp)
            else
             u=15.0*x(1)**0.13
            endif
            resp=t1*EXP(0.0548*wtemp)*EXP(0.03*u)*5.258
          endif
C
C --- Thornton and Lessem temperature effect
```

```
C --- age dependent values
C --- *******Arrhenius (1998)for age-0  changed te4 from 25 to 23 degrees******
C
      IF(iage.eq.0)then
        xk1=0.1
        xk2=0.98
        xk3=0.98
        xk4=0.01

C Base        te1=1.0
C Base        te2=15.0
C Base        te3=17.0
C Base        te4=23.0

        te1=8.0
        te2=10.897
        te3=11.310
        te4=12.552
      endif
C
      IF(iage.eq.1)then
        xk1=0.1
        xk2=0.98
        xk3=0.98
        xk4=0.01

C Base        te1=1.0
C Base        te2=15.0
C Base        te3=17.0
C Base        te4=25.0

        te1=8.0
        te2=10.897
        te3=11.310
        te4=12.966
      endif

      IF(iage.gt.1)then
        xk1=0.1
        xk2=0.98
        xk3=0.98
        xk4=0.01

C Base        te1=1.0
C Base        te2=13.0
C Base        te3=15.0
C Base        te4=23.0

        te1=8.0
        te2=10.483
        te3=10.897
```

```
          te4=12.552
        endif

        tt5=(1.0/(te2-te1))
        t5=tt5 * alog(0.98*(1.0-xk1)/(0.02*xk1))
        t4=exp(t5*(wtemp-te1))

        tt7 = 1.0/(te4-te3)
        t7=tt7*alog(0.98*(1.0-xk4)/(0.02*xk4))
        t6=exp(t7*(te4-wtemp))

        gcta=(xk1*t4)/(1.0+xk1*(t4-1.0))
        gctb=xk4*t6/(1.0+xk4*(t6-1.0))
        gctemp=gcta * gctb
        gcmax=0.642*tt1**0.256*gctemp
C
C --- multispecies functional response
C --- usse either this or adjust little p
C
C----- set vulnerabilities and k values for 3 zoop groups
C
    vul(1)=1.0
    vul(2)=1.0
    vul(3)=1.0

    k(1)=0.3638
    k(2)=0.0364
    k(3)=0.3638

c     k(1)=2000.0
c     k(2)=200.0
c     k(3)=2000.0

    cnum=zoop1(jjday)*vul(1)/k(1)+zoop2(jjday)*vul(2)/k(2)
   $     +zoop3(jjday)*vul(3)/k(3)
        c1=gcmax*zoop1(jjday)*vul(1)/k(1)
        c2=gcmax*zoop2(jjday)*vul(2)/k(2)
        c3=gcmax*zoop3(jjday)*vul(3)/k(3)
        con1=c1/(1.0+cnum)
        con2=c2/(1.0+cnum)
        con3=c3/(1.0+cnum)
        con=con1+con2+con3
C
C-----if using constant p rather than functional response, set p here
C --- to tune to observed size at age data. If using functional response
C --- comment the next line out
C
      con=0.6375*gcmax
C
C --- egestion
C
```

```
        f=0.16*con                  ! Base Case
        IF(iage.eq.0)f=0.125*con    ! Age-dependent – R.A. Klumb (26 Jan 2002)
C
C --- excretion
        e=0.1*(con-f)               ! Base Case
        IF(iage.eq.0)e=0.078*con    ! Age-dependent – R.A. Klumb (26 Jan 2002)
C
C --- Specific Dynamic Action
C
c------   *******Arrhenius (1998) age dependent SDA from 17.5% to 15% ****
        IF(iage.eq.0)sda=0.15*(con-f)     ! Base Case
        IF(iage.eq.0)sda=0.125*(con-f)    ! Age-dependent – R.A. Klumb (26 Jan 2002)
        IF(iage.ge.1)sda=0.175*(con-f)
C
C --- use the ratio of calories/g of zoop (2580) to calories/g of fish (5533)
C
C --- bioenergetics differential equation - constant energy density for herring
C
C         xdot(1)=(con-resp-f-e-sda)*x(1)*2580./5533.      ! Base Case
C
C    include seasonal variation of energy density for .ge. 2 yr olds
C
        if(iage.ge.2)then
          enMar1=5750.
          jdMar1=60
          enOct1=9800.
          jdOct1=274
          if(jjday.lt.60)then
              delen=(enMar1-enOct1)/151
              en=enOct1+(90+jjday)*delen
            end if
            if(jjday.ge.60.and.jjday.lt.274)then
              delen=(enOct1-enMar1)/(jdOct1-jdMar1)
              en=enMar1+(jjday-jdMar1)*delen
            end if
            if(jjday.ge.274)then
              delen=(enMar1-enOct1)/151
              en=enOct1+(jjday-jdOct1)*delen
            end if
          else
            en=4460.
          end if
        xdot(1)=(con-resp-f-e-sda)*x(1)*2580./en

        IF(wtemp.le.1.0)xdot(1)=0.0
C
C --- Spawning section. Assume loose 20% of body weight/day
C            t1=float(jjday)
c                   if(amod(t1,365.0) .ge. 152.0 .and.
c    &            amod(t1,365.0) .le. 156.0) then
c                     xdot(1)=(con-resp-f-e-sda-0.20)*x(1)*2580./5533.
```

```
c       endif

        RETURN
        END
```

Appendix 4 NEMURO.FISH (NEMURO FORTRAN code supplied by Yasuhiro Yamanaka) with the herring bioenergetic model (base case) (supplied by Bernard Megrey and Ken Rose). The herring model is linked to NEMURO in a one-way static link.

```
!***********************************************************************
!    NEMURO model     Jun 13, 2002  written by Yasuhiro Yamanaka
!***********************************************************************
 program NEMURO.FISH
     implicit none
!    ..... Control for Time Ingration .....
     character(19)    :: Cstart = '0001/07/20 00:00:00'  ! Starting date
     character(19)    :: Cend   = '0011/07/21 00:00:00'  ! Ending date
     character(19)    :: Cstep  = '0000/00/00 01:00:00'  ! Time step
     character(19)    :: Cmon   = '0000/00/01 00:00:00'  ! Monitor Interval
     character(19)    :: CTime
     real(8)          :: dt, TTime, Tbefore, Season, Tmon
     integer          :: Iyr, Imon, Iday, Ihour, Imin, Isec
!    ..... scale conversion .....
     real(8),parameter :: d2s       = 86400.0d0    ! day ---> sec
     real(8),parameter :: mcr       = 1.0d-6       ! micro
!    ..... Prognostic Variables (with initial conditions) and Thier Source Term .....
     real(8)          :: TPS    =  0.1D-6, QPS    ! Small Phytoplankton [molN/l]
     real(8)          :: TPL    =  0.1D-6, QPL    ! Large Phytoplankton
     real(8)          :: TZS    =  0.1D-6, QZS    ! Small Zooplankton
     real(8)          :: TZL    =  0.1D-6, QZL    ! Large Zooplankton
     real(8)          :: TZP    =  0.1D-6, QZP    ! Pradatory Zooplankton
     real(8)          :: TNO3   =  5.0D-6, QNO3   ! Nitrate
     real(8)          :: TNH4   =  0.1D-6, QNH4   ! Ammmonium
     real(8)          :: TPON   =  0.1D-6, QPON   ! Particulate Organic Nitrogen
     real(8)          :: TDON   =  0.1D-6, QDON   ! dissolved Organic Nitrogen
     real(8)          :: TSiOH4 = 10.0D-6, QSiOH4 ! Silicate
     real(8)          :: TOpal  =  0.1D-7, QOpal  ! Particulate Opal
!    ..... Prognostic Variables (with initial conditions) and Thier Source Term .....
!     real(8)          :: THrr   =  0.2D0,  QHrrl  ! Particulate Opal
!    ..... Light Condition Parameters .....
     real(8),parameter :: alpha1   = 4.0D-2     ! Light Dissipation coefficient of sea water[/m]
     real(8),parameter :: alpha2   = 4.0D4      ! PS+PL Selfshading coefficientS+PL      [l/molN/m]
     real(8),parameter :: IoptS    = 0.15D0     ! PS Optimum Light Intensity  S          [ly/min]
     real(8),parameter :: IoptL    = 0.15D0     ! PL Optimum Light Intensity             [ly/min]
     integer,parameter :: LLN      = 10         ! Number of sublayer for calculating of Lfc
     real(8)          :: LfcS                  ! Light factor for PS
     real(8)          :: LfcL                  ! Light factor for PL
     real(8)          :: kappa, Lint, dLint, LfcUS, LfcUL, LfcDS, LfcDL
     integer          :: L
!    ..... biological Parameters .....
     real(8),parameter :: VmaxS    = 0.4D0/d2s  ! PS Maximum Photosynthetic rate @0degC   [/s]
     real(8),parameter :: KNO3S    = 1.0D-6     ! PS Half satuation constant for Nitrate  [molN/l]
     real(8),parameter :: KNH4S    = 0.1D-6     ! PS Half satuation constant for Ammonium [molN/l]
     real(8),parameter :: PusaiS   = 1.5D6      ! PS Ammonium Inhibition Coefficient      [l/molN]
     real(8),parameter :: KGppS    = 6.93D-2    ! PS Temp. Coeff. for Photosynthetic Rate [/degC]
     real(8),parameter :: MorPS0   = 5.85D4/d2s ! PS Mortality Rate @0degC               [/s]
```

```
real(8),parameter :: KMorPS   = 6.93D-2    ! PS Temp. Coeff. for Mortality          [/degC]
real(8),parameter :: ResPS0   = 0.03D0/d2s ! PS Respiration Rate at @0degC          [/s]
real(8),parameter :: KResPS   = 0.0519D0   ! PS Temp. Coeff. for Respiration       [/degC]
real(8),parameter :: GammaS   = 0.135D0    ! PS Ratio of Extracell. Excret. to Photo.[(nodim)]
real(8),parameter :: VmaxL    = 0.8D0/d2s  ! PL Maximum Photosynthetic rate @0degC  [/s]
real(8),parameter :: KNO3L    = 3.00D-6    ! PL Half satuation constant for Nitrate  [molN/l]
real(8),parameter :: KNH4L    = 0.30D-6    ! PL Half satuation constant for Ammonium [molN/l]
real(8),parameter :: KSiL     = 6.00D-6    ! PL Half satuation constant for Silicate [molSi/l]
real(8),parameter :: PusaiL   = 1.50D6     ! PL Ammonium Inhibition Coefficient      [l/molN]
real(8),parameter :: KGppL    = 6.93D-2    ! PL Temp. Coeff. for Photosynthetic Rate [/degC]
real(8),parameter :: MorPL0   = 2.90D4/d2s ! PL Mortality Rate @0degC              [/s]
real(8),parameter :: KMorPL   = 6.93D-2    ! PL Temp. Coeff. for Mortality          [/degC]
real(8),parameter :: ResPL0   = 0.03D0/d2s ! PL Respiration Rate at @0degC          [/s]
real(8),parameter :: KResPL   = 0.0519D0   ! PL Temp. Coeff. for Respiration       [/degC]
real(8),parameter :: GammaL   = 0.135D0    ! PL Ratio of Extracell. Excret. to Photo.[(nodim)]
real(8),parameter :: GRmaxS   = 0.40D0/d2s ! ZS Maximum Rate of Grazing PS @0degC    [/s]
real(8),parameter :: KGraS    = 6.93D-2    ! ZS Temp. Coeff. for Grazing           [/degC]
real(8),parameter :: LamS     = 1.40D6     ! ZS Ivlev constant                     [l/molN]
real(8),parameter :: PS2ZSstar= 0.043D-6   ! ZS Threshold Value for Grazing PS      [molN/l]
real(8),parameter :: AlphaZS  = 0.70D0     ! ZS Assimilation Efficiency            [(nodim)]
real(8),parameter :: BetaZS   = 0.30D0     ! ZS Growth Efficiency                  [(nodim)]
real(8),parameter :: MorZS0   = 5.85D4/d2s ! ZS Mortality Rate @0degC              [/s]
real(8),parameter :: KMorZS   = 0.0693D0   ! ZS Temp. Coeff. for Mortality         [/degC]
real(8),parameter :: GRmaxLps = 0.10D0/d2s ! ZL Maximum Rate of Grazing PS @0degC    [/s]
real(8),parameter :: GRmaxLpl = 0.40D0/d2s ! ZL Maximum Rate of Grazing PL @0degC    [/s]
real(8),parameter :: GRmaxLzs = 0.40D0/d2s ! ZL Maximum Rate of Grazing ZS @0degC    [/s]
real(8),parameter :: KGraL    = 6.93D-2    ! ZL Temp. Coeff. for Grazing           [/degC]
real(8),parameter :: LamL     = 1.4000D6   ! ZL Ivlev constant                     [l/molN]
real(8),parameter :: PS2ZLstar= 4.00D-8    ! ZL Threshold Value for Grazing PS      [molN/l]
real(8),parameter :: PL2ZLstar= 4.00D-8    ! ZL Threshold Value for Grazing PL      [molN/l]
real(8),parameter :: ZS2ZLstar= 4.00D-8    ! ZL Threshold Value for Grazing ZS      [molN/l]
real(8),parameter :: AlphaZL  = 0.70D0     ! ZL Assimilation Efficiency            [(nodim)]
real(8),parameter :: BetaZL   = 0.30D0     ! ZL Growth Efficiency                  [(nodim)]
real(8),parameter :: MorZL0   = 5.85D4/d2s ! ZL Mortality Rate @0degC              [/s]
real(8),parameter :: KMorZL   = 0.0693D0   ! ZL Temp. Coeff. for Mortality         [/degC]
real(8),parameter :: GRmaxPpl = 0.20D0/d2s ! ZP Maximum rate of grazing PL @0degC    [/s]
real(8),parameter :: GRmaxPzs = 0.20D0/d2s ! ZP Maximum rate of grazing ZS @0degC    [/s]
real(8),parameter :: GRmaxPzl = 0.20D0/d2s ! ZP Maximum rate of grazing ZL @0degC    [/s]
real(8),parameter :: KGraP    = 6.93D-2    ! ZP Temp. Coeff. for grazing           [/degC]
real(8),parameter :: LamP     = 1.4000D6   ! ZP Ivlev constant                     [l/molN]
real(8),parameter :: PL2ZPstar= 4.00D-8    ! ZP Threshold Value for Grazing PL      [molN/l]
real(8),parameter :: ZS2ZPstar= 4.00D-8    ! ZP Threshold Value for Grazing ZS      [molN/l]
real(8),parameter :: ZL2ZPstar= 4.00D-8    ! ZP Threshold Value for Grazing ZL      [molN/l]
real(8),parameter :: PusaiPL  = 4.605D6    ! ZP Preference Coeff. for PL           [l/molN]
real(8),parameter :: PusaiZS  = 3.010D6    ! ZP Preference Coeff. for ZS           [l/molN]
real(8),parameter :: AlphaZP  = 0.70D0     ! ZP Assimilation Efficiency            [(nodim)]
real(8),parameter :: BetaZP   = 0.30D0     ! ZP Growth Efficiency                  [(nodim)]
real(8),parameter :: MorZP0   = 5.85D4/d2s ! ZP Mortality Rate @0degC              [/s]
real(8),parameter :: KMorZP   = 0.0693D0   ! ZP Temp. Coeff. for Mortality         [/degC]
real(8),parameter :: Nit0     = 0.03D0/d2s ! NH4 Nitrification Rate @0degC         [/s]
real(8),parameter :: KNit     = 0.0693D0   ! NH4 Temp. coefficient for Nitrification [/degC]
```

```
      real(8),parameter :: VP2N0    = 0.10D0/d2s ! PON Decomp. Rate to Ammonium @0degC     [/s]
      real(8),parameter :: KP2N     = 6.93D-2    ! PON Temp. Coeff. for Decomp. to Ammon.  [/degC]
      real(8),parameter :: VP2D0    = 0.10D0/d2s ! PON Decomp. Rate to DON @0degC          [/s]
      real(8),parameter :: KP2D     = 6.93D-2    ! PON Temp. Coeff. for Decomp. to DON     [/degC]
      real(8),parameter :: VD2N0    = 0.20D0/d2s ! DON Decomp. Rate to Ammonium @0degC     [/s]
      real(8),parameter :: KD2N     = 6.93D-2    ! DON Temp. Coeff. for Decomp. to Ammon.  [/degC]
      real(8),parameter :: VO2S0    = 0.10D0/d2s ! Opal Decomp. Rate to Silicate @0degC    [/s]
      real(8),parameter :: KO2S     = 6.93D-2    ! Opal Temp. Coeff. for Decomp.to Silicate[/degC]
      real(8),parameter :: RSiN     = 2.0D0         !Si/N ratio                  [molSi/molN]
      real(8),parameter :: RCN      = 106.0D0/16.0D0 !C/N ratio                  [molC/molN]
!     ..... bottom boundary Condition .....
      real(8),parameter :: setVPON  = 40.0D0/d2s ! Settling velocity of PON              [m/s]
      real(8),parameter :: setVOpal = 40.0D0/d2s ! Settling velocity of Opal             [m/s]
      real(8),parameter :: TNO3d   =  25.0d-6    ! Nitrate Concentraion in the Deep Layer  [molN/l]
      real(8),parameter :: TSiOH4d =  35.0d-6    ! Silicate Concentraion in the Deep Layer [molSi/l]
!     ..... Paramters of ZL Vertical Migration .....
      character(19)     :: CZup ='0000/04/01 00:00:00' ! Date Coming up to the Euphotic Layer
      character(19)     :: CZdwn='0000/09/01 00:00:00' ! Date Returning to the Deep Layer
      real(8)           :: TZup, TZdwn, TZLd, SVRate=0.2D0
      integer           :: IyrU, ImonU, IdayU ,IhourU, IminU, IsecU
      integer           :: IyrD, ImonD, IdayD ,IhourD, IminD, IsecD
!
      real(8)           :: GppPSn,  GppNPSn, GppAPSn, RnewS, ResPSn,  MorPSn,  ExcPSn
      real(8)           :: GppPLn,  GppNPLn, GppAPLn, RnewL, ResPLn,  MorPLn,  ExcPLn
      real(8)           :: GppPLsi, GppSiPLsi,              ResPLsi, MorPLsi, ExcPLsi
      real(8)           :: GraPS2ZSn, GraPS2ZLn,  GraPL2ZLn, GraPL2ZLsi, GraZS2ZLn
      real(8)           :: GraPL2ZPn, GraPL2ZPsi, GraZS2ZPn, GraZL2ZPn
      real(8)           :: EgeZSn, MorZSn, ExcZSn, EgeZLn, EgeZLsi, MorZLn, ExcZLn
      real(8)           ::                    EgeZPn, EgeZPsi, MorZPn, ExcZPn
      real(8)           :: DecP2N, DecP2D, DecD2N, DecO2S, Nit
      real(8)           :: ExpPON, ExpOpal,ExcNO3, ExcSiOH4
      integer           :: lt=0 , nt
!
!     ..... Environmental Condition .....
      real(8)           :: Temp                    ! Temperature [degC]
      real(8)           :: Lint0                   ! Light Intencity at sea surface [ly/min]
      real(8)           :: MLD = 30.0d0            ! Mixed Layer Depth [m]
      real(8)           :: ExcTime = 1.0d0 / (100.0d0*d2s) ! Exch. Coeff. between Sur-Deep [/s]
!     ..... statement function & def. type of functions .....
      real(8)           :: cd2tt, nd2tt
      character(19)     :: tt2cd
      real(8)           :: Td, GraF, Mich, a, b, c
      Td  (a,b)   = a * exp(b*Temp)
      GraF(a,b,c) = MAX( 0.0D0, 1.0 - exp(a * (b - c)))
      Mich(a,b)   = b / ( a + b )
!
!     ***** Initial Setting *****
!     ..... for time control .....
      TTime = cd2tt(Cstart)                  ! Starting Date
      CTime = TT2CD(TTime)                   ! present time (charactor form)
      dt    = cd2tt(Cstep) - cd2tt('0000/00/00 00:00:00')  ! Time Step (real8 form)
```

```
      Tmon  = cd2tt(Cmon)  - cd2tt('0000/00/00 00:00:00')  ! Monitor Interval (real8 form)
      nt = NINT( ( cd2tt(Cend) - cd2tt(Cstart) ) / dt )    ! Total Time Steps
!     ..... for Vertical Migration ......
      TZup  = CD2TT( CZup  )
      TZdwn = CD2TT( CZdwn )
      call TT2ND(IyrU, ImonU, IdayU ,IhourU, IminU, IsecU ,TZup )
      call TT2ND(IyrD, ImonD, IdayD ,IhourD, IminD, IsecD ,TZdwn)
      TZLd = TZL  ! ZL living in the deep layer at the initial condition
      TZL  = 0.0
!     ..... File Open for monitoring output .....
      open( 10, file='Results.csv', form='FORMATTED' )
      write(10,'(A,13(",", A))') 'Time(day)', &
                 'NO3'   , 'NH4'    , 'PS'    , 'PL'     , &
                 'ZS'    , 'ZL'     , 'ZP'    , 'PON'    , &
                 'DON'   , 'SiOH4'  , 'Opal'  , 'TotalN' , 'TotalSi'
      write(10,'(A,11(",", F8.4))') CTime, &
                 TNO3/mcr, TNH4  /mcr, TPS  /mcr, TPL /mcr, &
                 TZS /mcr, TZL   /mcr, TZP  /mcr, TPON/mcr, &
                 TDON/mcr, TSiOH4/mcr, TOpal/mcr
      open( 11, file='Forcing.csv', form='FORMATTED' )
      write(11,'(A,13(",", A))') 'Time(day)','Lint0', 'TMP', 'MLD', 'ExcTime'
      write(11,'(A,13(",", 1PE10.4))') CTime, Lint0, Temp, MLD, ExcTime*d2s
!
!     ****** Main Loop *****
      do lt = 1, nt
!       ..... time control (Season : 0 to 1, parcentage in a year).....
        Tbefore = TTime                          ! one step before present time
        TTime   = TTime + dt                       ! present time (real8 form)
        CTime = TT2CD(TTime)                           ! present time (charactor form)
        CALL TT2ND(Iyr, Imon, Iday ,Ihour, Imin, Isec ,TTime)
        Season = ( TTime                - ND2TT(Iyr  ,1,1,0,0,0) )/  &
                 ( ND2TT(Iyr+1,1,1,0,0,0) - ND2TT(Iyr  ,1,1,0,0,0) )
!
!       ..... Example of Boundray condition .....
        Lint0 = 0.1d0 * ( 1.0D0 + 0.3d0 * cos( 2.0d0*3.1415926536d0*(Season - 0.50D0) ) )
        Temp  =          6.0D0 + 4.0d0 * cos( 2.0d0*3.1415926536d0*(Season - 0.65D0) )
        if (Temp .lt. 4.0 ) then
          MLD = MLD + dt * (150.0d0 - MLD ) / ( 100.0d0 * d2s )
          ExcTime = ExcTime + dt * ( 1.0d0/( 40.0d0*d2s) - ExcTime ) / (100.0d0*d2s)
        else
          MLD = MLD + dt * ( 30.0d0 - MLD ) / (   5.0d0 * d2s )
          ExcTime = ExcTime + dt * ( 1.0d0/(100.0d0*d2s) - ExcTime ) / (  5.0d0*d2s)
        end if
!
!       ..... Light Factors (LfcS, LfcL).....
        Lint = Lint0
        LfcDS = Lint/IoptS * exp(1.0D0 - Lint/IoptS)
        LfcDL = Lint/IoptL * exp(1.0D0 - Lint/IoptL)
        LfcS  = 0.0D0
        LfcL  = 0.0D0
        Kappa = alpha1 + alpha2 * ( TPS + TPL )
```

```
      dLint = exp( -Kappa * (MLD/LLN) )
      do L = 1, LLN
        LfcUS  = LfcDS
        LfcUL  = LfcDL
        Lint   = Lint      * dLint
        LfcDS  = Lint/IoptS * exp( 1.0D0 - Lint/IoptS )
        LfcDL  = Lint/IoptL * exp( 1.0D0 - Lint/IoptL )
        LfcS   = LfcS + ( LfcUS + LfcDS ) * 0.5D0 / LLN
        LfcL   = LfcL + ( LfcUL + LfcDL ) * 0.5D0 / LLN
      end do
!     ..... Photosynthesis of PS .....
      GppNPSn   = Mich( KNO3S, TNO3 ) * exp( - PusaiS * TNH4 )
      GppAPSn   = Mich( KNH4S, TNH4 )
      GppPSn    = Td(VmaxS, KGppS) * LfcS * TPS * ( GppNPSn + GppAPSn )
      RnewS     = GppNPSn / ( GppNPSn + GppAPSn )
      ResPSn    = Td( ResPS0, KResPS ) * TPS
      MorPSn    = Td( MorPS0, KMorPS ) * TPS * TPS
      ExcPSn    = GammaS             * GppPSn
!     ..... Photosynthesis of PL .....
      GppNPLn   = Mich( KNO3L, TNO3   ) * exp( - PusaiL * TNH4 )
      GppAPLn   = Mich( KNH4L, TNH4   )
      GppSiPLsi = Mich( KSiL , TSiOH4 )
      GppPLn    = Td(VmaxL, KGppL) * LfcL * TPL * min( ( GppNPLn + GppAPLn ), GppSiPLsi )
      RnewL     = GppNPLn / ( GppNPLn + GppAPLn )
      ResPLn    = Td( ResPL0, KResPL ) * TPL
      MorPLn    = Td( MorPL0, KMorPL ) * TPL * TPL
      ExcPLn    = GammaL             * GppPLn
!     ..... Grazing PS, PL, ZS, ZL --> ZS, ZL, ZP .....
      GraPS2ZSn = Td(GRmaxS,  KGraS) *GraF(LamS,PS2ZSstar,TPS) *TZS
      GraPS2ZLn = Td(GRmaxLps,KGraL) *GraF(LamL,PS2ZLstar,TPS) *TZL
      GraPL2ZLn = Td(GRmaxLpl,KGraL) *GraF(LamL,PL2ZLstar,TPL) *TZL
      GraZS2ZLn = Td(GRmaxLzs,KGraL) *GraF(LamL,ZS2ZLstar,TZS) *TZL
      GraPL2ZPn = Td(GRmaxPpl,KGraP) *GraF(LamP,PL2ZPstar,TPL) *TZP * exp( -PusaiPL *(TZL
       + TZS))
      GraZS2ZPn = Td(GRmaxPzs,KGraP) *GraF(LamP,ZS2ZPstar,TZS) *TZP * exp( -PusaiZS * TZL )
      GraZL2ZPn = Td(GRmaxPzl,KGraP) *GraF(LamP,ZL2ZPstar,TZL) *TZP
!     ..... Mortality, Excration, Egestion for Zooplanktons
!     ..... Commented out after Saito-san Meeting at 19 Jun, 2000 .....
!     BetaZS = 0.3 ** (  1.0 + Mich( TPL, TPS )  )
      ExcZSn = (AlphaZS-  BetaZS)   * GraPS2ZSn
      EgeZSn = (1.0    - AlphaZS)   * GraPS2ZSn
      MorZSn = Td( MorZS0, KMorZS ) * TZS * TZS
      ExcZLn = (AlphaZL-  BetaZL)   * (GraPS2ZLn+GraPL2ZLn+GraZS2ZLn)
      EgeZLn = (1.0    - AlphaZL)   * (GraPS2ZLn+GraPL2ZLn+GraZS2ZLn)
      MorZLn = Td( MorZL0, KMorZL ) * TZL * TZL
      ExcZPn = (AlphaZP-  BetaZP)   * (GraPL2ZPn+GraZS2ZPn+GraZL2ZPn)
      EgeZPn = (1.0    - AlphaZP)   * (GraPL2ZPn+GraZS2ZPn+GraZL2ZPn)
      MorZPn = Td( MorZP0, KMorZP ) * TZP * TZP
!     ..... Decomposition PON, DON, Opal ---> NH4, DON, SiOH4 .....
      DecP2N    = Td( VP2N0  , KP2N ) * TPON
      DecP2D    = Td( VP2D0  , KP2D ) * TPON
```

```
      DecD2N    = Td( VD2N0  , KD2N ) * TDON
      DecO2S    = Td( VO2S0  , KO2S ) * TOpal
      Nit       = Td( Nit0   , KNit ) * TNH4
!     ..... silica fluxes .....
      GppPLsi    = GppPLn    * RSiN
      ResPLsi    = ResPLn    * RSiN
      MorPLsi    = MorPLn    * RSiN
      ExcPLsi    = ExcPLn    * RSiN
      GraPL2ZLsi = GraPL2ZLn * RSiN
      GraPL2ZPsi = GraPL2ZPn * RSiN
      EgeZLsi    = GraPL2ZLsi
      EgeZPsi    = GraPL2ZPsi
!
!     ..... Tendency Terms for biological processes .....
      QNO3   = -( GppPSn - ResPSn ) * RnewS   &
             -( GppPLn - ResPLn ) * RnewL + Nit
      QNH4   = -( GppPSn - ResPSn ) * (1.0 - RnewS)   &
             -( GppPLn - ResPLn ) * (1.0 - RnewL)   &
             - Nit + DecP2N + DecD2N + ExcZSn + ExcZLn + ExcZPn
      QPS    = GppPSn - ResPSn - MorPSn - ExcPSn - GraPS2ZSn - GraPS2ZLn
      QPL    = GppPLn - ResPLn - MorPLn - ExcPLn - GraPL2ZLn - GraPL2ZPn
      QZS    = GraPS2ZSn - GraZS2ZLn - MorZSn - ExcZSn - EgeZSn - GraZS2ZPn
      QZL    = GraPL2ZLn + GraZS2ZLn - MorZLn - ExcZLn - EgeZLn + GraPS2ZLn - GraZL2ZPn
      QZP    = GraPL2ZPn + GraZS2ZPn - MorZPn - ExcZPn - EgeZPn + GraZL2ZPn
      QPON   = MorPSn  + MorPLn  + MorZSn  + MorZLn + MorZPn   &
           + EgeZPn  + EgeZSn  + EgeZLn  - DecP2N - DecP2D
      QDON   = ExcPSn  + ExcPLn  + DecP2D  - DecD2N
      QSiOH4 =-GppPLsi + ResPLsi + ExcPLsi + DecO2S
      QOpal  = MorPLsi + EgeZLsi + EgeZPsi - DecO2S
!
!     ..... Exchange Fluxes between the Surface and Deep Layers .....
      ExpPON   = setVPON  / MLD * TPON
      ExpOpal  = setVOpal / MLD * TOpal
      ExcNO3   = ExcTime * ( TNO3d   - TNO3   )
      ExcSiOH4 = ExcTime * ( TSiOH4d - TSiOH4 )
      QNO3   = QNO3   + ExcNO3
      QSiOH4 = QSiOH4 + ExcSiOH4
      QPON   = QPON   - ExpPON
      QOpal  = QOpal  - ExpOpal
!
!     ..... Time Integration with Forward Scheme .....
      TNO3   = TNO3   + dt * QNO3
      TNH4   = TNH4   + dt * QNH4
      TPS    = TPS    + dt * QPS
      TPL    = TPL    + dt * QPL
      TZS    = TZS    + dt * QZS
      TZL    = TZL    + dt * QZL
      TZP    = TZP    + dt * QZP
      TPON   = TPON   + dt * QPON
      TDON   = TDON   + dt * QDON
      TSiOH4 = TSiOH4 + dt * QSiOH4
```

```
      TOpal  = TOpal  + dt * QOpal
!
!     ..... Vertical Migration of ZL .....
      TZdwn = ND2TT(Iyr, ImonD, IdayD ,IhourD, IminD, IsecD )
      TZup  = ND2TT(Iyr, ImonU, IdayU ,IhourU, IminU, IsecU )
      if ( (Tbefore .lt. TZdwn).and.(TTime .ge. TZdwn) ) then
        TZLd = TZL
        TZL  = 0.0
        write(*,*) '*** Down ***', CTime
      end if
      if ( (Tbefore .lt. TZup).and.(TTime .ge. TZup) ) then
        TZL = SVRate * TZLd
        write(*,*) '***  UP  ***', CTime
      end if
!
      call Herring(TTime, Tbefore, TZS, TZL, TZP, Temp)
!
!     ..... Monitor .....
      if ( int(TTime/Tmon).ne. int(Tbefore/Tmon) ) then
!       write(*,'(A,13(",", F8.4))') CTime, Season
        write(10,'(A,11(",", F8.4))') CTime, &
              TNO3/mcr, TNH4  /mcr, TPS  /mcr, TPL /mcr, &
              TZS /mcr, TZL   /mcr, TZP  /mcr, TPON/mcr, &
              TDON/mcr, TSiOH4/mcr, TOpal/mcr
        write(11,'(A,13(",", 1PE10.4))') CTime, Lint0, Temp, MLD, ExcTime*d2s
      end if
    end do
!
    close(10); close(11)
!
    stop
    end
!*******************************************************************************************
    Subroutine Herring(TTime, Tbefore, TZS, TZL, TZP, Temp)
!
    implicit none
    real(8)          :: TTime, Tbefore, TZS, TZL, TZP, Temp
    real(8),parameter :: d2s       = 86400.0d0    ! day ---> sec
    integer          :: Iyr, Imon, Iday, Ihour, Imin, Isec
    character(19)    :: CAge ='0000/07/19 00:00:00' ! Date of Aging ( JJday = 200 )
    character(19)    :: CTime
    real(8)          :: TAge
    integer          :: iage = 0
    integer, save    :: IyrA, ImonA, IdayA ,IhourA, IminA, IsecA
    integer          :: JJday
    real(8)          :: ZooP1, ZooP2, ZooP3, tt1
    real(8)          :: t1,t2,wtemp
    real(8)          :: x(1) =0.2d0, xdot(1)
    real(8)          :: cd2tt, nd2tt
    character(19)    :: tt2cd
    real(8)          :: vul(3), k(3)
```

```
      integer(4)        :: id(365)
      real(8)           :: zop1(365), zop2(365), zop3(365)
      real(8):: v, a, u, resp
     real(8) :: xk1,xk2,xk3,xk4,te1,te2,te3,te4,tt5,t5,t4,tt7,t7,t6, gcta,gctb,gctemp,gcmax
     real(8) :: cnum,c1,c2,c3,con1,con2,con3,con
     real(8) :: f,e, sda
!
      integer, save     :: First = 1
!
!     ==================
      if ( First .eq. 1 ) then; First = 0
        TAge  = CD2TT( CAge  )
        call TT2ND(IyrA, ImonA, IdayA ,IhourA, IminA, IsecA ,TAge )
        open( 20, file='Herring.csv', form='FORMATTED' )
!
!!!!        OPEN(UNIT=111,FILE='nemuro.txt',STATUS='unknown')
!!!!        -----read in the 3 zoop groups from Nemuro output last 3 columns
!!!!        do JJday=1,365
!!!!          READ(111,999)id(JJday),zop1(JJday),zop2(JJday),zop3(JJday)
!!!!  999      FORMAT(1x,i3,1x,3(e13.6,1x))
!!!!        end do
      end if
!     ==================
!
      CTime = TT2CD(TTime)                          ! present time (charactor form)
      CALL TT2ND(Iyr, Imon, Iday ,Ihour, Imin, Isec ,TTime)
      JJday = 1 + ( TTime - ND2TT(Iyr  ,1,1,0,0,0) ) / d2s
!
!------convert Nemuro zoop in uM N/L to g ww/m3
!------  tt1 is conversion from uM N/liter to g ww/m3
!------  14 ug N/uM * 1.0e-6 g/ug * 1 g dw/0.07 g N dw * 1 g ww/0.2 g dw *
!------       1.0e3 liters/m3
!
      tt1=14.0*1.0e-6*(1.0/0.07)*(1.0/0.2)*1.0e3
      zoop1 = TZS*tt1 *1.0d6
      zoop2 = TZL*tt1 *1.0d6
      zoop3 = TZP*tt1 *1.0d6
!!!!     zoop1 = zop1(JJday) * tt1
!!!!     zoop2 = zop2(JJday) * tt1
!!!!     zoop3 = zop3(JJday) * tt1
!
!     ..... Temperature Seting .....
!
      t1=float(jjday)
      t2=12.75-10.99*cos(0.0172*t1)-6.63*sin(0.0172*t1)
      wtemp=t2-5.0
      IF(wtemp.le.1.0)wtemp=1.0

!      write(*,*) TT2CD(cd2tt('0002/01/01 00:00:00')+200.0*86400.0)
!      stop
!     ..... Aging of Herring ......
```

```
      TAge = ND2TT(Iyr, ImonA, IdayA ,IhourA, IminA, IsecA )
      if ( (Tbefore .lt. TAge).and.(TTime .ge. TAge) ) then
          write(*,*) '*** Aging +1 of Herring ***', CTime
          iage = iage + 1
       end if
!
!--- Herring weight state variable = x(1)
!
!----- set vulnerabilities and k values for 3 zoop groups
!
      vul(1) =   1.0; vul(2) =  1.0; vul(3) =   1.0
      k  (1) = 0.3638; k  (2) = 0.0364; k  (3) = 0.3638
!
! --- weight affect on respiration
!
      tt1 = 1.0 / x(1)
      t1  = 0.0033 * tt1**0.227
! --- *********this is the new stuff from Ahhrenius for YOY only*********
! --- The 5.258 puts resp (g oxygen/fish) into units of g zoop/g fish/day
! --- [13560 joules/gram oxygen]/4.18 joules/cal = 3244 cal/gO2
! --- [2580 joules/gram zoop]/4.18 joules/cal = 617 cal/g zoop
! --- so respiration in grams/oxygen/g fish/day is multiplied by 3244/617 = 5.258
! --- to get food energy equivalents of a gram of oxygen respired
!
      IF (iage .eq. 0 )then
        IF(wtemp.le.15.0)then
          v = 5.76 * exp( 0.0238 * wtemp ) * x(1)**0.386
        else
          v = 8.6 * x(1)**0.386
        endif
        a=EXP((0.03-0.0*wtemp)*v)
        resp=t1*EXP(0.0548*wtemp)*a*5.258
! --- *********back to the old equations for respiration for age-1 and older********
      else   ! (iage .gt. 0)
        IF (wtemp.le.9.0)then
          u=3.9*x(1)**0.13*EXP(0.149*wtemp)
        else
          u=15.0*x(1)**0.13
        endif
          resp=t1*EXP(0.0548*wtemp)*EXP(0.03*u)*5.258
      endif
!C
!C --- Thornton and Lessem temperature effect
!C --- age dependent values
!C --- *******Arrhenius for age-0 he changed te4 from 25 to 23 degrees******
!C
      if ( iage .eq. 0 ) then
        xk1 = 0.1;  xk2 = 0.98;  xk3 = 0.98;  xk4 = 0.01
        te1 = 1.0;  te2 = 15.0;  te3 = 17.0;  te4 = 23.0
      else if ( iage .eq. 1 ) then
        xk1 = 0.1;  xk2 = 0.98;  xk3 = 0.98;  xk4 = 0.01
```

```
        te1 = 1.0;  te2 = 15.0;  te3 = 17.0;  te4 = 25.0
      else if( iage .gt. 1 ) then
        xk1 = 0.1;  xk2 = 0.98;  xk3 = 0.98;  xk4 = 0.01
        te1 = 1.0;  te2 = 13.0;  te3 = 15.0;  te4 = 23.0
      endif
!
      tt5 = ( 1.0 / ( te2 - te1 ) )
      t5  = tt5 * log( 0.98 * ( 1.0 - xk1 ) / ( 0.02 * xk1 ) )
      t4  = exp( t5 * ( wtemp - te1 ) )
!
      tt7 = 1.0 /( te4 - te3 )
      t7  = tt7 * log( 0.98 * ( 1.0 - xk4 ) / ( 0.02 * xk4 ) )
      t6  = exp( t7 * ( te4 - wtemp ) )
!
      gcta  = ( xk1 * t4 ) / ( 1.0 + xk1 * ( t4 - 1.0 ) )
      gctb  = xk4 * t6 / ( 1.0 + xk4 * ( t6 - 1.0 ) )
      gctemp= gcta * gctb
      gcmax = 0.642 * tt1**0.256 * gctemp
!
! --- multispecies functional response
! --- usse either this or adjust little p
!
      cnum=zoop1 * vul(1)/k(1) + zoop2*vul(2)/k(2) +zoop3 * vul(3)/k(3)
      c1=gcmax*zoop1*vul(1)/k(1)
      c2=gcmax*zoop2*vul(2)/k(2)
      c3=gcmax*zoop3*vul(3)/k(3)
      con1=c1/(1.0+cnum)
      con2=c2/(1.0+cnum)
      con3=c3/(1.0+cnum)
      con= con1+con2+con3
!
!-----if using constant p rather than functional response, set p here
! --- to tune to observed size at age data
!     con=0.425*gcmax
!
! --- egestion
!
          f=0.16*con
!
! --- excretion
          e=0.1*(con-f)
!
!
! --- Specific Dynamic Action
!
!c------   *******Arrhenius age dependent SDA from 17.5% to 15% ****
          IF ( iage .eq. 0 ) then
            sda=0.15*(con-f)
          else
            sda=0.175*(con-f)
          end if
```

```
!C
!C --- use the ratio of calories/g of zoop (2580) to calories/g of fish (5533)
!C
!C --- bioenergetics differential equation
!C
        xdot(1)=(con-resp-f-e-sda)*x(1)*2580./5533.
!
        IF(wtemp.le.1.0)xdot(1)=0.0
!C
!C --- Spawning section. Assume loose 20% of bosy weight/day
!C            t1=float(jjday)
!     if( mod(JJday,365) .ge. 152.0 .and. mod(JJday,365) .le. 156.0) then
!         xdot(1)=(con-resp-f-e-sda-0.20)*x(1)*2580./5533.
!         write(*,*) '### Spawning ###'
!     endif
!
!    if (iage .eq. 1 ) then
!     write(*,*) JJday, wtemp, x(1), xdot(1)
!     stop
!     end if
!     write(*,'(A,I4,3(1PE14.5))') Ctime, JJday, wtemp, x(1), xdot(1)
!
!    Time Integration
!
     x(1) = x(1) + 3600.0d0 /d2s * xdot(1)
!
!    ..... for Check .....
    if ( int(TTime/d2s) .ne. int(Tbefore/d2s) ) then
!!       write(*,'(A,I4,3(1PE14.5))') Ctime, JJday, wtemp, x(1), xdot(1)
!!        stop
!!     write(*,*) TZS, zop1(JJday), TZL,zop2(JJday), TZP,zop3(JJday)
!!     write(*,*) TZP*1.0d6, zop3(JJday)
       write(20,'(A,11(",", F12.4))') CTime, x(1), wtemp, gcmax
     end if
!
     return
!
     stop
     end
!*******************************************************************************
!* Utilities for Date Control  Writtien by Yasuhiro Yamanaka (galapen@ees.hokudai.ac.jp) *
!*******************************************************************************
!    exp. 1997/12/31 23:59:59 --> 6.223158719900000E+10
!    exp. 0000/01/01 00:00:00 --> 0.000000000000000E+00
!*******************************************************************************
     real(8) function CD2TT( Cdate )
!
     integer       :: Iyr, Imon, Iday , Ihour, Imin, Isec
     real(8)       :: ND2TT
     character(19) :: Cdate
!
```

```
    if ( len( Cdate ) .ne. 19 ) then
      write(*,*) '### Length of date is no good ###'
      stop
    end if
    read (Cdate( 1: 4),*)  Iyr
    read (Cdate( 6: 7),*)  Imon
    read (Cdate( 9:10),*)  Iday
    read (Cdate(12:13),*)  Ihour
    read (Cdate(15:16),*)  Imin
    read (Cdate(18:19),*)  Isec
!
    CD2TT = ND2TT(Iyr, Imon, Iday , Ihour, Imin, Isec)
!
    return
    end function
!**********************************************************************
!    exp. 6.223158719900000E+10 --> 1997/12/31 23:59:59
!**********************************************************************
    character(19) function TT2CD(tt)
!
    integer :: Iyr, Imon, Iday , Ihour, Imin, Isec
    real(8) :: tt
!
    call TT2ND( Iyr, Imon, Iday, Ihour, Imin, Isec , tt )
!
    write(TT2CD,'(I4.4,5(A,I2.2))') Iyr, '/', Imon, '/', Iday, &
                        ' ', Ihour, ':', Imin, ':', Isec
!
    return
    end function
!**********************************************************************
!    exp. 1997,12,31,23,59,59 --> 6.223158719900000E+10
!**********************************************************************
    real(8) function ND2TT(Iyr, Imon, Iday, Ihour, Imin, Isec)
!
    integer   :: IM2D(12,0:1) = &
      reshape( (/ 0,31,59,90,120,151,181,212,243,273,304,334,  &
                  0,31,60,91,121,152,182,213,244,274,305,335  /), (/12,2/) )
    integer   :: Iyr, Imon, Iday, Ihour, Imin, Isec
    integer   :: Iy4, Iy1, Ileap, Im, Itt
!
!
    Iy4 = 1461 * ( Iyr / 4 )
    Iy1 = 365 * mod( Iyr, 4 )
!
    if ( mod( Iyr, 4 ) .ne. 0 ) then
      Ileap = 0
    else
      Ileap = 1
    end if
    Im = IM2D( Imon, Ileap)
```

```
!
    Itt = Iy4 + Iy1 + Im + Iday - Ileap
!
    ND2TT = Ihour * 3600 + Imin * 60 + Isec
    ND2TT = ND2TT + Itt * 86400.0D0
!
    return
    end function
!**************************************************************************
!    exp. 6.223158719900000E+10 --> 1997,12,31,23,59,59
!**************************************************************************
    subroutine TT2ND(                                &
            Iyr   , Imon  , Iday   , Ihour, Imin, Isec,   & !O & I
            tt    )
!
    integer :: Iyr, Imon, Iday , Ihour, Imin, Isec
    integer :: Itt, Iy, Iy4, Iyd, Iy1, Ileap, Imd, Im, Its
    integer   :: IM2D(12,0:1) = &
      reshape( (/ 0,31,59,90,120,151,181,212,243,273,304,334,  &
                  0,31,60,91,121,152,182,213,244,274,305,335  /), (/12,2/) )
    integer :: IY2D(4) = (/0,366,731,1096/)
    real(8) :: tt, tt0, ND2TT
!
!
!    ..... ITT [day] .....
    Itt = 1 + tt / 86400.0D0
!
    Iy4   = (Itt-1) / 1461
    Iyd   = Itt - Iy4 * 1461
    do IY = 1, 4
      if ( IY2D(Iy) + 1 .le. Iyd ) then
        Iy1 = Iy
      end if
    end do
!
    Iyr   = Iy4 * 4 + Iy1 - 1
    if ( mod(Iyr,4) .ne. 0 ) then
      Ileap = 0
    else
      Ileap = 1
    end if
    IMD = IYD - IY2D(IY1)
!
    do IM = 1, 12
      if ( IM2D(IM,ILEAP)+1 .le. IMD ) then
        IMON = IM
      end if
    end do
    IDAY = IMD - IM2D(IMON,ILEAP)
!
    TT0 = ND2TT(IYR, IMON, IDAY ,0,0,0)
```

```
      ITS = nint(  TT - TT0 )
      Ihour = ITS / 3600
      Imin  = ( ITS - Ihour * 3600 ) / 60
      Isec  = ITS - Ihour * 3600 - Imin * 60
!
      return
      end subroutine
!
```

Appendix 5 NEMURO.FISH (NEMURO FORTRAN code supplied by Yasuhiro Yamanaka) with the saury bioenergetic model (base case) (supplied by Bernard Megrey and Ken Rose and modified by "team saury"). The saury model is linked to NEMURO in a one-way static link.

```
!*******************************************************************************
!    NEMURO model     Jun 13, 2002  written by Yasuhiro Yamanaka
!                          modified by Masahiko Fujii
!                                Shin-ichi Ito
!*******************************************************************************
      program NEMURO
      implicit none
!     ..... Control for Time Ingration .....
      character(19)     :: Cstart = '0001/02/01 00:00:00'  ! Starting date
      character(19)     :: Cend   = '0003/02/01 00:00:00'  ! Ending date
      character(19)     :: Cstep  = '0000/00/00 01:00:00'  ! Time step
      character(19)     :: Cmon   = '0000/00/01 00:00:00'  ! Monitor Interval
      character(19)     :: CTime
      real(8)           :: dt, TTime, Tbefore, Season, Tmon
      integer           :: Iyr, Imon, Iday, Ihour, Imin, Isec
!     ..... scale conversion .....
      real(8),parameter :: d2s       = 86400.0d0    ! day ---> sec
      real(8),parameter :: mcr       = 1.0d-6       ! micro
!     ..... Prognostic Variables (with initial conditions) and Thier Source Term .....
      real(8)           :: TPS    =  0.1D-6, QPS    ! Small Phytoplankton [molN/l]
      real(8)           :: TPL    =  0.1D-6, QPL    ! Large Phytoplankton
      real(8)           :: TZS    =  0.1D-6, QZS    ! Small Zooplankton
      real(8)           :: TZL    =  0.1D-6, QZL    ! Large Zooplankton
      real(8)           :: TZP    =  0.1D-6, QZP    ! Pradatory Zooplankton
      real(8)           :: TNO3   =  5.0D-6, QNO3   ! Nitrate
      real(8)           :: TNH4   =  0.1D-6, QNH4   ! Ammmonium
      real(8)           :: TPON   =  0.1D-6, QPON   ! Particulate Organic Nitrogen
      real(8)           :: TDON   =  0.1D-6, QDON   ! dissolved Organic Nitrogen
      real(8)           :: TSiOH4 = 10.0D-6, QSiOH4 ! Silicate
      real(8)           :: TOpal  =  0.1D-7, QOpal  ! Particulate Opal
!     ..... Prognostic Variables (with initial conditions) and Thier Source Term .....
!      real(8)          :: THrr   =  0.2D0,  QHrrl  ! Particulate Opal
!     ..... Light Condition Parameters .....
      real(8),parameter :: alpha1   = 4.0D-2     ! Light Dissipation coefficient of sea water[/m]
      real(8),parameter :: alpha2   = 4.0D4      ! PS+PL Selfshading coefficientS+PL      [l/molN/m]
      real(8),parameter :: IoptS    = 0.15D0     ! PS Optimum Light Intensity  S          [ly/min]
      real(8),parameter :: IoptL    = 0.15D0     ! PL Optimum Light Intensity             [ly/min]
      integer,parameter :: LLN      = 10         ! Number of sublayer for calculating of Lfc
      real(8)           :: LfcS                  ! Light factor for PS
      real(8)           :: LfcL                  ! Light factor for PL
      real(8)           :: kappa, Lint, dLint, LfcUS, LfcUL, LfcDS, LfcDL
      integer           :: L
!     ..... biological Parameters .....
      real(8),parameter :: VmaxS    = 0.4D0/d2s  ! PS Maximum Photosynthetic rate @0degC   [/s]
      real(8),parameter :: KNO3S    = 1.0D-6     ! PS Half satuation constant for Nitrate  [molN/l]
      real(8),parameter :: KNH4S    = 0.1D-6     ! PS Half satuation constant for Ammonium [molN/l]
```

```
real(8),parameter :: PusaiS   = 1.5D6      ! PS Ammonium Inhibition Coefficient      [l/molN]
real(8),parameter :: KGppS    = 6.93D-2    ! PS Temp. Coeff. for Photosynthetic Rate [/degC]
real(8),parameter :: MorPS0   = 5.85D4/d2s ! PS Mortality Rate @0degC                [/s]
real(8),parameter :: KMorPS   = 6.93D-2    ! PS Temp. Coeff. for Mortality           [/degC]
real(8),parameter :: ResPS0   = 0.03D0/d2s ! PS Respiration Rate at @0degC           [/s]
real(8),parameter :: KResPS   = 0.0519D0   ! PS Temp. Coeff. for Respiration         [/degC]
real(8),parameter :: GammaS   = 0.135D0    ! PS Ratio of Extracell. Excret. to Photo.[(nodim)]
real(8),parameter :: VmaxL    = 0.8D0/d2s  ! PL Maximum Photosynthetic rate @0degC   [/s]
real(8),parameter :: KNO3L    = 3.00D-6    ! PL Half satuation constant for Nitrate  [molN/l]
real(8),parameter :: KNH4L    = 0.30D-6    ! PL Half satuation constant for Ammonium [molN/l]
real(8),parameter :: KSiL     = 6.00D-6    ! PL Half satuation constant for Silicate [molSi/l]
real(8),parameter :: PusaiL   = 1.50D6     ! PL Ammonium Inhibition Coefficient      [l/molN]
real(8),parameter :: KGppL    = 6.93D-2    ! PL Temp. Coeff. for Photosynthetic Rate [/degC]
real(8),parameter :: MorPL0   = 2.90D4/d2s ! PL Mortality Rate @0degC               [/s]
real(8),parameter :: KMorPL   = 6.93D-2    ! PL Temp. Coeff. for Mortality           [/degC]
real(8),parameter :: ResPL0   = 0.03D0/d2s ! PL Respiration Rate at @0degC           [/s]
real(8),parameter :: KResPL   = 0.0519D0   ! PL Temp. Coeff. for Respiration         [/degC]
real(8),parameter :: GammaL   = 0.135D0    ! PL Ratio of Extracell. Excret. to Photo.[(nodim)]
real(8),parameter :: GRmaxS   = 0.40D0/d2s ! ZS Maximum Rate of Grazing PS @0degC    [/s]
real(8),parameter :: KGraS    = 6.93D-2    ! ZS Temp. Coeff. for Grazing             [/degC]
real(8),parameter :: LamS     = 1.40D6     ! ZS Ivlev constant                       [l/molN]
real(8),parameter :: PS2ZSstar= 0.043D-6   ! ZS Threshold Value for Grazing PS       [molN/l]
real(8),parameter :: AlphaZS  = 0.70D0     ! ZS Assimilation Efficiency              [(nodim)]
real(8),parameter :: BetaZS   = 0.30D0     ! ZS Growth Efficiency                    [(nodim)]
real(8),parameter :: MorZS0   = 5.85D4/d2s ! ZS Mortality Rate @0degC                [/s]
real(8),parameter :: KMorZS   = 0.0693D0   ! ZS Temp. Coeff. for Mortality           [/degC]
real(8),parameter :: GRmaxLps = 0.10D0/d2s ! ZL Maximum Rate of Grazing PS @0degC    [/s]
real(8),parameter :: GRmaxLpl = 0.40D0/d2s ! ZL Maximum Rate of Grazing PL @0degC    [/s]
real(8),parameter :: GRmaxLzs = 0.40D0/d2s ! ZL Maximum Rate of Grazing ZS @0degC    [/s]
real(8),parameter :: KGraL    = 6.93D-2    ! ZL Temp. Coeff. for Grazing             [/degC]
real(8),parameter :: LamL     = 1.4000D6   ! ZL Ivlev constant                       [l/molN]
real(8),parameter :: PS2ZLstar= 4.00D-8    ! ZL Threshold Value for Grazing PS       [molN/l]
real(8),parameter :: PL2ZLstar= 4.00D-8    ! ZL Threshold Value for Grazing PL       [molN/l]
real(8),parameter :: ZS2ZLstar= 4.00D-8    ! ZL Threshold Value for Grazing ZS       [molN/l]
real(8),parameter :: AlphaZL  = 0.70D0     ! ZL Assimilation Efficiency              [(nodim)]
real(8),parameter :: BetaZL   = 0.30D0     ! ZL Growth Efficiency                    [(nodim)]
real(8),parameter :: MorZL0   = 5.85D4/d2s ! ZL Mortality Rate @0degC                [/s]
real(8),parameter :: KMorZL   = 0.0693D0   ! ZL Temp. Coeff. for Mortality           [/degC]
real(8),parameter :: GRmaxPpl = 0.20D0/d2s ! ZP Maximum rate of grazing PL @0degC    [/s]
real(8),parameter :: GRmaxPzs = 0.20D0/d2s ! ZP Maximum rate of grazing ZS @0degC    [/s]
real(8),parameter :: GRmaxPzl = 0.20D0/d2s ! ZP Maximum rate of grazing ZL @0degC    [/s]
real(8),parameter :: KGraP    = 6.93D-2    ! ZP Temp. Coeff. for grazing             [/degC]
real(8),parameter :: LamP     = 1.4000D6   ! ZP Ivlev constant                       [l/molN]
real(8),parameter :: PL2ZPstar= 4.00D-8    ! ZP Threshold Value for Grazing PL       [molN/l]
real(8),parameter :: ZS2ZPstar= 4.00D-8    ! ZP Threshold Value for Grazing ZS       [molN/l]
real(8),parameter :: ZL2ZPstar= 4.00D-8    ! ZP Threshold Value for Grazing ZL       [molN/l]
real(8),parameter :: PusaiPL  = 4.605D6    ! ZP Preference Coeff. for PL             [l/molN]
real(8),parameter :: PusaiZS  = 3.010D6    ! ZP Preference Coeff. for ZS             [l/molN]
real(8),parameter :: AlphaZP  = 0.70D0     ! ZP Assimilation Efficiency              [(nodim)]
real(8),parameter :: BetaZP   = 0.30D0     ! ZP Growth Efficiency                    [(nodim)]
real(8),parameter :: MorZP0   = 5.85D4/d2s ! ZP Mortality Rate @0degC                [/s]
```

```
      real(8),parameter :: KMorZP   = 0.0693D0   ! ZP Temp. Coeff. for Mortality          [/degC]
      real(8),parameter :: Nit0     = 0.03D0/d2s ! NH4 Nitrification Rate @0degC          [/s]
      real(8),parameter :: KNit     = 0.0693D0   ! NH4 Temp. coefficient for Nitrification [/degC]
      real(8),parameter :: VP2N0    = 0.10D0/d2s ! PON Decomp. Rate to Ammonium @0degC    [/s]
      real(8),parameter :: KP2N     = 6.93D-2    ! PON Temp. Coeff. for Decomp. to Ammon.  [/degC]
      real(8),parameter :: VP2D0    = 0.10D0/d2s ! PON Decomp. Rate to DON @0degC         [/s]
      real(8),parameter :: KP2D     = 6.93D-2    ! PON Temp. Coeff. for Decomp. to DON     [/degC]
      real(8),parameter :: VD2N0    = 0.20D0/d2s ! DON Decomp. Rate to Ammonium @0degC    [/s]
      real(8),parameter :: KD2N     = 6.93D-2    ! DON Temp. Coeff. for Decomp. to Ammon.  [/degC]
      real(8),parameter :: VO2S0    = 0.10D0/d2s ! Opal Decomp. Rate to Silicate @0degC   [/s]
      real(8),parameter :: KO2S     = 6.93D-2    ! Opal Temp. Coeff. for Decomp.to Silicate[/degC]
      real(8),parameter :: RSiN     = 2.0D0      !Si/N ratio                  [molSi/molN]
      real(8),parameter :: RCN      = 106.0D0/16.0D0 !C/N ratio               [molC/molN]
!     ..... bottom boundary Condition .....
      real(8),parameter :: setVPON  = 40.0D0/d2s ! Settling velocity of PON          [m/s]
      real(8),parameter :: setVOpal = 40.0D0/d2s ! Settling velocity of Opal         [m/s]
      real(8),parameter :: TNO3d   =  25.0d-6    ! Nitrate Concentraion in the Deep Layer  [molN/l]
      real(8),parameter :: TSiOH4d =  35.0d-6    ! Silicate Concentraion in the Deep Layer [molSi/l]
!     ..... Paramters of ZL Vertical Migration .....
      character(19)     :: CZup ='0000/04/01 00:00:00' ! Date Coming up to the Euphotic Layer
      character(19)     :: CZdwn='0000/09/01 00:00:00' ! Date Returning to the Deep Layer
      real(8)           :: TZup, TZdwn, TZLd, SVRate=0.2D0
      integer           :: IyrU, ImonU, IdayU ,IhourU, IminU, IsecU
      integer           :: IyrD, ImonD, IdayD ,IhourD, IminD, IsecD
!
      real(8)           :: GppPSn,  GppNPSn, GppAPSn, RnewS, ResPSn,  MorPSn,  ExcPSn
      real(8)           :: GppPLn,  GppNPLn, GppAPLn, RnewL, ResPLn,  MorPLn,  ExcPLn
      real(8)           :: GppPLsi, GppSiPLsi,              ResPLsi, MorPLsi, ExcPLsi
      real(8)           :: GraPS2ZSn, GraPS2ZLn,  GraPL2ZLn, GraPL2ZLsi, GraZS2ZLn
      real(8)           :: GraPL2ZPn, GraPL2ZPsi, GraZS2ZPn, GraZL2ZPn
      real(8)           :: EgeZSn, MorZSn, ExcZSn, EgeZLn, EgeZLsi, MorZLn, ExcZLn
      real(8)           ::                    EgeZPn, EgeZPsi, MorZPn, ExcZPn
      real(8)           :: DecP2N, DecP2D, DecD2N, DecO2S, Nit
      real(8)           :: ExpPON, ExpOpal,ExcNO3, ExcSiOH4
      integer           :: lt=0 , nt
!
!     ..... Environmental Condition .....
      real(8)           :: Temp                    ! Temperature [degC]
      real(8)           :: Lint0                   ! Light Intencity at sea surface [ly/min]
      real(8)           :: MLD = 30.0d0            ! Mixed Layer Depth [m]
      real(8)           :: ExcTime = 1.0d0 / (100.0d0*d2s) ! Exch. Coeff. between Sur-Deep [/s]
!     ..... statement function & def. type of functions .....
      real(8)           :: cd2tt, nd2tt
      character(19)     :: tt2cd
      real(8)           :: Td, GraF, Mich, a, b, c
      Td  (a,b)   = a * exp(b*Temp)
      GraF(a,b,c) = MAX( 0.0D0, 1.0 - exp(a * (b - c)))
      Mich(a,b)   = b / ( a + b )
!
!     ***** Initial Setting *****
!     ..... for time control .....
```

```
      TTime = cd2tt(Cstart)                          ! Starting Date
      CTime = TT2CD(TTime)                           ! present time (charactor form)
      dt    = cd2tt(Cstep) - cd2tt('0000/00/00 00:00:00')  ! Time Step (real8 form)
      Tmon  = cd2tt(Cmon)  - cd2tt('0000/00/00 00:00:00')  ! Monitor Interval (real8 form)
      nt = NINT( ( cd2tt(Cend) - cd2tt(Cstart) ) / dt )    ! Total Time Steps
!     ..... for Vertical Migration ......
      TZup  = CD2TT( CZup  )
      TZdwn = CD2TT( CZdwn )
      call TT2ND(IyrU, ImonU, IdayU ,IhourU, IminU, IsecU ,TZup )
      call TT2ND(IyrD, ImonD, IdayD ,IhourD, IminD, IsecD ,TZdwn)
      TZLd = TZL  ! ZL living in the deep layer at the initial condition
      TZL  = 0.0
!     ..... File Open for monitoring output .....
      open( 10, file='Results.csv', form='FORMATTED' )
      write(10,'(A,13(",", A))') 'Time(day)', &
                 'NO3'   , 'NH4'     , 'PS'     , 'PL'      , &
                 'ZS'    , 'ZL'      , 'ZP'     , 'PON'     , &
                 'DON'   , 'SiOH4'   , 'Opal'   , 'TotalN'  , 'TotalSi'
      write(10,'(A,11(",", F8.4))') CTime, &
                 TNO3/mcr, TNH4  /mcr, TPS  /mcr, TPL /mcr, &
                 TZS /mcr, TZL   /mcr, TZP  /mcr, TPON/mcr, &
                 TDON/mcr, TSiOH4/mcr, TOpal/mcr
      open( 11, file='Forcing.csv', form='FORMATTED' )
      write(11,'(A,13(",", A))') 'Time(day)','Lint0', 'TMP', 'MLD', 'ExcTime'
      write(11,'(A,13(",", 1PE10.4))') CTime, Lint0, Temp, MLD, ExcTime*d2s
!
!     ****** Main Loop *****
      do lt = 1, nt
!       ..... time control (Season : 0 to 1, parcentage in a year).....
        Tbefore = TTime                              ! one step before present time
        TTime   = TTime + dt                         ! present time (real8 form)
        CTime = TT2CD(TTime)                         ! present time (charactor form)
        CALL TT2ND(Iyr, Imon, Iday ,Ihour, Imin, Isec ,TTime)
        Season = ( TTime                - ND2TT(Iyr  ,1,1,0,0,0) )/  &
                 ( ND2TT(Iyr+1,1,1,0,0,0) - ND2TT(Iyr  ,1,1,0,0,0) )
!
!       ..... Example of Boundray condition .....
        Lint0 = 0.1d0 * ( 1.0D0 + 0.3d0 * cos( 2.0d0*3.1415926536d0*(Season - 0.50D0) ) )
        Temp  =         6.0D0 + 4.0d0 * cos( 2.0d0*3.1415926536d0*(Season - 0.65D0) )
        if (Temp .lt. 4.0 ) then
          MLD = MLD + dt * (150.0d0 - MLD ) / ( 100.0d0 * d2s )
          ExcTime = ExcTime + dt * ( 1.0d0/( 40.0d0*d2s) - ExcTime ) / (100.0d0*d2s)
        else
          MLD = MLD + dt * ( 30.0d0 - MLD ) / (   5.0d0 * d2s )
          ExcTime = ExcTime + dt * ( 1.0d0/(100.0d0*d2s) - ExcTime ) / (  5.0d0*d2s)
        end if
!
!       ..... Light Factors (LfcS, LfcL).....
        Lint = Lint0
        LfcDS = Lint/IoptS * exp(1.0D0 - Lint/IoptS)
        LfcDL = Lint/IoptL * exp(1.0D0 - Lint/IoptL)
```

```
      LfcS  = 0.0D0
      LfcL  = 0.0D0
      Kappa = alpha1 + alpha2 * ( TPS + TPL )
      dLint = exp( -Kappa * (MLD/LLN) )
      do L = 1, LLN
        LfcUS  = LfcDS
        LfcUL  = LfcDL
        Lint   = Lint      * dLint
        LfcDS  = Lint/IoptS * exp( 1.0D0 - Lint/IoptS )
        LfcDL  = Lint/IoptL * exp( 1.0D0 - Lint/IoptL )
        LfcS   = LfcS + ( LfcUS + LfcDS ) * 0.5D0 / LLN
        LfcL   = LfcL + ( LfcUL + LfcDL ) * 0.5D0 / LLN
      end do
!     ..... Photosynthesis of PS .....
      GppNPSn   = Mich( KNO3S, TNO3 ) * exp( - PusaiS * TNH4 )
      GppAPSn   = Mich( KNH4S, TNH4 )
      GppPSn    = Td(VmaxS, KGppS) * LfcS * TPS * ( GppNPSn + GppAPSn )
      RnewS     = GppNPSn / ( GppNPSn + GppAPSn )

      ResPSn    = Td( ResPS0, KResPS ) * TPS
      MorPSn    = Td( MorPS0, KMorPS ) * TPS * TPS
      ExcPSn    = GammaS             * GppPSn
!     ..... Photosynthesis of PL .....
      GppNPLn   = Mich( KNO3L, TNO3   ) * exp( - PusaiL * TNH4 )
      GppAPLn   = Mich( KNH4L, TNH4   )
      GppSiPLsi = Mich( KSiL , TSiOH4 )
      GppPLn    = Td(VmaxL, KGppL) * LfcL * TPL * min( ( GppNPLn + GppAPLn ), GppSiPLsi )
      RnewL     = GppNPLn / ( GppNPLn + GppAPLn )
      ResPLn    = Td( ResPL0, KResPL ) * TPL
      MorPLn    = Td( MorPL0, KMorPL ) * TPL * TPL
      ExcPLn    = GammaL             * GppPLn
!     ..... Grazing PS, PL, ZS, ZL --> ZS, ZL, ZP .....
      GraPS2ZSn = Td(GRmaxS,  KGraS) *GraF(LamS,PS2ZSstar,TPS) *TZS
      GraPS2ZLn = Td(GRmaxLps,KGraL) *GraF(LamL,PS2ZLstar,TPS) *TZL
      GraPL2ZLn = Td(GRmaxLpl,KGraL) *GraF(LamL,PL2ZLstar,TPL) *TZL
      GraZS2ZLn = Td(GRmaxLzs,KGraL) *GraF(LamL,ZS2ZLstar,TZS) *TZL
      GraPL2ZPn = Td(GRmaxPpl,KGraP) *GraF(LamP,PL2ZPstar,TPL) *TZP * exp( -PusaiPL *(TZL
       + TZS))
      GraZS2ZPn = Td(GRmaxPzs,KGraP) *GraF(LamP,ZS2ZPstar,TZS) *TZP * exp( -PusaiZS * TZL )
      GraZL2ZPn = Td(GRmaxPzl,KGraP) *GraF(LamP,ZL2ZPstar,TZL) *TZP
!     ..... Mortality, Excration, Egestion for Zooplanktons
!     ..... Commented out after Saito-san Meeting at 19 Jun, 2000 .....
!     BetaZS = 0.3 ** (  1.0 + Mich( TPL, TPS )  )
      ExcZSn = (AlphaZS-  BetaZS)   * GraPS2ZSn
      EgeZSn = (1.0    - AlphaZS)   * GraPS2ZSn
      MorZSn = Td( MorZS0, KMorZS ) * TZS * TZS
      ExcZLn = (AlphaZL-  BetaZL)   * (GraPS2ZLn+GraPL2ZLn+GraZS2ZLn)
      EgeZLn = (1.0    - AlphaZL)   * (GraPS2ZLn+GraPL2ZLn+GraZS2ZLn)
      MorZLn = Td( MorZL0, KMorZL ) * TZL * TZL
      ExcZPn = (AlphaZP-  BetaZP)   * (GraPL2ZPn+GraZS2ZPn+GraZL2ZPn)
      EgeZPn = (1.0    - AlphaZP)   * (GraPL2ZPn+GraZS2ZPn+GraZL2ZPn)
```

```
      MorZPn = Td( MorZP0, KMorZP ) * TZP * TZP
!     ..... Decomposition PON, DON, Opal ---> NH4, DON, SiOH4 .....
      DecP2N    = Td( VP2N0  , KP2N ) * TPON
      DecP2D    = Td( VP2D0  , KP2D ) * TPON
      DecD2N    = Td( VD2N0  , KD2N ) * TDON
      DecO2S    = Td( VO2S0  , KO2S ) * TOpal
      Nit       = Td( Nit0   , KNit ) * TNH4
!     ..... silica fluxes .....
      GppPLsi    = GppPLn    * RSiN
      ResPLsi    = ResPLn    * RSiN
      MorPLsi    = MorPLn    * RSiN
      ExcPLsi    = ExcPLn    * RSiN
      GraPL2ZLsi = GraPL2ZLn * RSiN
      GraPL2ZPsi = GraPL2ZPn * RSiN
      EgeZLsi    = GraPL2ZLsi
      EgeZPsi    = GraPL2ZPsi
!
!     ..... Tendency Terms for biological processes .....
      QNO3   = -( GppPSn - ResPSn ) * RnewS   &
             -( GppPLn - ResPLn ) * RnewL + Nit
      QNH4   = -( GppPSn - ResPSn ) * (1.0 - RnewS)   &
             -( GppPLn - ResPLn ) * (1.0 - RnewL)   &
             - Nit + DecP2N + DecD2N + ExcZSn + ExcZLn + ExcZPn
      QPS    = GppPSn - ResPSn - MorPSn - ExcPSn - GraPS2ZSn - GraPS2ZLn
      QPL    = GppPLn - ResPLn - MorPLn - ExcPLn - GraPL2ZLn - GraPL2ZPn
      QZS    = GraPS2ZSn - GraZS2ZLn - MorZSn - ExcZSn - EgeZSn - GraZS2ZPn
      QZL    = GraPL2ZLn + GraZS2ZLn - MorZLn - ExcZLn - EgeZLn + GraPS2ZLn - GraZL2ZPn
      QZP    = GraPL2ZPn + GraZS2ZPn - MorZPn - ExcZPn - EgeZPn + GraZL2ZPn
      QPON   = MorPSn  + MorPLn  + MorZSn  + MorZLn + MorZPn   &
           + EgeZPn  + EgeZSn  + EgeZLn  - DecP2N - DecP2D
      QDON   = ExcPSn  + ExcPLn  + DecP2D  - DecD2N
      QSiOH4 =-GppPLsi + ResPLsi + ExcPLsi + DecO2S
      QOpal  = MorPLsi + EgeZLsi + EgeZPsi - DecO2S
!
!     ..... Exchange Fluxes between the Surface and Deep Layers .....
      ExpPON   = setVPON  / MLD * TPON
      ExpOpal  = setVOpal / MLD * TOpal
      ExcNO3   = ExcTime * ( TNO3d   - TNO3   )
      ExcSiOH4 = ExcTime * ( TSiOH4d - TSiOH4 )
      QNO3   = QNO3   + ExcNO3
      QSiOH4 = QSiOH4 + ExcSiOH4
      QPON   = QPON   - ExpPON
      QOpal  = QOpal  - ExpOpal
!
!     ..... Time Integration with Forward Scheme .....
      TNO3   = TNO3   + dt * QNO3
      TNH4   = TNH4   + dt * QNH4
      TPS    = TPS    + dt * QPS
      TPL    = TPL    + dt * QPL
      TZS    = TZS    + dt * QZS
      TZL    = TZL    + dt * QZL
```

```
      TZP    = TZP    + dt * QZP
      TPON   = TPON   + dt * QPON
      TDON   = TDON   + dt * QDON
      TSiOH4 = TSiOH4 + dt * QSiOH4
      TOpal  = TOpal  + dt * QOpal
!
!     ..... Vertical Migration of ZL .....
      TZdwn = ND2TT(Iyr, ImonD, IdayD ,IhourD, IminD, IsecD )
      TZup  = ND2TT(Iyr, ImonU, IdayU ,IhourU, IminU, IsecU )
      if ( (Tbefore .lt. TZdwn).and.(TTime .ge. TZdwn) ) then
        TZLd = TZL
        TZL  = 0.0
        write(*,*) '*** Down ***', CTime
      end if
      if ( (Tbefore .lt. TZup).and.(TTime .ge. TZup) ) then
        TZL = SVRate * TZLd
        write(*,*) '***  UP  ***', CTime
      end if
!
      call Saury(TTime, Tbefore, TZS, TZL, TZP, Temp)
!
!     ..... Monitor .....
      if ( int(TTime/Tmon).ne. int(Tbefore/Tmon) ) then
!       write(*,'(A,13(",", F8.4))') CTime, Season
        write(10,'(A,11(",", F8.4))') CTime, &
              TNO3/mcr, TNH4  /mcr, TPS  /mcr, TPL /mcr, &
              TZS /mcr, TZL   /mcr, TZP  /mcr, TPON/mcr, &
              TDON/mcr, TSiOH4/mcr, TOpal/mcr
        write(11,'(A,13(",", 1PE10.4))') CTime, Lint0, Temp, MLD, ExcTime*d2s
      end if
    end do
!
    close(10); close(11)
!
    stop
    end
!*******************************************************************************************
    Subroutine Saury(TTime, Tbefore, TZS, TZL, TZP, Temp)
!
    implicit none
    real(8)          :: TTime, Tbefore, TZS, TZL, TZP, Temp
    real(8),parameter :: d2s       = 86400.0d0    ! day ---> sec
    integer          :: Iyr, Imon, Iday, Ihour, Imin, Isec
    character(19)    :: CAge ='0000/03/01 00:00:00' ! Date of Aging ( JJday = 200 )
    character(19)    :: CTime
    character(19)    :: CAge2 ='0000/07/01 00:00:00' ! Date of Aging ( JJday = 200 )
    character(19)    :: CTime2
    real(8)          :: TAge
    real(8)          :: TAge2
    integer          :: iage = 0
    integer, save    :: IyrA, ImonA, IdayA ,IhourA, IminA, IsecA
```

```
      integer, save     :: IyrB, ImonB, IdayB ,IhourB, IminB, IsecB
      integer           :: JJday
      real(8)           :: ZooP1, ZooP2, ZooP3, tt1
      real(8)           :: t1,t2,wtemp
      real(8)           :: x(1) =0.2d0, xdot(1)
      real(8)           :: cd2tt, nd2tt
      character(19)     :: tt2cd
      real(8)           :: vul(3), k(3)
      integer(4)        :: id(365)
      real(8)           :: zop1(365), zop2(365), zop3(365)
      real(8):: v, a, u, resp
     real(8) :: xk1,xk2,xk3,xk4,te1,te2,te3,te4,tt5,t5,t4,tt7,t7,t6, gcta,gctb,gctemp,gcmax
     real(8) :: cnum,c1,c2,c3,con1,con2,con3,con
     real(8) :: f,e, sda
     real(8) :: phalf
!
      integer, save     :: First = 1
!
      PHalf=0.100

!     ==================
      if ( First .eq. 1 ) then; First = 0
        TAge  = CD2TT( CAge  )
        call TT2ND(IyrA, ImonA, IdayA ,IhourA, IminA, IsecA ,TAge )
        TAge2  = CD2TT( CAge2  )
        call TT2ND(IyrB, ImonB, IdayB ,IhourB, IminB, IsecB ,TAge2 )
        open( 20, file='saury.csv', form='FORMATTED' )

!
!!!!        OPEN(UNIT=111,FILE='nemuro.txt',STATUS='unknown')
!!!!        -----read in the 3 zoop groups from Nemuro output last 3 columns
!!!!        do JJday=1,365
!!!!          READ(111,999)id(JJday),zop1(JJday),zop2(JJday),zop3(JJday)
!!!!  999      FORMAT(1x,i3,1x,3(e13.6,1x))
!!!!        end do
      end if
!     ==================

!
      CTime = TT2CD(TTime)                          ! present time (charactor form)
      CALL TT2ND(Iyr, Imon, Iday ,Ihour, Imin, Isec ,TTime)
      JJday = 1 + ( TTime - ND2TT(Iyr  ,1,1,0,0,0) ) / d2s
!
!------convert Nemuro zoop in uM N/L to g ww/m3
!------  tt1 is conversion from uM N/liter to g ww/m3
!------  14 ug N/uM * 1.0e-6 g/ug * 1 g dw/0.07 g N dw * 1 g ww/0.2 g dw
!------       1.0e3 liters/m3
!
      tt1=14.0*1.0e-6*(1.0/0.07)*(1.0/0.2)*1.0e3
      zoop1 = TZS*tt1 *1.0d6
      zoop2 = TZL*tt1 *1.0d6
```

```
      zoop3 = TZP*tt1 *1.0d6
!!!!     zoop1 = zop1(JJday) * tt1
!!!!     zoop2 = zop2(JJday) * tt1
!!!!     zoop3 = zop3(JJday) * tt1
!
!     ..... Temperature Seting .....
!
      t1=float(jjday)
      t2=12.75-10.99*cos(0.0172*t1)-6.63*sin(0.0172*t1)
      wtemp=t2-5.0
      IF(wtemp.le.1.0)wtemp=1.0

!      write(*,*) TT2CD(cd2tt('0002/01/01 00:00:00')+200.0*86400.0)
!      stop
!     ..... Aging of saury ......
      TAge = ND2TT(Iyr, ImonA, IdayA ,IhourA, IminA, IsecA )
      if ( (Tbefore .lt. TAge).and.(TTime .ge. TAge) .and. (iage.eq.0)) then
           write(*,*) '*** Aging +1 of saury ***', CTime
           iage = iage + 1
      end if
      TAge2 = ND2TT(Iyr, ImonB, IdayB ,IhourB, IminB, IsecB )
      if ( (Tbefore .lt. TAge2).and.(TTime .ge. TAge2) .and. (iage.eq.1) ) then
           write(*,*) '*** Aging +1 of saury ***', CTime
           iage = iage + 1
      end if
!
!--- saury weight state variable = x(1)
!
!----- set vulnerabilities and k values for 3 zoop groups
!
      if ( iage .eq. 0 ) then
        vul(1) =   1.0; vul(2) =  0.0; vul(3) =   0.0
        k  (1) = phalf; k  (2) = phalf; k  (3) = phalf
      else if ( iage .eq. 1 ) then
        vul(1) =   1.0; vul(2) =  1.0; vul(3) =   0.0
        k  (1) = phalf; k  (2) = phalf; k  (3) = phalf
      else
        vul(1) =   0.0; vul(2) =  1.0; vul(3) =   1.0
        k  (1) = phalf; k  (2) = phalf; k  (3) = phalf
      endif
!
! --- weight affect on respiration
!
      tt1 = 1.0 / x(1)
      t1  = 0.0033 * tt1**0.227
! --- *********this is the new stuff from Ahhrenius for YOY only*********
! --- The 5.258 puts resp (g oxygen/fish) into units of g zoop/g fish/day
! --- [13560 joules/gram oxygen]/4.18 joules/cal = 3244 cal/gO2
! --- [2580 joules/gram zoop]/4.18 joules/cal = 617 cal/g zoop
! --- so respiration in grams/oxygen/g fish/day is multiplied by 3244/617 = 5.258
! --- to get food energy equivalents of a gram of oxygen respired
```

```
!
!ccc      IF (iage .eq. 0 )then
!ccc        IF(wtemp.le.15.0)then
!ccc          v = 5.76 * exp( 0.0238 * wtemp ) * x(1)**0.386
!ccc        else
!ccc          v = 8.6 * x(1)**0.386
!ccc        endif
!ccc        a=EXP((0.03-0.0*wtemp)*v)
!ccc        resp=t1*EXP(0.0548*wtemp)*a*5.258
! --- *********back to the old equations for respiration for age-1 and older********
!ccc      else   ! (iage .gt. 0)
!c         IF (wtemp.le.9.0)then
        IF (wtemp.le.12.0)then
!C           u=3.9*x(1)**0.13*EXP(0.149*wtemp)
          u=2.0*x(1)**0.33*EXP(0.149*wtemp)
        else
!c           u=15.0*x(1)**0.13
          u=11.7*x(1)**0.33
        endif
          resp=t1*EXP(0.0548*wtemp)*EXP(0.03*u)*5.258
!ccc      endif
!C
!C --- Thornton and Lessem temperature effect
!C --- age dependent values
!C --- *******Arrhenius for age-0 he changed te4 from 25 to 23 degrees******
!C
     if ( iage .eq. 0 ) then
!c        xk1 = 0.1;  xk2 = 0.98;  xk3 = 0.98;  xk4 = 0.01
!c        te1 = 1.0;  te2 = 15.0;  te3 = 17.0;  te4 = 23.0
        xk1 = 0.1;  xk2 = 0.98;  xk3 = 0.98;  xk4 = 0.5
        te1 = 5.0;  te2 = 20.0;  te3 = 26.0;  te4 = 30.0
     else if ( iage .eq. 1 ) then
!c        xk1 = 0.1;  xk2 = 0.98;  xk3 = 0.98;  xk4 = 0.01
!c        te1 = 1.0;  te2 = 15.0;  te3 = 17.0;  te4 = 25.0
        xk1 = 0.1;  xk2 = 0.98;  xk3 = 0.98;  xk4 = 0.5
        te1 = 5.0;  te2 = 16.0;  te3 = 20.0;  te4 = 30.0
     else if( iage .gt. 1 ) then
!c        xk1 = 0.1;  xk2 = 0.98;  xk3 = 0.98;  xk4 = 0.01
!c        te1 = 1.0;  te2 = 13.0;  te3 = 15.0;  te4 = 23.0
        xk1 = 0.1;  xk2 = 0.98;  xk3 = 0.98;  xk4 = 0.5
        te1 = 5.0;  te2 = 16.0;  te3 = 20.0;  te4 = 30.0
     endif
!
     tt5 = ( 1.0 / ( te2 - te1 ) )
     t5  = tt5 * log( xk2 * ( 1.0 - xk1 ) / ( (1.0-xk2) * xk1 ) )
     t4  = exp( t5 * ( wtemp - te1 ) )
!
     tt7 = 1.0 /( te4 - te3 )
     t7  = tt7 * log( xk3 * ( 1.0 - xk4 ) / ( (1.0-xk3) * xk4 ) )
     t6  = exp( t7 * ( te4 - wtemp ) )
!
```

```
      gcta  = ( xk1 * t4 ) / ( 1.0 + xk1 * ( t4 - 1.0 ) )
      gctb  = xk4 * t6 / ( 1.0 + xk4 * ( t6 - 1.0 ) )
      gctemp= gcta * gctb
!c      gcmax = 0.642 * tt1**0.256 * gctemp
      gcmax = 0.6 * tt1**0.256 * gctemp
!
! --- multispecies functional response
! --- usse either this or adjust little p
!
      cnum=zoop1 * vul(1)/k(1) + zoop2*vul(2)/k(2) +zoop3 * vul(3)/k(3)
      c1=gcmax*zoop1*vul(1)/k(1)
      c2=gcmax*zoop2*vul(2)/k(2)
      c3=gcmax*zoop3*vul(3)/k(3)
      con1=c1/(1.0+cnum)
      con2=c2/(1.0+cnum)
      con3=c3/(1.0+cnum)
      con= con1+con2+con3
!
!-----if using constant p rather than functional response, set p here
! --- to tune to observed size at age data
!     con=0.425*gcmax
!
! --- egestion
!
          f=0.16*con
!
! --- excretion
          e=0.1*(con-f)
!
!
! --- Specific Dynamic Action
!
!c------   *******Arrhenius age dependent SDA from 17.5% to 15% ****
          IF ( iage .eq. 0 ) then
            sda=0.15*(con-f)
          else
            sda=0.175*(con-f)
          end if
!C
!C --- use the ratio of calories/g of zoop (2580) to calories/g of fish (5533)
!C
!C --- bioenergetics differential equation
!C
         xdot(1)=(con-resp-f-e-sda)*x(1)*2580./5533.
!
         IF(wtemp.le.1.0)xdot(1)=0.0
!C
!C --- Spawning section. Assume loose 20% of bosy weight/day
!C            t1=float(jjday)
!      if( mod(JJday,365) .ge. 152.0 .and. mod(JJday,365) .le. 156.0) then
!         xdot(1)=(con-resp-f-e-sda-0.20)*x(1)*2580./5533.
```

```
!         write(*,*) '### Spawning ###'
!      endif
!
!     if (iage .eq. 1 ) then
!      write(*,*) JJday, wtemp, x(1), xdot(1)
!      stop
!      end if
!      write(*,'(A,I4,3(1PE14.5))') Ctime, JJday, wtemp, x(1), xdot(1)
!
!     Time Integration
!
      x(1) = x(1) + 3600.0d0 /d2s * xdot(1)
!
!     ..... for Check .....
     if ( int(TTime/d2s) .ne. int(Tbefore/d2s) ) then
!!       write(*,'(A,I4,3(1PE14.5))') Ctime, JJday, wtemp, x(1), xdot(1)
!!        stop
!!      write(*,*) TZS, zop1(JJday), TZL,zop2(JJday), TZP,zop3(JJday)
!!      write(*,*) TZP*1.0d6, zop3(JJday)
        write(20,'(A,11(",", F12.4))') CTime, x(1), wtemp, gcmax
      end if
!
      return
!
      stop
      end
!*******************************************************************************************
!* Utilities for Date Control  Writtien by Yasuhiro Yamanaka (galapen@ees.hokudai.ac.jp) *
!*******************************************************************************************
!     exp. 1997/12/31 23:59:59 --> 6.223158719900000E+10
!     exp. 0000/01/01 00:00:00 --> 0.000000000000000E+00
!*******************************************************************************************
      real(8) function CD2TT( Cdate )
!
      integer       :: Iyr, Imon, Iday , Ihour, Imin, Isec
      real(8)       :: ND2TT
      character(19) :: Cdate
!
      if ( len( Cdate ) .ne. 19 ) then
        write(*,*) '### Length of date is no good ###'
        stop
      end if
      read (Cdate( 1: 4),*)  Iyr
      read (Cdate( 6: 7),*)  Imon
      read (Cdate( 9:10),*)  Iday
      read (Cdate(12:13),*)  Ihour
      read (Cdate(15:16),*)  Imin
      read (Cdate(18:19),*)  Isec
!
      CD2TT = ND2TT(Iyr, Imon, Iday , Ihour, Imin, Isec)
!
```

```
    return
    end function
!**********************************************************************
!    exp. 6.223158719900000E+10 --> 1997/12/31 23:59:59
!**********************************************************************
    character(19) function TT2CD(tt)
!
    integer :: Iyr, Imon, Iday , Ihour, Imin, Isec
    real(8) :: tt
!
    call TT2ND( Iyr, Imon, Iday, Ihour, Imin, Isec , tt )
!
    write(TT2CD,'(I4.4,5(A,I2.2))') Iyr, '/', Imon, '/', Iday, &
                        ' ', Ihour, ':', Imin, ':', Isec
!
    return
    end function
!**********************************************************************
!    exp. 1997,12,31,23,59,59 --> 6.223158719900000E+10
!**********************************************************************
    real(8) function ND2TT(Iyr, Imon, Iday, Ihour, Imin, Isec)
!
    integer   :: IM2D(12,0:1) = &
      reshape( (/ 0,31,59,90,120,151,181,212,243,273,304,334,  &
                  0,31,60,91,121,152,182,213,244,274,305,335  /), (/12,2/) )
    integer   :: Iyr, Imon, Iday, Ihour, Imin, Isec
    integer   :: Iy4, Iy1, Ileap, Im, Itt
!
!
    Iy4 = 1461 * ( Iyr / 4 )
    Iy1 = 365 * mod( Iyr, 4 )
!
    if ( mod( Iyr, 4 ) .ne. 0 ) then
      Ileap = 0
    else
      Ileap = 1
    end if
    Im = IM2D( Imon, Ileap)
!
    Itt = Iy4 + Iy1 + Im + Iday - Ileap
!
    ND2TT = Ihour * 3600 + Imin * 60 + Isec
    ND2TT = ND2TT + Itt * 86400.0D0
!
    return
    end function
!**********************************************************************
!    exp. 6.223158719900000E+10 --> 1997,12,31,23,59,59
!**********************************************************************
    subroutine TT2ND(                                &
            Iyr   , Imon  , Iday   , Ihour, Imin, Isec,   & !O & I
```

```
            tt    )
!
    integer :: Iyr, Imon, Iday , Ihour, Imin, Isec
    integer :: Itt, Iy, Iy4, Iyd, Iy1, Ileap, Imd, Im, Its
    integer   :: IM2D(12,0:1) = &
      reshape( (/ 0,31,59,90,120,151,181,212,243,273,304,334,  &
                  0,31,60,91,121,152,182,213,244,274,305,335  /), (/12,2/) )
    integer :: IY2D(4) = (/0,366,731,1096/)
    real(8) :: tt, tt0, ND2TT
!
!
!   ..... ITT [day] .....
    Itt = 1 + tt / 86400.0D0
!
    Iy4   = (Itt-1) / 1461
    Iyd   = Itt - Iy4 * 1461
    do IY = 1, 4
      if ( IY2D(Iy) + 1 .le. Iyd ) then
        Iy1 = Iy
      end if
    end do
!
    Iyr   = Iy4 * 4 + Iy1 - 1
    if ( mod(Iyr,4) .ne. 0 ) then
      Ileap = 0
    else
      Ileap = 1
    end if
    IMD = IYD - IY2D(IY1)
!
    do IM = 1, 12
      if ( IM2D(IM,ILEAP)+1 .le. IMD ) then
        IMON = IM
      end if
    end do
    IDAY = IMD - IM2D(IMON,ILEAP)
!
    TT0 = ND2TT(IYR, IMON, IDAY ,0,0,0)
    ITS = nint(  TT - TT0 )
    Ihour = ITS / 3600
    Imin  = ( ITS - Ihour * 3600 ) / 60
    Isec  = ITS - Ihour * 3600 - Imin * 60
!
    return
    end subroutine
!
```